

PURINERGIC SIGNALLING IN THE FRAGILE X MOUSE CORTEX

ASTROCYTE-MEDIATED PURINERGIC SIGNALLING  
IN THE FRAGILE X MOUSE CORTEX

By

KATHRYN E. REYNOLDS, BSc (Hons), MSc

A Thesis  
Submitted to the School of Graduate Studies  
in Partial Fulfillment of the Requirements  
for the Degree

Doctor of Philosophy

McMaster University  
© Kathryn E. Reynolds, September 2021

DOCTOR OF PHILOSOPHY (2021)  
(Health Sciences – Neuroscience)

McMaster University  
Hamilton, Ontario

TITLE: Astrocyte-mediated purinergic signalling in the  
Fragile X mouse cortex  
AUTHOR: Kathryn E. Reynolds, BSc (Hons), MSc (University of Guelph)  
SUPERVISOR: Angela L. Scott, PhD  
PAGES: xviii, 236

## Lay Abstract

Autism spectrum disorders (ASDs) have become a serious health concern in recent years due to rapidly rising rates of diagnosis. Despite extensive research, there are still no effective treatments for these disorders of brain development. It is therefore important that we study the cellular events contributing to ASDs in order to design new therapeutic strategies. The most common inherited form of ASD is Fragile X syndrome (FXS), which is characterized by cognitive and motor disabilities, sensory hyperresponsivity, attention deficits, hyperactivity, and seizures. Using the *Fmr1* knockout (KO) mouse model of FXS, recent research has shown that many of these symptoms are related to disordered communication between brain cells within the cerebral cortex; specifically, between neurons and the helper-like cells known as astrocytes. One form of cellular signalling that supports this communication is known as the purinergic signalling pathway. Collectively, this thesis work is the first to show that purinergic signalling is increased in *Fmr1* KO mouse cortical astrocytes and that it impacts FXS neuronal connections. Specifically, *Fmr1* KO cortical astrocytes demonstrated increased communication using purinergic signalling, due to greater expression of P2Y<sub>2</sub> and P2Y<sub>6</sub> purinergic receptors and altered levels of the molecules that stimulate these receptors. Activation of *Fmr1* KO astrocyte P2Y receptors promoted expression of the neuronal connection-forming protein TSP-1 and stimulated additional astrocyte signalling pathways. As a result of these changes, when *Fmr1* KO neurons were grown in the presence of *Fmr1* KO astrocytes, they grew longer extensions and demonstrated greater activity than wildtype controls, in a manner consistent with the excitation-related symptoms of FXS. Selectively targeting P2Y<sub>2</sub>-driven purinergic pathways with drug treatments corrected this activity, thereby revealing a potential new therapeutic approach for FXS. Understanding excess astrocyte P2Y-driven purinergic communication within the brain may therefore provide a foundation for the future development of new FXS treatments.

## Abstract

Disordered communication between cortical neurons and glia underlies many of the characteristics of Fragile X syndrome (FXS), the most common monogenic form of intellectual disability and autism spectrum disorder (ASD). Despite extensive research, no effective treatments exist to comprehensively mitigate ASD- or FXS-related cognitive and motor disabilities, sensory hyperresponsivity, seizures, and other excitation-related symptoms. Glial-glial and glial-neuronal communication can be facilitated by purinergic signalling pathways, which utilize ATP, UTP, and their metabolites to influence both short-term and longer-term activation. The overall objective of this thesis work was to establish whether purinergic signalling is dysregulated within cortical astrocytes derived from the *Fmr1* KO mouse model of FXS, and furthermore, to determine whether astrocyte purinergic dysregulations contribute to aberrant *Fmr1* KO neuronal-glial interactions. Collectively, these studies provide the first reported evidence that P2Y receptor-driven purinergic signalling is elevated in *Fmr1* KO cortical astrocytes, and suggest that this impacts the formation and activity of neuronal circuitry in a manner consistent with FXS symptomatology. *Fmr1* KO cortical astrocyte dysregulations included elevated expression of P2Y<sub>2</sub> and P2Y<sub>6</sub> purinergic receptors, increased intracellular calcium release following P2Y activation, aberrant levels of intracellular purinergic signalling molecules, and increased ectonucleotidase glycosylation. UTP treatment promoted excess *Fmr1* KO astrocyte expression and secretion of the synaptogenic protein TSP-1 to potentially influence neuronal connectivity, as well as increased phosphorylation of transcription factor STAT3 to likely drive cortical immune responses. Both exogenous UTP and the presence of *Fmr1* KO astrocyte secretions promoted neurite outgrowth, while *Fmr1* KO astrocyte-neuron co-cultures demonstrated elevated neuronal burst frequency that was normalized through chronic and selective P2Y<sub>2</sub> antagonism. Together, these findings indicate novel and significant astrocyte P2Y-mediated purinergic upregulations within the *Fmr1* KO mouse cortex, and suggest that astrocyte purinergic signalling should be further investigated in the search for innovative FXS treatments.

## **Preface**

This thesis is prepared as a compilation of manuscripts written by the author, K.E. Reynolds, which have been published, submitted, or prepared for submission. A general literature review is included in Chapter One, four author-generated manuscripts are presented in Chapters Two through Five, and an overall discussion and conclusion is included in Chapter Six. As a result of this sandwich thesis structure, there may be a considerable amount of overlap between the topics presented in each chapter, especially within the introductory and discussion sections.

## Acknowledgements

First and foremost, **Dr. Angela Scott** – thank you for absolutely everything. I am immensely grateful that you took me under your wing and helped to guide this project down a path that neither of us could've seen coming. Thank you for nudging me into tackling the big projects, pushing me when I needed to be pushed, reassuring me when I doubted my decisions, and fostering an incredibly supportive and encouraging working relationship. It has been such a pleasure to be your first PhD student, and I am so thankful for your guidance throughout the years.

**Dr. Laurie Doering** – thank you for bringing me into the lab, for your encouragement and positivity as I started at McMaster, and for your support with scholarship applications. Thank you to my supervisory committee, **Dr. Ram Mishra** and **Dr. Kathy Murphy**, for your guidance throughout this degree. I am also extremely grateful for the financial support of the **Canadian Institutes of Health Research** throughout my degree.

This research would not be possible without significant help from my collaborators. **Dr. M. Kirk Green** and **Dr. Fan Fei** – when I naïvely showed up with plans to quantify purinergic signalling molecules using mass spectrometry, we never expected that this “little collaboration” would turn into a multiple year-long troubleshooting journey. Thank you for your expert advice and endless patience as we've worked through this deceptively difficult task of detecting UTP together. **Nadeem Murtaza** and **Dr. Karun Singh** – thank you for your guidance with microelectrode array optimization and for the use of your laboratory space and equipment.

So many graduate and undergraduate researchers have made the Scott Lab a productive and supportive place to work. **Gregory**, thank you for being a friend and the most supportive of colleagues throughout our years working together. **Chloe**, you're the reason I headed down the rabbit hole of astrocyte P2Y receptors, and you've provided me with never-ending encouragement for years after your graduation. **Eileen**, I appreciate your tireless work helping me to troubleshoot microelectrode array experiments more than you know. **Monica, Eliza** and **Aasritha**, thank you for never doubting me as I asked you to diligently plug away at endless neurite analyses. **Victoria, Eva**, and **Matt**, it has been a pleasure working alongside you in the lab and watching as our understanding of astrocyte and purinergic dysregulations continues to grow. To all the other Scott Lab members – thank you, too.

I am also incredibly grateful for the friends I've made and maintained along the way. My Guelph ladies, **Dendra, Julia**, and **Lisette** – thank you for your endless advice and opinions on work, life, and everything in between, and for helping me to keep things in perspective. To my McMaster crew, especially **Saurabh, Aya**, and **Ashley**, thank you for

all our pre-pandemic SOMA adventures, and for engaging in the most stimulating conversations about anything and everything brain-related.

*Mom & Dad* – thank you for supporting me in my working and writing from the cottage, and for humouring me every time I needed a Horseshoe Lake kayak to de-stress. More importantly, thank you for encouraging me to always strive for success and for believing that I have what it takes to get there. I am grateful to have grown up with not just one, but two researcher role models, and I am proud to become the second Dr. Reynolds in the family.

And last, but not least, *Mike* – thank you for selflessly celebrating my triumphs, empathizing with my struggles, solving my technical difficulties, and understanding when I needed to buckle down and when I needed a break from it all. You’ve been my greatest cheerleader, supporter, and a true partner throughout these past 4+ years. Despite distance, a pandemic, and all the other unexpected things that have come our way – here we are, about to start the next chapter as Dr. Reynolds and Dr. Zylstra. I’m so proud of both of us, and so grateful for you.

## Declaration of Academic Achievement

The majority of the work presented within this thesis was designed, conducted, analyzed, interpreted, and written by the author, Kathryn E. Reynolds, under the supervision of Dr. Angela L. Scott. Within each chapter, the *Author Contributions* subsection indicates the specific research contributions of each individual.

In addition to the published and submitted manuscripts included within this thesis, the author has presented these findings at the following scientific meetings:

1. Reynolds, K.E., Huang, E., Sabbineni, M., Wiseman, E., Wong, C.R. & Scott, A.L. Upregulated astrocyte purinergic signalling increases neurite extension and neuronal activity in a mouse model of Fragile X syndrome. Poster: Canadian Association for Neuroscience Annual Meeting; 2021 August 23-25; Virtual Format.
2. Reynolds, K.E. Purinergic signalling dysfunction in Fragile X cortical astrocytes. Guest Lecture: Topics in Physiology Seminar, McMaster University. 27 Oct 2020; Hamilton, ON.
3. Reynolds, K.E., Wong, C.R., Wiseman, E., Thotakura, A. & Scott, A.L. Pyrimidinergetic signalling alterations in the Fragile X Syndrome mouse cortex. Poster presentation: Canadian Association for Neuroscience Annual Meeting; 2020 May 31 – June 3; Toronto, ON. *\*\*Abstract accepted; conference cancelled due to COVID-19\*\**
4. Reynolds, K.E., Wong, C.R., Doering, L.C. & Scott, A.L. Astrocyte purinergic signalling and thrombospondin-1 expression are dysregulated within the Fragile X Syndrome mouse cortex. Poster: Society for Neuroscience; 2019 October 21; Chicago, IL.
5. Reynolds, K.E., Wong, C.R., Huang, E., Doering, L.C. & Scott, A.L. Pyrimidinergetic signalling alterations in the Fragile X Syndrome mouse cortex. Poster: Canadian Association for Neuroscience Annual Meeting; 2019 May 24; Toronto, ON.
6. Reynolds, K.E., Wong, C.R., Doering, L.C. & Scott, A.L. Pyrimidinergetic signalling alterations in the Fragile X Syndrome mouse cortex. Invited Presentation: Faculty of Health Sciences Research Plenary; 2019 May 16; Hamilton, ON.
7. Reynolds, K.E., Wong, C.R., Doering, L.C. & Scott, A.L. Astrocyte thrombospondin-1 expression is altered in Fragile X syndrome following treatment with exogenous UTP. Poster: Society for Neuroscience; 2018 November 3-7; San Diego, CA.

8. Reynolds, K.E., Scott, A.L. & Doering, L.C. Astrocyte thrombospondin-1 expression is altered in Fragile X syndrome following treatment with exogenous UTP. Poster: Cold Spring Harbor Glia in Health and Disease Meeting; 2018 July 21; Cold Spring Harbor, NY.
9. Reynolds, K.E., Scott, A.L. & Doering, L.C. Exploring alterations in astrocyte thrombospondin-1 expression in Fragile X Syndrome. Invited Oral Presentation: McMaster University Faculty of Health Sciences Research Plenary; 2018 May 17; Hamilton, ON.
10. Reynolds, K.E., Scott, A.L. & Doering, L.C. Astrocyte thrombospondin-1 expression is altered in Fragile X Syndrome following treatment with exogenous UTP. Poster: Southern Ontario Neuroscience Association Annual Meeting; 2018 May 4; Guelph, ON.
11. Reynolds, K.E., Scott, A.L. & Doering, L.C. Alterations in astrocyte thrombospondin-1 expression in Autism Spectrum Disorders. Poster: McMaster University PNB & MiNDS Graduate Research Day; 2017 December 7; Hamilton, ON.
12. Reynolds, K.E., Scott, A.L. & Doering, L.C. Alterations in astrocyte thrombospondin-1 expression in Autism Spectrum Disorders. Poster: Society for Neuroscience Annual Meeting; 2017 November 12; Washington, DC.
13. Reynolds, K.E. & Doering, L.C. Alterations in astrocyte thrombospondin-1 (TSP-1) expression in Autism Spectrum Disorders. 3 Minute Thesis: Neuroscience Graduate Program (MiNDS) 10 Year Anniversary Event; 2017 September 23; Hamilton, ON.

Kathryn E. Reynolds has also contributed to the field through the following works that are currently in preparation, and are not included within the thesis:

1. Reynolds, K.E., Poxon, A.F., Andrews, S. & Scott, A.L. P2X-mediated astrocyte purinergic signalling mediates neurite outgrowth and excitability in the Fragile X mouse cortex. To be submitted to *Purinergic Signaling*.
2. Reynolds, K.E., Chowdhury, H., Sabbineni, M., Benaini, A., Shin, D., Shoeib, A. & Scott, A.L. Adenosine signalling in the Fragile X mouse cortex leads to enhanced circuit excitation. To be submitted to *Molecular Neurobiology*.

In recognition of these academic achievements, the author has received the following scholarships and awards:

Canadian Institutes of Health Research Doctoral Award (CIHR CGS-D)	September 2017 – August 2020
<i>*COVID-19 CGS-D funding extension</i>	August 2020 – December 2020
Faculty of Health Sciences Research Plenary Excellence in Oral Presentation Award	May 30, 2018

## Table of Contents

<b>LAY ABSTRACT .....</b>	<b>III</b>
<b>ABSTRACT.....</b>	<b>IV</b>
<b>PREFACE.....</b>	<b>V</b>
<b>ACKNOWLEDGEMENTS .....</b>	<b>VI</b>
<b>DECLARATION OF ACADEMIC ACHIEVEMENT.....</b>	<b>VIII</b>
<b>LIST OF FIGURES AND TABLES.....</b>	<b>XIV</b>
<b>LIST OF ABBREVIATIONS .....</b>	<b>XVI</b>
<b>1. CHAPTER ONE: INTRODUCTION.....</b>	<b>1</b>
1.1. AUTISM SPECTRUM DISORDER.....	1
1.1.1. <i>Prevalence</i> .....	1
1.1.2. <i>Symptoms</i> .....	1
1.1.3. <i>Genetic and Environmental Factors</i> .....	2
1.2. FRAGILE X SYNDROME .....	2
1.2.1. <i>Prevalence</i> .....	2
1.2.2. <i>Symptoms</i> .....	3
1.2.3. <i>Current Therapeutic Approaches</i> .....	3
1.2.4. <i>The Genetic Basis of FXS</i> .....	4
1.2.5. <i>FMRP Expression</i> .....	5
1.2.6. <i>FMRP-Mediated mRNA Binding and Translational Regulation</i> .....	5
1.2.7. <i>The Fmr1 Knockout Mouse Model of FXS</i> .....	6
1.3. THE CEREBRAL CORTEX .....	8
1.3.1. <i>Structure and Function</i> .....	8
1.3.2. <i>Cortical Neurons</i> .....	9
1.3.3. <i>Neurite Extension</i> .....	9
1.3.3.1. <i>Neurite Outgrowth and Branching in FXS</i> .....	10
1.3.4. <i>Cortical Astrocytes</i> .....	11
1.3.5. <i>Synaptogenesis</i> .....	13
1.3.5.1. <i>Synaptic Characteristics in FXS</i> .....	14
1.3.5.1.1. <i>Converging Synptogenic and Immune Regulation in FXS</i> .....	16
1.3.6. <i>Synaptic Activity</i> .....	16
1.3.6.1. <i>Neuronal Network Activity in FXS</i> .....	17
1.4. PURINERGIC SIGNALLING.....	18
1.4.1. <i>Purinergic Receptors</i> .....	18
1.4.2. <i>P2Y Receptors</i> .....	19
1.4.3. <i>UTP Synthesis and Breakdown</i> .....	20
1.4.4. <i>Calcium Waves</i> .....	23
1.4.5. <i>Signal Transduction</i> .....	25
1.5. P2Y RECEPTORS IN CORTICAL DEVELOPMENT AND CONNECTIVITY .....	26

1.5.1. <i>Neurite Outgrowth and Branching</i> .....	26
1.5.2. <i>Synaptogenesis</i> .....	27
1.5.3. <i>Purinergic Dysregulation in Fragile X and Autism Spectrum Disorder</i> .....	28
1.6. RESEARCH OBJECTIVE .....	29
1.7. AIMS AND HYPOTHESES .....	29
1.8. REFERENCES .....	31
<b>2. CHAPTER TWO:.....</b>	<b>44</b>
<b>ASTROCYTE-MEDIATED PURINERGIC SIGNALLING IS UPREGULATED IN A MOUSE MODEL OF FRAGILE X SYNDROME .....</b>	<b>44</b>
2.1. PREFACE .....	44
2.2. STUDY SIGNIFICANCE .....	44
2.3. AIMS AND HYPOTHESES .....	45
2.4. PUBLICATION STATUS .....	45
2.5. AUTHOR CONTRIBUTIONS .....	47
2.6. ABSTRACT .....	47
2.7. INTRODUCTION .....	48
2.8. MATERIALS AND METHODS .....	51
2.9. RESULTS .....	59
2.10. DISCUSSION .....	72
2.11. PERSPECTIVES AND SIGNIFICANCE .....	81
2.12. REFERENCES .....	84
<b>3. CHAPTER THREE:.....</b>	<b>93</b>
<b>DYSREGULATED PURINERGIC SIGNALLING MOLECULES IN FRAGILE X MOUSE CORTICAL ASTROCYTES .....</b>	<b>93</b>
3.1. PREFACE .....	93
3.2. STUDY SIGNIFICANCE .....	93
3.3. AIMS AND HYPOTHESES .....	94
3.4. PUBLICATION STATUS .....	94
3.5. AUTHOR CONTRIBUTIONS .....	95
3.6. ABSTRACT .....	95
3.7. INTRODUCTION .....	96
3.8. METHODS .....	99
3.9. RESULTS .....	103
3.10. DISCUSSION .....	109
3.11. REFERENCES .....	117
<b>4. CHAPTER FOUR: .....</b>	<b>122</b>
<b>CONVERGING PURINERGIC AND IMMUNE SIGNALLING PATHWAYS DRIVE IL-6 SECRETION BY FRAGILE X CORTICAL ASTROCYTES VIA STAT3 .....</b>	<b>122</b>
4.1. PREFACE .....	122

4.2.	STUDY SIGNIFICANCE .....	122
4.3.	AIMS AND HYPOTHESES.....	123
4.4.	PUBLICATION STATUS.....	123
4.5.	AUTHOR CONTRIBUTIONS.....	125
4.6.	ABSTRACT .....	125
4.7.	INTRODUCTION .....	126
4.8.	METHODS.....	128
4.9.	RESULTS .....	133
4.10.	DISCUSSION .....	143
4.11.	CONCLUSION.....	149
4.12.	REFERENCES .....	151
<b>5.</b>	<b>CHAPTER FIVE: .....</b>	<b>157</b>
	<b>ASTROCYTE-DERIVED PURINERGIC SIGNALLING MEDIATES NEURITE OUTGROWTH AND EXCITABILITY IN THE FRAGILE X MOUSE CORTEX</b> .....	<b>157</b>
5.1.	PREFACE .....	157
5.2.	STUDY SIGNIFICANCE .....	157
5.3.	AIMS AND HYPOTHESES.....	158
5.4.	PUBLICATION STATUS.....	158
5.4.	AUTHOR CONTRIBUTIONS.....	159
5.5.	ABSTRACT .....	159
5.6.	INTRODUCTION .....	160
5.7.	METHODS.....	163
5.8.	RESULTS .....	170
5.9.	DISCUSSION .....	189
5.10.	SUMMARY .....	200
5.11.	REFERENCES .....	201
<b>6.</b>	<b>CHAPTER SIX: .....</b>	<b>209</b>
	<b>DISCUSSION AND CONCLUSIONS .....</b>	<b>209</b>
6.1.	REFERENCES .....	223
<b>7.</b>	<b>APPENDIX: COPYRIGHT TRANSFER AGREEMENTS.....</b>	<b>229</b>

## List of Figures and Tables

### Chapter One: Introduction

Figure 1. Timeline of mouse cortical neurodevelopment. ....	12
Table 1. Members of the metabotropic P2Y purinergic receptor subfamily .....	20
Figure 2. Astrocyte synthesis and breakdown of uridine-based purinergic signalling molecules. ....	22
Figure 3. P2Y-mediated astrocyte calcium signalling. ....	24

### Chapter Two: Astrocyte-mediated purinergic signalling is upregulated in a mouse model of Fragile X syndrome

Figure 1. High resolution intracellular calcium recording of primary astrocytes isolated from <i>Fmr1</i> KO and WT P1 cortices. ....	60
Figure 2. High-resolution intracellular calcium recordings of <i>Fmr1</i> KO and WT primary cortical astrocytes following P2Y receptor agonism and antagonism. ....	62
Figure 3. <i>In vitro</i> quantitative Western blotting analysis and immunocytochemistry of P2Y receptors in primary astrocytes cultured from P1 WT and <i>Fmr1</i> KO cortices. ....	64
Figure 4. Quantitative protein expression of P2Y receptors in acutely dissociated P1 cortical astrocytes (As) versus astrocyte-depleted fraction of other cells (Oth), isolated via magnetic cell separation. ....	65
Figure 5. Astrocyte secretion of TSP-1 following 12 h UTP treatment. ....	68
Figure 6. TSP-1 expression in WT and <i>Fmr1</i> KO primary astrocyte culture following 12 h UTP treatment. ....	69
Figure 7. Quantitative Western blotting analysis of TSP-1 expression .....	71
Figure 8. Purinergic signalling is upregulated in early postnatal <i>Fmr1</i> KO cortical astrocytes. ....	73
Supplementary Figure 1. Assessment of astrocyte health following UTP treatment. ....	83

### Chapter Three: Dysregulated purinergic signalling molecules in Fragile X mouse cortical astrocytes

Table 1. Optimized gradient utilized for LC/MS nucleotide analysis. ....	102
Figure 1. LC/MS quantification of intracellular UTP, UDP, and UMP in WT and <i>Fmr1</i> KO primary cortical astrocytes. ....	105
Figure 2. LC/MS quantification of intracellular ATP, ADP, and AMP in WT and <i>Fmr1</i> KO primary cortical astrocytes. ....	106
Figure 3. LC/MS quantification of intracellular nucleosides in WT and <i>Fmr1</i> KO primary cortical astrocytes. ....	107

Figure 4. Western blotting quantification of WT and <i>Fmr1</i> KO primary cortical astrocyte membrane-bound ectonucleotidases. ....	108
--	-----

**Chapter Four: Converging purinergic and immune signalling pathways drive IL-6 secretion by Fragile X cortical astrocytes via STAT3**

Figure 1. Secreted and cell-associated TNC following application of exogenous UTP to WT and <i>Fmr1</i> KO cortical astrocyte cultures. ....	134
Figure 2. Proportion of tyrosine-phosphorylated STAT3 vs total STAT3 in WT and <i>Fmr1</i> KO cortical astrocyte cultures treated with exogenous UTP and TNC. ....	135
Figure 3. IL-6 secretion from WT and <i>Fmr1</i> KO cortical astrocytes following STAT3 knockdown. ....	137
Figure 4. IL-6 secretion from WT and <i>Fmr1</i> KO cortical astrocytes following TLR4 antagonism. ....	140
Figure 5. Soluble/bound IL-6 receptor (s/IL-6R) association with WT and <i>Fmr1</i> KO cortical astrocytes following 3 h treatment with TNC. ....	142
Figure 6. Proposed model of purinergic and immune interactions in cortical astrocytes. ....	145

**Chapter Five: Astrocyte-derived purinergic signalling mediates neurite outgrowth and excitability in the Fragile X mouse cortex**

Figure 1. Extension of the longest neurite in WT and <i>Fmr1</i> KO primary neurons cultured for 5DIV in combination with either WT or <i>Fmr1</i> KO astrocyte-conditioned media, and treated with the P2Y agonist UTP. ....	171
Figure 2. Sholl analysis of WT and <i>Fmr1</i> KO primary neurons cultured in WT or <i>Fmr1</i> KO astrocyte-conditioned media in the presence of UTP. ....	175
Figure 3. Quantification of P2Y <sub>1</sub> , P2Y <sub>2</sub> , P2Y <sub>4</sub> , and P2Y <sub>6</sub> excitatory purinergic receptors in neurons cultured from WT and <i>Fmr1</i> KO embryonic (E15) cortex. ....	178
Figure 4. Firing characteristics of WT and <i>Fmr1</i> KO co-cultured neurons between 7-35DIV. ....	181
Figure 5. Normalization of aberrant neuronal <i>Fmr1</i> KO bursting with P2Y <sub>2</sub> antagonism. ....	185

## List of Abbreviations

ACM	astrocyte-conditioned media
ACSA-2	astrocyte cell surface antigen
ADP	adenosine diphosphate
Akt	protein kinase B
AMP	adenosine monophosphate
AMPA	alpha-amino-3-hydroxy-5-methyl-4-isoxazolepropionic acid
ANOVA	analysis of variance
AP-5	(2 <i>R</i> )-amino-5-phosphonovaleric acid
AR-C 118925XX	5-[[5-(2,8-Dimethyl-5 <i>H</i> -dibenzo[a,d]cyclohepten-5-yl)-3,4-dihydro-2-oxo-4-thioxo-1(2 <i>H</i> )-pyrimidinyl]methyl]- <i>N</i> -2 <i>H</i> -tetrazol-5-yl-2-furancarboxamide
ASD	autism spectrum disorder
ATP	adenosine triphosphate
BDNF	brain-derived neurotrophic factor
BzATP	2'(3')- <i>O</i> -(4-Benzoylbenzoyl)adenosine-5'-triphosphate tri(triethylammonium) salt
cAMP	cyclic adenosine monophosphate
CMF-HBSS	calcium- and magnesium-free Hanks' buffered saline solution
CNQX	6-cyano-7-nitroquinoxaline-2,3-dioneis ( <i>aka.</i> cyanquixaline)
CNT2	concentrative nucleoside transporter 2
DAPI	4',6-diamidino-2-phenylindole
DC	detergent compatible
DIV	days <i>in vitro</i>
DMSO	dimethyl sulfoxide
DSM-5	Diagnostic and Statistical Manual of Mental Disorders (DSM-5)
E	embryonic day
ECM	extracellular matrix
ecto-NTPDase	ecto-nucleoside triphosphate diphosphohydrolase ( <i>aka.</i> CD39)
EDTA	ethylenediaminetetraacetic acid
ERK	extracellular signal-regulated kinase
exTNC	exogenous tenascin C
FITC	fluorescein isothiocyanate
FGF2	fibroblast growth factor 2
<i>Fmr1</i> KO	<i>Fmr1</i> knockout
FXS	Fragile X syndrome
GABA	gamma-aminobutyric acid

GFAP	glial fibrillary acidic protein
GLT1	glutamate transporter 1
GluR	glutamate receptor
gp130	glycoprotein 130
GPCR	G protein-coupled receptor
GSK3	glycogen synthase kinase 3
HILIC	hydrophilic interaction liquid chromatography
ID	intellectual disability
IL-1 $\beta$	interleukin-1 beta
IL-6	interleukin-6
IL-6R	interleukin-6 receptor
IL-8	interleukin-8
IP <sub>3</sub>	inositol triphosphate
iPSC	induced pluripotent stem cell
JAK	Janus kinase
kDa	kilodalton
KO	knockout
KOACM	<i>Fmr1</i> knockout astrocyte-conditioned media
KON	<i>Fmr1</i> knockout neuron
LC	liquid chromatography
LC/MS	liquid chromatography/mass spectrometry
LPS	lipopolysaccharide
LPS-RS	lipopolysaccharide from <i>Rhodobacter sphaeroides</i>
MAP1b	microtubule-associated protein 1b
MAP2	microtubule-associated protein 2
MAPK	mitogen-activated protein kinase
MEA	microelectrode array
MEK	mitogen-activated protein kinase kinase
mGluR5	metabotropic glutamate receptor 5
mRNA	messenger ribonucleic acid
MRS 2578	<i>N,N'</i> -1,4-Butanediylbis[ <i>N'</i> -(3-isothiocyanatophenyl)thiourea
MS	mass spectrometry
mTOR	mechanistic target of rapamycin
NF- $\kappa$ B	nuclear factor kappa-light-chain-enhancer of activated B cells
NMDA	N-methyl-D-aspartic acid
NMM	neuronal maintenance media
NDP kinase	nucleoside-diphosphate kinase
NT-3	neurotrophin-3

P	postnatal day
PBS	phosphate buffered saline
PEI	polyethylenimine
PI3K	phosphoinositide 3-kinase
PKC	protein kinase C
PLC	phospholipase C
PLL	poly-L-lysine
PSD-95	postsynaptic density-95
pSTAT3	phosphorylated signal transducer and activator of transcription factor 3
RIPA	radioimmunoprecipitation assay buffer
RGC	radial glial cell
RNA	ribonucleic acid
ROUT	robust regression and outlier removal
ROI	region of interest
SEM	standard error of the mean
sIL-6R	soluble IL-6 receptor
siRNA	small interfering ribonucleic acid
SPARC	secreted protein acidic and rich in cysteine
SSRI	selective serotonin reuptake inhibitor
STAT3	signal transducer and activator of transcription 3
TBS-T	tris-buffered saline solution with Tween-20
TLR4	toll-like receptor 4
TNC	tenascin C
TNF $\alpha$	tumour necrosis factor alpha
trypsin-EDTA	trypsin-ethylenediaminetetraacetic acid
TSP-1	thrombospondin-1
UDP	uridine diphosphate
UMP	uridine monophosphate
$\mu$ M	micromolar
UTP	uridine triphosphate
VZ	ventricular zone
WT	wildtype
WTACM	wildtype astrocyte-conditioned media
WTN	wildtype neuron

## **Chapter One: Introduction**

### **1.1. Autism Spectrum Disorder**

#### ***1.1.1. Prevalence***

Autism spectrum disorder (ASD) is currently one of the fastest growing neurological syndromes in Canada. The prevalence of this neurodevelopmental disorder has steadily risen across Canada throughout the 21<sup>st</sup> century (Ouellette-Kuntz et al., 2014), with the most recent report by the Canadian National Autism Spectrum Disorder Surveillance System estimating that as of 2015, 1 in every 66 Canadian children between the ages of 5-17 has been diagnosed with ASD (Ofner et al., 2018). It is therefore becoming increasingly important to investigate the genetic, cellular, and molecular bases of the ASD phenotype. Due to the reliability of genetic models for experimentation, particular attention is paid to heritable conditions which consistently demonstrate ASD symptoms, such as Fragile X syndrome, the most common monogenic disorder to exhibit the ASD phenotype.

#### ***1.1.2. Symptoms***

ASD is characterized in the Diagnostic and Statistical Manual of Mental Disorders (DSM-5) by a combination of impaired social interactions and repetitive behaviours, with common symptoms of aberrant verbal and nonverbal social communication, hyperfixation, behavioural stereotypies, hyperresponsivity to auditory and tactile stimuli, attention deficits and/or hyperactivity (American Psychiatric Association, 2013). Intellectual disabilities, mood disorders, and seizures are also frequently coincident with a diagnosis of ASD. The various forms of this disorder fall within a broad spectrum of symptomatic severity, with some individuals experiencing significant impairments while others are comparatively mildly affected. Approximately 56% of Canadian children diagnosed with ASD have received this diagnosis by the age of 6, and ~75% by the age of 8, demonstrating the developmental nature of this disorder. A

clear sex difference has also been observed, with 1 in 42 Canadian males receiving an ASD diagnosis in comparison to only 1 in 165 females (Ofner et al., 2018).

### **1.1.3. Genetic and Environmental Factors**

ASDs are linked on a cellular level by altered and hyperexcitable signalling in brain regions including the cerebral cortex, hippocampus, and striatum, which largely arise during critical periods of early childhood brain development (reviewed in Zoghbi & Bear, 2012). Over 100 ASD risk genes have been identified in recent years, including mutations in *Fmr1*, *SHANK*, and *CNTNAP2* (Satterstrom et al., 2020). In addition, factors including maternal health, birth complications, and prenatal exposure to oxidative stress-producing environmental exposures have been associated with increased ASD incidence (Modabbernia, Velthorst, & Reichenberg, 2017). This confluence of risk factors is particularly challenging for drug discovery and development, and as a result, no effective treatments that comprehensively combat ASD symptoms currently exist.

## **1.2. Fragile X Syndrome**

### **1.2.1. Prevalence**

The most common monogenic form of intellectual disability is Fragile X syndrome (FXS), an X-linked dominant condition which closely overlaps with the symptomatic spectrum of ASD and is therefore widely considered to be the most prevalent heritable form of ASD. FXS is characterized by mutation-induced silencing of the *Fmr1* gene and the subsequent absence of its gene product, FMRP protein. Currently, 1 in 4000 Canadian males and 1 in 6000-8000 females are estimated to be affected (Aubertin, 2015), with similar rates of incidence reported across the United States of America and United Kingdom (Turner, Webb, Wake, & Robinson, 1996; Youings et al., 2000). Males are more frequently and severely impacted than females due to the X-linked nature of this disorder, as females with a single silenced *Fmr1* allele possess a second unaffected allele that can facilitate compensatory production of FMRP (Kirchgesner, Warren, & Willard, 1995).

### ***1.2.2. Symptoms***

Individuals with FXS exhibit cognitive symptoms of intellectual disability and delayed development of both language and motor skills (Meguid et al., 2012; Zingerevich et al., 2009), with males typically displaying moderate impairments and females displaying less severe phenotypes. Recent estimates suggest that 60-90% of males diagnosed with FXS also meet the diagnostic criteria for ASD due to similarities in social and behavioural phenotypes (Hernandez et al., 2009; Zingerevich et al., 2009). Common FXS/ASD symptoms associated with neural excitation include epilepsy, sensory hypersensitivities, attention deficit/hyperactivity, and hyperarousal (Musumeci et al., 1999; Sullivan et al., 2006), while other frequently reported FXS symptoms aligning with the ASD spectrum include anxiety, repetitive behaviours, and poor nonverbal social communication (Cordeiro, Ballinger, Hagerman, & Hessler, 2011; Oakes et al., 2016). Unlike ASD, diagnoses of FXS are not determined solely on the basis of symptoms, but through pre- or postnatal genetic screening to detect the presence of the *Fmr1* mutation.

### ***1.2.3. Current Therapeutic Approaches***

Current clinical management of FXS consists of a combination of behavioural and pharmacological interventions chosen to individually target each symptom, as effective therapeutic approaches to comprehensively combat the range of cognitive and behavioural symptoms associated with FXS have not yet been developed. Speech-language therapy is often suggested to improve communication skills, physical or occupational therapy is utilized to target motor impairments, selective serotonin reuptake inhibitors (SSRIs) are prescribed to manage anxiety, and stimulants are administered to improve attention deficits and hyperactivity (reviewed in Ciaccio et al., 2017). SSRIs in particular have been found to be effective in only ~60% of FXS patients (Berry-Kravis & Potanos, 2004), demonstrating a need for more effective therapeutic approaches. Recent research has investigated the efficacy of treatments which aim to selectively normalize common dysregulations in FXS, including an imbalance in glutamatergic signalling; however, novel

and highly anticipated glutamate receptor antagonists such as mavoglurant and basimglurant have not been effective enough to succeed in clinical trials (reviewed in Erickson et al., 2017). It is therefore clear that the cellular events underlying the pathogenesis of FXS must be more clearly understood in order to inform more targeted and effective therapeutic approaches.

#### **1.2.4. The Genetic Basis of FXS**

FXS arises due to a dominant mutation in the *Fmr1* gene which prompts epigenetic silencing. This gene is located on the long arm of the X chromosome at position Xq27.3, comprised of 17 exons and spanning a total of 38 kilobases (Eichler, Richards, Gibbs, & Nelson, 1993). *Fmr1* typically encodes a 3.9 kilobase-long mRNA, though several uncommon splice variants have also been identified. The *Fmr1* 5' untranslated region contains a series of CGG repeats that become expanded and epigenetically silenced in FXS, and are visible as a “fragile” region at the tip of the X chromosome. Unaffected individuals typically possess 5-44 CGG trinucleotide repeats at this locus, while the FXS full mutation allele is clinically characterized by the presence of >200 CGG repeats (Maddalena et al., 2001). In individuals with the full mutation, excess CGG repeats lead to DNA methyltransferase 1-mediated hypermethylation of cytosine residues within the expanded repeat region, as well as within CpG islands at the *Fmr1* promoter. This hypermethylation prevents initiation of transcription, resulting in an absence of *Fmr1* mRNA (Sutcliffe et al., 1992; Verkerk et al., 1991). The resulting *Fmr1* gene product, FMRP protein, is unable to be expressed, leading to widespread neural signalling dysfunctions.

CGG expansions ranging from 55-200 trinucleotide repeats constitute an FXS premutation associated with an increased risk of the premutation-specific FXS-related disorders Fragile X Associated Tremor/Ataxia Syndrome in males, and Fragile X Premature Ovarian Insufficiency in females (reviewed in Brouwer, Willemsen, & Oostra, 2009). Like FXS, premutation-associated disorders are also characterized by a reduction in FMRP, but this arises due to a different mechanism: increased histone acetylation at the

premutation allele upregulates transcription (Todd et al., 2010), which leads to the formation of hairpin structures that are thought to inhibit ribosomal activity and thereby reduce FMRP translation (Handa, Saha, & Usdin, 2003). Individuals with the premutation do not have FXS, but are considered to be carriers for this syndrome, since the maternal premutation allele is unstable and may expand to >200 repeats when inherited by offspring (Nolin et al., 2003).

### ***1.2.5. FMRP Expression***

The 70-80 kDa, 632 amino acid-long FMRP protein is detectable throughout the body, but is notably expressed at high levels in neurons. Neuronal FMRP is primarily localized to the cytoplasm, dendrites, and postsynaptic dendritic spines, with minimal nuclear expression (Antar, Dichtenberg, Plociniak, Afroz, & Bassell, 2005; Feng et al., 1997). FMRP is also found in non-neuronal cells of the brain during early development; specifically, those co-expressing markers denoting astrocytic and oligodendrocytic lineages (Pacey & Doering, 2007). Consistent with a role in brain development, expression of both neuronal and glial FMRP has been shown to peak during the developmental period broadly associated with synaptogenesis, followed by an age-related reduction in expression (Pacey & Doering, 2007; Singh, Gaur, & Prasad, 2007). FMRP is also upregulated in response to synaptic activity, as seen following sensory inputs within the rat somatosensory cortex (Todd & Mack, 2000), suggesting that this protein may be instrumental in activity-dependent synaptic modulation.

### ***1.2.6. FMRP-Mediated mRNA Binding and Translational Regulation***

FMRP is classified as an RNA-binding protein due to the presence of four distinct RNA-binding domains: two ribonucleoprotein K homology domains, one N-terminal NDF domain, and one C-terminal RGG box; as well as nuclear localization signals and nuclear export signals (reviewed in Zalfa & Bagni, 2004). These domains, in particular the RGG box, permit FMRP to form complexes that bind and chaperone a plethora of mRNAs. Recent work suggests that nearly 4% of the mRNAs expressed within the human brain

associate with FMRP (V. Brown et al., 2001), including those encoding ~30% of both the presynaptic and postsynaptic proteomes. Well-known targets of FMRP include mRNAs that encode proteins related to neuronal morphology, synaptogenesis, and signalling, such as microtubule-associated protein 1b (MAP1b), postsynaptic density-95 (PSD-95), and various subunits of AMPA receptors (GluRs) (Darnell et al., 2011).

Not only does FMRP bind mRNA to potentially impact its localization; more importantly, it modulates its translation. FMRP strongly associates with neuronal polyribosomes, suggesting an active role in translational regulation (Stefani, Fraser, Darnell, & Darnell, 2004). Indeed, incubation of FMRP with target mRNAs *in vitro* significantly prevented their translation, while mRNA co-incubation with multiple recombinant forms of FMRP produced normal protein levels (Laggerbauer, Ostareck, Keidel, Ostareck-Lederer, & Fischer, 2001). This was first shown to result from impairments in the assembly of the 80S ribosome translational initiation complex (Laggerbauer et al., 2001), though more recent research suggests that the complete ribosome is present yet becomes stalled during translocation (Darnell et al., 2011). The majority of FMRP target mRNAs are translationally inhibited by FMRP; however, not all target mRNAs are regulated equally, as FMRP also increases translation of a subset of mRNAs through poorly defined mechanisms. Lack of FMRP in the FXS brain therefore leads to an inability to regulate translation and localization of target mRNAs, resulting in an overall overabundance of numerous developmentally significant proteins (Qin, Kang, Burlin, Jiang, & Smith, 2005). Although it is well-known that FMRP is absent in FXS, the consequences for cortical signalling are still being discovered, due in part to the diversity of mRNA targets and subsequent downstream protein interactions involved in developmental regulation.

### ***1.2.7. The Fmr1 Knockout Mouse Model of FXS***

The use of a model system permits the isolation or targeting of single cell-types within the brain to identify morphological and functional aberrations, as well as the use of

experimental drug treatments both *in vitro* and *in vivo* to correct these dysfunctions. To this end, FXS model systems have been generated in *Mus musculus*, as well as *Drosophila melanogaster*, *Rattus norvegicus*, and recently, in patient-derived human induced pluripotent stem cells. The mouse model is one of the most commonly used FXS models, owing to its practicality while also maintaining translational validity. Importantly, mouse *Fmr1* shares 95% homology with human *Fmr1*, while mouse FMRP is over 98% similar to the human protein (Ashley et al., 1993). The mouse timeline of brain development is also significantly shortened yet relatively similar to humans, allowing developmental research to be performed efficiently.

The well-characterized *Fmr1* knockout (*Fmr1* KO) mouse model was generated in 1994, using homologous recombination to globally edit the mouse *Fmr1* gene out of the genome and thereby prevent expression of the mouse FMRP protein (The Dutch-Belgian Fragile X Consortium et al., 1994). This model recapitulates the molecular consequences of FMRP loss at the cellular and molecular levels, with *Fmr1* KO mice reproducibly demonstrating pathologies seen in human patients, such as increased excitatory and decreased inhibitory signalling, increased synaptic density, and altered connectivity (M. S. Brown, Singel, Hepburn, & Rojas, 2013; El Idrissi et al., 2005; Galvez, Gopal, & Greenough, 2003; Grossman, Elisseou, McKinney, & Greenough, 2006; Higashimori et al., 2016; Nimchinsky, Oberlander, & Svoboda, 2001; Puts et al., 2017; Wallingford, Scott, Rodrigues, & Doering, 2017) which are further discussed in *Sections 1.3.3.1, 1.3.5.1, and 1.3.6.1*. Importantly, this model also generally recreates a number of the ASD symptoms observed in individuals with FXS, including hyperactivity, attention deficit, seizures, and repetitive or stereotypic behaviours, indicating that the aforementioned deficits lead to physiologically relevant outcomes in the mouse model (reviewed in Kazdoba, Leach, Silverman, & Crawley, 2014). Similar to the variable symptomatic presentation across individuals with FXS, *Fmr1* KO mouse studies have shown considerable heterogeneity among the behavioural characteristics reported. Despite this variability, pharmacological treatments have generally performed similarly between *Fmr1* KO mouse studies and

clinical trials, indicating that *Fmr1* KO mouse models provide a significant degree of predictive validity for translational research (Kazdoba et al., 2014).

### **1.3. The Cerebral Cortex**

#### ***1.3.1. Structure and Function***

Many of the intellectual and sensory processes that are impaired in FXS stem from disordered signalling events within the cerebral cortex. The largest region of the mammalian brain, the cortex is functionally classified into sensory, motor, and association areas. Cognition and attention are generally governed by activity within the prefrontal cortex, while processing of visual and auditory inputs is controlled by their respective visual and auditory cortices, and voluntary motor movement is governed by signalling within motor areas. Each of these cortical regions are organized into six distinct layers, with layers I-III responsible for corticocortical connectivity, while layers IV and V-VI connect the cortex with the thalamus and subcortical structures, respectively. Within those layers exists a predictable columnar organization allowing for the formation of local neural circuits (Tau & Peterson, 2010).

A series of coordinated events contribute to the ongoing development and refinement of cortical signalling throughout the gestational period and into the early stages of postnatal development, leading to an 88% increase in human cortical volume by the end of the first postnatal year (Knickmeyer et al., 2008). Both mouse and human cortices are populated by homologous types and proportions of cells, including neurons and three main types of glial cells: astrocytes, which interface with neurons to regulate their activity and connectivity; microglia, which regulate cortical immune function; and oligodendrocytes, which myelinate neuronal axons to improve the speed of neuronal signalling (Tau & Peterson, 2010). As this work specifically investigates the crosstalk between cortical neurons and astrocytes, the contribution of microglia and oligodendrocytes will therefore not be discussed in detail.

### ***1.3.2. Cortical Neurons***

Neurons are the electrically active cells of the cortex, propagating unidirectional action potentials to facilitate thoughts and behaviours. The most abundant neuronal subtype is the excitatory pyramidal neuron, which comprises ~80% of the total neuron population within the adult mouse cortex (Molyneaux, Arlotta, Menezes, & Macklis, 2007). These glutamatergic neurons possess a single long axon extending from the neuronal soma to transmit neuronal signals, as well as numerous branched dendrites radiating from the soma to receive neuronal excitation. Glutamatergic pyramidal neurons are generated through the asymmetric division of radial glial cells (RGCs) to produce one excitatory postmitotic neuron while also retaining the RGC population, beginning in the first human trimester (~E42) and comparatively later in gestation in the mouse (~E10-13) (reviewed in Wodarz & Huttner, 2003). Newborn glutamatergic cortical neurons travel from the edge of the lateral ventricles (ventricular zone; VZ) to form the layers of the cortex in an inside-out manner, following RGC projections spanning from the VZ to the pial surface. Excitatory signalling is tempered by the complementary GABAergic inhibitory cortical interneuron population, which is generated from medial ganglionic eminences and migrates tangentially (reviewed in Nadarajah & Parnavelas, 2002). The neuronal population is largely formed by mid-gestation (~E108) in the human and by late gestation (~E17-18) in the mouse, though migration of upper-layer neurons continues on in the mouse until ~P7 (reviewed in Farhy-Tselnicker & Allen, 2018). In mouse models, primary neuron cultures are created by dissecting the cortex between embryonic day 15-17, ensuring that a large population of excitatory neurons are obtained while preventing contamination with glia.

### ***1.3.3. Neurite Extension***

Newly generated neurons form the growing neuronal network by extending their axonal and dendritic processes, collectively termed neurites, through rapid remodeling of the actin cytoskeleton. A growth cone located at the distal end of the growing axon mediates both the length and direction of axonal extension, drawing information about its trajectory

from attractive or repulsive guidance cues within the extracellular environment. These guidance cues are largely neurotrophic factors, such as neurotrophin-3 and netrin-1 (Marsick, Flynn, Santiago-Medina, Bamburg, & Letourneau, 2010), and are released from nearby neurons and glia to mediate the formation of a coordinated neural network. To facilitate axonal and dendritic extension, actin is rapidly depolymerized and repolymerized to permit the addition of new monomers, with actin-severing proteins such as cofilin modulating the rate of this remodeling process (Dent, Gupton, & Gertler, 2011). This period of extension and branching continues throughout the first four postnatal weeks in the mouse, and is coupled with an extended period of axonal myelination that promotes speed of action potential transmission (Tau & Peterson, 2010). The combination of axonal growth, dendritic arborization, and myelination leads to a widespread increase in cortical volume and thickness that is visible by the third human trimester (Garel et al., 2001; Huttenlocher & Dabholkar, 1997), though these processes are significantly delayed until after birth in the mouse. Astrocytes also prioritize the extension of their processes during the first several postnatal weeks of mouse development, allowing them to contact numerous neurons and facilitate synaptic connections (Farhy-Tselnicker & Allen, 2018).

#### ***1.3.3.1. Neurite Outgrowth and Branching in FXS***

A lack of FMRP in FXS impacts both dendritic and axonal length, suggesting potential consequences for the formation of appropriate neural networks. The complexity of dendritic arbors was found to be elevated in *Drosophila* lacking functional FMRP, while axons were also improperly targeted, leading to increased number and length of axonal projections with poor spatial localization (Pan, Zhang, Woodruff, & Broadie, 2004). Furthermore, increased dendritic arborization was observed by Galvez et al. (2003) within *Fmr1* KO mouse barrel cortical tissue. As these studies were conducted in intact preparations containing both neurons and astrocytes, it is unclear whether these effects result from the absence of neuronal or astrocyte FMRP, or the precise signalling interactions that led to aberrant neurite extension. Further *in vitro* work has suggested that aberrant neurite length and branching are primarily a consequence of dysregulated

astrocyte-secreted factor secretion, strongly implicating the role of astrocytes in the determination of neuronal morphology (Hodges et al., 2017; Jacobs & Doering, 2010).

#### ***1.3.4. Cortical Astrocytes***

The most prominent cell-type populating the cerebral cortex is the astrocyte, which supports neuronal function and modulates neuronal signalling. They are traditionally thought to be 10 times more prevalent than cortical neurons, though recent research has suggested that the true cortical ratio of astrocytes to neurons may be closer to 3:1 or 4:1 (von Bartheld, Bahney, & Herculano-Houzel, 2016). Mature astrocytes are large, star-shaped glial cells which densely populate the cortex, residing throughout all cortical regions and layers in a non-overlapping pattern. They can be broadly classified based on their localization and morphology: highly branched protoplasmic astrocytes are localized to grey matter where they extensively contact synapses and endothelial cells; while fibrous astrocytes possess longer, thinner processes and are found within white matter (Tabata, 2015). Astrocytes are generated around the time of birth (~E18-19/P0 in the mouse), when remaining RGCs undergo a Notch1/STAT-mediated signal switch that halts neurogenesis and permits RGCs to differentiate into glia (Bonni et al., 1997; Namihira et al., 2009). Unlike neurons, they undergo local cell division following migration to increase cortical astrocyte density, as the remaining RGCs are insufficient to populate the entire cortex (Tabata, 2015). The process of gliogenesis ultimately continues for the first ~28 postnatal days in the mouse, and into the first year of life in the human (Silbereis, Pochareddy, Zhu, Li, & Sestan, 2016). Exploiting this developmental timeline, primary astrocyte cultures are generated by dissecting the mouse cortex during gliogenesis between P0-P3, and culturing cells in a glial-selective media which is insufficient for the maturation and survival of neurons.

Historically, research regarding the role of astrocytes has focused on their function as passive modulators of neuronal health, as they produce glucose to fuel neuronal activity, manage neuronal waste, and interface with epithelial cells to form the blood-brain barrier

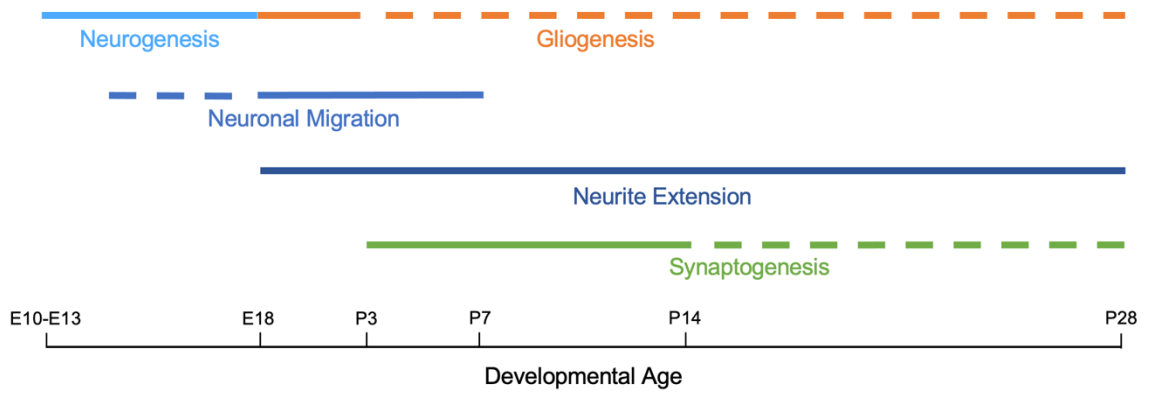


Figure 1. Timeline of mouse cortical neurodevelopment. Dotted lines indicate time frames at which these processes occur at lower levels. E: embryonic day; P: postnatal day (compiled from Farhy-Tselnicker & Allen, 2018; Schuz & Palm, 1989; Wodarz & Huttner, 2003).

(Kimelberg & Nedergaard, 2010). Astrocyte communication is facilitated through the propagation of calcium waves, which will be presented in detail in *Section 1.4.4*. Importantly, recent studies have shown that the function of astrocytes extends far beyond solely supporting neurons, as they are highly involved in not only establishing synaptic connections, but also modulating the degree of neuronal firing. Astrocyte-specific dysfunctions in FXS continue to be uncovered, and these will be further discussed in the context of their relationship with synaptogenesis and neural connectivity in the proceeding sections.

### ***1.3.5. Synaptogenesis***

Neurons and astrocytes interface at the tripartite synapse, a structure which establishes a connection between a presynaptic axon, postsynaptic dendrite, and interfacing astrocyte to permit neuronal signalling. Synaptogenesis begins with axonal localization to a target dendrite through actin remodeling at the axonal growth cone, followed by presynaptic vesicular and postsynaptic receptor recruitment, and finally, the anchoring of pre- and postsynaptic terminals (Shen & Cowan, 2010). The number of synaptic connections is rapidly and excessively upregulated during synaptogenesis, to approximately 150% of adult synaptic density (Semple, Blomgren, Gimlin, Ferriero, & Noble-Haeusslein, 2013). Human cortical synaptogenesis begins as early as the fifth gestational week (GW5) and continues throughout the first several years of childhood, while in the mouse, this process is largely restricted to the postnatal period (Huttenlocher, 1990; Huttenlocher & Dabholkar, 1997). Elevated rates of mouse cortical synaptogenesis begin around P3 and extend to P14, then continue at lower levels until P21-P28, ultimately leading to the formation of an average 8,200 connections made per cortical neuron (Schüz & Palm, 1989).

Astrocytes locally influence neuronal connectivity by secreting pro- and anti-synaptogenic proteins in a calcium-dependent manner to modulate the formation of cortical synapses. Release of these astrocyte-secreted proteins is in fact necessary for the initiation

of rapid connectivity during synaptogenesis, as neurons cultured in the absence of astrocytes or their secreted factors are unable to form sufficient synaptic connections (Ullian, Sapperstein, Christopherson, & Barres, 2001). Key astrocyte-secreted factors that influence the formation of excitatory synapses include glypicans, hevin, SPARC, interleukin-6, and thrombospondin-1, of which the latter is discussed further in *Sections 1.4.5. and 1.5.2.* (Allen et al., 2012; Christopherson et al., 2005; Farhy-Tselnicker et al., 2017; Kucukdereli et al., 2011; Wei et al., 2012), while a number of astrocyte-secreted factors promoting inhibitory synaptogenesis have also been identified (Diniz et al., 2014; Elmariah, Oh, Hughes, & Balice-Gordon, 2005). While these and other synaptogenic factors are generally expressed during peak synaptogenic periods, their levels vary across cortical layers and regions, thereby serving as a method to generate functional specificity across cortical subregions (Farhy-Tselnicker & Allen, 2018).

Following this phase of rapid connectivity, the neural network must be refined and streamlined to ensure efficient and targeted signalling. Since neurogenesis produces significantly more neurons than necessary, excess proliferating cells at the VZ are eliminated, along with any postmitotic neurons forming insufficient or inefficient connections (Ferrer, Soriano, Del Rio, Alcántara, & Auladell, 1992). Network refinement is also accomplished through astrocyte- and microglial-mediated pruning of less active synaptic connections, taking place between 1-4 postnatal months in the mouse cortex (Chung et al., 2013) or ~1.5-5 years after birth in humans (Huttenlocher & Dabholkar, 1997) and resulting in region-specific reductions in cortical size. Astrocytes also undergo pruning of unneeded extensions at the end of the first rodent postnatal month to further streamline the connectivity of the neuronal network (Farhy-Tselnicker & Allen, 2018).

#### ***1.3.5.1. Synaptic Characteristics in FXS***

As the brain region responsible for both executive functions and sensory processing, it is unsurprising that the cerebral cortex displays cellular dysfunctions in FXS. A predictable synaptic phenotype has emerged in FXS, largely owing to research performed in *Fmr1* KO mouse models. Most notably, FXS neurons within the cortex and other brain

regions are characterized by their elevated numbers of long and thin dendritic spines, which are indicative of an immature spine morphology (Galvez et al., 2003; Grossman et al., 2006; Nimchinsky et al., 2001). It remains somewhat unclear how and when these spines mature, and whether this process is disrupted in FXS. However, this elevated spine density is consistent with findings of increased excitatory synaptic puncta during early postnatal development (Wallingford et al., 2017).

The ability of FXS neurons to form stable and appropriate numbers of synaptic connections is likely influenced by the translation and secretion of astrocyte soluble factors. Elevated dendritic spine density has been observed in *Fmr1* KO mouse models as early as within a single postnatal week (Nimchinsky et al., 2001), while increased thalamocortical synaptic puncta were also observed after two weeks *in vitro* (Wallingford et al., 2017). Notably, cortical levels of the pro-synaptogenic protein hevin were elevated in *Fmr1* KO mouse by a yet-unknown mechanism, occurring in tandem with decreased levels of anti-synaptogenic SPARC at time points consistent with synaptogenesis (Wallingford et al., 2017). The astrocyte-secreted extracellular matrix glycoprotein tenascin C (TNC), which is involved in synaptic remodeling, was also found to be upregulated in the cortex between 2-4 postnatal weeks *in vivo*, along with altered expression and secretion of the pro-inflammatory cytokine interleukin-6 which promotes excitatory synaptogenesis (Krasovska & Doering, 2018; Wei et al., 2011). Such alterations in astrocyte soluble factor secretion have important behavioural consequences, as a targeted deletion of *Fmr1* in mouse astrocytes produced morphological alterations neurons of the motor cortex, leading altered motor skill learning (Hodges et al., 2017) and thereby suggesting a potential mechanism behind delayed motor development in FXS.

It is possible that elevated FXS synaptic density may also result from glial-driven pruning dysfunctions, a common hypothesis in the field of ASD and FXS research. Deficits in synaptic pruning have indeed been identified in both individuals with FXS and the *Fmr1* KO mouse (Galvez et al., 2003; Patel, Loerwald, Huber, & Gibson, 2014). However, dysregulated hevin, SPARC, and IL-6 expression coupled with the fact that excess FXS

synapses were observed within a single week *in vitro* (Nimchinsky et al., 2001) suggests that pro-synaptogenic processes are also likely at play. FMRP, localized within dendritic spines, is also known to regulate the translation of numerous pre- and postsynaptic mRNAs (Satterstrom et al., 2020) which are overexpressed in its absence, suggesting an additional neuronal synaptogenic link. Regardless of the mechanism, the presence of excess synaptic puncta at early developmental stages suggests the potential for increased excitatory signalling, which is consistent with the hyperexcitatory and hyperresponsive characteristics observed in FXS patients and mouse models.

#### **1.3.5.1.1. *Converging Synptogenic and Immune Regulation in FXS***

Elevated secretion of IL-6 from *Fmr1* KO astrocytes not only suggests that excitatory synaptogenesis might be altered in the FXS cortex, but also provides evidence of upregulated immune responses. Recent work has indeed demonstrated immune dysregulation within the brains of individuals with ASD and FXS, including increased astrocyte secretion of the pro-inflammatory cytokines tumour necrosis factor  $\alpha$  (TNF $\alpha$ ) and interleukin-1 $\beta$  (IL-1 $\beta$ ), as well as IL-6 (Ashwood et al., 2011; Krasovska & Doering, 2018; X. Li et al., 2009). Elevated IL-6 in particular is associated with neurological impairments and a neuronal phenotype strikingly similar to that of FXS (Campbell et al., 1993). IL-6 secretion is downstream of the astrocyte soluble extracellular matrix glycoprotein TNC, which is overexpressed by *Fmr1* KO astrocytes (Krasovska & Doering, 2018). It is also associated with the activation of purinergic receptors and phosphorylation of STAT3 transcription factor, and this relationship will be further discussed in *Section 1.4.5*. While this FXS immune response has been identified, the role of cortical astrocytes in *Fmr1* KO cytokine regulation are still being elucidated.

#### **1.3.6. *Synaptic Activity***

Once neuronal networks are established through neurite outgrowth and synaptogenesis, their activity is closely modulated by the action of astrocytes. In response to local excitation in the form of intracellular calcium, astrocytes engage in targeted

synaptic release of gliotransmitters, including glutamate, ATP, and GABA (Santello & Volterra, 2009). In addition to secreting gliotransmitters and proteins to modulate synaptic activity, they are involved in clearing the synapse of signalling molecules following the initiation of an action potential. Astrocyte-expressed glutamate transporters facilitate glutamate reuptake following neuronal release, while inward rectifier potassium channels rapidly reuptake potassium following an action potential, thereby modulating neuronal depolarization (Walz, 2000). Astrocytes also modulate neuronal activity by releasing, reuptaking and/or hydrolyzing ATP and UTP, which will be further discussed in *Section 1.4.3*. Deficits in these processes therefore promote neuronal hyperexcitation, with a lack of glutamate or potassium reuptake in particular leading to the onset of seizures.

#### ***1.3.6.1. Neuronal Network Activity in FXS***

The aforementioned deficits characterized in FXS models lead to altered connectivity of neural networks. Within the *Fmr1* KO mouse cortex, both regional structural and functional connectivity were found to be elevated relative to unaffected controls, with increased neuronal connections formed between neurons within localized cortical areas (Haberl et al., 2015). This is consistent with findings of substantially greater overall cortical volume and thickness in the cortex of male children with FXS (Meguid et al., 2012), as well as a transient increase in the total brain volume of males with ASD, lasting for the first ~2 years of postnatal development (Courchesne, Campbell, & Solso, 2011).

In addition to these structural changes, increased regional excitation has been consistently observed in the FXS cortex. This may result from an imbalance in excitatory versus inhibitory signalling, recognized as the excitation-inhibition imbalance hypothesis (Lee, Lee, & Kim, 2017; Rubenstein & Merzenich, 2003). This hypothesis posits that the ASD brain is more highly excitable due to an inability to modulate excitatory versus inhibitory signalling, and that correcting this excitatory imbalance can mitigate ASD symptoms. Increased firing of glutamatergic neurons was indeed found in *Fmr1* KO sensory cortex, and was concurrent with a deficit in excitatory projections to inhibitory

neurons (Gibson, Bartley, Hays, & Huber, 2008), suggesting an overall increase in excitatory signalling that is consistent with hyperexcitation- and hypersensitivity-related symptoms. In both ASD and FXS, numerous studies have supported this hypothesis through demonstration of an increase in glutamatergic signalling and glutamate availability, as well as a reduction in GABAergic inhibition, ultimately driving increased neuronal activity in FXS (M. S. Brown et al., 2013; El Idrissi et al., 2005; Puts et al., 2017; L. Wang et al., 2016). Notably, astrocyte-specific absence of FMRP has recently been associated with reduced GLT1 glutamate transporter activity, which prolongs the reuptake of glutamate from the synapse and contributes to neuronal hyperexcitation (Higashimori et al., 2016). Given this astrocyte-specific role in elevated cortical excitation, the role of astrocytes should therefore be further explored in relation to excitatory imbalances in FXS circuitry.

#### **1.4. Purinergic Signalling**

Given the aberrant neuronal circuitry in FXS and the ability of astrocytes to influence neuronal connectivity and activity, it is important to investigate the signalling pathways associated with glial-neuronal communication in FXS. One of the most common pathways used to facilitate glial-neuronal crosstalk within the cerebral cortex is the purinergic signalling pathway. This form of intercellular signalling utilizes nucleoside triphosphates (UTP, ATP) and their metabolites to exert a strong influence on neuronal morphology and activity (Abbracchio, Burnstock, Verkhratsky, & Zimmermann, 2009), with considerable overlap between the processes governed by purinergic signalling and those that are dysregulated in FXS. This section will primarily focus on the role of the P2Y subfamily of purinergic receptors and their activation by uridine-based ligands, as well as their potential roles in the neurodevelopmental processes which are altered in FXS.

##### **1.4.1. Purinergic Receptors**

Purinergic receptors can be broadly categorized into P1 and P2 receptor families based on their ligand affinities. The four adenosine-sensitive purinergic receptors are

known as P1 receptors, and they serve both excitatory ( $A_{2A}$ ,  $A_{2B}$ ) and inhibitory ( $A_1$ ,  $A_3$ ) roles in the control of neurotransmitter release (reviewed in Stockwell, Jakova, & Cayabyab, 2017). The larger class of P2 receptors are responsive to nucleotide tri- and diphosphates, and are further classified as P2X and P2Y receptors based on their receptor structure. The seven fast-acting ionotropic P2X receptors are responsive to ATP, and they increase intracellular calcium to promote neuronal depolarization and drive synaptic firing (reviewed in Abbracchio et al., 2009). In contrast, P2Y receptors are slower-acting metabotropic receptors which can be activated by UTP and UDP as well as ATP and ADP, and are adept at fine-tuning synaptic transmission.

#### ***1.4.2. P2Y Receptors***

Eight P2Y receptors have been identified to date: P2Y<sub>1</sub>, P2Y<sub>2</sub>, P2Y<sub>4</sub>, P2Y<sub>6</sub>, P2Y<sub>11</sub>, P2Y<sub>12</sub>, P2Y<sub>13</sub>, and P2Y<sub>14</sub>. Of these, the P2Y<sub>1</sub>, P2Y<sub>2</sub>, P2Y<sub>4</sub>, P2Y<sub>6</sub>, and P2Y<sub>11</sub> receptors are excitatory in nature, and are G<sub>q</sub>/G<sub>11</sub>-coupled receptors which activate phospholipase C to promote intracellular calcium release (Abbracchio et al., 2009). The remaining P2Y receptors, P2Y<sub>12</sub>, P2Y<sub>13</sub>, and P2Y<sub>14</sub>, are inhibitory G<sub>i/o</sub>-linked receptors which inhibit adenylyl cyclase. This leads to a decrease in cyclic AMP production, hyperpolarization of the neuronal membrane, and ultimately, the inhibition of voltage-sensitive calcium channel activity (Abbracchio et al., 2009). The P2Y receptors are differentially activated by ATP, ADP, UTP, and UDP, as shown in Table 1.

All eight P2Y receptors share structural similarities owing to their G protein-coupled identities, including seven hydrophobic transmembrane domains connected by intra- and extracellular loops, as well as two extracellular disulfide bridges between loops. Despite these similarities, as well as considerable overlap in the ligands which agonize each P2Y receptor, their amino acid sequences are quite variable (reviewed in von Kugelgen & Hoffmann, 2016). The structure of P2Y receptors permits their coupling with other purinergic receptors to reciprocally influence activation; for instance, P2Y<sub>2</sub>, P2Y<sub>4</sub>, and P2Y<sub>6</sub> are all commonly found as homodimers, while P2Y<sub>4</sub> and P2Y<sub>6</sub> can be linked to form

heterodimers (D'Ambrosi, Iafrate, Saba, Rosa, & Volonté, 2007). While P2Y receptor expression has previously been found to be altered in disorders of neuronal excitation, including a notable increase in P2Y<sub>2</sub> expression associated with temporal lobe epilepsy, the levels of P2Y receptor expression within FXS and ASD have remained undetermined (Alves et al., 2017).

Table 1. Members of the metabotropic P2Y purinergic receptor subfamily (compiled from Dobolyi et al., 2011; Erb & Weisman, 2012)

RECEPTOR	AGONIST(S)
<b>G<sub>Q</sub>/G<sub>11</sub>-LINKED</b>	
P2Y <sub>1</sub>	ADP>ATP
P2Y <sub>2</sub>	UTP = ATP
P2Y <sub>4</sub>	UTP>ATP *ATP acts as an antagonist in humans
P2Y <sub>6</sub>	UDP
P2Y <sub>11</sub>	ATP
<b>G<sub>1/O</sub>-LINKED</b>	
P2Y <sub>12</sub>	ADP>ATP
P2Y <sub>13</sub>	ADP, ATP
P2Y <sub>14</sub>	UDP-sugars

### 1.4.3. UTP Synthesis and Breakdown

The pyrimidines UDP and UTP, which specifically activate P2Y<sub>2</sub>, P2Y<sub>4</sub>, and P2Y<sub>6</sub> receptors, are derived from the nucleoside uridine. Uridine itself is not a purinergic agonist, but its presence is crucial for the maintenance of UTP and UDP to facilitate purinergic signalling. Uridine is most frequently obtained through dietary sources, easily crossing the blood-brain barrier by way of the nucleoside transporter CNT2, though it can also be synthesized within in the brain when needed (reviewed in Cansev, 2006; Dobolyi, Juhasz, Kovacs, & Kardos, 2011). Though neither uridine nor UTP levels have been measured

within the brains of individuals with FXS or ASD, plasma uridine levels have been shown to be elevated in children with ASD, suggesting the potential for purinergic dysregulations in these neurodevelopmental disorders (Adams et al., 2011).

UTP is generated through the phosphorylation of uridine, utilizing both uridine- and adenosine-based purinergic signalling molecules to reciprocally regulate their expression. In the first step of this pathway, uridine kinase transfers a single phosphate group from ATP to uridine, forming UMP and ADP in the process. UTP acts as a regulator of this enzyme such that uridine is most frequently phosphorylated when there is a need for additional cellular UTP. UMP kinase then mediates the transfer of an additional phosphate group from ATP to UMP, thereby producing UDP along with the byproduct of another ADP molecule; NDP kinase facilitates a further exchange of phosphates to produce UTP alongside ADP (Dobolyi et al., 2011). The creation of uridine-based molecules for purinergic signalling may therefore also promote the adenosine-based agonism of P2Y receptors, since ADP acts as an agonist of P2Y<sub>6</sub> as well as various other P2Y receptors.

Following astrocyte release into the synapse, reuptake of nucleoside triphosphates by neuronal and glial nucleoside transporters, coupled with rapid breakdown down by membrane-bound ectonucleotidases, controls the strength and duration of signalling (Dobolyi et al., 2011). Given that both nucleoside di- and triphosphates act as signalling molecules, this may reduce activity at one purinergic receptor subtype while also facilitating signalling at another. The ecto-nucleoside triphosphate diphosphohydrolase (ecto-NTPDase) CD39 hydrolyzes UTP into UDP and UMP, respectively, and also facilitates a similar conversion for adenosine-based transmitters (Dobolyi et al., 2011). Further reduction to their nucleoside forms is accomplished through the action of the ecto-5'-nucleotidase CD73, which removes a phosphate group to convert UMP into uridine (Zimmermann, 1996). Through these reversible enzymatic reactions, the availability of purinergic signalling molecules can be tightly controlled to modulate purinergic receptor activation and thereby influence the generation of intracellular calcium responses, as shown

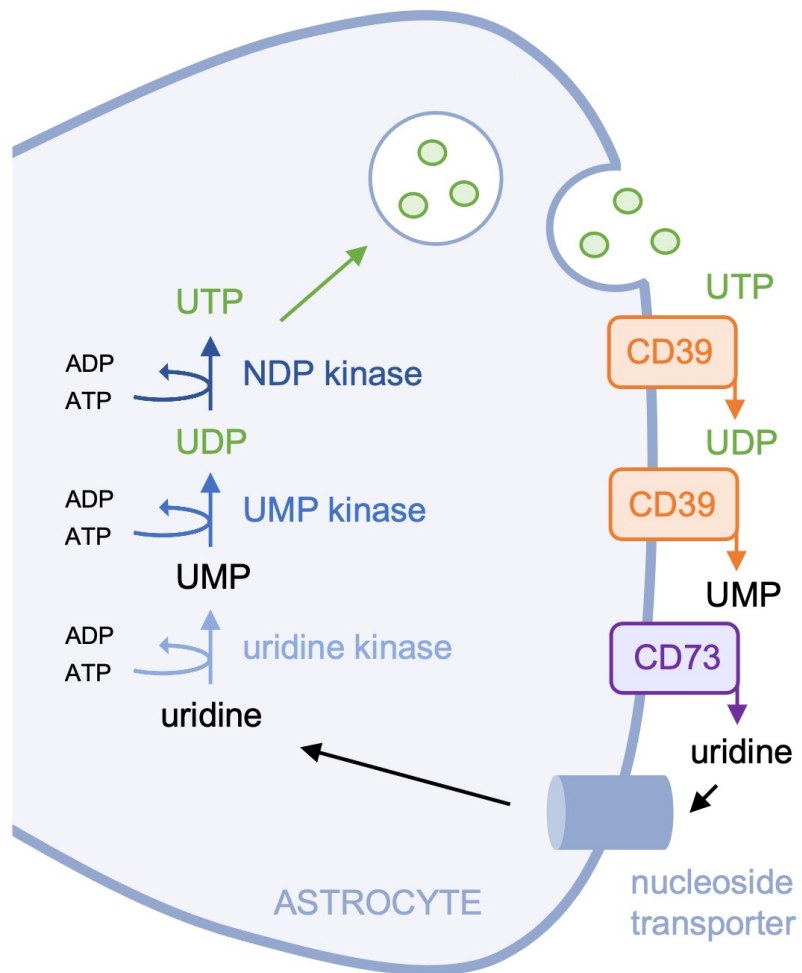


Figure 2. Astrocyte synthesis and breakdown of uridine-based purinergic signalling molecules. Secreted UTP and UDP are hydrolyzed to UMP and then to uridine by the action of membrane-bound CD39 and CD73 ectonucleotidases, respectively. Kinases utilize ATP as a substrate to phosphorylate uridine, UMP, and UDP to facilitate the formation of UTP.

in Figure 2. It is currently unclear whether the ectonucleotidases associated with extracellular UTP availability are altered in the ASD or FXS cortex.

#### ***1.4.4. Calcium Waves***

The activation of G<sub>q</sub>/G<sub>11</sub>-coupled P2Y receptors triggers the release of endoplasmic reticulum calcium stores to propagate a calcium wave (Figure 3), the primary means of astrocyte-to-astrocyte communication. A calcium wave is defined as an increase in astrocyte intracellular calcium which spreads throughout the cytosol, often extends to nearby astrocytes, and impacts ion channel and transporter activity (eg. K<sup>+</sup> channels, Ca<sup>2+</sup>-ATPase, Na<sup>+</sup>/Ca<sup>+</sup> exchangers) as well as gliotransmitter and protein release. Purinergic-induced calcium waves are initiated by the activation of P2Y G<sub>q</sub>/G<sub>11</sub>-coupled receptors as well as the faster-acting P2X receptors. Through the P2Y pathway, purinergic binding at P2Y/G<sub>q</sub>/G<sub>11</sub> receptors activates phospholipase C (PLC), which subsequently increases inositol triphosphate (IP<sub>3</sub>) (reviewed in Scemes & Giaume, 2006). IP<sub>3</sub> binding at endoplasmic reticulum (ER)-bound IP<sub>3</sub> receptors triggers the release of ER calcium stores and ultimately drives the spread of calcium ions throughout the cytosol. Released calcium may trigger an IP<sub>3</sub>-mediated response in gap junction-connected astrocytes, continuing the calcium wave throughout the astrocyte network. Intercellular calcium waves have been reproducibly observed within both primary astrocyte cultures and intact cortical slice preparations, and have been shown to travel at an approximate rate of 15-20 μm/s (Scemes & Giaume, 2006). Though a calcium wave is commonly thought of as a large-scale increase in calcium, smaller intracellular calcium waves within individual astrocyte processes may also respond to and regulate neuronal activity in a more localized manner (Di Castro et al., 2011).

The transmission of intercellular calcium waves is not limited to astrocytes in physical proximity with each other, as the spread of intracellular calcium also influences vesicular release of glutamate and P2Y receptor agonists (*e.g.* ATP) (Scemes & Giaume, 2006). Accordingly, intercellular calcium waves have previously been detected between

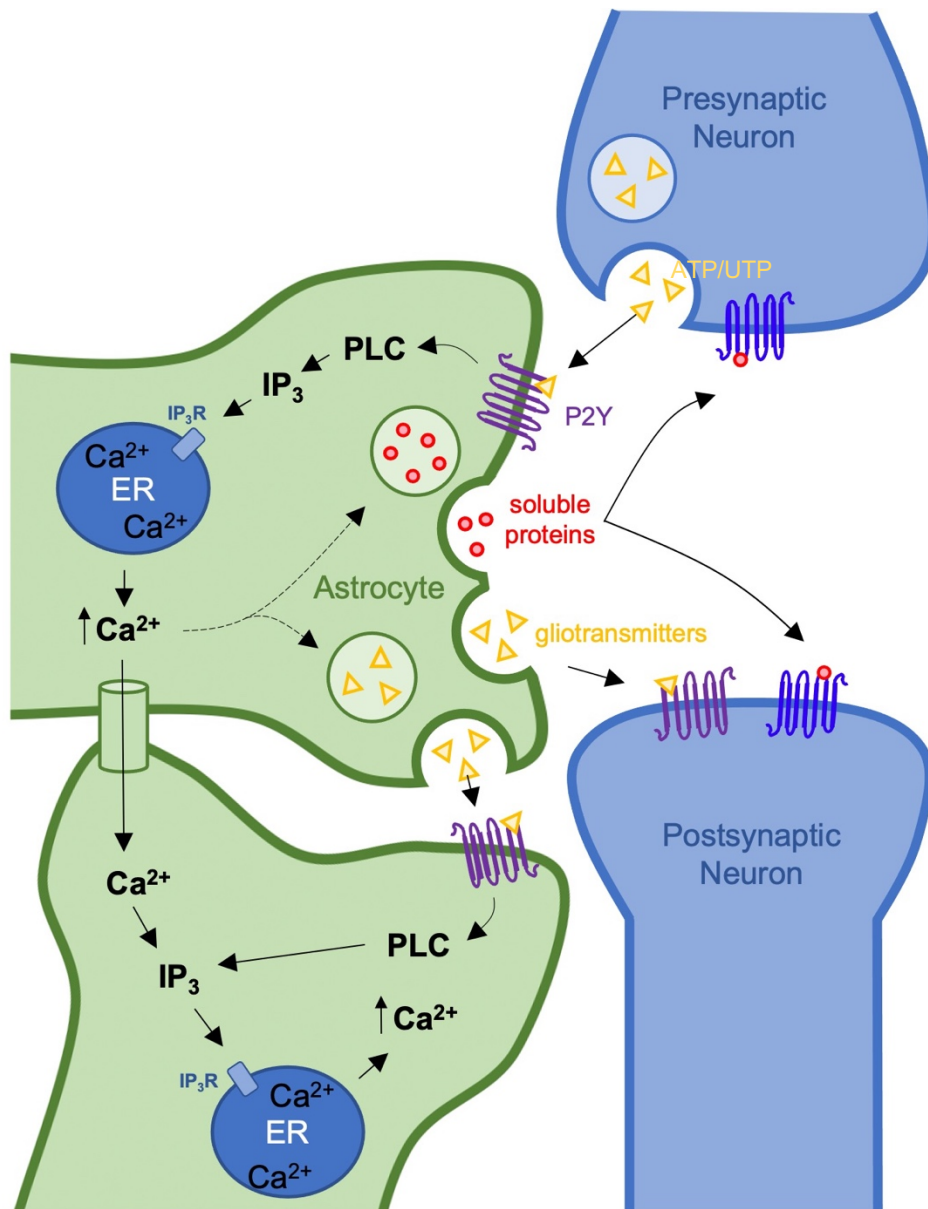


Figure 3. P2Y-mediated astrocyte calcium signalling. Purinergic signalling molecules (*e.g.* ATP, UTP) bind to P2Y receptors to activate PLC and IP<sub>3</sub>, thereby triggering the release of endoplasmic reticulum-stored calcium. Calcium ions can pass through gap junctions to increase IP<sub>3</sub> and facilitate calcium release from adjacent astrocytes, thereby propagating intercellular calcium waves. In addition, increased intracellular calcium levels indirectly influence the expression and secretion of astrocyte soluble proteins, as well as the release of gliotransmitters.

astrocytes which are physically separated in culture (Hassinger, Guthrie, Atkinson, Bennett, & Kater, 1996). The combination of purinergic gliotransmitter secretion and gap junction-mediated calcium transmission may therefore initiate feed-forward pathways which powerfully increase intercellular calcium wave propagation. It has remained unclear whether the initiation and/or propagation of astrocyte calcium waves, and their impact on related signalling processes, might be altered in the FXS cortex.

#### ***1.4.5. Signal Transduction***

In addition to the effects of P2Y receptor activation attributable to calcium release, the activation of G<sub>q</sub>/G<sub>11</sub>-coupled receptors also initiates signal transduction to promote longer-term modulation of gene expression. In primary astrocyte culture, a number of signal transduction cascades have been shown to be initiated in response to P2Y receptor binding, with the most well-characterized of these being P2Y-associated phosphorylation of extracellular signal-regulated protein kinase (ERK). In this cascade, protein kinase C (PKC) is activated following P2Y receptor binding to promote ERK phosphorylation and its subsequent nuclear translocation. This was demonstrated in rat cortical culture, when P2Y<sub>2</sub> receptor activation with specific agonists was unable to phosphorylate ERK in the absence of PKC (Neary et al., 1999). While PKC can be activated as a result of IP<sub>3</sub>-driven calcium release, P2Y has also been found to enable PKC activity through a calcium-independent mechanism, as specific inhibition of calcium-dependent PKC isoforms was unable to prevent P2Y-driven ERK phosphorylation (Neary et al., 1999). Astrocyte expression of the astrocyte-secreted synaptogenic protein TSP-1 in particular has been shown to be upregulated through this process (Tran & Neary, 2006), suggesting its importance in the establishment of cortical synapses.

Expression of astrocyte TSP-1 has additionally been linked to the phosphorylation of Akt kinases by way of PI3K activation, as treatment with a phosphoinositide 3-kinase (PI3K) antagonist largely prevented P2Y-driven TSP-1 expression (Tran & Neary, 2006). Similarly, a lack of P2Y<sub>6</sub> receptors has been recently shown to reduce phosphorylation of

Akt in NK cells (Z. Li et al., 2020), further demonstrating the role of P2Y receptors and this signal transduction cascade. Though the PI3k/Akt pathway is more commonly known for its role in cell proliferation than gene expression, the work of Tran and Neary (2006) suggests that it additionally contributes to transcription factor-mediated modulation of astrocyte gene expression.

P2Y receptor activity also promotes phosphorylation of signal transducer and activator 3 (STAT3), which leads to its dimerization, nuclear translocation, and subsequent function as a transcription factor. Treatment with the P2Y-specific agonist UTP has been shown to increase STAT3 phosphorylation in rat cortical astrocytes, while the pan-purinergic antagonist suramin prevented STAT3 phosphorylation, confirming the involvement of P2Y receptors in the initiation of this pathway (Washburn & Neary, 2006). Interestingly, ERK is able to promote STAT3 phosphorylation at serine residues, while STAT3 can also be phosphorylated independently of ERK at tyrosine residues by Janus kinase (JAK), suggesting a potential convergence of these signal transduction pathways (Decker & Kovarik, 2000). As STAT3 is involved in the regulation of a plethora of genes, including those encoding the pro-inflammatory cytokine IL-6 (S. W. Wang & Sun, 2014), this pathway may also underlie the expression of astrocyte factors influencing neural network formation, as well as immune responses in the FXS cortex. However, the extent to which each of the aforementioned signal transduction cascades are modulated by purinergic signalling to promote astrocyte-mediated influence of FXS neural networks remains unclear.

## **1.5. P2Y Receptors in Cortical Development and Connectivity**

### ***1.5.1. Neurite Outgrowth and Branching***

The purinergic signalling system is associated with a number of processes that are crucial for appropriate cortical development and activity. The first of these is the control of neuronal extension, which has been demonstrated in the neuron-like PC12 cell line. Following P2Y<sub>2</sub> receptor activation through a combination of immune signalling and UTP

treatment, both neurite outgrowth and branching were found to be elevated as a result of calcium-dependent processes (Peterson et al., 2013; Pooler, Guez, Benedictus, & Wurtman, 2005). This calcium-mediated increase in neurite length was correlated with phosphorylation of the actin-severing protein cofilin, thereby governing the remodeling of the actin cytoskeleton (Peterson et al., 2013). As neurite extension requires dynamic cytoskeletal remodeling (Basu & Lamprecht, 2018), alterations in the activation of neuronal P2Y<sub>2</sub> receptors by purinergic ligands could therefore exert a strong influence on neuronal morphology and connectivity, potentially driving the neuronal phenotypes seen in FXS.

### ***1.5.2. Synaptogenesis***

Purinergic signalling has also been found to regulate the expression and release of the astrocyte-secreted synaptogenic glycoprotein thrombospondin-1 (TSP-1) (Tran & Neary, 2006). TSP-1 is an adhesive glycoprotein which is transiently expressed by astrocytes during postnatal development, and reaches peak levels in the mouse cortex during the first two weeks of postnatal development (Risher et al., 2018). Following its release from astrocytes, TSP-1 increases excitatory synapse numbers, modulates synaptic alignment, and controls localization of molecules within the synapse. This protein establishes immature excitatory synapses through binding at  $\alpha 2\delta$ -1 neuronal receptors, thereby facilitating postsynaptic recruitment of synaptic adhesion and scaffolding proteins to strengthen the connection between pre- and postsynaptic neurons, though the precise timing and mechanism by which these synapses may become mature are still under investigation (Eroglu et al., 2009). In rat astrocyte culture, treatment with exogenous UTP led to an increase in both the expression and release of TSP-1. This phenomenon was hypothesized to be regulated through the activation of purinergic P2Y<sub>4</sub> receptors by way of ERK and Akt phosphorylation and subsequent transcription factor activation (Tran & Neary, 2006).

In addition, P2Y-mediated signalling indirectly influences synaptogenesis through the activation of astrocyte immune responses. In addition to its upregulated expression and

release in the *Fmr1* KO mouse cortical astrocyte cultures, the cytokine IL-6 has been shown to be elevated following UTP-specific agonism of P2Y receptors (Braun, Lu, Aroonsakool, & Insel, 2010; Caraccio et al., 2005; Krasovska & Doering, 2018). IL-6 not only exerts immune functions, but also promotes excitatory synaptogenesis (Wei et al., 2012). IL-6 levels are known to be modulated through phosphorylation of STAT3, and accordingly, STAT3 phosphorylation was increased in both human keratinocytes and rat primary astrocytes *in vitro* as a consequence of UTP-specific P2Y receptor activation (Jokela et al., 2017; Washburn & Neary, 2006), providing a potential mechanism behind P2Y-induced IL-6 upregulation. Astrocyte purinergic signalling is therefore capable of modulating the expression of astrocyte soluble synaptogenic proteins through distinct processes, and dysregulations in astrocyte purinergic signalling could therefore result in altered synaptogenesis during development, consistent with FXS synaptogenic defects.

### ***1.5.3. Purinergic Dysregulation in Fragile X and Autism Spectrum Disorder***

It is clear that considerable overlap exists between the cellular processes that are dysregulated in FXS and those controlled by purinergic signalling. Specifically, the structural and functional changes seen in FXS, including increased synaptic puncta, aberrant neuronal morphology and neuronal hyperexcitation, are largely consistent with the changes observed following an increase in P2Y receptor activation. Though the role of P2Y receptors has been seldom studied in ASD, and never explored in FXS until this work, there is reason to believe that P2Y activation by UTP and its metabolites may be associated with ASD. Levels of the circulating precursor uridine have been positively correlated with brain UDP concentrations, demonstrated by injecting mice with uridine and measuring the resultant increase in UDP levels within the brain (Steculorum et al., 2015). Children diagnosed with ASD indeed demonstrate elevated levels of plasma uridine (Adams et al., 2011), suggesting that UDP and/or other uridine-derived ligands may also be elevated in the ASD brain. Further, P2Y receptor expression is also elevated in FXS-comorbid epilepsies, suggesting that P2Y receptors may promote pathological excitation (Alves et al., 2017; Sukigara et al., 2014). These upregulations paired with functional overlap

therefore suggest that the purinergic signalling pathway may be upregulated in FXS, and may be an important pathway associated with the development of altered FXS circuitry.

## **1.6. Research Objective**

The overarching goal of this research was to identify whether purinergic signalling is dysregulated within astrocytes of the FXS mouse cortex, and following that, to determine whether astrocyte purinergic dysregulations contribute to the aberrant neuronal-glia interactions observed in FXS.

## **1.7. Aims and Hypotheses**

To address the overarching objective of this research, three aims and associated hypotheses were developed:

Aim 1: Establish whether astrocyte purinergic signalling is dysregulated as a result of an absence of FMRP in the *Fmr1* KO mouse cortex.

Hypothesis: Astrocyte purinergic receptors and/or ligands are differentially expressed in the *Fmr1* KO mouse cortex, leading to increased activation of purinergic pathways and changes in downstream soluble factor expression.

Aim 2: Determine whether purinergic signalling alters the activation of the immune-regulating STAT3 signal transduction pathway in *Fmr1* KO cortical astrocytes.

Hypothesis: Purinergic agonism promotes the phosphorylation of astrocyte STAT3, with downstream consequences for cortical immune regulation in the *Fmr1* KO mouse cortex.

Aim 3: Determine the functional outcomes of purinergic signalling on neural circuitry.

Hypothesis: Elevated astrocyte purinergic signalling increases neuronal activity and connectivity in *Fmr1* KO co-cultures, and can be targeted for potential therapeutic interventions.

## 1.8. References

- Abbracchio, M. P., Burnstock, G., Verkhatsky, A., & Zimmermann, H. (2009). Purinergic signalling in the nervous system: an overview. *Trends Neurosci*, 32(1), 19-29. doi:10.1016/j.tins.2008.10.001
- Adams, J. B., Audhya, T., McDonough-Means, S., Rubin, R. A., Quig, D., Geis, E., . . . Lee, W. (2011). Nutritional and metabolic status of children with autism vs. neurotypical children, and the association with autism severity. *Nutr Metab (Lond)*, 8(1), 34. doi:10.1186/1743-7075-8-34
- Allen, N. J., Bennett, M. L., Foo, L. C., Wang, G. X., Chakraborty, C., Smith, S. J., & Barres, B. A. (2012). Astrocyte glypicans 4 and 6 promote formation of excitatory synapses via GluA1 AMPA receptors. *Nature*, 486(7403), 410-414. doi:10.1038/nature11059
- Alves, M., Gomez-Villafuertes, R., Delanty, N., Farrell, M. A., O'Brien, D. F., Miras-Portugal, M. T., . . . Engel, T. (2017). Expression and function of the metabotropic purinergic P2Y receptor family in experimental seizure models and patients with drug-refractory epilepsy. *Epilepsia*, 58(9), 1603-1614. doi:10.1111/epi.13850
- American Psychiatric Association. (2013). *Diagnostic and Statistical Manual of Mental Disorders*, (5th ed.).
- Antar, L. N., Dichtenberg, J. B., Plociniak, M., Afroz, R., & Bassell, G. J. (2005). Localization of FMRP-associated mRNA granules and requirement of microtubules for activity-dependent trafficking in hippocampal neurons. *Genes Brain Behav*, 4(6), 350-359. doi:10.1111/j.1601-183X.2005.00128.x
- Ashley, C. T., Sutcliffe, J. S., Kunst, C. B., Leiner, H. A., Eichler, E. E., Nelson, D. L., & Warren, S. T. (1993). Human and murine FMR-1: alternative splicing and translational initiation downstream of the CGG-repeat. *Nature Genetics*, 4(3), 244-251. doi:10.1038/ng0793-244
- Ashwood, P., Krakowiak, P., Hertz-Picciotto, I., Hansen, R., Pessah, I., & Van de Water, J. (2011). Elevated plasma cytokines in autism spectrum disorders provide evidence of immune dysfunction and are associated with impaired behavioral outcome. *Brain, Behavior, and Immunity*, 25(1), 40-45. doi:10.1016/j.bbi.2010.08.003
- Aubertin, G. (2015). *Fragile X Syndrome in Canada: A Canadian Paediatric Surveillance Program Study*. Paper presented at the Paediatr Child Health.
- Basu, S., & Lamprecht, R. (2018). The Role of Actin Cytoskeleton in Dendritic Spines in the Maintenance of Long-Term Memory. *Frontiers in Molecular Neuroscience*, 11, 143-143. doi:10.3389/fnmol.2018.00143

- Berry-Kravis, E., & Potanos, K. (2004). Psychopharmacology in fragile X syndrome--present and future. *Ment Retard Dev Disabil Res Rev*, *10*(1), 42-48. doi:10.1002/mrdd.20007
- Bonni, A., Sun, Y., Nadal-Vicens, M., Bhatt, A., Frank, D. A., Rozovsky, I., . . . Greenberg, M. E. (1997). Regulation of gliogenesis in the central nervous system by the JAK-STAT signaling pathway. *Science*, *278*(5337), 477-483. doi:10.1126/science.278.5337.477
- Braun, O. Ö., Lu, D., Aroonsakool, N., & Insel, P. A. (2010). Uridine triphosphate (UTP) induces profibrotic responses in cardiac fibroblasts by activation of P2Y2 receptors. *Journal of Molecular and Cellular Cardiology*, *49*(3), 362-369. doi:10.1016/j.yjmcc.2010.05.001
- Brouwer, J. R., Willemsen, R., & Oostra, B. A. (2009). The FMR1 gene and fragile X-associated tremor/ataxia syndrome. *Am J Med Genet B Neuropsychiatr Genet*, *150b*(6), 782-798. doi:10.1002/ajmg.b.30910
- Brown, M. S., Singel, D., Hepburn, S., & Rojas, D. C. (2013). Increased glutamate concentration in the auditory cortex of persons with autism and first-degree relatives: a (1)H-MRS study. *Autism Res*, *6*(1), 1-10. doi:10.1002/aur.1260
- Brown, V., Jin, P., Ceman, S., Darnell, J. C., O'Donnell, W. T., Tenenbaum, S. A., . . . Warren, S. T. (2001). Microarray Identification of FMRP-Associated Brain mRNAs and Altered mRNA Translational Profiles in Fragile X Syndrome. *Cell*, *107*(4), 477-487. doi:doi.org/10.1016/S0092-8674(01)00568-2
- Campbell, I. L., Abraham, C. R., Masliah, E., Kemper, P., Inglis, J. D., Oldstone, M. B., & Mucke, L. (1993). Neurologic disease induced in transgenic mice by cerebral overexpression of interleukin 6. *Proceedings of the National Academy of Sciences of the United States of America*, *90*(21), 10061-10065. doi:10.1073/pnas.90.21.10061
- Cansev, M. (2006). Uridine and cytidine in the brain: Their transport and utilization. *Brain Research Reviews*, *52*(2), 389-397. doi:doi.org/10.1016/j.brainresrev.2006.05.001
- Caraccio, N., Monzani, F., Santini, E., Cuccato, S., Ferrari, D., Callegari, M. G., . . . Solini, A. (2005). Extracellular adenosine 5'-triphosphate modulates interleukin-6 production by human thyrocytes through functional purinergic P2 receptors. *Endocrinology*, *146*(7), 3172-3178. doi:10.1210/en.2004-1527
- Christopherson, K. S., Ullian, E. M., Stokes, C. C., Mallowney, C. E., Hell, J. W., Agah, A., . . . Barres, B. A. (2005). Thrombospondins are astrocyte-secreted proteins that promote CNS synaptogenesis. *Cell*, *120*(3), 421-433. doi:10.1016/j.cell.2004.12.020

- Chung, W. S., Clarke, L. E., Wang, G. X., Stafford, B. K., Sher, A., Chakraborty, C., . . . Barres, B. A. (2013). Astrocytes mediate synapse elimination through MEGF10 and MERTK pathways. *Nature*, *504*(7480), 394-400. doi:10.1038/nature12776
- Ciaccio, C., Fontana, L., Milani, D., Tabano, S., Miozzo, M., & Esposito, S. (2017). Fragile X syndrome: a review of clinical and molecular diagnoses. *Italian Journal of Pediatrics*, *43*(1), 39. doi:10.1186/s13052-017-0355-y
- Cordeiro, L., Ballinger, E., Hagerman, R., & Hessel, D. (2011). Clinical assessment of DSM-IV anxiety disorders in fragile X syndrome: prevalence and characterization. *J Neurodev Disord*, *3*(1), 57-67. doi:10.1007/s11689-010-9067-y
- Courchesne, E., Campbell, K., & Solso, S. (2011). Brain growth across the life span in autism: age-specific changes in anatomical pathology. *Brain Res*, *1380*, 138-145. doi:10.1016/j.brainres.2010.09.101
- D'Ambrosi, N., Iafrate, M., Saba, E., Rosa, P., & Volonté, C. (2007). Comparative analysis of P2Y4 and P2Y6 receptor architecture in native and transfected neuronal systems. *Biochimica et Biophysica Acta (BBA) - Biomembranes*, *1768*(6), 1592-1599. doi:10.1016/j.bbamem.2007.03.020
- Darnell, J. C., Van Driesche, S. J., Zhang, C., Hung, K. Y., Mele, A., Fraser, C. E., . . . Darnell, R. B. (2011). FMRP stalls ribosomal translocation on mRNAs linked to synaptic function and autism. *Cell*, *146*(2), 247-261. doi:10.1016/j.cell.2011.06.013
- Decker, T., & Kovarik, P. (2000). Serine phosphorylation of STATs. *Oncogene*, *19*(21), 2628-2637. doi:10.1038/sj.onc.1203481
- Dent, E. W., Gupton, S. L., & Gertler, F. B. (2011). The growth cone cytoskeleton in axon outgrowth and guidance. *Cold Spring Harbor Perspectives in Biology*, *3*(3). doi:10.1101/cshperspect.a001800
- Di Castro, M. A., Chuquet, J., Liaudet, N., Bhaukaurally, K., Santello, M., Bouvier, D., . . . Volterra, A. (2011). Local Ca<sup>2+</sup> detection and modulation of synaptic release by astrocytes. *Nat Neurosci*, *14*(10), 1276-1284. doi:10.1038/nn.2929
- Diniz, L. P., Tortelli, V., Garcia, M. N., Araújo, A. P. B., Melo, H. M., Seixas da Silva, G. S., . . . Gomes, F. C. A. (2014). Astrocyte transforming growth factor beta 1 promotes inhibitory synapse formation via CaM kinase II signaling. *Glia*, *62*(12), 1917-1931. doi:doi.org/10.1002/glia.22713
- Dobolyi, A., Juhasz, G., Kovacs, Z., & Kardos, J. (2011). Uridine function in the central nervous system. *Curr Top Med Chem*, *11*(8), 1058-1067. doi:10.2174/156802611795347618

- Eichler, E. E., Richards, S., Gibbs, R. A., & Nelson, D. L. (1993). Fine structure of the human FMR1 gene. *Hum Mol Genet*, 2(8), 1147-1153. doi:10.1093/hmg/2.8.1147
- El Idrissi, A., Ding, X. H., Scalia, J., Trenkner, E., Brown, W. T., & Dobkin, C. (2005). Decreased GABA(A) receptor expression in the seizure-prone fragile X mouse. *Neurosci Lett*, 377(3), 141-146. doi:10.1016/j.neulet.2004.11.087
- Elmariah, S. B., Oh, E. J., Hughes, E. G., & Balice-Gordon, R. J. (2005). Astrocytes Regulate Inhibitory Synapse Formation via Trk-Mediated Modulation of Postsynaptic GABA<sub>A</sub> Receptors. *The Journal of Neuroscience*, 25(14), 3638-3650. doi:10.1523/jneurosci.3980-04.2005
- Erickson, C. A., Davenport, M. H., Schaefer, T. L., Wink, L. K., Pedapati, E. V., Sweeney, J. A., . . . Berry-Kravis, E. (2017). Fragile X targeted pharmacotherapy: lessons learned and future directions. *J Neurodev Disord*, 9, 7. doi:10.1186/s11689-017-9186-9
- Eroglu, C., Allen, N. J., Susman, M. W., O'Rourke, N. A., Park, C. Y., Ozkan, E., . . . Barres, B. A. (2009). Gabapentin receptor alpha2delta-1 is a neuronal thrombospondin receptor responsible for excitatory CNS synaptogenesis. *Cell*, 139(2), 380-392. doi:10.1016/j.cell.2009.09.025
- Farhy-Tselnicker, I., & Allen, N. J. (2018). Astrocytes, neurons, synapses: a tripartite view on cortical circuit development. *Neural Development*, 13(1), 7. doi:10.1186/s13064-018-0104-y
- Farhy-Tselnicker, I., van Casteren, A. C. M., Lee, A., Chang, V. T., Aricescu, A. R., & Allen, N. J. (2017). Astrocyte-Secreted Glypican 4 Regulates Release of Neuronal Pentraxin 1 from Axons to Induce Functional Synapse Formation. *Neuron*, 96(2), 428-445.e413. doi:10.1016/j.neuron.2017.09.053
- Feng, Y., Gutekunst, C.-A., Eberhart, D. E., Yi, H., Warren, S. T., & Hersch, S. M. (1997). Fragile X Mental Retardation Protein: Nucleocytoplasmic Shuttling and Association with Somatodendritic Ribosomes. *The Journal of Neuroscience*, 17(5), 1539-1547. doi:10.1523/jneurosci.17-05-01539.1997
- Ferrer, I., Soriano, E., Del Rio, J. A., Alcántara, S., & Auladell, C. (1992). Cell death and removal in the cerebral cortex during development. *Progress in Neurobiology*, 39(1), 1-43. doi:doi.org/10.1016/0301-0082(92)90029-E
- Galvez, R., Gopal, A. R., & Greenough, W. T. (2003). Somatosensory cortical barrel dendritic abnormalities in a mouse model of the fragile X mental retardation syndrome. *Brain Res*, 971(1), 83-89. doi:10.1016/s0006-8993(03)02363-1

- Garel, C., Chantrel, E., Brisse, H., Elmaleh, M., Luton, D., Oury, J.-F., . . . Hassan, M. (2001). Fetal Cerebral Cortex: Normal Gestational Landmarks Identified Using Prenatal MR Imaging. *American Journal of Neuroradiology*, 22(1), 184-189.
- Gibson, J. R., Bartley, A. F., Hays, S. A., & Huber, K. M. (2008). Imbalance of neocortical excitation and inhibition and altered UP states reflect network hyperexcitability in the mouse model of fragile X syndrome. *Journal of Neurophysiology*, 100(5), 2615-2626. doi:10.1152/jn.90752.2008
- Grossman, A. W., Elisseou, N. M., McKinney, B. C., & Greenough, W. T. (2006). Hippocampal pyramidal cells in adult Fmr1 knockout mice exhibit an immature-appearing profile of dendritic spines. *Brain Res*, 1084(1), 158-164. doi:10.1016/j.brainres.2006.02.044
- Haberl, M. G., Zerbi, V., Veltien, A., Ginger, M., Heerschap, A., & Frick, A. (2015). Structural-functional connectivity deficits of neocortical circuits in the Fmr1 (-/y) mouse model of autism. *Science Advances*, 1(10), e1500775-e1500775. doi:10.1126/sciadv.1500775
- Handa, V., Saha, T., & Usdin, K. (2003). The fragile X syndrome repeats form RNA hairpins that do not activate the interferon-inducible protein kinase, PKR, but are cut by Dicer. *Nucleic Acids Res*, 31(21), 6243-6248. doi:10.1093/nar/gkg818
- Hassinger, T. D., Guthrie, P. B., Atkinson, P. B., Bennett, M. V., & Kater, S. B. (1996). An extracellular signaling component in propagation of astrocytic calcium waves. *Proceedings of the National Academy of Sciences of the United States of America*, 93(23), 13268-13273. doi:10.1073/pnas.93.23.13268
- Hernandez, R. N., Feinberg, R. L., Vaurio, R., Passanante, N. M., Thompson, R. E., & Kaufmann, W. E. (2009). Autism spectrum disorder in fragile X syndrome: a longitudinal evaluation. *Am J Med Genet A*, 149a(6), 1125-1137. doi:10.1002/ajmg.a.32848
- Higashimori, H., Schin, C. S., Chiang, M. S., Morel, L., Shoneye, T. A., Nelson, D. L., & Yang, Y. (2016). Selective Deletion of Astroglial FMRP Dysregulates Glutamate Transporter GLT1 and Contributes to Fragile X Syndrome Phenotypes In Vivo. *J Neurosci*, 36(27), 7079-7094. doi:10.1523/jneurosci.1069-16.2016
- Hodges, J. L., Yu, X., Gilmore, A., Bennett, H., Tjia, M., Perna, J. F., . . . Zuo, Y. (2017). Astrocytic Contributions to Synaptic and Learning Abnormalities in a Mouse Model of Fragile X Syndrome. *Biological Psychiatry*, 82(2), 139-149. doi:doi.org/10.1016/j.biopsych.2016.08.036
- Huttenlocher, P. R. (1990). Morphometric study of human cerebral cortex development. *Neuropsychologia*, 28(6), 517-527.

- Huttenlocher, P. R., & Dabholkar, A. S. (1997). Regional differences in synaptogenesis in human cerebral cortex. *J Comp Neurol*, 387(2), 167-178.
- Jacobs, S., & Doering, L. C. (2010). Astrocytes Prevent Abnormal Neuronal Development in the Fragile X Mouse. *The Journal of Neuroscience*, 30(12), 4508-4514. doi:10.1523/jneurosci.5027-09.2010
- Jokela, T., Kärnä, R., Rauhala, L., Bart, G., Pasonen-Seppänen, S., Oikari, S., . . . Tammi, R. H. (2017). Human Keratinocytes Respond to Extracellular UTP by Induction of Hyaluronan Synthase 2 Expression and Increased Hyaluronan Synthesis. *The Journal of Biological Chemistry*, 292(12), 4861-4872. doi:10.1074/jbc.M116.760322
- Kazdoba, T. M., Leach, P. T., Silverman, J. L., & Crawley, J. N. (2014). Modeling fragile X syndrome in the Fmr1 knockout mouse. *Intractable Rare Dis Res*, 3(4), 118-133. doi:10.5582/irdr.2014.01024
- Kimelberg, H. K., & Nedergaard, M. (2010). Functions of astrocytes and their potential as therapeutic targets. *Neurotherapeutics*, 7(4), 338-353. doi:10.1016/j.nurt.2010.07.006
- Kirchgessner, C. U., Warren, S. T., & Willard, H. F. (1995). X inactivation of the FMR1 fragile X mental retardation gene. *J Med Genet*, 32(12), 925-929. doi:10.1136/jmg.32.12.925
- Knickmeyer, R. C., Gouttard, S., Kang, C., Evans, D., Wilber, K., Smith, J. K., . . . Gilmore, J. H. (2008). A Structural MRI Study of Human Brain Development from Birth to 2 Years. *The Journal of Neuroscience*, 28(47), 12176-12182. doi:10.1523/jneurosci.3479-08.2008
- Krasovska, V., & Doering, L. C. (2018). Regulation of IL-6 Secretion by Astrocytes via TLR4 in the Fragile X Mouse Model. *Frontiers in Molecular Neuroscience*, 11, 272-272. doi:10.3389/fnmol.2018.00272
- Kucukdereli, H., Allen, N. J., Lee, A. T., Feng, A., Ozlu, M. I., Conatser, L. M., . . . Eroglu, C. (2011). Control of excitatory CNS synaptogenesis by astrocyte-secreted proteins Hevin and SPARC. *Proceedings of the National Academy of Sciences of the United States of America*, 108(32), E440-449. doi:10.1073/pnas.1104977108
- Laggerbauer, B., Ostareck, D., Keidel, E.-M., Ostareck-Lederer, A., & Fischer, U. (2001). Evidence that fragile X mental retardation protein is a negative regulator of translation. *Human Molecular Genetics*, 10(4), 329-338. doi:10.1093/hmg/10.4.329

- Lee, E., Lee, J., & Kim, E. (2017). Excitation/Inhibition Imbalance in Animal Models of Autism Spectrum Disorders. *Biol Psychiatry*, *81*(10), 838-847. doi:10.1016/j.biopsych.2016.05.011
- Li, X., Chauhan, A., Sheikh, A. M., Patil, S., Chauhan, V., Li, X.-M., . . . Malik, M. (2009). Elevated immune response in the brain of autistic patients. *Journal of Neuroimmunology*, *207*(1), 111-116. doi:10.1016/j.jneuroim.2008.12.002
- Li, Z., He, C., Wei, H., Zhang, H., Hu, L., & Jiang, W. (2020). Purinergic Receptor P2Y 6 Inhibits the Maturation and Function of NK Cells by Suppressing mTOR Signaling Pathway. *iScience, Preview ahead of print*. doi:doi.org/10.2139/ssrn.3565015
- Maddalena, A., Richards, C. S., McGinniss, M. J., Brothman, A., Desnick, R. J., Grier, R. E., . . . Wolff, D. J. (2001). Technical standards and guidelines for fragile X: the first of a series of disease-specific supplements to the Standards and Guidelines for Clinical Genetics Laboratories of the American College of Medical Genetics. Quality Assurance Subcommittee of the Laboratory Practice Committee. *Genet Med*, *3*(3), 200-205. doi:10.1097/00125817-200105000-00010
- Marsick, B. M., Flynn, K. C., Santiago-Medina, M., Bamburg, J. R., & Letourneau, P. C. (2010). Activation of ADF/cofilin mediates attractive growth cone turning toward nerve growth factor and netrin-1. *Dev Neurobiol*, *70*(8), 565-588. doi:10.1002/dneu.20800
- Meguid, N. A., Fahim, C., Sami, R., Nashaat, N. H., Yoon, U., Anwar, M., . . . Evans, A. C. (2012). Cognition and lobar morphology in full mutation boys with fragile X syndrome. *Brain Cogn*, *78*(1), 74-84. doi:10.1016/j.bandc.2011.09.005
- Modabbernia, A., Velthorst, E., & Reichenberg, A. (2017). Environmental risk factors for autism: an evidence-based review of systematic reviews and meta-analyses. *Mol Autism*, *8*, 13. doi:10.1186/s13229-017-0121-4
- Molyneaux, B. J., Arlotta, P., Menezes, J. R. L., & Macklis, J. D. (2007). Neuronal subtype specification in the cerebral cortex. *Nature Reviews Neuroscience*, *8*(6), 427-437. doi:10.1038/nrn2151
- Musumeci, S. A., Hagerman, R. J., Ferri, R., Bosco, P., Bernardina, B. D., Tassinari, C. A., . . . Elia, M. (1999). Epilepsy and EEG Findings in Males with Fragile X Syndrome. *Epilepsia*, *40*(8), 1092-1099. doi:doi.org/10.1111/j.1528-1157.1999.tb00824.x
- Nadarajah, B., & Parnavelas, J. G. (2002). Modes of neuronal migration in the developing cerebral cortex. *Nature Reviews Neuroscience*, *3*(6), 423-432. doi:10.1038/nrn845

- Namihira, M., Kohyama, J., Semi, K., Sanosaka, T., Deneen, B., Taga, T., & Nakashima, K. (2009). Committed neuronal precursors confer astrocytic potential on residual neural precursor cells. *Dev Cell*, *16*(2), 245-255. doi:10.1016/j.devcel.2008.12.014
- Neary, J. T., Kang, Y., Bu, Y., Yu, E., Akong, K., & Peters, C. M. (1999). Mitogenic signaling by ATP/P2Y purinergic receptors in astrocytes: involvement of a calcium-independent protein kinase C, extracellular signal-regulated protein kinase pathway distinct from the phosphatidylinositol-specific phospholipase C/calcium pathway. *The Journal of Neuroscience*, *19*(11), 4211-4220. doi:10.1523/JNEUROSCI.19-11-04211.1999
- Nimchinsky, E. A., Oberlander, A. M., & Svoboda, K. (2001). Abnormal Development of Dendritic Spines in FMR1 Knock-Out Mice. *The Journal of Neuroscience*, *21*(14), 5139-5146. doi:10.1523/jneurosci.21-14-05139.2001
- Nolin, S. L., Brown, W. T., Glicksman, A., Houck, G. E., Jr., Gargano, A. D., Sullivan, A., . . . Sherman, S. L. (2003). Expansion of the fragile X CGG repeat in females with premutation or intermediate alleles. *Am J Hum Genet*, *72*(2), 454-464. doi:10.1086/367713
- Oakes, A., Thurman, A. J., McDuffie, A., Bullard, L. M., Hagerman, R. J., & Abbeduto, L. (2016). Characterising repetitive behaviours in young boys with fragile X syndrome. *J Intellect Disabil Res*, *60*(1), 54-67. doi:10.1111/jir.12234
- Ofner, M., Coles, A., Decou, M. L., Do, M. T., Bienek, A., Snider, J., & Ugnat, A.-M. (2018). *Autism Spectrum Disorder Among Children and Youth in Canada 2018: A Report of the National Autism Spectrum Disorder Surveillance System*. Retrieved from <https://www.canada.ca/en/public-health/services/publications/diseases-conditions/autism-spectrum-disorder-children-youth-canada-2018.html>
- Ouellette-Kuntz, H., Coo, H., Lam, M., Breitenbach, M. M., Hennessey, P. E., Jackman, P. D., . . . Chung, A. M. (2014). The changing prevalence of autism in three regions of Canada. *J Autism Dev Disord*, *44*(1), 120-136. doi:10.1007/s10803-013-1856-1
- Pacey, L. K., & Doering, L. C. (2007). Developmental expression of FMRP in the astrocyte lineage: implications for fragile X syndrome. *Glia*, *55*(15), 1601-1609. doi:10.1002/glia.20573
- Pan, L., Zhang, Y. Q., Woodruff, E., & Broadie, K. (2004). The Drosophila Fragile X Gene Negatively Regulates Neuronal Elaboration and Synaptic Differentiation. *Current Biology*, *14*(20), 1863-1870. doi:10.1016/j.cub.2004.09.085

- Patel, A. B., Loerwald, K. W., Huber, K. M., & Gibson, J. R. (2014). Postsynaptic FMRP promotes the pruning of cell-to-cell connections among pyramidal neurons in the L5A neocortical network. *J Neurosci*, *34*(9), 3413-3418. doi:10.1523/jneurosci.2921-13.2014
- Peterson, T. S., Thebeau, C. N., Ajit, D., Camden, J. M., Woods, L. T., Wood, W. G., . . . Weisman, G. A. (2013). Up-regulation and activation of the P2Y(2) nucleotide receptor mediate neurite extension in IL-1 $\beta$ -treated mouse primary cortical neurons. *Journal of Neurochemistry*, *125*(6), 885-896. doi:10.1111/jnc.12252
- Pooler, A. M., Guez, D. H., Benedictus, R., & Wurtman, W. J. (2005). Uridine enhances neurite outgrowth in nerve growth factor-differentiated pheochromocytoma cells. *Neuroscience*, *134*, 207-214.
- Putz, N. A. J., Wodka, E. L., Harris, A. D., Crocetti, D., Tommerdahl, M., Mostofsky, S. H., & Edden, R. A. E. (2017). Reduced GABA and altered somatosensory function in children with autism spectrum disorder. *Autism Res*, *10*(4), 608-619. doi:10.1002/aur.1691
- Qin, M., Kang, J., Burlin, T. V., Jiang, C., & Smith, C. B. (2005). Postadolescent changes in regional cerebral protein synthesis: an in vivo study in the FMR1 null mouse. *J Neurosci*, *25*(20), 5087-5095. doi:10.1523/jneurosci.0093-05.2005
- Risher, W. C., Kim, N., Koh, S., Choi, J.-E., Mitev, P., Spence, E. F., . . . Eroglu, C. (2018). Thrombospondin receptor  $\alpha 2\delta$ -1 promotes synaptogenesis and spinogenesis via postsynaptic Rac1. *Journal of Cell Biology*, *217*(10), 3747-3765. doi:10.1083/jcb.201802057
- Rubenstein, J. L., & Merzenich, M. M. (2003). Model of autism: increased ratio of excitation/inhibition in key neural systems. *Genes Brain Behav*, *2*(5), 255-267. doi:10.1034/j.1601-183x.2003.00037.x
- Santello, M., & Volterra, A. (2009). Synaptic modulation by astrocytes via Ca<sup>2+</sup>-dependent glutamate release. *Neuroscience*, *158*(1), 253-259. doi:doi.org/10.1016/j.neuroscience.2008.03.039
- Satterstrom, F. K., Kosmicki, J. A., Wang, J., Breen, M. S., De Rubeis, S., An, J.-Y., . . . Buxbaum, J. D. (2020). Large-Scale Exome Sequencing Study Implicates Both Developmental and Functional Changes in the Neurobiology of Autism. *Cell*, *180*(3), 568-584.e523. doi:10.1016/j.cell.2019.12.036
- Scemes, E., & Giaume, C. (2006). Astrocyte calcium waves: what they are and what they do. *Glia*, *54*(7), 716-725. doi:10.1002/glia.20374

- Schüz, A., & Palm, G. (1989). Density of neurons and synapses in the cerebral cortex of the mouse. *Journal of Comparative Neurology*, 286(4), 442-455. doi:doi.org/10.1002/cne.902860404
- Semple, B. D., Blomgren, K., Gimlin, K., Ferriero, D. M., & Noble-Haeusslein, L. J. (2013). Brain development in rodents and humans: Identifying benchmarks of maturation and vulnerability to injury across species. *Progress in Neurobiology*, 106-107, 1-16. doi:10.1016/j.pneurobio.2013.04.001
- Shen, K., & Cowan, C. W. (2010). Guidance molecules in synapse formation and plasticity. *Cold Spring Harbor Perspectives in Biology*, 2(4), a001842. doi:10.1101/cshperspect.a001842
- Silbereis, J. C., Pochareddy, S., Zhu, Y., Li, M., & Sestan, N. (2016). The Cellular and Molecular Landscapes of the Developing Human Central Nervous System. *Neuron*, 89(2), 248-268. doi:10.1016/j.neuron.2015.12.008
- Singh, K., Gaur, P., & Prasad, S. (2007). Fragile x mental retardation (Fmr-1) gene expression is down regulated in brain of mice during aging. *Mol Biol Rep*, 34(3), 173-181. doi:10.1007/s11033-006-9032-8
- Steculorum, S. M., Paeger, L., Bremser, S., Evers, N., Hinze, Y., Idzko, M., . . . Brüning, J. C. (2015). Hypothalamic UDP Increases in Obesity and Promotes Feeding via P2Y6-Dependent Activation of AgRP Neurons. *Cell*, 162(6), 1404-1417. doi:10.1016/j.cell.2015.08.032
- Stefani, G., Fraser, C. E., Darnell, J. C., & Darnell, R. B. (2004). Fragile X Mental Retardation Protein Is Associated with Translating Polyribosomes in Neuronal Cells. *The Journal of Neuroscience*, 24(33), 7272-7276. doi:10.1523/jneurosci.2306-04.2004
- Stockwell, J., Jakova, E., & Cayabyab, F. S. (2017). Adenosine A1 and A2A Receptors in the Brain: Current Research and Their Role in Neurodegeneration. *Molecules*, 22(4). doi:10.3390/molecules22040676
- Sukigara, S., Dai, H., Nabatame, S., Otsuki, T., Hanai, S., Honda, R., . . . Itoh, M. (2014). Expression of astrocyte-related receptors in cortical dysplasia with intractable epilepsy. *J Neuropathol Exp Neurol*, 73(8), 798-806. doi:10.1097/nen.0000000000000099
- Sullivan, K., Hatton, D., Hammer, J., Sideris, J., Hooper, S., Ornstein, P., & Bailey, D., Jr. (2006). ADHD symptoms in children with FXS. *Am J Med Genet A*, 140(21), 2275-2288. doi:10.1002/ajmg.a.31388

- Sutcliffe, J. S., Nelson, D. L., Zhang, F., Pieretti, M., Caskey, C. T., Saxe, D., & Warren, S. T. (1992). DNA methylation represses FMR-1 transcription in fragile X syndrome. *Hum Mol Genet*, *1*(6), 397-400. doi:10.1093/hmg/1.6.397
- Tabata, H. (2015). Diverse subtypes of astrocytes and their development during corticogenesis. *Frontiers in Neuroscience*, *9*(114). doi:10.3389/fnins.2015.00114
- Tau, G. Z., & Peterson, B. S. (2010). Normal development of brain circuits. *Neuropsychopharmacology*, *35*(1), 147-168. doi:10.1038/npp.2009.115
- The Dutch-Belgian Fragile X Consortium, Bakker, C. E., Verheij, C., Willemsen, R., van der Helm, R., Oerlemans, F., . . . Willems, P. J. (1994). Fmr1 knockout mice: a model to study fragile X mental retardation. The Dutch-Belgian Fragile X Consortium. *Cell*, *78*(1), 23-33.
- Todd, P. K., & Mack, K. J. (2000). Sensory stimulation increases cortical expression of the fragile X mental retardation protein in vivo. *Molecular Brain Research*, *80*(1), 17-25. doi:doi.org/10.1016/S0169-328X(00)00098-X
- Todd, P. K., Oh, S. Y., Krans, A., Pandey, U. B., Di Prospero, N. A., Min, K. T., . . . Paulson, H. L. (2010). Histone deacetylases suppress CGG repeat-induced neurodegeneration via transcriptional silencing in models of fragile X tremor ataxia syndrome. *PLoS Genet*, *6*(12), e1001240. doi:10.1371/journal.pgen.1001240
- Tran, M. D., & Neary, J. T. (2006). Purinergic signaling induces thrombospondin-1 expression in astrocytes. *Proceedings of the National Academy of Sciences of the United States of America*, *103*(24), 9321-9326. doi:10.1073/pnas.0603146103
- Turner, G., Webb, T., Wake, S., & Robinson, H. (1996). Prevalence of fragile X syndrome. *Am J Med Genet*, *64*(1), 196-197.
- Ullian, E. M., Sapperstein, S. K., Christopherson, K. S., & Barres, B. A. (2001). Control of synapse number by glia. *Science*, *291*(5504), 657-661. doi:10.1126/science.291.5504.657
- Verkerk, A. J. M. H., Pieretti, M., Sutcliffe, J. S., Fu, Y.-H., Kuhl, D. P. A., Pizzuti, A., . . . Warren, S. T. (1991). Identification of a gene (FMR-1) containing a CGG repeat coincident with a breakpoint cluster region exhibiting length variation in fragile X syndrome. *Cell*, *65*(5), 905-914. doi:doi.org/10.1016/0092-8674(91)90397-H
- von Bartheld, C. S., Bahney, J., & Herculano-Houzel, S. (2016). The search for true numbers of neurons and glial cells in the human brain: A review of 150 years of cell counting. *J Comp Neurol*, *524*(18), 3865-3895. doi:10.1002/cne.24040

- von Kugelgen, I., & Hoffmann, K. (2016). Pharmacology and structure of P2Y receptors. *Neuropharmacology*, *104*, 50-61. doi:10.1016/j.neuropharm.2015.10.030
- Wallingford, J., Scott, A. L., Rodrigues, K., & Doering, L. C. (2017). Altered Developmental Expression of the Astrocyte-Secreted Factors Hevin and SPARC in the Fragile X Mouse Model. *Frontiers in Molecular Neuroscience*, *10*, 268-268. doi:10.3389/fnmol.2017.00268
- Walz, W. (2000). Role of astrocytes in the clearance of excess extracellular potassium. *Neurochem Int*, *36*(4-5), 291-300. doi:10.1016/s0197-0186(99)00137-0
- Wang, L., Wang, Y., Zhou, S., Yang, L., Shi, Q., Li, Y., . . . Yang, Q. (2016). Imbalance between Glutamate and GABA in Fmr1 Knockout Astrocytes Influences Neuronal Development. *Genes*, *7*(8), 45. doi:10.3390/genes7080045
- Wang, S. W., & Sun, Y. M. (2014). The IL-6/JAK/STAT3 pathway: potential therapeutic strategies in treating colorectal cancer. *Int J Oncol*, *44*(4), 1032-1040. doi:10.3892/ijo.2014.2259
- Washburn, K. B., & Neary, J. T. (2006). P2 purinergic receptors signal to STAT3 in astrocytes: Difference in STAT3 responses to P2Y and P2X receptor activation. *Neuroscience*, *142*(2), 411-423. doi:10.1016/j.neuroscience.2006.06.034
- Wei, H., Chadman, K. K., McCloskey, D. P., Sheikh, A. M., Malik, M., Brown, W. T., & Li, X. (2012). Brain IL-6 elevation causes neuronal circuitry imbalances and mediates autism-like behaviors. *Biochimica et Biophysica Acta (BBA) - Molecular Basis of Disease*, *1822*(6), 831-842. doi:doi.org/10.1016/j.bbadis.2012.01.011
- Wei, H., Zou, H., Sheikh, A. M., Malik, M., Dobkin, C., Brown, W. T., & Li, X. (2011). IL-6 is increased in the cerebellum of autistic brain and alters neural cell adhesion, migration and synaptic formation. *J Neuroinflammation*, *8*, 52. doi:10.1186/1742-2094-8-52
- Wodarz, A., & Huttner, W. B. (2003). Asymmetric cell division during neurogenesis in *Drosophila* and vertebrates. *Mech Dev*, *120*(11), 1297-1309. doi:10.1016/j.mod.2003.06.003
- Youngs, S. A., Murray, A., Dennis, N., Ennis, S., Lewis, C., McKechnie, N., . . . Jacobs, P. (2000). FRAXA and FRAXE: the results of a five year survey. *J Med Genet*, *37*(6), 415-421. doi:10.1136/jmg.37.6.415
- Zalfa, F., & Bagni, C. (2004). Molecular insights into mental retardation: multiple functions for the Fragile X mental retardation protein? *Curr Issues Mol Biol*, *6*(2), 73-88.

- Zhong, X., Malhotra, R., Woodruff, R., & Guidotti, G. (2001). Mammalian Plasma Membrane Ecto-nucleoside Triphosphate Diphosphohydrolase 1, CD39, Is Not Active Intracellularly: THE N-GLYCOSYLATION STATE OF CD39 CORRELATES WITH SURFACE ACTIVITY AND LOCALIZATION\*. *Journal of Biological Chemistry*, 276(44), 41518-41525. doi:doi.org/10.1074/jbc.M104415200
- Zimmermann, H. (1996). BIOCHEMISTRY, LOCALIZATION AND FUNCTIONAL ROLES OF ECTO-NUCLEOTIDASES IN THE NERVOUS SYSTEM. *Progress in neurobiology*, 49(6), 589-618. doi:doi.org/10.1016/0301-0082(96)00026-3
- Zingerevich, C., Greiss-Hess, L., Lemons-Chitwood, K., Harris, S. W., Hessel, D., Cook, K., & Hagerman, R. J. (2009). Motor abilities of children diagnosed with fragile X syndrome with and without autism. *J Intellect Disabil Res*, 53(1), 11-18. doi:10.1111/j.1365-2788.2008.01107.x
- Zoghbi, H. Y., & Bear, M. F. (2012). Synaptic dysfunction in neurodevelopmental disorders associated with autism and intellectual disabilities. *Cold Spring Harbor Perspectives in Biology*, 4(3). doi:10.1101/cshperspect.a009886

## Chapter Two:

### **Astrocyte-mediated purinergic signalling is upregulated in a mouse model of Fragile X syndrome**

#### **2.1. Preface**

Synaptic dysregulations are observed in both FXS patients and *Fmr1* KO mouse models, and contribute to a lack of appropriate connections within the FXS brain. Recent evidence indicates that the loss of FMRP in astrocytes leads to disordered dendritic growth and aberrant synaptogenesis in developing neurons; however, the astrocyte-derived factors impacted by this loss of FMRP are largely unknown. The purinergic signalling pathway is one of the most ubiquitous signalling systems utilized to facilitate glial-neuronal and glial-glial crosstalk, and notably, it is associated with the regulation of astrocyte-secreted synaptogenic proteins. Accordingly, this pathway may contribute to the modulation of astrocyte function in FXS, though its role in this neurodevelopmental disorder has remained unexplored. This chapter will therefore investigate whether purinergic signalling is dysregulated within the FXS mouse cortex, and whether this dysregulation contributes to aberrant intercellular communication.

#### **2.2. Study Significance**

This study is the first to identify novel and significant purinergic signalling elevations in FXS cortical astrocytes. Levels of *Fmr1* KO astrocyte P2Y<sub>2</sub> and P2Y<sub>6</sub> receptors were increased both *in vitro* and in acutely dissociated astrocytes, while evoked intracellular calcium responses were heightened following P2Y agonism and abolished with pan-purinergic antagonism, strongly implicating P2Y receptors in FXS astrocyte dysfunction. P2Y receptor activation also regulated the expression and release of the synaptogenic protein TSP-1, which was transiently elevated in the *Fmr1* KO cortex, indicating that this combination of increased intracellular calcium and upregulation of TSP-1 may act to increase cortical excitation and promote glial-mediated cortical

synaptogenesis. Together, these findings suggest that elevated purinergic pathways may be targeted to mitigate the signalling aberrations observed in the FXS cortex.

### **2.3. Aims and Hypotheses**

This research was designed to address the first aim of this thesis work:

Aim 1: Establish whether astrocyte purinergic signalling is dysregulated as a result of *Fmr1* mutation in the KO mouse cortex.

Hypothesis: Astrocyte purinergic receptors and/or ligands are differentially expressed in the *Fmr1* KO mouse cortex, leading to increased activation of purinergic pathways and changes in downstream soluble factor expression.

### **2.4. Publication Status**

The following manuscript is an author-generated version of work previously published in *Glia*, and is reproduced here with permission (see Appendix: Copyright Transfer Agreements):

Reynolds, KE, Wong, CR, Scott, AL. Astrocyte-mediated purinergic signalling is upregulated in a mouse model of Fragile X syndrome. *Glia*. 2021; 69(7): 1816–1832. doi.org/10.1002/glia.23997

**Title: Astrocyte-mediated purinergic signalling is upregulated in a mouse model of Fragile X syndrome**

**Authors:**

Kathryn E. Reynolds<sup>1</sup>, Chloe R. Wong<sup>2</sup> & Angela L. Scott<sup>1,2</sup>

1. Neuroscience Graduate Program, McMaster University, Hamilton, Ontario, Canada

2. Department of Pathology and Molecular Medicine, McMaster University,  
Hamilton, Ontario, Canada

**Correspondence:**

Angela L. Scott  
Department of Pathology and Molecular Medicine  
McMaster University  
1200 Main Street West, Hamilton, Ontario L8N 3Z5, Canada.  
scottan@mcmaster.ca

**Funding Information:**

Canadian Institutes of Health Research; Brain Canada; FRAXA Research Foundation

**Acknowledgements:**

We sincerely thank Ashley Chen, Connie Cheng, and Laurie Doering for the range of technical assistance and support provided for the successful completion of this work. This work was supported by a partnership grant from Brain Canada and the Azrieli Foundation, as well as a fellowship award from the FRAXA Foundation to AS. KR was funded by a Canadian Institutes of Health Research Canada Graduate Scholarship (CIHR CGS-D).

**Conflict of Interests:**

None

**Keywords:**

astrocyte, ATP, cortex, Fragile X syndrome, P2Y, purinergic s, thrombospondin-1, UTP

**Main Points:**

- Purinergic signalling is upregulated in Fragile X astrocytes.

- Absence of FMRP increases astrocyte P2Y<sub>2</sub> and P2Y<sub>6</sub> receptor expression, enhances calcium release, and transiently upregulates synaptogenic protein TSP-1.

## 2.5. Author Contributions

This study was designed by A.L. Scott and K.E. Reynolds. K.E. Reynolds designed, executed, and analyzed all experiments involved TSP-1 expression, secretion, and *in vivo* abundance (Figures 5-7), as well as all supplementary analysis (Supplementary Figure 1), while C.R. Wong assisted with Western blotting to detect astrocyte P2Y receptors *in vitro* and in acutely dissociated tissue (Figures 3, 4). Experiments involving astrocyte calcium signalling (Figures 1, 2) were designed, conducted, and analyzed by A.L. Scott. The manuscript was written by K.E. Reynolds and A.L. Scott, and was reviewed and edited by all authors prior to publication.

## 2.6. Abstract

Fragile X syndrome (FXS) is the leading monogenic cause of intellectual disability and autism spectrum disorders. With increasing investigation into the molecular mechanisms underlying FXS, there is growing evidence that perturbations in glial signalling are widely associated with neurological pathology. Purinergic signalling, which utilizes nucleoside triphosphates as signalling molecules, provides one of the most ubiquitous signalling systems for glial-neuronal and glial-glial crosstalk. Here, we sought to identify whether purinergic signalling is dysregulated within the FXS mouse cortex, and whether this dysregulation contributes to aberrant intercellular communication. In primary astrocyte cultures derived from the *Fmr1* knockout (KO) mouse model of FXS, we found that application of exogenous ATP and UTP evoked elevated intracellular calcium responses compared to wildtype levels. Accordingly, purinergic P2Y<sub>2</sub> and P2Y<sub>6</sub> receptor expression was increased in *Fmr1* KO astrocytes both *in vitro* and in acutely dissociated tissue, while P2Y antagonism via suramin prevented intracellular calcium elevations, suggesting a role for these receptors in aberrant FXS astrocyte activation. To investigate the impact of elevated purinergic signalling on astrocyte-mediated synaptogenesis, we

quantified synaptogenic protein TSP-1, known to be regulated by P2Y activation. TSP-1 secretion and expression were both heightened in *Fmr1* KO vs wildtype astrocytes following UTP application, while naïve TSP-1 cortical expression was also transiently elevated *in vivo*, indicating increased potential for excitatory TSP-1-mediated synaptogenesis in the FXS cortex. Together, our results demonstrate novel and significant purinergic signalling elevations in *Fmr1* KO astrocytes, which may serve as a potential therapeutic target to mitigate the signalling aberrations observed in FXS.

## 2.7. Introduction

Neurodevelopmental diseases such as intellectual disability (ID) and autism spectrum disorders (ASDs) pose an ever-growing challenge, as ~3% of the world's population is currently afflicted and the rate of prevalence continues to rise (Olusanya et al., 2018). In the race to successfully reduce incidence of disease or develop effective treatments, it is becoming increasingly urgent that we understand potentially convergent modes of pathophysiology. Etiological assessments predict that up to one-half of ID and ASD cases are due to genetic mutations, several of which co-occur with other disorders (reviewed in Verma, Paul, Amrapali Vishwanath, Vaidya, & Clement, 2019). The most common monogenic form of ID and ASD is due to a genetic variation that is associated with Fragile X syndrome (FXS). The expansion and hypermethylation of CGG repeats within the *Fmr1* gene effectively silences the gene and prevents the expression of FMRP protein (Pieretti et al., 1991), leading many FXS patients to present with learning difficulties, memory impairments, cognitive and social deficiencies, repetitive behaviors, hypersensitivity to sensory stimuli, and seizure activity (Zoghbi & Bear, 2012). Imbalances to excitatory and inhibitory neural networks are believed to underlie many of the clinical features associated with FXS; however, the cellular and molecular mechanisms regulating these network changes are largely unknown.

During development, glial cells play a prominent role in the regulation of growth, refinement, and function of neural circuits, through a number of complex intercellular

signalling systems. Astrocytes, in particular, can govern the formation, elimination, and maintenance of both excitatory and inhibitory synapses via the expression of synaptogenic molecules. For example, the adhesion glycoprotein thrombospondin-1 (TSP-1) is secreted by astrocytes during early development and promotes the formation of excitatory synapses through its interaction with the neuronal  $\alpha 2\delta$ -1 voltage-gated calcium channel subunit, otherwise known as the gabapentin receptor (Eroglu et al., 2009). Indeed, transgenic mice that lack either TSP-1 or  $\alpha 2\delta$ -1 expression display network imbalances due to significantly reduced numbers of excitatory synapses (Christopherson et al., 2005; Eroglu et al., 2009). Changes to excitatory circuitry are particularly apparent during cortical development in FXS, with heightened levels of cortical excitation contributing to hypersensitivity and the onset of seizures. In an animal model of FXS, the *Fmr1* knockout (KO) mouse, cortical neurons display increased spine density, immature spine morphology, and prolonged spine turnover (Galvez, Gopal, & Greenough, 2003; Grossman, Elisseou, McKinney, & Greenough, 2006). Interestingly, the presence of wildtype (WT) astrocytes effectively normalizes these neuronal changes in co-culture systems (Cheng, Lau, & Doering, 2016; Jacobs & Doering, 2010). This suggests that FMRP expression in astrocytes is particularly important for regulating astrocyte-mediated synaptogenic factors that are required to correct aberrant neuron spine density and morphology during development. Further studies regarding the impact of FMRP deletion on astrocytes specifically revealed variations in astrocyte glutamate transmission (Higashimori et al., 2016) and synaptogenic factor expression (Wallingford, Scott, Rodrigues, & Doering, 2017), providing evidence of an inherent role for astrocyte-neuronal interactions in the pathophysiology of FXS.

A plethora of regulatory molecules has been identified in astrocyte-neuronal interactions responsible for neuronal growth, pathfinding, and synapse development. Among those, the purinergic signalling system is the most ubiquitously expressed in both glial and neuronal cell-types during these key developmental periods. Purinergic signalling, via nucleoside triphosphates and their metabolites, influences neuronal growth and activity through two receptor families, P1 and P2 (Abbracchio, Burnstock, Verkhratsky, & Zimmermann, 2009). P2 receptors, further sub-classified as ionotropic P2X and

metabotropic P2Y receptors, are transiently expressed in the cortex during embryonic and early postnatal development (Abbracchio et al., 2009). Both P2Y and P2X subtypes work to modulate neuronal and astrocyte activity within the developing brain via calcium-dependent mechanisms. Interestingly, P2Y receptor activation in astrocytes promotes not only mobilization of intracellular calcium but also propagation of calcium into neighboring cells, effectively producing intercellular calcium waves to expand the activated region (Gallagher & Salter, 2003). Increased astrocyte P2Y activation has also been associated with enhanced expression of synaptogenic factors; for instance, exogenous application of uridine triphosphate (UTP), a specific P2Y agonist, led to a significant increase in TSP-1 expression and secretion by rat astrocytes (Tran & Neary, 2006). While elevated levels of plasma uridine, the nucleoside precursor to UTP, have been found in children with ASD (Adams et al., 2011), potential aberrations of P2Y receptor expression and/or activation in FXS have yet to be reported.

Given the importance of glial-neuronal crosstalk in cortical development, as well as the numerous instances of aberrant neuronal connectivity in FXS, we examined whether purinergic signalling is dysregulated within the FXS mouse cortex. Here, we show that P2Y receptor agonists ATP and UTP abnormally enhanced intracellular calcium transients in *Fmr1* KO cortical astrocytes, a response that was normalized by application of suramin, a nonspecific P2Y antagonist. Likely underpinning these aberrant calcium responses was a heightened expression of P2Y<sub>2</sub> and P2Y<sub>6</sub> receptors in *Fmr1* KO astrocytes, both *in vitro* and in acutely dissociated tissue. Furthermore, exogenous UTP also resulted in aberrant elevations of *Fmr1* KO astrocyte TSP-1 secretion and expression, while *in vivo* quantification demonstrated transient elevations in cortical TSP-1, suggesting that purinergic dysregulation in the *Fmr1* KO cortex may have potential downstream consequences for synaptogenesis. Together, our results suggest that purinergic signalling is elevated in *Fmr1* KO astrocytes, and through its regulation of TSP-1, may warrant further investigation as a promising therapeutic target to correct synaptic abnormalities in FXS.

## 2.8. Materials and Methods

### *Animals*

*Fmr1*<sup>+/+</sup> (WT) and *Fmr1*<sup>-/-</sup> (*Fmr1* KO; FVB.129P2[B6]-*Fmr1*<sup>tm1Cgr</sup>) mice were bred and housed in the McMaster Health Sciences Central Animal Facility until removal at various postnatal developmental time points, including postnatal day (P) 1–3, P7, P14, and P21. All housing conditions and experiments involving mice were approved by the McMaster Animal Ethics Board (Animal Utilization Protocol 17–04-11) and complied with the guidelines and regulations outlined by the Canadian Council on Animal Care.

### *Primary Astrocyte Culture*

Cortical brain tissue was isolated from WT and *Fmr1* KO mice at P1-3, dissociated, and cultured in astrocyte-selective glial media as described by Jacobs and Doering (2009). Briefly, three mice per culture were euthanized by decapitation, and brains were placed into ice-cold calcium- and magnesium-free Hanks' buffered saline solution (Invitrogen, Waltham, MA). Meninges and hippocampi were removed under a Zeiss Stemi SR stereo microscope (Carl Zeiss, Oberkochen, Germany) to isolate the cerebral cortex. Cortical tissue was homogenized in 1 mg/ml DNase (Roche Applied Science) and 0.25% trypsin (Invitrogen) prior to plating in a glial-selective media comprised of minimum essential media (Gibco, Waltham, MA), 10% horse serum (Gibco), and 0.6% D-(+)-glucose (Sigma-Aldrich, St. Louis, MO; Jacobs & Doering, 2009). Primary astrocyte cultures were maintained at 37°C and 5% CO<sub>2</sub> for 6–8 days *in vitro* (DIV). Half media changes took place 24 hr after plating, and every subsequent 2–3 days until astrocytes reached 75–90% confluency.

Once cells reached confluency, they were prepared for calcium imaging, or lifted with 0.05% trypsin-ethylenediaminetetraacetic acid (trypsin–EDTA; Gibco) and re-plated onto 1 mg/ml poly-L-lysine- (PLL; Sigma-Aldrich) and 10 µg/ml laminin- (Invitrogen) coated dishes. Astrocytes intended for astrocyte-conditioned media (ACM) collection

and/or Western blotting were plated onto PLL/laminin-coated 6-well plates (Corning, NY) at a density of 100,000 cells/well, while astrocytes intended for immunocytochemistry were plated onto PLL/laminin-coated 12 mm coverslips (Neuvitro, Vancouver, WA) at a density of 5,000 cells/well. Re-plated cortical astrocyte cultures were maintained for an additional 4.5 DIV at 37°C and 5% CO<sub>2</sub>, and were switched to serum-free media (minimum essential media plus 0.6% D-(+)-glucose) prior to treatment and/or collection to permit the accurate measurement of secreted proteins, following protocols from Krasovska and Doering (2018). Cells were then collected for Western blotting, fixed for immunocytochemistry, or treated for 12 hr with a series of UTP treatments prepared in 0.1 M phosphate-buffered saline (PBS; Life Technologies, Waltham, MA): PBS vehicle, 0.1 μM UTP, 1 μM UTP, 10 μM UTP, or 100μM UTP (ThermoFisher, Waltham, MA).

### ***Calcium Imaging***

Ratiometric Ca<sup>2+</sup> imaging techniques were used to measure changes to intracellular free Ca<sup>2+</sup> concentrations ([Ca<sup>2+</sup>]<sub>i</sub>) in cultured primary astrocytes. Astrocytes were cultured according to techniques described above. Dissociated cells were plated at a density of 5,000 cells/dish onto modified 35 mm culture dishes coated with a thin layer of Matrigel (Collaborative Research, Bedford, MA), and maintained for 6–8 DIV. Astrocyte cultures were then pre-loaded with a fluorescent Ca<sup>2+</sup> indicator, fura-2 AM (2.5 μM; Molecular Probes, Eugene, OR, USA), for 30 min at 37°C. Astrocytes were then continuously perfused with a standard bicarbonate-buffered solution (24 mM NaHCO<sub>3</sub>, 115 mM NaCl, 10 mM glucose, 12 mM sucrose, 5 mM KCl, 2 mM CaCl<sub>2</sub>, 1 mM MgCl<sub>2</sub>) in the presence or absence of the following agents: adenosine triphosphate (ATP; 10 μM; 30 s; Tocris Bioscience, Bristol, UK), UTP (10 μM; 30 s; ThermoFisher), suramin alone (100 μM; 30 s; Tocris Bioscience), or suramin with either ATP or UTP (30 s). All perfusions were performed at room temperature, bubbled with 5% CO<sub>2</sub>, and maintained at an extracellular pH of approximately 7.4. For WT values, each data point represented the averaged responses of 3–6 cells/dish across 4–10 dishes produced by a single primary culture isolated from pups of individual litters (6–7 litters for each experiment were used). For *Fmr1* KO values, each

data point represented the averaged responses of 4–19 cells/dish across 1–5 dishes produced by a single primary culture isolated from pups of different litters (6–10 litters were used for each group/experiment). Specifically, for ATP treatment alone, recordings were taken from 164 primary WT cells (38 dishes) that were produced from seven individual litters ( $n = 7$ ; 22–38 cells/litter); and 118 primary *Fmr1* KO cells (33 dishes) that were produced from 7 litters ( $n = 7$ ; 4–19 cells/litter). For combined ATP and suramin experiments, measurements were acquired from 156 primary WT cells (36 dishes) produced from 6 litters ( $n = 6$ ); and 103 primary *Fmr1* KO cells (25 dishes) produced from 7 litters ( $n = 7$ ). For UTP treatment alone, measurements were taken from 134 primary WT cells (32 dishes) produced from 9 individual litters ( $n = 9$ ); and 75 primary *Fmr1* KO cells (21 dishes) were produced from 6 litters ( $n = 6$ ). For UTP and suramin combined treatment, recordings were acquired from 152 primary WT cells (38 dishes) produced from 10 individual litters ( $n = 10$ ); and 98 primary *Fmr1* KO cells (25 dishes) produced from 7 litters ( $n = 7$ ).

Measurements of  $[Ca^{2+}]_i$  were acquired as previously described by Scott, Zhang, and Nurse (2015). The cells were visualized with a Nikon Eclipse TE2000-U inverted microscope (Nikon, Mississauga, Canada) with a Lambda DG-4 ultra-high-speed wavelength changer (Sutter Instrument Co., Novato, CA, USA), a Hamamatsu OCRCA-ET digital CCD camera (Hamamatsu, Sewickley, PA, USA), and a Nikon S-Fluor 40X oil-immersion objective. Images were acquired simultaneously at 340 nm and 380 nm excitations (510 nm emission) every 2 s, with an exposure time of 100 ms. Ratiometric measurements were collected using Simple PCI software version 5.3 and  $[Ca^{2+}]_i$  was calculated according to the Grynkiewicz equation (described in Grynkiewicz, Poenie, & Tsien, 1985). The concentration of intracellular calcium was expressed as either a total  $[Ca^{2+}]_i$  (cumulative response above baseline) during single drug treatments or an average  $[Ca^{2+}]_i$  (average response above baseline over a specified period of time) when more than one treatment was given during an experiment. Thus, analysis of changes to  $[Ca^{2+}]_i$  for single treatments included parameters such as peak change and duration of response since they were measured from the start of the response until the return to baseline; however,

analysis of the relative changes to ATP/UTP in the presence or absence of suramin was limited to 30 s durations (during treatment) in order to standardize the analysis.

### ***Western Blotting***

Western blotting lysates were prepared from WT and *Fmr1* KO mouse cortex, as well as from WT and *Fmr1* KO primary astrocyte culture and astrocyte-conditioned media. Time points chosen for *in vivo* cortical lysate collection and analysis were P1, P7, P14, and P21, which correspond with peak astrocyte proliferation and synaptogenesis in the mouse cortex (Martynoga, Drechsel, & Guillemot, 2012; Semple, Blomgren, Gimlin, Ferriero, & Noble-Haeusslein, 2013). Acutely dissociated P1 astrocyte-separated cortical tissue was also collected for Western blotting, following magnetic-activated cell sorting protocols described in Wallingford et al. (2017). Briefly, WT and *Fmr1* KO cortical tissue was incubated with a blocking reagent, then with magnetic beads bound to an astrocyte cell surface antigen (ACSA-2) antibody (Miltenyi Biotec, Bergisch Gladbach, Germany). Bound astrocytes were run through a magnetic filtration column to isolate astrocytes from all other cells of the cortex. Finally, to analyze astrocyte-secreted TSP-1 levels, ACM was obtained by incubating confluent astrocytes with fresh serum-free glial media (minimum essential media (Gibco) with 0.6% D-(+)-glucose (Sigma-Aldrich)), then collecting media following 12 hr astrocyte UTP treatment. ACM was filtered using a 0.22 $\mu$ m PES syringe filter (MilliporeSigma, Burlington, MA) and concentrated using a 50 kDa molecular weight cutoff ultrafiltration device (Vivaspin, GE Healthcare, Chicago, IL) to ensure appropriate dilutions for Western blotting, as described in Krasovska and Doering (2018).

For all P2Y Western blots, samples were flash frozen in liquid nitrogen and stored at  $-80^{\circ}\text{C}$  until homogenization, then mechanically homogenized in RIPA lysis buffer (150 mM NaCl, 1% NP-40, 0.5% deoxycholic acid, 1% SDS, 50 mM Tris, Roche ULTRA protease inhibitor, Roche PhoSTOP phosphatase inhibitor) following protocols described in Krasovska and Doering (2018). For all TSP-1 Western blots, 1X Brain Extraction Buffer (25 mM HEPES pH 7.3, 150 mM KCl, 8% glycerol, 0.1% NP-40, Roche ULTRA protease

inhibitor, Roche PhoSTOP phosphatase inhibitor; Vessey et al., 2012) was utilized for homogenization, due to a need for gentler methods to preserve and detect TSP-1.

Prior to Western blotting, total protein levels within each lysate were quantified using a DC protein assay (BioRad, Mississauga, ON, Canada). All Western blotting was performed on precast polyacrylamide TGX Stain-Free 4–12% gradient gels (BioRad), loaded with samples comprised of 30 µg protein lysate in 2.5% β-mercaptoethanol and Laemmli sample buffer (BioRad). Human recombinant TSP-1 protein (0.1 ng; R&D Systems, Minneapolis, MN, USA) was also loaded as a positive control for TSP-1 Western blotting. Following gel electrophoresis, gels were UV activated for 45 s to activate BioRad Stain-Free technology, permitting the visualization of tryptophan amino acids in each sample for use as a “total protein” loading control. After UV activation, proteins were transferred onto polyvinylidene difluoride (PVDF; BioRad) membranes using the TransBlot Turbo system (BioRad), then membranes were imaged to quantify loading controls for densitometry normalization. Membranes were blocked in 5% non-fat milk prepared in 1X Tris-buffered saline solution with Tween-20 (TBS-T), then incubated overnight in one of the following primary antibodies: P2Y<sub>1</sub> (rabbit polyclonal; 1:200; Alomone Labs, Jerusalem, Israel Cat# APR-009, RRID:AB\_2040070; 66 kDa; Cui et al., 2016), P2Y<sub>2</sub> (rabbit polyclonal; 1:200; Alomone Labs Cat# APR-010, RRID: AB\_2040078; 47 kDa; Cui et al., 2016), P2Y<sub>4</sub> (rabbit polyclonal; 1:200; Alomone Labs Cat# APR-006, RRID:AB\_2040080; 80 kDa), P2Y<sub>6</sub> (rabbit polyclonal; 1:200; Alomone Labs Cat# APR-106, RRID:AB\_2040082; 42 kDa; Vazquez-Cuevas, Zarate-Diaz, Garay, & Arellano, 2010), and TSP-1 (rabbit polyclonal; 1:250; Abcam, Cambridge, UK Cat# ab85762, RRID:AB\_10674322; double band at 155 kDa; Sidoryk-Wegrzynowicz et al., 2017). Following 2 hr secondary antibody incubation (donkey anti-rabbit horseradish peroxidase; 1:2500; GE Healthcare) and development in enhanced chemiluminescence (ECL) substrate (BioRad), membranes were imaged using a ChemiDoc imaging system (BioRad). Bands of interest were quantified using the ImageLab 6.0.1 software (BioRad) and normalized to total protein density, then expressed as fold change relative to mean WT protein levels.

## ***Immunocytochemistry***

Primary astrocyte cultures were processed for immunocytochemistry according to previously reported protocols in Krasovska and Doering (2018). Astrocytes, grown on 12 mm PLL/laminin-coated coverslips prior to immunocytochemistry, were fixed in 4% paraformaldehyde (Sigma-Aldrich), permeabilized with 0.1% Triton X-100 (BDH Chemicals, Radnor, PA), blocked in 1% bovine serum albumin (BSA; Sigma-Aldrich), and incubated in primary antibody overnight at 4°C. The following primary antibodies, diluted in PBS, were utilized: P2Y<sub>1</sub> (rabbit polyclonal; 1:200; Alomone Labs, Jerusalem, Israel Cat# APR-009, RRID:AB\_2040070; Filippov, Choi, Simon, Barnard, & Brown, 2006), P2Y<sub>2</sub> (rabbit polyclonal; 1:200; Alomone Labs Cat# APR-010, RRID:AB\_2040078; Choi et al., 2013), P2Y<sub>4</sub> (rabbit polyclonal; 1:200; Alomone Labs Cat# APR-006, RRID:AB\_2040080; Certal et al., 2015), P2Y<sub>6</sub> (rabbit polyclonal; 1:200; Alomone Labs Cat# APR-106, RRID:AB\_2040082; Apolloni et al., 2010), TSP-1 (mouse monoclonal; 1:100; Thermo Fisher Scientific Cat# MA5-13398, RRID:AB\_10984611; Kim et al., 2016) and glial fibrillary acidic protein (GFAP; chicken polyclonal; 1:1000; OriGene, Rockville, MD, USA Cat# TA309150). Following primary antibody incubation, the following secondary antibodies, diluted in PBS, were applied at room temperature: donkey anti-rabbit AlexaFluor 568 (1:200; Invitrogen Cat# A10042), donkey anti-mouse AlexaFluor 594 (1:500; Invitrogen Cat# A21203) and/or donkey anti-chicken fluorescein isothiocyanate (FITC; 1:100; Jackson ImmunoResearch, West Grove, PA, USA Cat# 703-095-155). Coverslips were mounted onto slides using ProlongGold antifade mounting medium plus 40,6-diamidino-2-phenylindole (DAPI) nuclear stain (Invitrogen). All cells were imaged at 20X objective magnification using a Zeiss Axio Imager.M2 epifluorescent microscope (Carl Zeiss), Axiocam 506 camera (Carl Zeiss), and ZEN Blue (Carl Zeiss) acquisition software.

### *Image Analysis*

Images of TSP-1- and P2Y-labelled primary cortical astrocytes were analyzed for intracellular distribution and staining intensity using ImageJ software (National Institutes of Health, Bethesda, MD, USA). Intensity measurements were averaged across three regions of interest per astrocyte. Regions of interest (ROI) were 5  $\mu\text{m}$  thick and spanned the entire length of the astrocyte process, beginning from the outer edge of the nucleus. Each intensity measurement for each region of interest was normalized to the background fluorescence intensity of an adjacent area outside the cell. Mean intensities were compiled by measuring 3–4 astrocytes per sample, across eight separate coverslips (n) prepared from four individual litters, for a total of 24–30 astrocytes measured per experimental condition.

TSP-1-positive astrocytes in 100  $\mu\text{M}$  UTP- and vehicle-treated conditions were assessed for GFAP positivity, cell death, and size to ensure that UTP treatment did not negatively impact astrocyte health. Differentiated astrocytes were identified as those staining positively for GFAP. Cells with an absence of GFAP staining, indicating possible non-astrocytic identity, were noted in GFAP analyses in order to determine the percentage of GFAP-positive cells, but were excluded from TSP-1 cell death and morphology analyses. Additionally, a minimal number of astrocytes visibly expressed intense levels of GFAP staining. These cells were similarly noted as not belonging to the GFAP-positive percentage of healthy, quantified astrocytes (Figure S1b), and were also excluded from cell death and morphology analyses due to the likelihood that these cells possessed a highly reactive astrocyte phenotype. Cell death rates were compared between genotypes and treatment conditions by counting GFAP-positive cells which displayed apoptotic condensed or fragmented nuclei vs. healthy nuclei, visualized using DAPI nuclear staining. To assess GFAP staining and cell death, three distinct fields of view within a single coverslip were counted by a blinded observer at 10X objective magnification and averaged to form one experimental sample, then repeated over six separate coverslips (n) prepared from three individual litters. Total astrocyte size was measured by tracing outlines of astrocytes imaged at  $\times 20$  objective magnification and calculating the resulting intracellular

area and perimeter using ImageJ software. Mean perimeter and area were compiled by measuring 3–4 astrocytes per sample, across eight separate coverslips (n) prepared from four individual litters, for a total of 24–30 astrocytes measured per experimental condition.

### ***Statistics***

Graphing and statistical analyses were conducted using GraphPad Prism 8.0 software (GraphPad Software, San Diego, CA). All statistical comparisons between two means, including P2Y primary culture and *in vivo* TSP-1 cortical Western blots, were made using unpaired two-tailed t-tests with significance at  $p < .05$ . Statistical comparisons between three or more means, including TSP-1 secretion Western blots and TSP-1 immunostaining intensity analyses, were made using one-way analysis of variance (ANOVA) plus a post-hoc Sidak correction for selected multiple comparisons with significance at  $p < .05$ ; reported statistics are adjusted p values following Sidak correction. When we aimed to determine the relative effect of genotype or drug treatments to a collective data set, as in calcium imaging results, we used two-way ANOVA to determine significant relationships. The robust regression and outlier removal (ROUT) method (Motulsky & Brown, 2006) was utilized to detect and remove data outliers where applicable. All data are represented in dot plots (displaying each n value) with the means  $\pm$  SEM presented unless otherwise indicated.

## 2.9. Results

### *Differentially enhanced $[Ca^{2+}]_i$ in *Fmr1* KO astrocytes following purinergic stimulation*

Purinergic signalling is known to induce intracellular calcium oscillations in astrocytes and lead to astrocyte-mediated neuronal excitation (Shen, Nikolic, Meunier, Pfrieger, & Audinat, 2017). Using ratiometric fura-2  $Ca^{2+}$  imaging, we tested whether the acute application of exogenous ATP (10  $\mu$ M) evoked differential intracellular  $Ca^{2+}$  transients ( $[Ca^{2+}]_i$ ) in WT compared to *Fmr1* KO cultured astrocytes. This concentration of ATP consistently showed changes in  $[Ca^{2+}]_i$  in our preliminary studies using WT astrocytes that promptly recovered and could be repetitively induced without response decay. In Figure 1a, a 30 s ATP exposure led to a significant  $\Delta[Ca^{2+}]_i$  in both WT (n = 6) and *Fmr1* KO (n = 7) astrocytes; however, the magnitude appeared much greater in *Fmr1* KO astrocytes. As illustrated in Figure 1a' and b', it is important to note that fura2 primarily labeled the astrocyte soma (ROI) rather than distal processes, so measurements taken prior to (a') and following (b') ATP application were more representative of slower global cell responses (s–min) than faster local transients (ms). In *Fmr1* KO astrocytes, both the peak of the response (Figure 1b, p = .021) and the duration of response (Figure 1c, p = .011) to ATP were significantly greater than in WT astrocytes. Given the higher mean peak and longer lasting  $[Ca^{2+}]_i$  response in *Fmr1* KO astrocytes, the integrated area representative of the total  $\Delta[Ca^{2+}]_i$  mediated via ATP was approximately three times greater in *Fmr1* KO astrocytes compared to WT (p = .008; Figure 1d).

The increased  $\Delta[Ca^{2+}]_i$  in response to ATP observed in *Fmr1* KO astrocytes was significantly reduced with co-application of suramin, a general purinergic receptor antagonist (Mallard, Marshall, Sithers, & Spriggs, 1992; Figure 2a). For these experiments, we compared the integrated  $\Delta[Ca^{2+}]_i$  in WT (n = 6) and *Fmr1* KO (n = 7) astrocytes for the duration of each application +30 s (1 min total), using the following protocol: 30 s ATP (10  $\mu$ M), 2–5 min washout, 30 s suramin (100  $\mu$ M), 30 s ATP (10  $\mu$ M) plus suramin (100  $\mu$ M), 2–5 min washout, followed by 30 s ATP (10  $\mu$ M) recovery control. There was a main effect

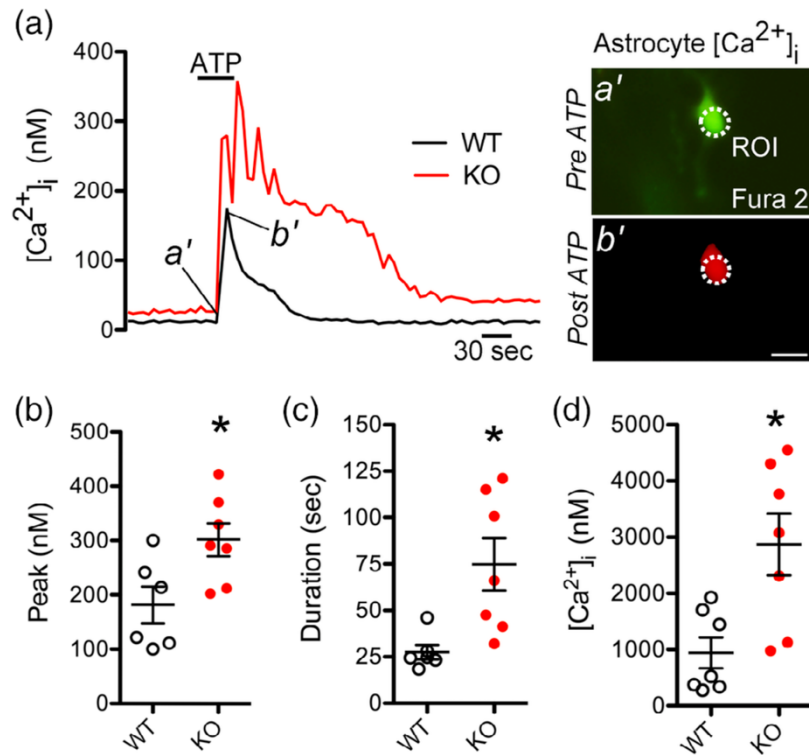


Figure 1. High resolution intracellular calcium recording of primary astrocytes isolated from *Fmr1* KO and WT P1 cortices. (a) Representative traces (left panel) and images (right panel) of intracellular calcium observed in WT (black line) or *Fmr1* KO (red line) astrocytes loaded with fura2 calcium indicator, prior to (a') and following 10  $\mu$ M ATP exposure (30 s; b'). Intracellular calcium response (b) peak, (c) duration, and (d) quantity following 10  $\mu$ M ATP exposure, showing an elevated intracellular calcium response in *Fmr1* KO astrocytes relative to WT (n = 7). Data presented as means  $\pm$  SEM. \*, significant differences between WT and *Fmr1* KO, p < .05. Scale bar: 50  $\mu$ m.

of genotype on integrated  $\Delta[\text{Ca}^{2+}]_i$  responses, with *Fmr1* KO astrocytes being affected by exogenous ATP and suramin to a greater extent ( $p = .04$ ) than WT. This is clearly demonstrated by the selection of random traces presented that were chosen from one culture preparation from each genotype (Figure 2a). As in the previous experiments, pairwise comparisons showed that *Fmr1* KO astrocytes had a significantly greater response to ATP application compared to WT (means of 1799 nm vs. 1002 nm,  $p = .017$ ). Furthermore, responses to ATP were considerably reduced in each genotype with the application of suramin (372.2 nm for KO,  $p < .0001$  and 346.9 nm for WT,  $p < .001$ ; Figure 2b). Notably, the  $\Delta[\text{Ca}^{2+}]_i$  mediated by ATP in combination with suramin did not significantly differ between genotypes, and suramin did not induce any change in  $[\text{Ca}^{2+}]_i$  from baseline in either WT or *Fmr1* KO astrocytes.

Similarly to purines, pyrimidine-mediated stimulation via UTP and uracil-based metabolites also increases  $[\text{Ca}^{2+}]_i$  in astrocytes, but activation is limited to P2Y receptor activity (Ralevic & Burnstock, 1998). In order to further discern the mechanism of differential purinergic signalling in FXS, we tested  $\Delta[\text{Ca}^{2+}]_i$  in primary WT and *Fmr1* KO astrocytes in response to exogenous UTP (10  $\mu\text{M}$ ) application, and to UTP (10  $\mu\text{M}$ ) in the presence of suramin (100  $\mu\text{M}$ ). Similarly to our findings with ATP, UTP-evoked  $\Delta[\text{Ca}^{2+}]_i$  was greater in *Fmr1* KO astrocytes ( $n = 6$ ) than WT ( $n = 6$ ), but this effect was limited to the duration of the response ( $p = .011$ ) and not the peak change ( $p = .967$ ; Figure 2c–e). Responses to UTP were completely inhibited by suramin in both genotypes (Figure 2f; UTP versus UTP + suramin,  $p < .0001$  for both WT and *Fmr1* KO). Notably in Figure 2f, the analysis of  $\Delta[\text{Ca}^{2+}]_i$  was limited to the short duration of treatment application (30 s per treatment), so differences between WT and *Fmr1* KO astrocyte  $\Delta[\text{Ca}^{2+}]_i$  following UTP treatment were not detectable in this analysis.

### ***Elevated P2Y<sub>2</sub> and P2Y<sub>6</sub> receptor expression in Fmr1 KO cortical astrocytes***

Given the clear effects of both ATP and UTP on  $\Delta[\text{Ca}^{2+}]_i$  in astrocytes, and the differential response in those derived from *Fmr1* KO mice, we next tested for possible

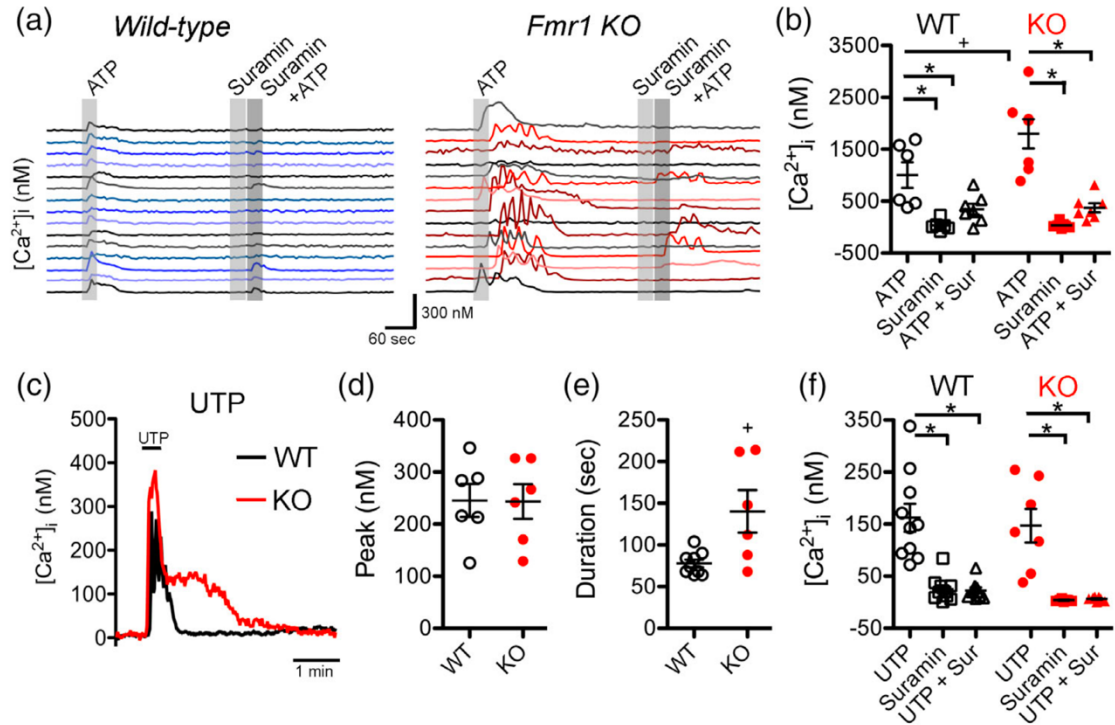


Figure 2. High-resolution intracellular calcium recordings of *Fmr1* KO and WT primary cortical astrocytes following P2Y receptor agonism and antagonism. (a) Representative traces of intracellular calcium observed in WT (left panel) or *Fmr1* KO (right panel) astrocytes loaded with fura2 calcium indicator, following treatment with 10  $\mu$ M ATP (30 s; first shaded area), 100  $\mu$ M suramin (30 s; second shaded area), and 100  $\mu$ M suramin +10  $\mu$ M ATP (30 s; third shaded area). (b) Average intracellular calcium quantities following ATP, suramin, and ATP + suramin application show significant decreases of responses with suramin application in both *Fmr1* KO and WT primary astrocytes. (c) Representative traces of intracellular calcium observed in WT (black line) or *Fmr1* KO (red line) astrocytes loaded with fura2 and treated with 10  $\mu$ M UTP (30 s). Intracellular calcium response (d) peak and (e) duration following 10  $\mu$ M UTP exposure, showing an elevated duration of intracellular calcium response in *Fmr1* KO astrocytes relative to WT (n = 6). Intracellular calcium levels were reduced (f) following suramin and suramin + UTP treatments in both WT and *Fmr1* KO astrocytes. Data presented as means  $\pm$  SEM. \*, significant differences between treatments; +, significant differences between WT and *Fmr1* KO; p < .05.

differences in P2Y receptor expression in WT and *Fmr1* KO cortical astrocytes. Excitatory P2Y<sub>1</sub>, P2Y<sub>2</sub>, P2Y<sub>4</sub>, and P2Y<sub>6</sub> receptors were each highly and consistently expressed in astrocytes of both genotypes, along with numerous other members of the P2Y family (data not shown). P2Y<sub>2</sub> receptors appeared more widely distributed in *Fmr1* KO astrocytes (n = 9, 27 cells) compared to WT (n = 5, 16 cells; Figure 3c), and P2Y<sub>2</sub> receptor expression was significantly greater in the majority of *Fmr1* KO astrocyte cultures (n = 6) compared to low levels of expression in WTs (n = 8, p = .0096; Figure 3d). The expression of the P2Y<sub>6</sub> receptor was also greater in *Fmr1* KO astrocyte cultures (n = 8) than in WT cultures (n = 8, p = .0114; Figure 3h), with a higher intensity of P2Y<sub>6</sub> receptors occurring on the distal portion of the *Fmr1* KO cells (n = 7, 23 cells) compared to WT (n = 6, 18 cells; Figure 3g). In contrast, P2Y<sub>1</sub> receptor distribution was similar between the cultured WT (n = 8, 32 cells) and *Fmr1* KO astrocytes (n = 17, 51 cells; Figure 3a), and protein levels were equally abundant between genotypes (WT, n = 7 and *Fmr1* KO, n = 8; p = .660; Figure 3b). This was also true for the distribution pattern of the P2Y<sub>4</sub> receptor (WT, n = 6, 23 cells; *Fmr1* KO, n = 8, 24 cells), as well as the overall levels of P2Y<sub>4</sub> protein expression in WT (n = 8) and *Fmr1* KO astrocytes (n = 8, p = .220; Figure 3e,f).

Analysis of *in vivo* protein expression of the above P2Y receptors showed that there were no overall differences in receptor abundance between *Fmr1* KO and WT cortical tissue at P1 (data not shown), a time period characterized by abundant gliogenesis and the rapid incorporation of astrocytes into the developing cortex. However, P2Y receptors are widely expressed across many cell-types in the brain (other glial cells, neurons, endothelial cells, *etc.*), so we isolated astrocytes from *Fmr1* KO and WT cortices and compared relative receptor abundance within cortical astrocytes to that found in all other cortical cell-types. Here, we limited our examination to P2Y<sub>2</sub>, P2Y<sub>4</sub>, and P2Y<sub>6</sub> due to their abundance during early cortical development and their relatively high affinity for pyrimidines, which are known to regulate expression and secretion of the synaptogenic protein TSP-1. Interestingly, the relative intensity of each P2Y receptor was significantly higher in astrocytes than in other cell-types isolated from *Fmr1* KO cortices, yet in WT cortices, the density of receptor expression in astrocytes was equivalent to other cell-types. Specifically,

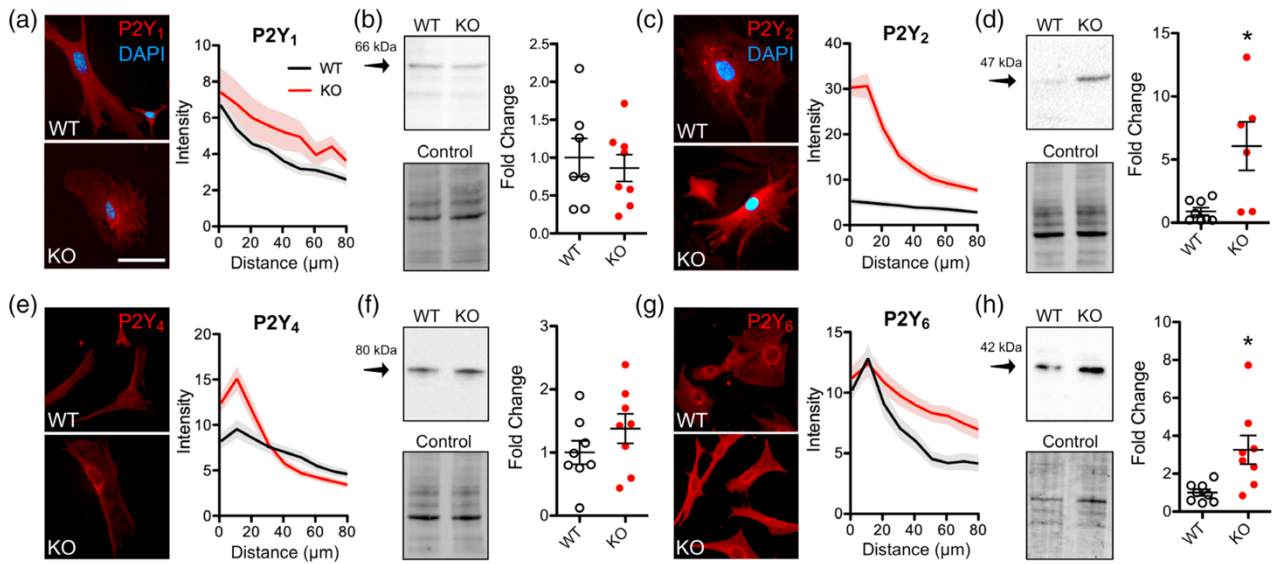


Figure 3. *In vitro* quantitative Western blotting analysis and immunocytochemistry of P2Y receptors in primary astrocytes cultured from P1 WT and *Fmr1* KO cortices. (a, e) Both P2Y<sub>1</sub> and P2Y<sub>4</sub> receptors had similar cellular distribution in WT (n=7) astrocytes as compared to *Fmr1* KO (n=8) (P2Y receptor, red; DAPI, blue). Expression levels of (b) P2Y<sub>1</sub> (66 kDa) and (f) P2Y<sub>4</sub> (80 kDa) were also similar between WT and *Fmr1* KO astrocytes. (c) The P2Y<sub>2</sub> receptor showed significantly greater distribution within *Fmr1* KO astrocytes (n=6; red) over WT (n=7; black), as well as (d) greater quantitative expression (band at 47 kDa). (g) The P2Y<sub>6</sub> receptor also showed greater distribution in the distal portion of *Fmr1* KO astrocytes (n=8) in comparison to WT astrocytes (n=7), and (h) a 2-fold higher quantitative expression (band at 42 kDa). Data presented as means +/- SEM. \*, significant differences between WT and *Fmr1* KO, p<0.05. Scale bar: 50  $\mu$ m.

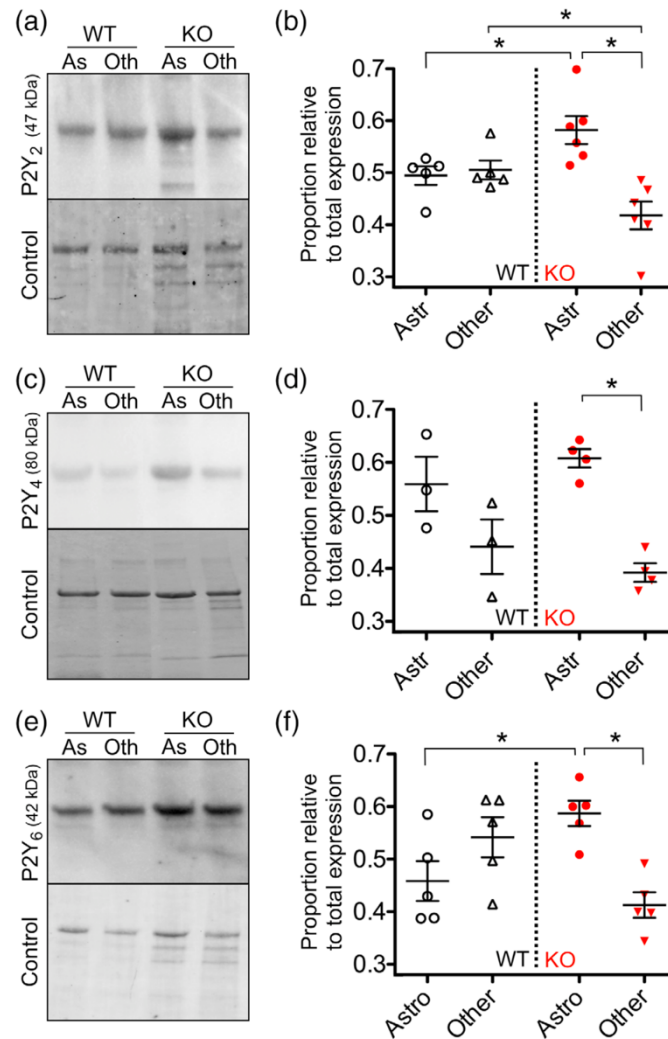


Figure 4. Quantitative protein expression of P2Y receptors in acutely dissociated P1 cortical astrocytes (As) versus astrocyte-depleted fraction of other cells (Oth), isolated via magnetic cell separation. (a,b) The proportion of P2Y<sub>2</sub> receptor expression in *Fmr1* KO cortex (n=6; red) was highest in acutely dissociated astrocytes compared to the paired astrocyte-depleted sample. Equal proportions of P2Y<sub>2</sub> were found in WT acutely dissociated astrocytes compared to the other cell fractions (n=5, black), but each WT fraction (*As* and *Oth*) was significantly different from *Fmr1* KO levels (*Fmr1* KO > WT in *As*; *Fmr1* KO < WT in *Oth*). (c,d) In *Fmr1* KO cortices (n=4), astrocytes made up a much greater proportion of P2Y<sub>4</sub> receptor expression than the other cell fraction, but no differences were evident between WT (n=3) and *Fmr1* KO P2Y<sub>4</sub> expression. (e,f) *Fmr1* KO acutely dissociated astrocytes (n=5) also comprised a greater proportion of P2Y<sub>6</sub> receptor expression compared to the astrocyte-depleted fraction, and possessed a greater proportion of P2Y<sub>6</sub> compared to WT astrocytes (n=5), but no significant differences were observed between cell fractions in WT cortices. Data presented as means +/- SEM. \*, significant differences between groups, p<0.05.

the relative expression of P2Y<sub>2</sub> (Figure 4a,b) showed a greater abundance in *Fmr1* KO astrocytes (n = 6), both compared to other *Fmr1* KO cell-types (p = .0015) and to WT astrocytes (n = 5, p = .029). Notably, there was lower expression of P2Y<sub>2</sub> in *Fmr1* KO non-astrocytic cells compared to WT (p = .0015), demonstrating that dysregulation of P2Y<sub>2</sub> expression in *Fmr1* KO cortices occurs differentially in different cell-types. For P2Y<sub>4</sub>, expression in *Fmr1* KO astrocytes (n = 4) was only greater than in other cell-types of the same genotype (p = .0026), but did not differ from the abundance found in WT astrocytes (n = 3; Figure 4c,d). Similar to P2Y<sub>2</sub>, relative expression of the P2Y<sub>6</sub> receptor was greater in *Fmr1* KO astrocytes (n = 5) compared to other *Fmr1* KO cell-types (p = .0057) and to WT astrocytes (n = 5, p = .0214; Figure 4e,f). For the P2Y<sub>2</sub> and P2Y<sub>6</sub> receptors, there was a statistically significant overall effect of genotype on the relative protein expression in astrocytes (P2Y<sub>2</sub>, p = .018; P2Y<sub>6</sub>, p = .0010) but not for the P2Y<sub>4</sub> receptor.

#### ***Differential regulation of soluble factor TSP-1 in WT and Fmr1 KO cortical astrocytes via P2Y receptors***

To assess the possibility that elevated purinergic signalling in *Fmr1* KO astrocytes might affect neuronal connectivity and activity, we chose to investigate the expression and secretion of astrocyte TSP-1, due to its identity as an astrocyte-secreted synaptogenic protein (Christopherson et al., 2005) and its known regulation by UTP (Tran & Neary, 2006). Following 12 hr application, UTP treatment resulted in contrasting patterns of TSP-1 secretion in WT and *Fmr1* KO astrocytes. While both genotypes secreted approximately the same quantity of TSP-1 following vehicle (PBS) treatment, the level of TSP-1 secretion from *Fmr1* KO astrocytes following 100 µM UTP treatment (n = 4) was significantly greater than from WT (n = 4; p = .0240; Figure 5a). Quantitative analysis demonstrated that TSP-1 secretion from WT astrocytes is normally downregulated following chronic P2Y activation with high levels of UTP (10 µM and 100 µM; n = 4; p = .0159 and p = .0087 respectively; Figure 5b) but not low levels of UTP (0.1 µM and 1 µM; n = 4; p = .9623 and p = .2009 respectively; Figure 5b). In contrast, TSP-1 secretion from *Fmr1* KO astrocytes did not appear to be influenced by either low dose UTP (0.1 µM and 1 µM; n = 5; p = .9546

and  $p = .9614$ , respectively) or high dose UTP application (10  $\mu\text{M}$ :  $n = 5$ ,  $p = .9551$ ; 100  $\mu\text{M}$ :  $n = 4$ ,  $p = .4823$ ; Figure 5c).

Given the differences in the overall UTP-driven TSP-1 secretion by *Fmr1* KO astrocytes in comparison to WT, we also examined the expression and distribution of TSP-1 within cultured astrocytes. Here, we observed that TSP-1 levels in vehicle-treated primary astrocytes were relatively low and largely isolated to the nuclear-adjacent regions of the soma ( $<10 \mu\text{m}$  from nucleus; Figure 6a–c). Similar to observed UTP effects on TSP-1 secretion, treatment with lower UTP concentrations (0.1  $\mu\text{M}$  and 1  $\mu\text{M}$  UTP) had little effect on the mean intensity or distribution of TSP-1 in WT astrocytes ( $n = 8$ ,  $p = .1439$  and  $p = .0903$ , respectively; Figure 6a,d). In contrast, higher concentrations (10  $\mu\text{M}$  and 100  $\mu\text{M}$  UTP) significantly increased the mean intensity of TSP-1 in WT astrocytes ( $p = .0404$  and  $p = .0097$ , respectively; Figure 6a,d). In *Fmr1* KO astrocytes ( $n = 8$ ), however, all doses of UTP led to large increases in the mean intensity of TSP-1 labeling relative to vehicle, regardless of treatment concentration (0.1  $\mu\text{M}$ :  $p = .0047$ ; 1  $\mu\text{M}$ :  $p = .0125$ ; 10  $\mu\text{M}$ :  $p = .0285$ ; 100  $\mu\text{M}$ :  $p = .0204$ ; Figure 6a,e).

A series of control experiments were also conducted to ensure that these results were not due to adverse effects on astrocyte health following UTP treatment. Rates of condensed and fragmented apoptotic nuclei were unchanged between WT and *Fmr1* KO astrocytes ( $n = 6$ ), as well as between vehicle (PBS) and UTP-treated (100  $\mu\text{M}$  UTP) astrocytes of each genotype ( $p = .2415$ ; Figure S1a). Quantification of GFAP immunostaining revealed that the proportion of moderately GFAP-positive astrocytes remained the same between treatment groups and genotypes ( $p = .5079$ ; Figure S1b). Measurements of astrocyte size and shape also indicated that treatment or genotype differences were not associated with differences in the area ( $p = .1168$ ) or perimeter ( $p = .5085$ ) of cultured astrocytes (Figure S1c,d).

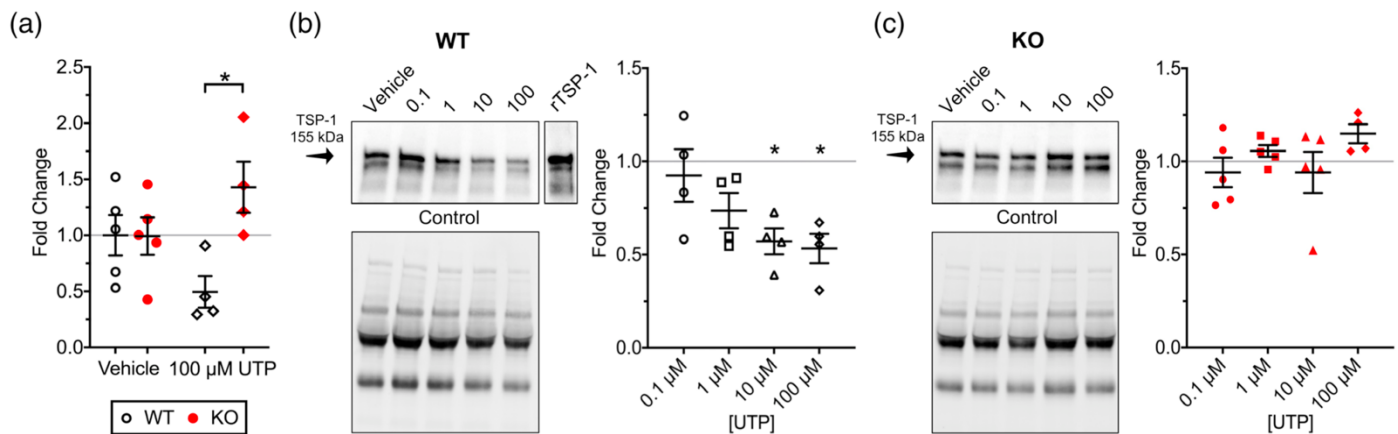


Figure 5. Astrocyte secretion of TSP-1 following 12 h UTP treatment with 0.1  $\mu\text{M}$  UTP, 1  $\mu\text{M}$  UTP, 10  $\mu\text{M}$  UTP, 100  $\mu\text{M}$  UTP or vehicle (PBS). (a) Comparison of TSP-1 secretion between WT ( $n=4$ ) and *Fmr1* KO ( $n=5$ ) astrocytes following 100  $\mu\text{M}$  UTP treatment, relative to WT vehicle, showing increased TSP-1 secretion from *Fmr1* KO astrocytes following high dose UTP treatment. (b) Secretion of TSP-1 from WT astrocytes following UTP treatment, relative to WT vehicle secretion levels. Recombinant human TSP-1 protein (rTSP-1; 0.1 ng) was utilized as a positive control. (c) Secretion of TSP-1 from *Fmr1* KO astrocytes following UTP treatment, relative to *Fmr1* KO vehicle secretion levels. Double bands at 155 kDa normalized to total protein control and expressed as fold change relative to vehicle means; vehicle means denoted by grey vertical lines. Vehicle means denoted by grey horizontal lines. Data presented as means  $\pm$  SEM. \*, significant differences between groups,  $p < 0.05$ .

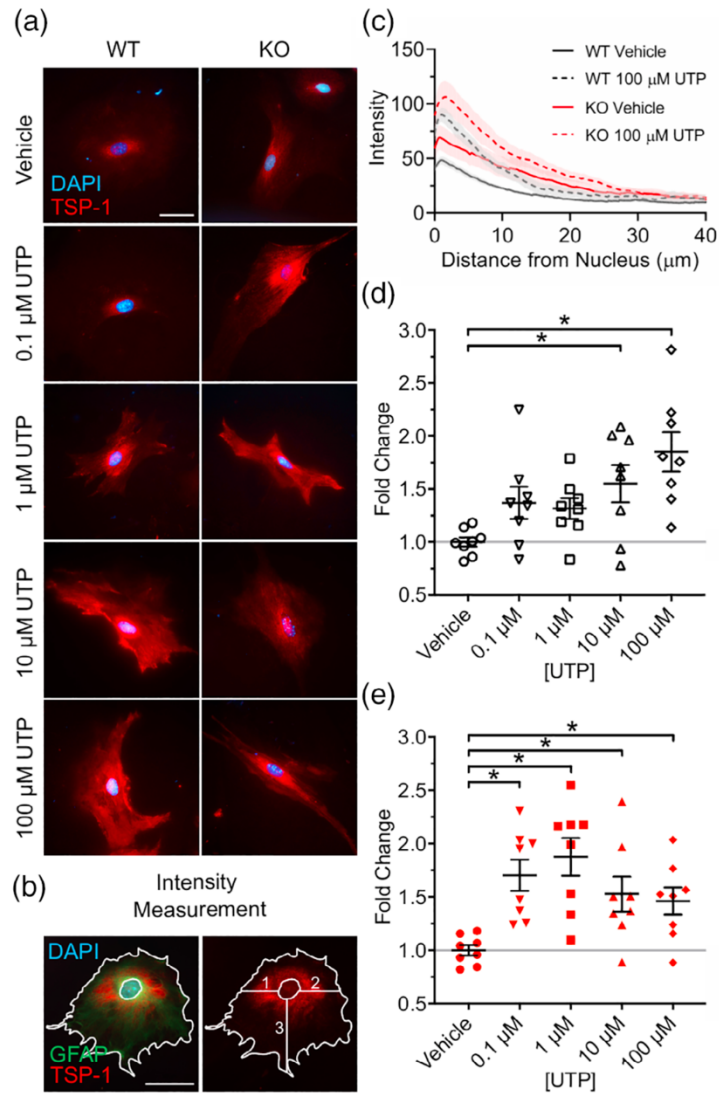


Figure 6. TSP-1 expression in WT and *Fmr1* KO primary astrocyte culture following 12 h UTP treatment with 0.1  $\mu\text{M}$ , 1  $\mu\text{M}$ , 10  $\mu\text{M}$ , 100  $\mu\text{M}$  UTP or vehicle (PBS). (a) Representative images of TSP-1 immunostaining following UTP treatment (TSP-1, red; DAPI, blue). (b) Schematic depicting intensity measurement protocol. Mean intensity of TSP-1 staining was measured from 3 locations per astrocyte, from the edge of the nucleus to the distal border of the astrocyte. (c) Average traces of intensity measurement in WT and *Fmr1* KO vehicle-treated astrocytes vs. astrocytes treated with 100  $\mu\text{M}$  UTP (n=8). (d) Mean WT TSP-1 staining intensity following UTP treatment, relative to vehicle. (e) Mean *Fmr1* KO TSP-1 staining intensity following UTP treatment, relative to vehicle. Vehicle means denoted by grey horizontal lines. Data presented as means  $\pm$  SEM. \*, significant differences between groups,  $p < 0.05$ . Scale bar: 50  $\mu\text{m}$ .

### ***Transiently elevated TSP-1 expression in Fmr1 KO cortex***

The collective findings of increased purinergic receptor expression (P2Y<sub>2</sub> and P2Y<sub>6</sub>), enhanced [Ca<sup>2+</sup>]<sub>i</sub> via purine and pyrimidine stimulation, and elevated TSP-1 following UTP treatment in *Fmr1* KO cortical astrocytes suggest that TSP-1 would be also be elevated in the *Fmr1* KO cortex *in vivo*. To test this, we examined TSP-1 expression within WT and *Fmr1* KO mouse whole cortex across key developmental periods (P1-21), simultaneously capturing both extracellular secreted TSP-1 and astrocyte intracellular TSP-1, as well as any intracellular TSP-1 that might be found in other cortical cell-types. We noted multiple bands in our TSP-1 Western blots, which have also been observed in previous literature (Jana et al., 2018; Smeda et al., 2018) and may be explained by a combination of multiple glycosylation sites on the TSP-1 protein (Hofsteenge et al., 2001) as well as matrix metalloproteinase cleavage of the full-length protein (Jana et al., 2018). Here, we quantified only the TSP-1 band at the predicted molecular weight of 155 kDa (second band from top) but noted that the results were unchanged if these multiple bands were also quantified (data not shown). We observed that TSP-1 expression within the WT cortex was low at P1 (n=7) and at P7 (n=8) but peaked at P14 (n=8) before falling again at P21 (n = 8; Figure 7a–d left lanes). This transient pattern of expression was also observed in the *Fmr1* KO cortex; however, the increase in TSP-1 expression occurred earlier and to a greater extent than in WT cortex. TSP-1 expression at P7 in *Fmr1* KO cortex was significantly greater than in WT cortex at the same age (p = .0049; Figure 7b). Significant differences in TSP-1 expression between genotypes were also observed in the cortex at P14, with *Fmr1* KO TSP-1 expression again greater than WT (p = .0439; Figure 7c). In contrast, there were no differences between WT and *Fmr1* KO cortical TSP-1 expression at P1 (p = .8350; Figure 7a), or at P21 (p = .6231; Figure 7d).

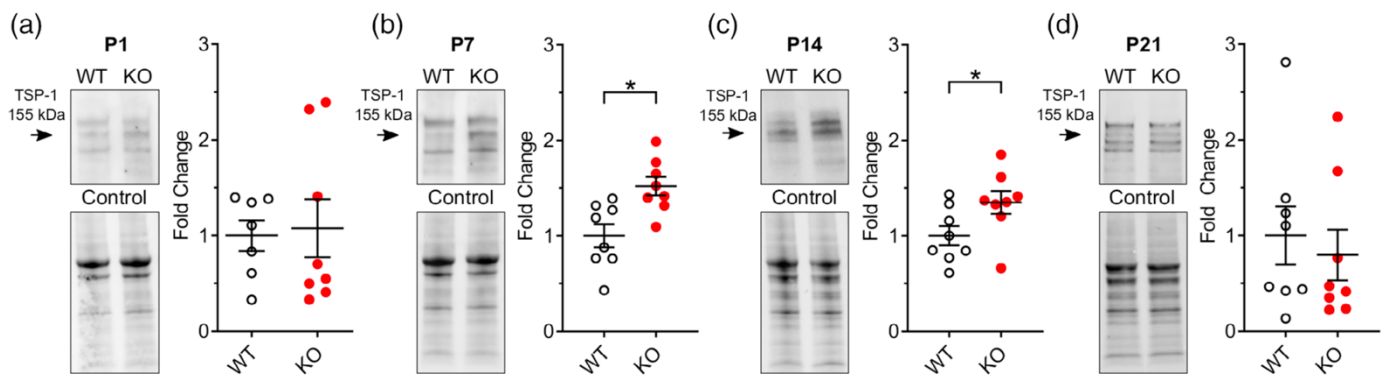


Figure 7. Quantitative Western blotting analysis of TSP-1 expression in WT and *Fmr1* KO cortex, at (a) postnatal day (P) 1, (b) P7, (c) P14, and (d) P21. Bands at 155 kDa (2<sup>nd</sup> band from top) normalized to total protein control; note that results were unchanged if the other visible bands at similar molecular weights, signifying additional post-translational modifications, were also quantified (data not shown). n=8; one outlier removed from P1 WT. Data presented as means  $\pm$  SEM. \*, significant differences between WT and *Fmr1* KO;  $p < 0.05$ .

## 2.10. Discussion

In the developing nervous system, astrocyte health and proper function are required for the formation and maintenance of appropriate connections within the brain. Evidence for astrocyte dysfunction contributing to the pathology of several neurodevelopmental disorders continues to grow, and it appears FXS is no exception. Notably, several studies have shown that synaptic abnormalities, present in both *Fmr1* KO mouse models and FXS patients, can be induced when the loss of FMRP in astrocytes leads to abnormal dendritic growth and aberrant synapse formation in developing neurons; yet, the astrocyte-derived factors impacted by the mutation are largely unknown. Our current findings highlight novel glial interactions in the developing FXS brain that broaden our understanding of the many signalling events at play within FXS, and may provide new ideas for therapeutic approaches. Here, we propose a model of the early postnatal FXS cortex wherein absence of FMRP results in elevated expression of G<sub>q</sub>-coupled astrocyte P2Y<sub>2</sub> and P2Y<sub>6</sub> purinergic receptors, leading to increased mobilization of intracellular calcium stores as well as enhanced expression and release of astrocyte synaptogenic factor TSP-1 (Figure 8). We suggest that this combination of increased intracellular calcium and upregulation of TSP-1 may act to both increase cortical excitation and promote glial-mediated cortical synaptogenesis, thereby potentially contributing, in part, to the altered cortical signalling observed in FXS.

### ***P2Y receptor activation leads to elevated intracellular calcium mobilization in *Fmr1* KO astrocytes***

Purinergic signalling is known to elicit calcium-mediated activation of secondary systems within astrocytes that can lead to a host of downstream effects, including transmitter release, transmitter uptake, and protein expression. Here, we observed increases in the strength and duration of *Fmr1* KO astrocyte intracellular calcium mobilization following treatment with ATP and UTP, displaying increased capacity for excitatory signalling propagation by FXS cells that influences intercellular communication.

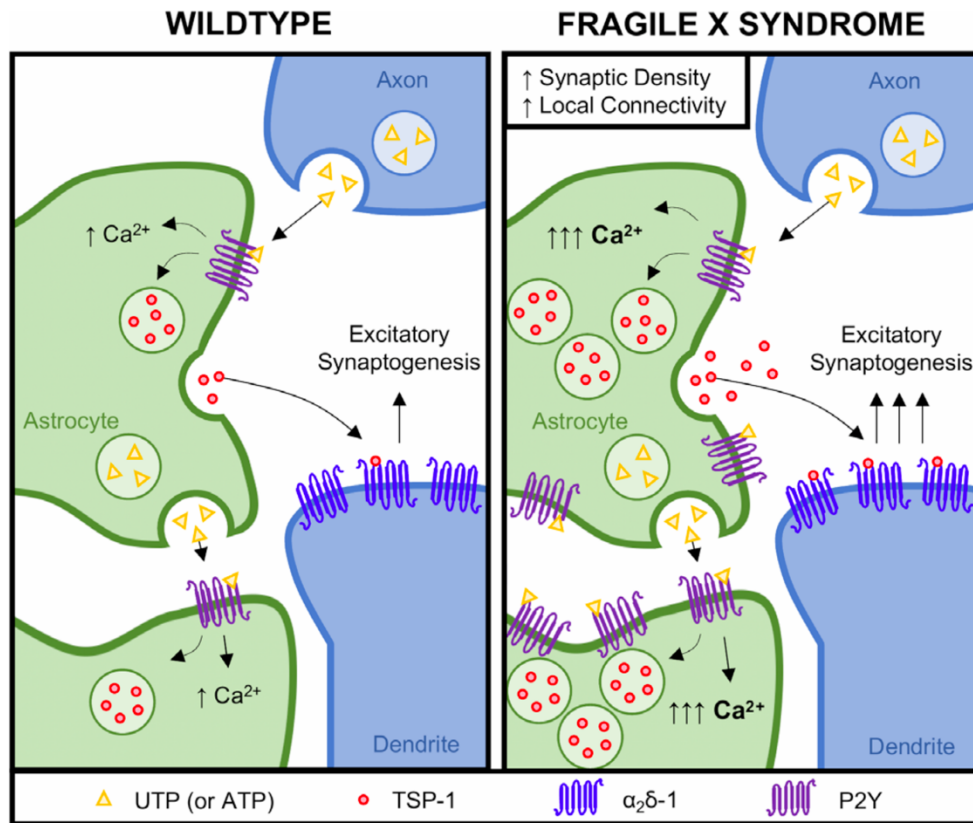


Figure 8. Purinergic signalling is upregulated in early postnatal *Fmr1* KO cortical astrocytes. Schematic demonstrating our findings of increased astrocyte P2Y<sub>2</sub> and P2Y<sub>6</sub> receptor expression (*purple*), permitting elevated ATP- and UTP-driven (*yellow*) intracellular calcium responses and elevating TSP-1 secretion and expression (*red*). We propose that these purinergic signalling aberrations contribute to pathologically increased excitatory signalling in FXS, as heightened TSP-1 binding to neuronal  $\alpha_2\delta-1$  receptors (*blue*) mediates increased excitatory synaptogenesis, and increased P2Y receptor activation promotes phospholipase-C-inositol triphosphate pathways to release intracellular calcium stores, allowing for elevated propagation of glial-glia calcium waves.

In response to basal or pathological excitation, numerous cell-types secrete purinergic ligands, including ATP, UTP, and their metabolites, into the extracellular space. These ligands subsequently bind to a host of purinergic receptors, including G<sub>q</sub>-coupled members of the P2Y family, which trigger activation of the phospholipase C-inositol triphosphate pathway. This pathway releases endoplasmic reticulum-bound intracellular calcium stores, and in turn promotes astrocyte-astrocyte communication via gap junction-mediated calcium waves (reviewed in Erb & Weisman, 2012). Indeed, in primary spinal astrocyte cultures, P2Y<sub>1</sub> and P2Y<sub>2</sub> purinergic receptor activation was required for the propagation of glial calcium waves, with P2Y<sub>2</sub> receptors promoting faster and longer-lasting waves than P2Y<sub>1</sub> (Gallagher & Salter, 2003). During calcium wave propagation, astrocytes also release gliotransmitters including ATP, which bind additional purinergic receptors to further drive signalling (Guthrie et al., 1999). In this way, purine-mediated intracellular calcium mobilization can act widely to influence both astrocyte and neuron communication within the brain, and the potential dysregulation of this signalling system could also lead to widespread pathology.

The aberrant intracellular calcium mobilization we observed here is likely mediated by the increased P2Y<sub>2</sub> and P2Y<sub>6</sub> receptor expression on *Fmr1* KO cortical astrocytes. Firstly, elevated P2Y<sub>2</sub> and P2Y<sub>6</sub> receptor density on the *Fmr1* KO astrocyte cell surface vastly increases the likelihood of receptor-ligand binding to activate calcium release pathways and drive calcium mobilization. Further, the abolishment of ATP- and UTP-driven intracellular calcium mobilization by the general P2 antagonist suramin; the relatively slow timescale of observed effects; and the fact that P2X receptors are largely UTP-insensitive (Ralevic & Burnstock, 1998); confirms that the vast majority of calcium mobilization following agonist application results from activation of UTP-sensitive, G<sub>q</sub>-coupled P2Y receptors. P2Y<sub>2</sub> receptors possess strong and equipotent affinity for both ATP and UTP (Soltoff, Avraham, Avraham, & Cantley, 1998), while P2Y<sub>6</sub> receptors display strong affinity for UDP along with weaker affinity for UTP and ADP (Communi, Parmentier, & Boeynaems, 1996), indicating the potential for both these receptors to contribute to upregulated ATP- or UTP-mediated intracellular calcium release. Given that

P2Y<sub>2</sub> and P2Y<sub>6</sub> were the only UTP-sensitive receptors to show elevated expression in *Fmr1* KO astrocytes, and are both effectively blocked with suramin, we concluded that suramin normalization of calcium signalling in *Fmr1* KO astrocytes must have occurred largely via blockade of these receptors in particular.

Along with astrocyte P2Y expression differences *in vitro*, we observed an increase in the proportion of P2Y<sub>2</sub> and P2Y<sub>6</sub> receptors on acutely dissociated *Fmr1* KO astrocytes, relative to their expression on other cell-types within the brain. This proportional expression was not conserved in WT, suggesting that the early postnatal upregulation of P2Y<sub>2</sub> and P2Y<sub>6</sub> receptors in FXS is primarily astrocyte-specific. It should be noted that these receptor changes were observed very early in cortical development (postnatal days 1–3), so whether they persist for longer periods or are transiently dysregulated during critical formative stages remains unclear. Not only was receptor expression elevated, both *in vitro* and in acutely dissociated *Fmr1* KO astrocytes, but intracellular distribution also differed between genotypes. *In vitro*, all four WT astrocyte P2Y receptors studied were localized in close proximity to the nucleus, consistent with their role in initiating signalling cascades that act on the endoplasmic reticulum. In comparison, *Fmr1* KO astrocyte P2Y<sub>2</sub> and P2Y<sub>6</sub> receptors were not only highly localized to nuclear-adjacent areas but were also abundant in more distal regions. This rise in distal receptor expression suggests that these receptors could more precisely control localized signalling events in FXS, as many G proteins are capable of regulating local membrane excitability or localized mRNA translation to selectively modulate astrocyte-secreted factors in a single distal astrocyte process (reviewed in Tréfier et al., 2018). The additional capacity for local translation, as observed widely in FXS, would increase astrocytes' ability to express and release synaptic factors, thereby upregulating synaptogenesis and plasticity during developmentally sensitive periods.

Enhanced excitatory P2Y receptor expression in the FXS cortex is consistent with previous findings of heightened excitatory signalling and excitation-inhibition imbalances in FXS (Gibson, Bartley, Hays, & Huber, 2008) associated with common symptoms such

as hypersensitivity and seizure activity. Indeed, elevated P2Y<sub>2</sub> receptor expression and increased astrocyte calcium signalling have been reported in other neurodevelopmental disorders with common FXS comorbidity, such as epilepsy. P2Y<sub>1</sub> and P2Y<sub>2</sub> receptors were upregulated in the brains of temporal lobe epilepsy patients (Alves et al., 2017), while patients with focal cortical dysplasia also displayed increased expression of P2Y<sub>1</sub>, P2Y<sub>2</sub>, and P2Y<sub>4</sub> receptors compared to neurotypical controls (Sukigara et al., 2014). However, from these studies, it remains unclear whether receptor upregulation increases seizure activity, or whether purinergic signalling is upregulated in early postnatal *Fmr1* KO cortical astrocytes.

Along with astrocyte P2Y expression differences *in vitro*, we observed an increase in the proportion of P2Y<sub>2</sub> and P2Y<sub>6</sub> receptors on acutely dissociated *Fmr1* KO astrocytes, relative to their expression on other cell-types within the brain. This proportional expression was not conserved in WT, suggesting that the early postnatal seizures lead to heightened P2Y expression. Nevertheless, given the similar characteristics of cortical hyperexcitability and P2Y expression between epilepsy and FXS, as well as their frequent co-occurrence, it is likely that elevated purinergic signalling in the FXS cortex is closely associated with early postnatal pathological functions.

### ***Upregulated P2Y activation increases synaptogenic protein TSP-1 in Fmr1 KO astrocytes***

Excitatory purinergic signalling is likely to act, at least in part, on cortical synaptogenesis by influencing astrocyte TSP-1 expression and secretion. TSP-1 establishes immature excitatory synapses through binding at  $\alpha 2\delta$ -1 neuronal receptors, thereby facilitating postsynaptic recruitment of synaptic adhesion and scaffolding proteins (Eroglu et al., 2009). Purinergic signalling has been shown to regulate TSP-1, as UTP treatment led to increased TSP-1 secretion and expression in WT rat astrocyte primary cultures (Tran & Neary, 2006). Our choice to focus solely on UTP agonism was strengthened by the fact that only a select number of P2Y purinergic receptors are stimulated by UTP/UDP, in contrast

to ATP/ADP, which binds all P2Y receptors in addition to the vast number of P2X receptors (Abbracchio et al., 2009). Here, we observed novel patterns of UTP-driven TSP-1 secretion and expression in *Fmr1* KO cortical astrocytes. TSP-1 secretion in *Fmr1* KO astrocyte culture was unchanged following all UTP doses but was markedly higher than the secretion of WT astrocytes following high doses of UTP, suggesting increased availability of TSP-1 in FXS upon strong local or widespread purinergic agonism. The decreasing TSP-1 secretion pattern observed in WT astrocytes suggests that during normal conditions, TSP-1 secretion is downregulated with high levels of sustained P2Y activation. It is logical that during 12 hr treatments, WT astrocytes modulate their response to purinergic stimulation and engage in compensatory mechanisms that would restrict excess synaptogenesis; however, *Fmr1* KO astrocytes appeared to be delayed in their ability to modulate TSP-1 release and, therefore, continued to release large quantities of TSP-1 following sustained purinergic agonism.

In contrast to TSP-1 secretion, intracellular TSP-1 expression increased in parallel with exogenous UTP concentration in WT astrocytes, and maximal levels were observed in the highest dose treatment group. Comparatively, in *Fmr1* KO astrocytes, both low- and high-dose treatments resulted in maximal intracellular TSP-1 levels. Thus, like WT astrocytes, *Fmr1* KO astrocytes were capable of upregulating TSP-1 expression with P2Y activation but demonstrated elevated levels of sensitivity, potentially as a result of increased receptor availability, ligand availability, or downstream signal transduction pathways. It is likely that purinergic-mediated TSP-1 regulation is largely driven via ERK and Akt phosphorylation and subsequent transcription factor activation. The majority of P2Y receptors have been shown to influence ERK and Akt phosphorylation, and inhibition of either ERK or Akt downregulated the effects of purinergic-driven TSP-1 expression (Tran & Neary, 2006). P2Y<sub>2</sub>, in particular, utilizes phospholipase C to activate protein kinase C to initiate a Ras/Raf/MEK/ERK signal transduction cascade, while many P2Y receptors are also able to trigger PI3K/Akt/mTOR cascades (reviewed in Van Kolen & Slegers, 2006). Other P2 receptors can also utilize the ERK signal transduction cascade to promote synaptic plasticity, as astrocyte P2X receptors have been shown to transiently upregulate cortical

astrocyte expression of P2Y<sub>2</sub> *in vitro* via ERK activation (D'Alimonte et al., 2007). Hyperphosphorylation of both ERK and Akt have been well documented in FXS (Gross et al., 2010; Wang et al., 2012), and pharmacological inhibition of ERK phosphorylation has been shown to have beneficial therapeutic outcomes for individuals with FXS (Pellerin et al., 2016). Heightened ERK and/or Akt phosphorylation in FXS may indeed underlie the TSP-1 expression patterns we observed following purinergic stimulation, whereby the combination of increased P2Y receptor expression, genotypic elevations in phosphorylation, and agonist treatment may aberrantly activate *Fmr1* KO signal transduction pathways to upregulate astrocyte soluble factors such as TSP-1.

We also observed a transient elevation in TSP-1 expression *in vivo* within P7 and P14 *Fmr1* KO cortical tissue. In contrast to primary astrocyte culture, cortical lysates preserve all TSP-1 found within the cortex, including extracellular secreted TSP-1, astrocyte intracellular TSP-1, and any intracellular TSP-1 that might be found in other cortical cell-types. While we cannot definitively rule out that the increases in TSP-1 are associated with expression in other cell-types, TSP-1 is known to be robustly and transiently expressed and secreted by astrocytes but not neurons, and our UTP treatment results indicate the capacity for cortical astrocytes to increase their TSP-1 expression and secretion. It is possible that either a lack of TSP-1 secretion or an excess of astrocyte TSP-1 production could be responsible for our observations of increased TSP-1 in both *Fmr1* KO UTP-treated cultured cortical astrocytes and P7-P14 *Fmr1* KO cortex; however, given our secretion findings, it is more likely that the excess TSP-1 is being actively secreted and utilized than inactively stored intracellularly. This timeframe of elevated *Fmr1* KO cortical TSP-1 is aligned with a critical period in the establishment of cortical synapses (Semple et al., 2013), as well as peak TSP-1 expression in WT cortex (Risher et al., 2018). Indeed, FXS mouse models demonstrate marked synaptic aberrations *in vitro* and *in vivo*, including transiently elevated spine formation and increased density of immature dendritic spines in motor cortex (Hodges et al., 2017). This finding also holds true in human ASD patients, as in post-mortem studies, Hutsler and Zhang (2010) observed greater spine density on superficial cortical pyramidal cells of male ASD brains, and Irwin et al. (2001) reported

elevated density of both immature and distal dendritic spines in pyramidal neurons within temporal and visual cortices of FXS males.

Elevations in secreted proteins are one of many ways by which astrocytes can promote connectivity, and TSP-1 is not the first astrocyte-secreted synaptogenic factor to be transiently elevated in FXS. Astrocyte-secreted proteins hevin and SPARC act antagonistically to modulate pre- and post-synaptic linkage of neurexin-1 $\alpha$  and neuroligin-1B (Kucukdereli et al., 2011; Singh et al., 2016). Expression of pro-synaptogenic hevin was elevated in *Fmr1* KO mouse cortical tissue at P14, while anti-synaptogenic SPARC was reduced in *Fmr1* KO mouse cortical tissue between P7-P14 (Wallingford et al., 2017). These findings were correlated with increased synaptic density in WT cortical and thalamic neurons grown with *Fmr1* KO cortical astrocytes over 14 DIV, relative to WT neurons grown with WT astrocytes (Wallingford et al., 2017). Thus, elevation of TSP-1 during a similar time frame is consistent with a transient overall dysregulation in *Fmr1* KO astrocyte synaptogenic factors, and the combined dysregulation of astrocyte-derived TSP-1, hevin, SPARC, and other yet unidentified factors may potentially contribute to the overall FXS cortical phenotype.

### ***Purinergic signalling influences synaptic transmission***

The effects of elevated purinergic signalling in the *Fmr1* KO cortex may extend beyond calcium wave propagation and TSP-1-mediated synaptogenesis, as the purinergic signalling system also influences transmission at established synapses. For instance, in the prefrontal cortex, ATP is known to trigger astrocyte vesicular glutamate release, which directly acts on neuronal metabotropic mGluR receptors (Wirkner et al., 2007). Meanwhile, expression of the mGluR5 receptor was found to be upregulated in the prefrontal cortex of FXS patients (Lohith et al., 2013), and partial knockout of the gene encoding mGluR5 glutamatergic receptors rescued numerous phenotypes in *Fmr1* KO mice, including aberrant cortical dendritic spine density (Dölen & Bear, 2008). Additionally, the glutamate transporter GLT1, which facilitates reuptake of excess synaptic glutamate following

synaptic release, is dysregulated following astrocyte-selective deletion of FMRP. This selective deletion promotes aberrant spine density and enhanced neuronal excitability, both of which are corrected by upregulating GLT1 expression (Higashimori et al., 2016). Therefore, antagonizing highly expressed astrocyte P2Y<sub>2</sub> and P2Y<sub>6</sub> receptors in FXS could potentially serve a dual therapeutic purpose – namely, reducing pathological glutamate-mediated neuronal excitation in addition to decreasing astrocyte-mediated synaptogenesis.

In this context, it is also important to consider the impact of P2Y<sub>2</sub> and P2Y<sub>6</sub> upregulation and heightened activation on other purinergic receptors. Mobilization of intracellular calcium drives vesicular release of purines, which can further act on both neuronal P2Y and P2X receptors (Ralevic & Burnstock, 1998) to powerfully influence synaptic activity. In addition to the G protein-mediated effects of P2Y receptor activation, fast-acting neuronal P2X receptors promote cationic inward currents and drive excitatory synaptic transmission (Pankratov, Lalo, Krishtal, & Verkhratsky, 2003). Indeed, sustained strong purinergic activation of P2X has been associated with pathological long-term potentiation (reviewed in Lalo, Verkhratsky, Burnstock, & Pankratov, 2012). While G<sub>i</sub>-coupled inhibitory astrocyte P2Y receptors including P2Y<sub>12</sub>, P2Y<sub>13</sub>, and P2Y<sub>14</sub> inhibit cAMP formation to keep excitation in check, the ability of these compensatory mechanisms to prevent excess cortical excitation when the excitatory-inhibitory receptor balance is disrupted remains unclear.

### ***Purinergic signalling influences widespread cellular health and communication***

Aside from the specific trophic effects of purinergic signalling on TSP-1 regulation, it is possible that astrocyte purinergic upregulation in FXS may lead to widespread impacts on cellular health, growth, and plasticity during development. Notably, P2Y activation in rat cortical astrocyte cultures upregulates mRNA encoding brain-derived neurotrophic factor (BDNF; Takasaki et al., 2008), a neurotrophic factor known to promote neuronal growth and synaptogenesis, and drives astrocyte BDNF re-release following endocytosis (Vignoli & Canossa, 2017). Additionally, ATP and UTP can also act in conjunction with

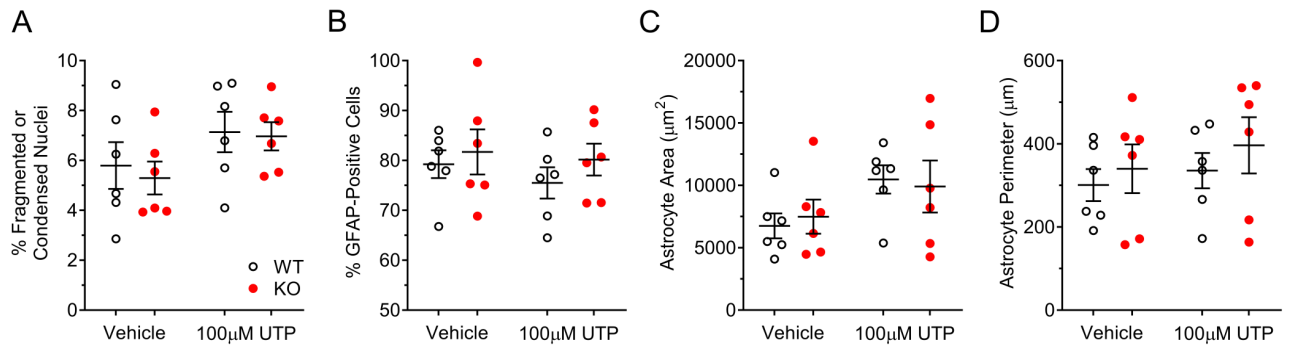
FGF2 to enhance ERK-mediated cyclin A and cyclin D1 expression and then promote FGF2-mediated cell cycle re-entry (Neary, Kang, & Shi, 2005). Perhaps of particular interest for the model proposed here, purinergic receptor stimulation can also transiently remodel the actin cytoskeleton to indirectly modulate synaptic plasticity, given that the creation and maturation of dendritic spines relies on robust actin polymerization (reviewed in Basu & Lamprecht, 2018). In fibroblast cultures, ATP transiently decreased parallel F-actin fiber density, which was inhibited through co-treatment with a  $\text{Ca}^{2+}$ -ATPase pump inhibitor, indicating a role for  $\text{Ca}^{2+}$ -mobilizing P2Y receptors (Goldman, Chandler-Militello, Langevin, Nedergaard, & Takano, 2013). P2Y<sub>2</sub> pre-activation with pro-inflammatory cytokines followed by UTP treatment also led to calcium-dependent cofilin phosphorylation and actin depolymerization in mouse cortical neuron cultures (Peterson et al., 2013). Unsurprisingly, dysregulated actin remodeling is associated with aberrant dendritic spine density within *in vitro* FXS models (Scharkowski, Frotscher, Lutz, Korte, & Michaelson-Preusse, 2017), suggesting that actin remodeling may be another potential mechanism by which astrocyte purinergic signalling elevations impact the FXS cortex. It is, therefore, clear that acute or chronically elevated purinergic signalling may have far-reaching trophic consequences for a host of cellular processes, and that unraveling these complex signal transduction pathways is increasingly important for our understanding of disorders such as FXS.

## **2.11. Perspectives and Significance**

Our findings demonstrating *Fmr1* KO astrocyte purinergic dysregulation have notable clinical relevance for FXS, as well as, more broadly, for ASD. Here, normalization of transiently elevated *Fmr1* KO astrocyte intracellular calcium levels by suramin treatment not only confirmed P2Y involvement, but also suggested an underlying mechanism for suramin action in the FXS cortex. Suramin is a nonspecific purinergic antagonist which acts broadly on P2Y<sub>1</sub>, P2Y<sub>2</sub>, P2Y<sub>6</sub>, P2Y<sub>11</sub>, and P2Y<sub>13</sub> receptors (reviewed in von Kugelgen & Hoffmann, 2016), as well as several P2X<sub>7</sub> and ryanodine receptors (Jacobson et al., 2006). The efficacy of suramin for ASD symptom reduction has recently been investigated,

albeit with the goal of reducing purinergic-driven metabolic syndrome (J. C. Naviaux et al., 2014; R. K. Naviaux et al., 2017) rather than correcting aberrant astrocyte P2Y signalling. If elevated purinergic signalling indeed drives pathological cortical excitability in FXS through astrocyte P2Y receptor upregulation and enhanced intracellular calcium mobilization, as we propose, this is consistent with reports of symptomatic improvement in both mice and ASD patients following suramin treatment (J. C. Naviaux et al., 2014; R. K. Naviaux et al., 2017). However, given that the purinergic signalling pathway is both complex and highly expressed throughout the body, systemic and/or long-term delivery of suramin likely remains prone to adverse effects (Arlt, Reincke, Siekmann, Winkelmann, & Allolio, 1994; Kaplan et al., 1987; Rosen et al., 1996). As our results indicate that expression of P2Y<sub>2</sub> and P2Y<sub>6</sub> receptors is elevated in FXS astrocytes, with consequences for calcium signalling and cortical excitation, we suggest that specific antagonism of these receptors may warrant further investigation as potential alternatives for ASD therapeutic development.

In summary, our work identifies novel perturbations to the glial-mediated purinergic signalling system within the *Fmr1* KO mouse cortex. These changes, including increased P2Y<sub>2</sub> and P2Y<sub>6</sub> receptor expression, enhanced mobilization of intracellular calcium stores, and upregulation of the purinergic-regulated synaptogenic protein TSP-1, promote aberrant excitatory astrocyte communication that may, in part, act to influence cortical excitatory synaptogenesis. Our findings are consistent with common hallmarks of FXS pathology, including heightened density of immature dendritic spines, increased local cortical excitation and connectivity, hypersensitivity, and seizure activity. We therefore propose that these elevations in FXS astrocyte purinergic signalling, with particular focus on the increased expression of P2Y<sub>2</sub> and P2Y<sub>6</sub> receptors, may warrant further investigation as a potential therapeutic target for future treatment of FXS.



Supplementary Figure 1. Assessment of astrocyte health following UTP treatment. A. Percentage of fragmented or condensed nuclei in cortical astrocyte culture. B. Quantification of GFAP-positive astrocytes, (C) mean astrocyte area, and (D) mean astrocyte perimeter in cortical astrocyte culture. Data presented as means  $\pm$  SEM; n=6; all results nonsignificant at  $p < 0.05$ .

## 2.12. References

- Abbracchio, M. P., Burnstock, G., Verkhratsky, A., & Zimmermann, H. (2009). Purinergic signalling in the nervous system: An overview. *Trends in Neurosciences*, 32(1), 19–29. <https://doi.org/10.1016/j.tins.2008.10.001>
- Adams, J. B., Audhya, T., McDonough-Means, S., Rubin, R. A., Quig, D., Geis, E., ... Lee, W. (2011). Nutritional and metabolic status of children with autism vs. neurotypical children, and the association with autism severity. *Nutrition & Metabolism (London)*, 8(1), 34. <https://doi.org/10.1186/1743-7075-8-34>
- Alves, M., Gomez-Villafuertes, R., Delanty, N., Farrell, M. A., O'Brien, D. F., Miras-Portugal, M. T., ... Engel, T. (2017). Expression and function of the metabotropic purinergic P2Y receptor family in experimental seizure models and patients with drug-refractory epilepsy. *Epilepsia*, 58 (9), 1603–1614. <https://doi.org/10.1111/epi.13850>
- Apolloni, S., Finocchi, P., D'Agnano, I., Alloisio, S., Nobile, M., D'Ambrosi, N., & Volonte, C. (2010). UDP exerts cytostatic and cytotoxic actions in human neuroblastoma SH-SY5Y cells over-expressing P2Y6 receptor. *Neurochemistry International*, 56(5), 670–678. <https://doi.org/10.1016/j.neuint.2010.02.003>
- Arlt, W., Reincke, M., Siekmann, L., Winkelmann, W., & Allolio, B. (1994). Suramin in adrenocortical cancer: Limited efficacy and serious toxicity. *Clinical Endocrinology*, 41, 299–307.
- Basu, S., & Lamprecht, R. (2018). The role of Actin cytoskeleton in dendritic spines in the maintenance of long-term memory. *Frontiers in Molecular Neuroscience*, 11, 143–143. <https://doi.org/10.3389/fnmol.2018.00143>
- Certal, M., Vinhas, A., Pinheiro, A. R., Ferreirinha, F., Barros-Barbosa, A. R., Silva, I., ... Correia-de-Sa, P. (2015). Calcium signaling and the novel anti-proliferative effect of the UTP-sensitive P2Y11 receptor in rat cardiac myofibroblasts. *Cell Calcium*, 58(5), 518–533. <https://doi.org/10.1016/j.ceca.2015.08.004>
- Cheng, C., Lau, S. K. M., & Doering, L. C. (2016). Astrocyte-secreted thrombospondin-1 modulates synapse and spine defects in the Fragile X mouse model. *Molecular Brain*, 9(1), 74. <https://doi.org/10.1186/s13041-016-0256-9>

- Choi, R. C., Chu, G. K., Siow, N. L., Yung, A. W., Yung, L. Y., Lee, P. S., ... Tsim, K. W. (2013). Activation of UTP-sensitive P2Y2 receptor induces the expression of cholinergic genes in cultured cortical neurons: A signaling cascade triggered by Ca<sup>2+</sup> mobilization and extracellular regulated kinase phosphorylation. *Molecular Pharmacology*, 84(1), 50–61. <https://doi.org/10.1124/mol.112.084160>
- Christopherson, K. S., Ullian, E. M., Stokes, C. C., Mallowney, C. E., Hell, J. W., Agah, A., ... Barres, B. A. (2005). Thrombospondins are astrocyte-secreted proteins that promote CNS synaptogenesis. *Cell*, 120(3), 421–433. <https://doi.org/10.1016/j.cell.2004.12.020>
- Communi, D., Parmentier, M., & Boeynaems, J.-M. (1996). Cloning, functional expression and tissue distribution of the human P2Y6 receptor. *Biochemical and Biophysical Research Communications*, 222(2), 303–308. <https://doi.org/10.1006/bbrc.1996.0739>
- Cui, J. D., Xu, M. L., Liu, E. Y. L., Dong, T. T. X., Lin, H. Q., Tsim, K. W. K., & Bi, C. W. C. (2016). Expression of globular form acetylcholinesterase is not altered in P2Y1R knock-out mouse brain. *Chemico-Biological Interactions*, 259 (Pt B), 291–294. <https://doi.org/10.1016/j.cbi.2016.06.028>
- D'Alimonte, I., Ciccarelli, R., Diiorio, P., Nargi, E., Buccella, S., Giuliani, P., ... Ballerini, P. (2007). Activation of P2X7 receptors stimulates the expression of P2Y2 receptor mRNA in astrocytes cultured from rat brain. *International Journal of Immunopathology and Pharmacology*, 20 (2), 301–316. <https://doi.org/10.1177/039463200702000210>
- Dölen, G., & Bear, M. F. (2008). Role for metabotropic glutamate receptor 5 (mGluR5) in the pathogenesis of Fragile X syndrome. *The Journal of Physiology*, 586(6), 1503–1508. <https://doi.org/10.1113/jphysiol.2008.150722>
- Erb, L., & Weisman, G. A. (2012). Coupling of P2Y receptors to G proteins and other signaling pathways. *Wiley Interdisciplinary Reviews: Membrane Transport and Signaling*, 1(6), 789–803. <https://doi.org/10.1002/wmts.62>
- Eroglu, C., Allen, N. J., Susman, M. W., O'Rourke, N. A., Park, C. Y., Ozkan, E., ... Barres, B. A. (2009). Gabapentin receptor alpha2delta-1 is a neuronal thrombospondin receptor responsible for excitatory CNS synaptogenesis. *Cell*, 139(2), 380–392. <https://doi.org/10.1016/j.cell.2009.09.025>
- Filippov, A. K., Choi, R. C., Simon, J., Barnard, E. A., & Brown, D. A. (2006). Activation of P2Y1 nucleotide receptors induces inhibition of the M-type K<sup>+</sup> current in rat hippocampal pyramidal neurons. *The Journal of Neuroscience*, 26(36), 9340–9348. <https://doi.org/10.1523/JNEUROSCI.2635-06.2006>

- Gallagher, C. J., & Salter, M. W. (2003). Differential properties of astrocyte calcium waves mediated by P2Y1 and P2Y2 receptors. *The Journal of Neuroscience*, 23(17), 6728–6739. <https://doi.org/10.1523/jneurosci.23-17-06728.2003>
- Galvez, R., Gopal, A. R., & Greenough, W. T. (2003). Somatosensory cortical barrel dendritic abnormalities in a mouse model of the Fragile X mental retardation syndrome. *Brain Research*, 971(1), 83–89. [https://doi.org/10.1016/s0006-8993\(03\)02363-1](https://doi.org/10.1016/s0006-8993(03)02363-1)
- Gibson, J. R., Bartley, A. F., Hays, S. A., & Huber, K. M. (2008). Imbalance of neocortical excitation and inhibition and altered UP states reflect network hyperexcitability in the mouse model of Fragile X syndrome. *Journal of Neurophysiology*, 100(5), 2615–2626. <https://doi.org/10.1152/jn.90752.2008>
- Goldman, N., Chandler-Militello, D., Langevin, H. M., Nedergaard, M., & Takano, T. (2013). Purine receptor mediated Actin cytoskeleton remodeling of human fibroblasts. *Cell Calcium*, 53(4), 297–301. <https://doi.org/10.1016/j.ceca.2013.01.004>
- Gross, C., Nakamoto, M., Yao, X., Chan, C.-B., Yim, S. Y., Ye, K., ... Bassell, G. J. (2010). Excess phosphoinositide 3-kinase subunit synthesis and activity as a novel therapeutic target in Fragile X syndrome. *The Journal of Neuroscience*, 30(32), 10624–10638. <https://doi.org/10.1523/jneurosci.0402-10.2010>
- Grossman, A. W., Elisseou, N. M., McKinney, B. C., & Greenough, W. T. (2006). Hippocampal pyramidal cells in adult *Fmr1* knockout mice exhibit an immature-appearing profile of dendritic spines. *Brain Research*, 1084(1), 158–164. <https://doi.org/10.1016/j.brainres.2006.02.044>
- Grynkiewicz, G., Poenie, M., & Tsien, R. Y. (1985). A new generation of Ca<sup>2+</sup> indicators with greatly improved fluorescence properties. *Journal of Biological Chemistry*, 260(6), 3440–3450.
- Guthrie, P. B., Knappenberger, J., Segal, M., Bennett, M. V., Charles, A. C., & Kater, S. B. (1999). ATP released from astrocytes mediates glial calcium waves. *The Journal of Neuroscience*, 19(2), 520–528. <https://doi.org/10.1523/jneurosci.19-02-00520.1999>
- Higashimori, H., Schin, C. S., Chiang, M. S., Morel, L., Shoneye, T. A., Nelson, D. L., & Yang, Y. (2016). Selective deletion of Astroglial FMRP Dysregulates glutamate transporter GLT1 and contributes to Fragile X syndrome phenotypes *in vivo*. *The Journal of Neuroscience*, 36(27), 7079–7094. <https://doi.org/10.1523/jneurosci.1069-16.2016>

- Hodges, J. L., Yu, X., Gilmore, A., Bennett, H., Tjia, M., Perna, J. F., ... Zuo, Y. (2017). Astrocytic contributions to synaptic and learning abnormalities in a mouse model of Fragile X syndrome. *Biological Psychiatry*, 82(2), 139–149. <https://doi.org/10.1016/j.biopsych.2016.08.036>
- Hofsteenge, J., Huwiler, K. G., Macek, B., Hess, D., Lawler, J., Mosher, D. F., & Peter-Katalinic, J. (2001). C-mannosylation and O-fucosylation of the thrombospondin type 1 module. *The Journal of Biological Chemistry*, 276(9), 6485–6498. <https://doi.org/10.1074/jbc.M008073200>
- Hutsler, J. J., & Zhang, H. (2010). Increased dendritic spine densities on cortical projection neurons in autism spectrum disorders. *Brain Research*, 1309, 83–94. <https://doi.org/10.1016/j.brainres.2009.09.120>
- Irwin, S. A., Patel, B., Idupulapati, M., Harris, J. B., Crisostomo, R. A., Larsen, B. P., ... Greenough, W. T. (2001). Abnormal dendritic spine characteristics in the temporal and visual cortices of patients with Fragile-X syndrome: A quantitative examination. *American Journal of Medical Genetics*, 98(2), 161–167. [https://doi.org/10.1002/10968628\(20010115\)98:2<161::Aid-ajmg1025>3.0.Co;2-b](https://doi.org/10.1002/10968628(20010115)98:2<161::Aid-ajmg1025>3.0.Co;2-b)
- Jacobs, S., & Doering, L. C. (2009). Primary dissociated astrocyte and neuron co-culture. In L. C. Doering (Ed.), *Protocols for Neural Cell Culture* (4th ed., pp. 269–284). New York, NY: Humana.
- Jacobs, S., & Doering, L. C. (2010). Astrocytes prevent abnormal neuronal development in the Fragile X mouse. *The Journal of Neuroscience*, 30 (12), 4508–4514. <https://doi.org/10.1523/jneurosci.5027-09.2010>
- Jacobson, K. A., Costanzi, S., Joshi, B. V., Besada, P., Shin, D. H., Ko, H., ... Mamedova, L. (2006). Agonists and antagonists for P2 receptors. *Novartis Foundation Symposium*, 276, 58–281. <https://doi.org/10.1002/9780470032244.ch6>
- Jana, S., Zhang, H., Lopaschuk, G. D., Freed, D. H., Sergi, C., Kantor, P. F., ... Kassiri, Z. (2018). Disparate remodeling of the extracellular matrix and proteoglycans in failing pediatric versus adult hearts. *Journal of the American Heart Association*, 7(19), e010427–e010427. <https://doi.org/10.1161/JAHA.118.010427>
- Kaplan, L. D., Wolfe, P. R., Volberding, P. A., Feorino, P., Levy, J. A., Abrams, D. I., ... Gottlieb, M. S. (1987). Lack of response to suramin in patients with AIDS and AIDS-related complex. *The American Journal of Medicine*, 82, 615–620.

- Kim, S. K., Hayashi, H., Ishikawa, T., Shibata, K., Shigetomi, E., Shinozaki, Y., ... Nabekura, J. (2016). Cortical astrocytes rewire somatosensory cortical circuits for peripheral neuropathic pain. *The Journal of Clinical Investigation*, 126(5), 1983–1997. <https://doi.org/10.1172/JCI82859>
- Krasovska, V., & Doering, L. C. (2018). Regulation of IL-6 secretion by astrocytes via TLR4 in the Fragile X mouse model. *Frontiers in Molecular Neuroscience*, 11, 272–272. <https://doi.org/10.3389/fnmol.2018.00272>
- Kucukdereli, H., Allen, N. J., Lee, A. T., Feng, A., Ozlu, M. I., Conatser, L. M., ... Eroglu, C. (2011). Control of excitatory CNS synaptogenesis by astrocyte-secreted proteins Hevin and SPARC. *Proceedings of the National Academy of Sciences of the United States of America*, 108(32), E440–E449. <https://doi.org/10.1073/pnas.1104977108>
- Lalo, U., Verkhatsky, A., Burnstock, G., & Pankratov, Y. (2012). P2X receptor-mediated synaptic transmission. *Wiley Interdisciplinary Reviews: Membrane Transport and Signaling*, 1(3), 297–309. <https://doi.org/10.1002/wmts.28>
- Lohith, T. G., Osterweil, E. K., Fujita, M., Jenko, K. J., Bear, M. F., & Innis, R. B. (2013). Is metabotropic glutamate receptor 5 upregulated in prefrontal cortex in Fragile X syndrome? *Molecular Autism*, 4(1), 15. <https://doi.org/10.1186/2040-2392-4-15>
- Mallard, N., Marshall, R., Sithers, A., & Spriggs, B. (1992). Suramin: A selective inhibitor of purinergic neurotransmission in the rat isolated vas deferens. *European Journal of Pharmacology*, 220(1), 1–10. [https://doi.org/10.1016/0014-2999\(92\)90004-N](https://doi.org/10.1016/0014-2999(92)90004-N)
- Martynoga, B., Drechsel, D., & Guillemot, F. (2012). Molecular control of neurogenesis: A view from the mammalian cerebral cortex. *Cold Spring Harbor Perspectives in Biology*, 4(10), a008359. <https://doi.org/10.1101/cshperspect.a008359>
- Motulsky, H. J., & Brown, R. E. (2006). Detecting outliers when fitting data with nonlinear regression - a new method based on robust nonlinear regression and the false discovery rate. *BMC Bioinformatics*, 7, 123. <https://doi.org/10.1186/1471-2105-7-123>
- Naviaux, J. C., Schuchbauer, M. A., Li, K., Wang, L., Risbrough, V. B., Powell, S. B., & Naviaux, R. K. (2014). Reversal of autism-like behaviors and metabolism in adult mice with single-dose antipurinergic therapy. *Translational Psychiatry*, 4, e400. <https://doi.org/10.1038/tp.2014.33>
- Naviaux, R. K., Curtis, B., Li, K., Naviaux, J. C., Bright, A. T., Reiner, G. E., ... Townsend, J. (2017). Low-dose suramin in autism spectrum disorder: A small, phase I/II, randomized clinical trial. *Annals of Clinical Translational Neurology*, 4(7), 491–505. <https://doi.org/10.1002/acn3.424>

- Neary, J. T., Kang, Y., & Shi, Y.-F. (2005). Cell cycle regulation of astrocytes by extracellular nucleotides and fibroblast growth factor-2. *Purinergic Signaling*, 1(4), 329–336. <https://doi.org/10.1007/s11302-0058075-y>
- Olusanya, B. O., Davis, A. C., Wertlieb, D., Boo, N.-Y., Nair, M. K. C., Halpern, R., ... Kassebaum, N. J. (2018). Developmental disabilities among children younger than 5 years in 195 countries and territories, 1990–2016: A systematic analysis for the Global Burden of Disease Study 2016. *The Lancet Global Health*, 6(10), e1100–e1121. [https://doi.org/10.1016/S2214-109X\(18\)30309-7](https://doi.org/10.1016/S2214-109X(18)30309-7)
- Pankratov, Y., Lalo, U., Krishtal, O., & Verkhratsky, A. (2003). P2X receptor-mediated excitatory synaptic currents in somatosensory cortex. *Molecular and Cellular Neurosciences*, 24(3), 842–849. [https://doi.org/10.1016/s1044-7431\(03\)00233-1](https://doi.org/10.1016/s1044-7431(03)00233-1)
- Pellerin, D., Çaku, A., Fradet, M., Bouvier, P., Dubé, J., & Corbin, F. (2016). Lovastatin corrects ERK pathway hyperactivation in Fragile X syndrome: Potential of platelet's signaling cascades as new outcome measures in clinical trials. *Biomarkers*, 21(6), 497–508. <https://doi.org/10.3109/1354750X.2016.1160289>
- Peterson, T. S., Thebeau, C. N., Ajit, D., Camden, J. M., Woods, L. T., Wood, W. G., ... Weisman, G. A. (2013). Up-regulation and activation of the P2Y(2) nucleotide receptor mediate neurite extension in IL-1 $\beta$ -treated mouse primary cortical neurons. *Journal of Neurochemistry*, 125(6), 885–896. <https://doi.org/10.1111/jnc.12252>
- Pieretti, M., Zhang, F. P., Fu, Y. H., Warren, S. T., Oostra, B. A., Caskey, C. T., & Nelson, D. L. (1991). Absence of expression of the FMR-1 gene in Fragile X syndrome. *Cell*, 66(4), 817–822. [https://doi.org/10.1016/0092-8674\(91\)90125-i](https://doi.org/10.1016/0092-8674(91)90125-i)
- Ralevic, V., & Burnstock, G. (1998). Receptors for purines and pyrimidines. *Pharmacological Reviews*, 50(3), 413–492.
- Risher, W. C., Kim, N., Koh, S., Choi, J.-E., Mitev, P., Spence, E. F., ... Eroglu, C. (2018). Thrombospondin receptor  $\alpha 2\delta$ -1 promotes synaptogenesis and spinogenesis via postsynaptic Rac1. *Journal of Cell Biology*, 217(10), 3747–3765. <https://doi.org/10.1083/jcb.201802057>
- Rosen, P. J., Mendoza, E. F., Landaw, E. M., Mondino, B., Graves, M. C., McBride, J. H., ... Belldegrun, A. (1996). Suramin in hormone-refractory metastatic prostate cancer: A drug with limited efficacy. *Journal of Clinical Oncology*, 14(5), 1626–1636.

- Scharkowski, F., Frotscher, M., Lutz, D., Korte, M., & Michaelsen-Preusse, K. (2017). Altered connectivity and synapse maturation of the hippocampal mossy fiber pathway in a mouse model of the Fragile X syndrome. *Cerebral Cortex*, 28(3), 852–867. <https://doi.org/10.1093/cercor/bhw408>
- Scott, A. L., Zhang, M., & Nurse, C. A. (2015). Enhanced BDNF signalling following chronic hypoxia potentiates catecholamine release from cultured rat adrenal chromaffin cells. *The Journal of Physiology*, 593(15), 3281–3299. <https://doi.org/10.1113/jp270725>
- Semple, B. D., Blomgren, K., Gimlin, K., Ferriero, D. M., & Noble-Haeusslein, L. J. (2013). Brain development in rodents and humans: Identifying benchmarks of maturation and vulnerability to injury across species. *Progress in Neurobiology*, 106–107, 1–16. <https://doi.org/10.1016/j.pneurobio.2013.04.001>
- Shen, W., Nikolic, L., Meunier, C., Pfrieger, F., & Audinat, E. (2017). An autocrine purinergic signaling controls astrocyte-induced neuronal excitation. *Scientific Reports*, 7(1), 11280–11280. <https://doi.org/10.1038/s41598-017-11793-x>
- Sidoryk-Wegrzynowicz, M., Gerber, Y. N., Ries, M., Sastre, M., Tolkovsky, A. M., & Spillantini, M. G. (2017). Astrocytes in mouse models of tauopathies acquire early deficits and lose neurosupportive functions. *Acta Neuropathologica Communications*, 5(1), 89. <https://doi.org/10.1186/s40478-017-0478-9>
- Singh, S. K., Stogsdill, J. A., Pulimood, N. S., Dingsdale, H., Kim, Y. H., Pilaz, L. J., ... Eroglu, C. (2016). Astrocytes assemble thalamocortical synapses by bridging NRX1alpha and NL1 via Hevin. *Cell*, 164(1–2), 183–196. <https://doi.org/10.1016/j.cell.2015.11.034>
- Smeda, M., Kieronska, A., Proniewski, B., Jaształ, A., Selmi, A., Wandzel, K., ... Chlopicki, S. (2018). Dual antiplatelet therapy with clopidogrel and aspirin increases mortality in 4T1 metastatic breast cancer-bearing mice by inducing vascular mimicry in primary tumour. *Oncotarget*, 9 (25), 17810–17824. <https://doi.org/10.18632/oncotarget.24891>
- Soltoff, S. P., Avraham, H., Avraham, S., & Cantley, L. C. (1998). Activation of P2Y2 receptors by UTP and ATP stimulates mitogen-activated kinase activity through a pathway that involves related adhesion focal tyrosine kinase and protein kinase C. *The Journal of Biological Chemistry*, 273(5), 2653–2660. <https://doi.org/10.1074/jbc.273.5.2653>

- Sukigara, S., Dai, H., Nabatame, S., Otsuki, T., Hanai, S., Honda, R., ... Itoh, M. (2014). Expression of astrocyte-related receptors in cortical dysplasia with intractable epilepsy. *Journal of Neuropathology and Experimental Neurology*, 73(8), 798–806. <https://doi.org/10.1097/nen>.
- Takasaki, I., Takarada, S., Tatsumi, S., Azegami, A., Yasuda, M., Fukuchi, M., ... Tsuda, M. (2008). Extracellular adenosine 50-triphosphate elicits the expression of brain-derived neurotrophic factor exon IV mRNA in rat astrocytes. *Glia*, 56(13), 1369–1379. <https://doi.org/10.1002/glia.20704>
- Tran, M. D., & Neary, J. T. (2006). Purinergic signaling induces thrombospondin-1 expression in astrocytes. *Proceedings of the National Academy of Sciences of the United States of America*, 103(24), 9321–9326. <https://doi.org/10.1073/pnas.0603146103>
- Tréfier, A., Pellissier, L. P., Musnier, A., Reiter, E., Guillou, F., & Crépieux, P. (2018). G protein-coupled receptors as regulators of localized translation: The forgotten pathway? *Frontiers in Endocrinology*, 9, 17–17. <https://doi.org/10.3389/fendo.2018.00017>
- Van Kolen, K., & Slegers, H. (2006). Integration of P2Y receptor-activated signal transduction pathways in G protein-dependent signalling networks. *Purinergic Signaling*, 2(3), 451–469. <https://doi.org/10.1007/s11302-006-9008-0>
- Vazquez-Cuevas, F. G., Zarate-Diaz, E. P., Garay, E., & Arellano, R. O. (2010). Functional expression and intracellular signaling of UTP-sensitive P2Y receptors in theca-interstitial cells. *Reproductive Biology and Endocrinology*, 8, 88. <https://doi.org/10.1186/1477-78278-88>
- Verma, V., Paul, A., Amrapali Vishwanath, A., Vaidya, B., & Clement, J. P. (2019). Understanding intellectual disability and autism spectrum disorders from common mouse models: Synapses to behaviour. *Open Biology*, 9(6), 180265. <https://doi.org/10.1098/rsob.180265>
- Vessey, J. P., Amadei, G., Burns, S. E., Kiebler, M. A., Kaplan, D. R., & Miller, F. D. (2012). An asymmetrically localized Staufen2-dependent RNA complex regulates maintenance of mammalian neural stem cells. *Cell Stem Cell*, 11(4), 517–528. <https://doi.org/10.1016/j.stem.2012.06.010>
- Vignoli, B., & Canossa, M. (2017). Glioactive ATP controls BDNF recycling in cortical astrocytes. *Communicative & Integrative Biology*, 10(1), e1277296. <https://doi.org/10.1080/19420889.2016.1277296>

- von Kugelgen, I., & Hoffmann, K. (2016). Pharmacology and structure of P2Y receptors. *Neuropharmacology*, 104, 50–61. <https://doi.org/10.1016/j.neuropharm.2015.10.030>
- Wallingford, J., Scott, A. L., Rodrigues, K., & Doering, L. C. (2017). Altered developmental expression of the astrocyte-secreted factors Hevin and SPARC in the Fragile X mouse model. *Frontiers in Molecular Neuroscience*, 10, 268–268. <https://doi.org/10.3389/fnmol.2017.00268>
- Wang, X., Snape, M., Klann, E., Stone, J. G., Singh, A., Petersen, R. B., ... Zhu, X. (2012). Activation of the extracellular signal-regulated kinase pathway contributes to the behavioral deficit of Fragile x-syndrome. *Journal of Neurochemistry*, 121(4), 672–679. <https://doi.org/10.1111/j.1471-4159.2012.07722.x>
- Wirkner, K., Gunther, A., Weber, M., Guzman, S. J., Krause, T., Fuchs, J., ... Illes, P. (2007). Modulation of NMDA receptor current in layer V pyramidal neurons of the rat prefrontal cortex by P2Y receptor activation. *Cerebral Cortex*, 17(3), 621–631. <https://doi.org/10.1093/cercor/bhk012>
- Zoghbi, H. Y., & Bear, M. F. (2012). Synaptic dysfunction in neurodevelopmental disorders associated with autism and intellectual disabilities. *Cold Spring Harbor Perspectives in Biology*, 4(3), a009886. <https://doi.org/10.1101/cshperspect.a009886>

## Chapter Three:

### Dysregulated purinergic signalling molecules in Fragile X mouse cortical astrocytes

#### 3.1. Preface

In the previous chapter, P2Y receptor levels were shown to be elevated in *Fmr1* KO cortical astrocytes. The activity of these overexpressed P2Y receptors, as well as that of P1 and P2X purinergic receptors, is dependent on the secretion of purinergic signalling molecules. Nucleoside triphosphate agonists are released by astrocytes in response to excitation (*e.g.* purinergic-mediated intracellular calcium release) to modulate purinergic receptor activity, and the strength and duration of their action is further controlled by astrocyte membrane-bound CD39 and CD73 ectonucleotidase enzymes that facilitate their extracellular breakdown. This chapter will investigate the relative abundance of *Fmr1* KO versus WT astrocyte purinergic molecules available for secretion, as well as the presence of associated astrocyte-bound ectonucleotidases, in order to elucidate a clearer understanding of astrocyte purinergic signalling dysregulation within the *Fmr1* KO mouse cortex.

#### 3.2. Study Significance

In this work, levels of *Fmr1* KO and WT intracellular nucleoside triphosphates and their metabolites are compared using a novel hydrophilic interaction liquid chromatography (HILIC) method coupled with mass spectrometry. This method provides a new and highly sensitive approach for the quantification of astrocyte intracellular purinergic molecules, while also comparing the amounts of purinergic molecules able to be secreted by *Fmr1* KO versus WT astrocytes. This study demonstrates that the P2Y<sub>6</sub> ligand UDP is substantially more abundant within *Fmr1* KO astrocytes than WTs, while ATP and adenosine are both less abundant; and that breakdown of these nucleoside tri- and diphosphates within the extracellular space may also be elevated due to excess glycosylation of *Fmr1* KO CD39. Overall, this research suggests that the ability of *Fmr1* KO astrocytes to secrete and utilize

purinergic ligands is altered in FXS, thereby affecting the activity of purinergic receptors; and furthermore, that the uridine and adenosine families of purinergic molecules are distinctly dysregulated in *Fmr1* KO astrocytes.

### **3.3. Aims and Hypotheses**

This research was designed to address the first aim of this thesis work:

Aim 1: Establish whether astrocyte purinergic signalling is dysregulated as a result of an absence of FMRP within the *Fmr1* KO mouse cortex.

Hypothesis: Astrocyte purinergic ligands and/or enzymes are differentially expressed in the *Fmr1* KO mouse cortex

### **3.4. Publication Status**

The following manuscript will be submitted to *Purinergic Signaling* following approval from all co-authors. Optimization of protocols to detect secreted purinergic molecules is ongoing, and this data will be included in the final manuscript if optimization can be accomplished in a timely manner.

**Title: Dysregulated purinergic signalling molecules in Fragile X mouse cortical astrocytes**

**Authors:**

Kathryn E. Reynolds<sup>1</sup>, Fan Fei<sup>1,2</sup>, M. Kirk Green<sup>1,2</sup> & Angela L. Scott<sup>1</sup>

1. Department of Pathology and Molecular Medicine, McMaster University, Hamilton, Ontario, Canada
2. McMaster Regional Centre for Mass Spectrometry, McMaster University, Hamilton, Ontario, Canada

**Correspondence:**

Angela L. Scott

Department of Pathology and Molecular Medicine

McMaster University

1200 Main Street West, Hamilton, Ontario L8N 3Z5, Canada.

scottan@mcmaster.ca

**Conflict of Interest:**

None

**3.5. Author Contributions**

This study was designed by K.E. Reynolds and A.L. Scott. K.E. Reynolds, F. Fei, and M.K. Green developed and optimized liquid chromatography/mass spectrometry protocols. K.E. Reynolds performed all experiments and data analysis. The manuscript was written by K.E. Reynolds with editorial assistance from A.L. Scott.

**3.6. Abstract**

The symptoms of the heritable autism spectrum disorder Fragile X syndrome (FXS) have been increasingly linked to disordered astrocyte signalling within the cerebral cortex. We have recently demonstrated that the purinergic signalling pathway, which utilizes nucleoside triphosphates and their metabolites to facilitate bidirectional glial and glial-neuronal interactions, is upregulated in cortical astrocytes derived from the *Fmr1* knockout (KO) model of FXS. Heightened *Fmr1* KO P2Y purinergic receptor levels were correlated with prolonged intracellular calcium release and elevated synaptogenic protein secretion, suggesting that this pathway may drive pathological upregulations in FXS cortical circuitry. However, the levels of purinergic ligands present and able to be secreted to activate these purinergic receptors remains unknown, due in part to a lack of suitably sensitive and reproducible quantification methods. We therefore developed novel hydrophilic interaction liquid chromatography (HILIC) protocols coupled with mass spectrometry to compare the

abundance of intracellular purinergic molecules between wildtype and *Fmr1* KO mouse astrocytes. Significant dysregulations were detected in the levels of UDP, ATP, AMP, and adenosine intracellular stores within *Fmr1* KO astrocytes relative to WT, implying the potential for their dysregulated release or metabolism. Glycosylation of the astrocyte membrane-bound CD39 ectonucleotidase, which facilitates ligand breakdown following synaptic release, was also elevated in *Fmr1* KO astrocyte cultures. Consistent with our previous P2Y receptor characterization, these differences are indicative of a profoundly dysregulated purinergic signalling system within *Fmr1* KO cortical astrocytes, and may lead to significant alterations in FXS purinergic receptor activation.

### **3.7. Introduction**

Affecting approximately 1:4000 males and 1:6000-1:8000 females, Fragile X syndrome (FXS) is the leading monogenic cause of intellectual disability and autism spectrum disorder (ASD) (Turner, Webb, Wake, & Robinson, 1996; Youings et al., 2000). This X-linked dominant syndrome is caused by an expansion of CGG trinucleotide repeats within the *Fmr1* gene, leading to an absence of FMRP RNA-binding protein (Pieretti et al., 1991; Sutcliffe et al., 1992; Verkerk et al., 1991). FMRP regulates the localization and translation of numerous mRNAs with critical roles in brain development (Brown et al., 2001), and its absence leads to widespread increased translation with significant downstream effects, many of which are still being uncovered. Though an absence of FMRP is strongly associated with hyperexcitable cortical circuitry, including symptoms such as sensory hyperresponsivity, attention deficit, hyperactivity, and seizures (Farzin et al., 2006; Musumeci et al., 1999), the precise molecular and cellular mechanisms that underlie this abnormal circuitry remain under investigation.

Recent research from our group and others indicates an emerging role of astrocytes in the pathogenesis of FXS. A lack of astrocyte FMRP has been shown to alter synaptogenic factor expression and release, impair glutamate reuptake, and strongly influence the morphology and activity of wildtype neurons, indicating that astrocytes are powerful

modulators of neural circuitry (Higashimori et al., 2016; Hodges et al., 2017; Jacobs & Doering, 2010; Reynolds, Wong, & Scott, 2021; Wallingford, Scott, Rodrigues, & Doering, 2017). Most recently, we have shown that a lack of FMRP leads to elevated astrocyte purinergic signalling, a pathway that utilizes nucleoside triphosphates and their metabolites to facilitate astrocyte-astrocyte and astrocyte-neuron communication (Abbracchio, Burnstock, Verkhratsky, & Zimmermann, 2009; Reynolds, Wong & Scott, 2021). Numerous purinergic receptors are expressed by astrocytes, and are classified based on their structure and ligand affinity. The P1 subfamily of purinergic receptors consists of metabotropic adenosine receptors, while excitatory ionotropic P2X and metabotropic P2Y receptors are activated by nucleoside di- and triphosphates to increase intracellular calcium levels, thereby facilitating the propagation of astrocyte calcium waves and promoting signal transduction pathway activation (Abbracchio et al., 2009). In response to calcium signalling, astrocytes also release nucleoside triphosphates to further drive the activity of glial and neuronal purinergic receptors (Abbracchio et al., 2009). Using an *Fmr1* knockout (KO) mouse model of FXS, we demonstrated that ATP/UTP-specific P2Y<sub>2</sub> and UDP/UTP-sensitive P2Y<sub>6</sub> receptor levels are elevated in *Fmr1* KO cortical astrocytes, and this was correlated with prolonged upregulation of UTP-evoked *Fmr1* KO astrocyte intracellular calcium as well as increased secretion of the synaptogenic protein TSP-1 (Reynolds et al., 2021). Elevated astrocyte purinergic pathways are therefore capable of upregulating excitatory signalling in both astrocytes and neurons to potentially underlie FXS symptoms.

To fully grasp the degree of purinergic dysregulation in FXS, it is important to also consider the levels of each purinergic ligand available to agonise their respective receptors, as ligand availability may become either a limiting or driving factor that influences receptor stimulation. However, quantification of specific intracellular and secreted purinergic molecules, especially UTP, has traditionally been challenging due to limited sensitive and reproducible methods. As a result, it is currently unclear whether the release of purinergic signalling molecules from FXS astrocytes is altered, and if so, what impact that might have on the stimulation of astrocyte and neuronal purinergic receptors.

The activity of astrocyte-associated enzymes also strongly influences the ability of secreted nucleoside triphosphates to engage in purinergic signalling. The uridine-based signalling molecules utilized by P2Y receptors are generated through a combination of *de novo* synthesis pathways and the action of intracellular kinases, which transfer phosphate residues from ATP to facilitate the creation of UMP, UDP, and UTP (Dobolyi, Juhasz, Kovacs, & Kardos, 2011). Following their secretion, purinergic signalling molecules are rapidly broken down by ectonucleotidase enzymes to limit their action, and ultimately taken back up by astrocyte nucleoside transporters to facilitate their recycling and re-release. Extracellular ATP and UTP are rapidly hydrolyzed to their di- and monophosphate forms by the glial membrane-bound ectonucleoside triphosphate diphosphohydrolase enzyme CD39, while CD73, or ecto-5'-nucleotidase, removes single phosphates from AMP and UMP to produce adenosine and uridine (Dobolyi et al., 2011; Zimmermann, 1996). The action of ectonucleotidases thereby modulates the duration of purinergic agonism at P2X and P2Y receptors, while also controlling the availability of adenosine to facilitate P1 receptor activity. While these membrane-bound ectonucleotidases are known to be expressed on the surface of rodent astrocytes (Lie et al., 1999; Wink et al., 2003), their abundance and activity have not been investigated in relation to FXS. Characterizing potential differences in astrocyte-bound CD39 and CD73 will therefore be important in order to fully understand the purinergic signalling dysregulations occurring in FXS.

While our previous work has shown increased expression of FXS cortical astrocyte P2Y receptors, the availability of secreted purinergic ligands to activate these receptors remains unknown. We therefore developed novel hydrophilic interaction liquid chromatography (HILIC) protocols coupled with mass spectrometry, the current gold standard method for nucleoside detection, in order to compare the abundance of intracellular purinergic molecules between wildtype and *Fmr1* KO mouse astrocytes and thereby suggesting their capacity for purinergic release. We also investigated levels of astrocyte-bound CD39 and CD73 ectonucleotidases responsible for the extracellular metabolism of ATP and UTP to further characterize dysregulations in FXS astrocyte purinergic signalling.

### 3.8. Methods

**Animals.** Two genotypes of mice, wildtype (WT) and *Fmr1*<sup>-/-</sup> (Fmr1 KO; FVB.129P2[B6]-*Fmr1*<sup>tm1Cgr</sup>), were bred and housed at the McMaster Health Sciences Central Animal Facility. All mouse housing, handling, and euthanization protocols followed the standards set by the Canadian Council on Animal Care and were authorized by the McMaster Animal Ethics Board (Animal Utilization Protocol 17-04-11). Pups of both sexes were euthanized by decapitation at postnatal day (P) 1-3 for astrocyte dissection and primary culture.

**Primary Astrocyte Culture.** WT and *Fmr1* KO primary cortical astrocyte cultures were prepared and maintained following protocols described by Jacobs and Doering (2009). Six cortical hemispheres, obtained from three P1-3 mouse pups, were pooled per genotype to form a single primary culture. Cells of the developing cerebral cortex were isolated by removing the hippocampus and meninges from each cortical hemisphere under a Zeiss Stemi SR stereo microscope (Carl Zeiss, Oberkochen, Germany), then dissociating cortical tissue in ice-cold Hanks' buffered saline solution (HBSS; Invitrogen, Waltham, MA, USA) with 1 mg/mL DNase (Roche Applied Science) and 0.25% trypsin (Invitrogen). Cells were plated in a glial-selective medium consisting of minimum essential medium (Gibco, Waltham, MA, USA) supplemented with 10% horse serum (Gibco) and 0.6% D-(+)-glucose (Sigma-Aldrich, St. Louis, MO, USA), and were maintained in a humidified incubator at 37°C and 5% CO<sub>2</sub> (NuAire, Plymouth, MN, USA). Primary cultures received half media changes every 2-3 days, starting at 24h post-dissection, until cells were 75-90% confluent (~6-8 days).

**Liquid Chromatography/Mass Spectrometry Sample Preparation.** After reaching 75-90% confluence, primary astrocyte cultures intended for liquid chromatography/mass spectrometry (LC/MS) were lifted with 0.05% trypsin-ethylenediaminetetraacetic acid (trypsin-EDTA; Gibco) for reseeding. Astrocytes were reseeded in six-well plates (Corning, NY, USA) pre-coated with 1 mg/mL poly-L-lysine (Sigma-Aldrich) and 10 µg/mL laminin (Invitrogen), at a density of 85 000 cells/well. After 24h, glial media was

replaced with a serum-free glial media comprised of minimum essential media (Gibco) plus 0.6% D-(+)-glucose (Sigma-Aldrich), then cultures were maintained at 37°C and 5% CO<sub>2</sub> for an additional 48h.

For sample collection, plates were placed on ice and washed 2x with ice-cold phosphate buffered saline (Gibco, Waltham, MA, USA) to halt ectonucleotidase activity. Astrocytes intended for LC/MS were mechanically lifted with a cell scraper (Corning) in 500 µL ice-cold LC/MS-grade methanol (Fisher Scientific, Waltham, MA, USA), while those intended for representative cell counts were lifted with 0.05% trypsin-EDTA. All six wells per plate were collected and pooled per sample to obtain sufficient quantities for nucleoside triphosphate detection, while a seventh well was collected to obtain a representative cell count for normalization. LC/MS cell suspensions were vortexed vigorously for 2 min, then stored at -80°C until extraction.

Isotopically labelled adenosine-<sup>13</sup>C<sub>5</sub> (Toronto Research Chemicals, North York, ON, Canada) was added to each cell suspension to act as an internal control, achieving a final internal standard concentration of 2.5 ng/µL. Cell suspensions were vigorously vortexed for 2 min and centrifuged at 10 000 rpm for 5 min (4°C), then supernatants were retained for LC/MS analysis. The extraction process was repeated twice with an additional 500 µL methanol, for a total of 3 pooled extractions per sample. The final pooled sample was dried with nitrogen gas and stored at -80°C until analysis. Samples were resuspended in 5 mM NH<sub>4</sub>OAc (50 µL; Sigma-Aldrich) immediately prior to LC/MS.

***Liquid Chromatography/Mass Spectrometry.*** A Luna NH<sub>2</sub> HILIC column with dimensions of 2.0 x 150 mm, 100 Å pore size, and 5 µm particle size (Cat# 00F-4378-B0, Phenomenex, Torrance, CA, USA) was utilized to separate purineric targets for analysis of intracellular sample preparations. LC was performed with a flow rate of 0.4 mL/min and an injection volume of 2 µL. Nucleoside mono-, di-, and triphosphates, with the exception of UMP, were separated using the following aqueous and organic mobile phases: (A) 100 mM ammonium acetate (NH<sub>4</sub>OAc; Sigma Aldrich) in water, adjusted to pH 9 with

ammonium hydroxide (NH<sub>4</sub>OH; Caledon); and (B) 100% acetonitrile (CH<sub>3</sub>CN; Fisher Scientific), respectively. Adenosine, uridine, cytidine, and UMP were poorly detected using these parameters but were robustly detected when the concentration of mobile phase A was reduced to 10 mM NH<sub>4</sub>OAc pH 9. As this lower concentration of NH<sub>4</sub>OAc could not be optimized to produce sharp nucleoside triphosphate peaks, samples were run twice, first with A: 100 mM NH<sub>4</sub>OAc pH 9 to detect ATP, ADP, AMP, UTP, UDP, and inosine, and again with A: 10 mM NH<sub>4</sub>OAc pH 9, to permit quantification of UMP, adenosine, uridine, and cytidine. The same LC/MS gradient was utilized for both applications, and is summarized in Table 1. The LC system was paired with an Agilent 6550 iFunnel Q-TOF Mass Spectrometer (Agilent, Santa Clara, CA, USA) for purinergic detection. MS parameters included negative electrospray ionization, and high sensitivity detection with 2GHz extended dynamic range.

Prior to sample analysis, standards specific to each purinergic target (Sigma-Aldrich) were quantified to optimize LC/MS parameters and to confirm peak identities and retention times. Standards specific to the following targets were analyzed using negative ionization mode: ATP (505.9985 m/z; 8.6635 min), ADP (426.0221 m/z; 8.3574 min), AMP (346.0558 m/z; 7.9346 min), UTP (482.9613 m/z; 8.4813 min), UDP (402.9949 m/z; 5.6737 min), UMP (323.0286 m/z; 7.747 min), adenosine (266.0895 m/z; 4.169 min), uridine (243.0623; 4.152 min), cytidine (242.0782; 5.656 min), inosine (267.0735 m/z; 5.0687 min), and the internal standard adenosine-<sup>13</sup>C<sub>5</sub> (271.1068 m/z). Within each genotype, the experimental sample consisted of 6 individual cultures (n=6) prepared from 4 separate litters, and run in duplicate or triplicate. Selected targets were identified using Agilent MassHunter Qualitative Analysis 10.0 software (Agilent), then analyzed using Agilent MassHunter Quantitative Analysis 10.1 software (Agilent). Mean nucleoside abundance was normalized to representative cell counts, as well as to the relative abundance of adenosine-<sup>13</sup>C<sub>5</sub> internal standard.

Table 1. Optimized gradient utilized for LC/MS nucleotide analysis.

<b>Time (min)</b>	<b>Mobile Phase</b>	
	<b>A (%)</b>	<b>B (%)</b>
0	5	95
0.5	5	95
5.5	50	50
5.6	92	8
10	95	5
15	95	5
15.1	5	95
30	5	95

**Western Blotting.** After reaching 75-90% confluence, primary astrocyte cultures intended for western blotting were lifted with 0.05% trypsin-EDTA and pelleted, then flash frozen in liquid nitrogen and stored at -80°C until homogenization. A total of 15 WT (n=15) and 14 *Fmr1* KO (n=14) samples were used for CD39 western blotting, and 8 samples per genotype (n=8) were used for CD73 western blotting, obtained from individual cultures prepared from separate litters. Samples were homogenized on ice in brain extraction buffer (25 mM HEPES pH 7.3, 150 mM KCl, 8% glycerol, 0.1% NP-40, one Roche ULTRA protease inhibitor tablet, and one Roche PhoSTOP phosphatase inhibitor tablet) (Reynolds et al., 2021), then total protein content was quantified within lysates (DC protein assay; BioRad, Mississauga, ON, Canada) to determine gel loading dilutions.

Western blotting samples were prepared with Laemmli sample buffer plus 2.5%  $\beta$ -mercaptoethanol (BioRad) to achieve a dilution of 10  $\mu$ g protein per lane. Samples were run on polyacrylamide TGX Stain-Free 4-12% gradient gels (BioRad) to separate proteins, activated with UV light for 45 s to permit visualization of “total protein” (tryptophan), then transferred to polyvinylidene difluoride (BioRad) membranes. Stain-free total protein

loading control images were acquired using a ChemiDoc imaging system (BioRad), then membranes were blocked with 5% non-fat milk for 1 h. Primary antibodies against CD39 (rabbit monoclonal; 1:500; Abcam, Cambridge, UK Cat# ab223842, RRID:AB\_2889212) or CD73 (mouse monoclonal; 1:500; R7D Systems, Minneapolis, MN, USA Cat# MAB57951) were applied overnight (4°C), followed by the corresponding secondary antibodies donkey anti-rabbit horseradish peroxidase (1:2500; GE Healthcare, Chicago, IL, USA) or donkey anti-mouse horseradish peroxidase (1:5000; GE Healthcare). Bands for astrocyte membrane-bound CD39 were detected at ~75 kDa and ~52 kDa, corresponding to glycosylated (active) and unglycosylated (immature) forms of the enzyme, respectively (Zhong, Malhotra, Woodruff, & Guidotti, 2001). Membrane-bound glycosylated CD73 was detected at ~62 kDa (Adzic & Nedeljkovic, 2018; Zhou et al., 2019). Membranes were developed using Clarity MAX enhanced chemiluminescence (ECL) substrate (BioRad), and chemiluminescence images were acquired using the ChemiDoc imaging system (BioRad). Densitometry was performed using ImageLab 6.0.1 software (BioRad) to normalize bands of interest to the density of total protein bands.

**Statistics.** All statistical analyses were conducted using GraphPad Prism 8.0 software (GraphPad Software, San Diego, CA, USA). Comparisons between WT and *Fmr1* KO are expressed as fold change relative to WT means, and were obtained using unpaired two-tailed t-tests with significance at  $p < 0.05$ .

### 3.9. Results

#### ***Intracellular abundance of UDP is elevated in Fmr1 KO astrocytes***

Here, we utilized a novel hydrophilic interaction liquid chromatography (HILIC) protocol paired with mass spectrometry to detect intracellular purinergic signalling molecules within *Fmr1* KO and WT astrocytes. We observed several differences in intracellular nucleoside tri-, di-, and monophosphate abundance between WT and *Fmr1* KO astrocytes. Within the uridine-based family of ligands, intracellular UTP levels were unchanged in WT vs *Fmr1* KO astrocytes ( $n=6$ ,  $p=0.2673$ ; Fig. 1A,B), while levels of

intracellular UDP were elevated in *Fmr1* KO astrocytes relative to WT (n=6, p=0.0118; Fig. 1C,D). The abundance of astrocyte intracellular UMP was also unchanged between genotypes (WT n=5/*Fmr1* KO n=6, p=0.7292; Fig. 1E,F). The internal standard adenosine-<sup>13</sup>C<sub>5</sub> was used to normalize all ligand measurements and showed minimal variability, both within and between genotypes (data not shown).

### ***Levels of intracellular ATP and adenosine are reduced in Fmr1 KO astrocytes***

In contrast, the adenosine-based family of ligands showed somewhat opposite patterns of intracellular levels between WT and *Fmr1* KO astrocytes. Intracellular ATP levels were notably reduced in *Fmr1* KO astrocytes in comparison to WT (n=6, p=0.0425; Fig. 2A,B), while intracellular ADP quantities did not change between genotypes (n=6, p=0.4195; Fig. 2C,D). However, intracellular levels of AMP were elevated in *Fmr1* KO astrocytes relative to WT (n=6, p=0.0122; Fig. 2E,F).

### ***Intracellular adenosine levels are reduced in Fmr1 KO astrocytes***

Intracellular nucleosides function as nucleoside mono-, di-, and triphosphate precursors, while the nucleoside adenosine also acts as a gliotransmitter by binding to the P1 purinergic receptor subfamily to exert both excitatory and inhibitory effects. Here, adenosine abundance was reduced in *Fmr1* KO astrocytes (WT n=5/*Fmr1* KO n=6, p=0.0494; Fig. 3A,B). However, intracellular levels of uridine (n=5, p=0.6328; Fig. 3C,D), inosine (n=6, p=0.6111; Fig. 3E,F), and cytidine (WT n=5/*Fmr1* KO n=6, p=0.7062; Fig. 3G,H) were unchanged.

### ***Glycosylated CD39 levels are elevated in Fmr1 KO astrocyte culture, but CD73 abundance does not differ***

The abundance of purinergic ligands is governed in part by the action of the CD39 ectonucleoside triphosphate diphosphohydrolase enzyme, which breaks down UTP and ADP into their di- and monophosphate forms. Active CD39 is localized to the plasma membrane, where it was detectable at the commonly observed molecular weight of

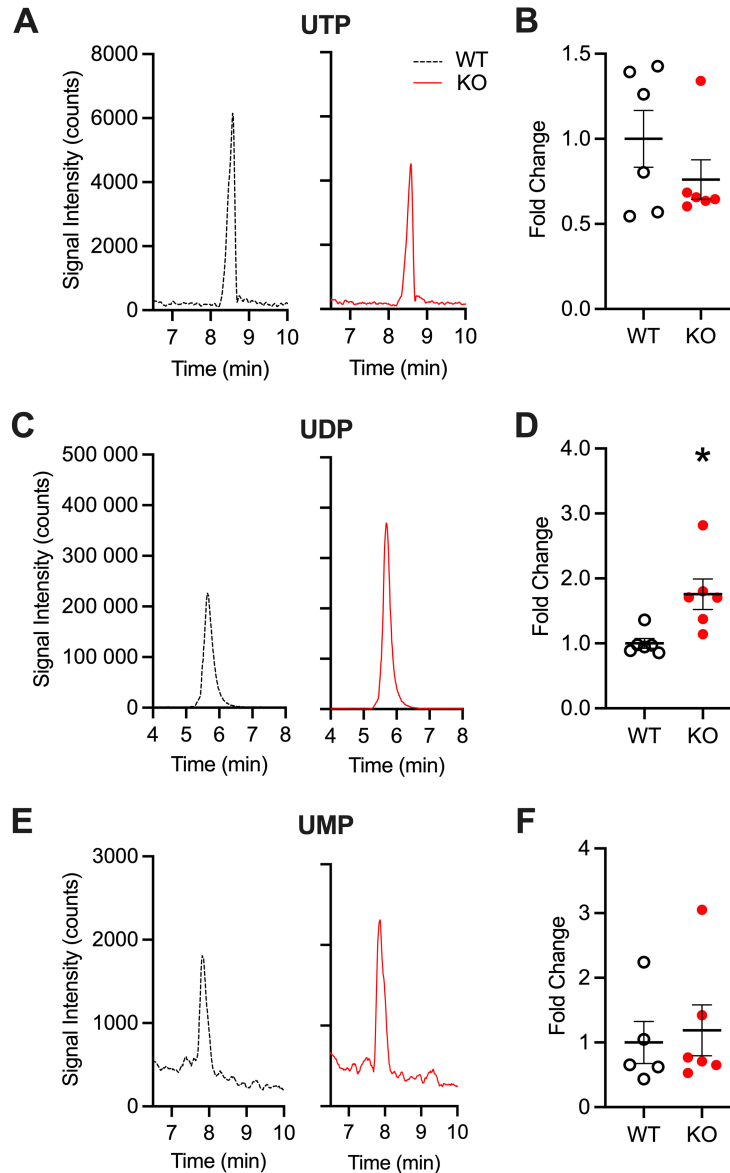


Figure 1. LC/MS quantification of intracellular UTP, UDP, and UMP in WT and *Fmr1* KO primary cortical astrocytes. Representative extracted ion chromatograms of WT and *Fmr1* KO astrocyte intracellular UTP (A), UDP (C), and UMP (E). Relative abundance of intracellular UTP (B), UDP (D), and UMP (F) in WT and *Fmr1* KO cultured astrocytes, showing increased UDP levels in *Fmr1* KO astrocytes. Abundance is presented as fold change relative to mean WT signal intensity, and is normalized to both representative cell count and adenosine-<sup>13</sup>C<sub>5</sub> internal standard signal intensity. Data presented as means  $\pm$  SEM. n=6, with the exception of WT UMP n=5; \* p<0.05.

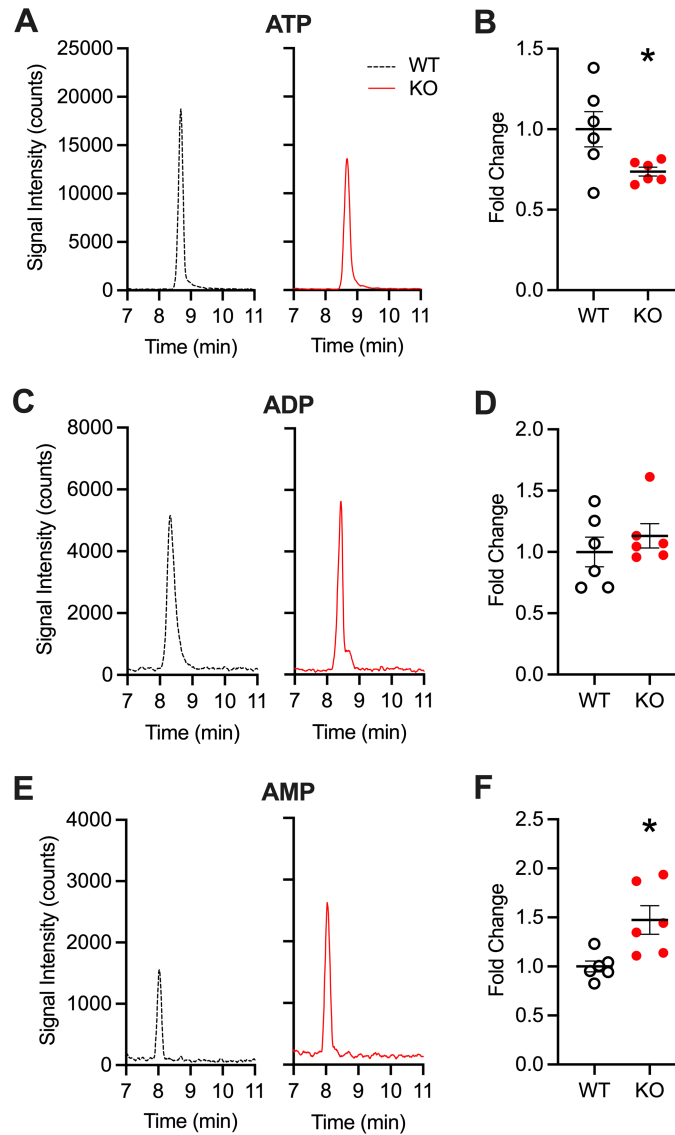


Figure 2. LC/MS quantification of intracellular ATP, ADP, and AMP in WT and *Fmr1* KO primary cortical astrocytes. Representative extracted ion chromatograms of WT and *Fmr1* KO astrocyte intracellular ATP (A), ADP (C), and AMP (E). Relative abundance of intracellular ATP (B), ADP (D), and AMP (F) in WT and *Fmr1* KO cultured astrocytes, showing reduced ATP levels and elevated AMP levels in *Fmr1* KO astrocytes. Abundance is presented as fold change relative to mean WT signal intensity, and is normalized to both representative cell count and adenosine- $^{13}\text{C}_5$  internal standard intensity. Data presented as means  $\pm$  SEM. n=6; \* p<0.05.

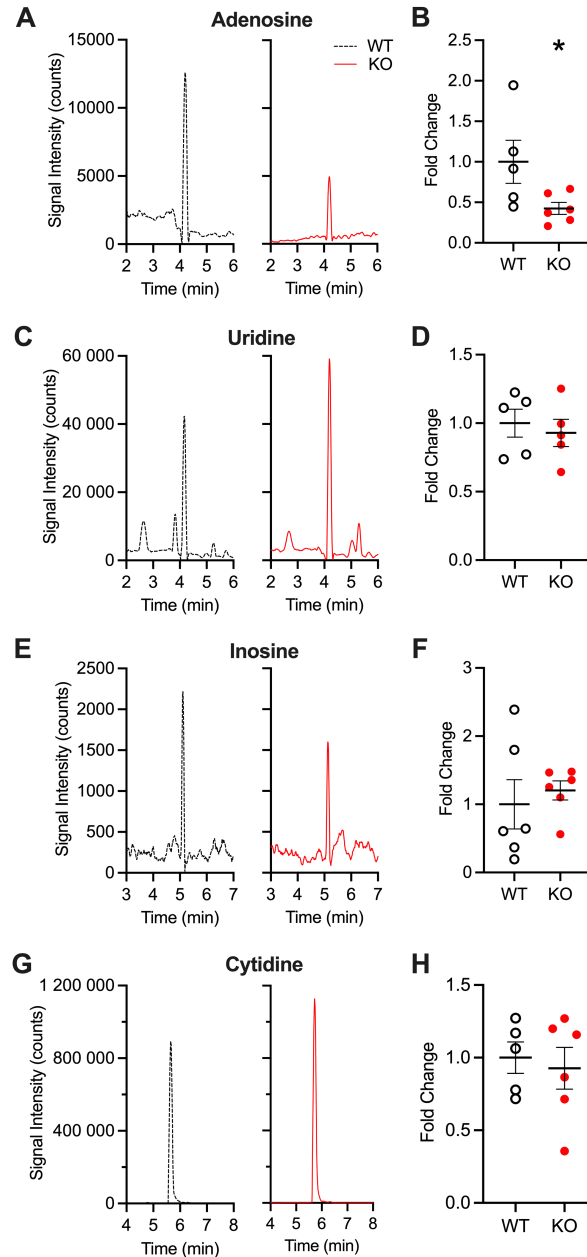


Figure 3. LC/MS quantification of intracellular nucleosides in WT and *Fmr1* KO primary cortical astrocytes. Representative extracted ion chromatograms of adenosine (A), uridine (C), inosine (E), and cytidine (G). Relative abundance of intracellular adenosine (B), uridine (D), inosine (F), and cytidine (H) in WT and *Fmr1* KO cultured astrocytes, showing decreased adenosine levels in *Fmr1* KO astrocytes. Abundance is presented as fold change relative to mean WT signal intensity, and is normalized to both representative cell count and adenosine- $^{13}\text{C}_5$  internal standard signal intensity. Data presented as means  $\pm$  SEM. WT n=5, with the exception of WT inosine n=6; *Fmr1* KO n=6; \* p<0.05.

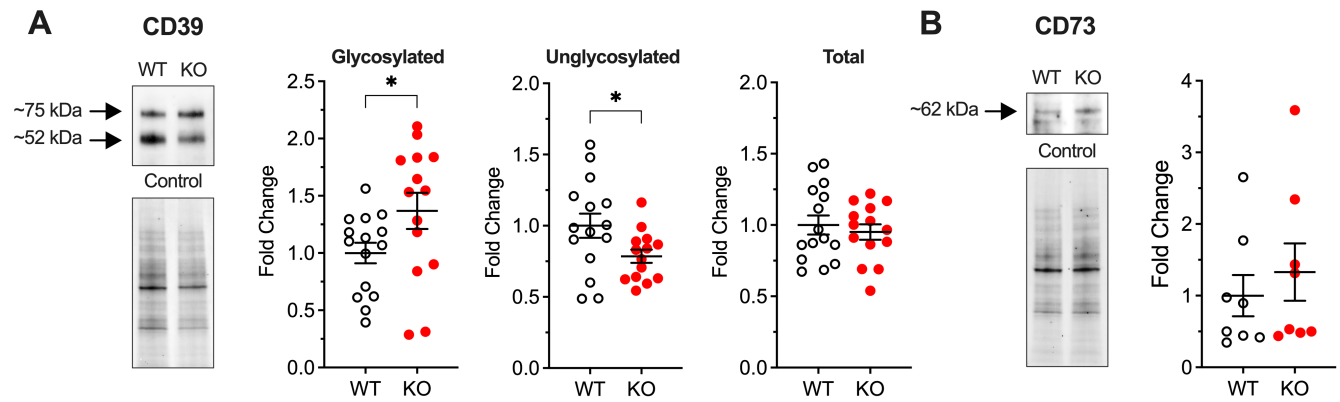


Figure 4. Western blotting quantification of WT and *Fmr1* KO primary cortical astrocyte membrane-bound ectonucleotidases. A. Representative western blot of astrocyte membrane-bound CD39 ectonucleotidase and corresponding total protein (tryptophan) control, showing bands for both glycosylated (~75 kDa) and unglycosylated (~52 kDa) CD39. B. Glycosylated (*i.e.* active) CD39 levels were elevated in *Fmr1* KO astrocyte cultures (n=14) relative to WT (n=15), while unglycosylated (*i.e.* immature) CD39 levels (C) were reduced in *Fmr1* KO; when both forms were added together, the total levels of CD39 were unchanged between genotypes. D. Representative western blot and corresponding total protein image of WT and *Fmr1* KO astrocyte-associated CD73. E. Astrocyte-bound CD73 was present at similar levels in WT and *Fmr1* KO (n=8) cultures. Enzyme abundance is normalized to total protein and is presented as fold change relative to mean WT levels. Data presented as means  $\pm$  SEM; \*  $p < 0.05$ .

~75 kDa. The ~52 kDa CD39 band we observed here has previously been shown to be indicative of an intracellularly localized form that only becomes active once it is glycosylated and incorporated within the plasma membrane (Zhong, Malhotra, Woodruff, & Guidotti, 2001). Here, we found that the glycosylated, active form of CD39 (~75 kDa) was more highly expressed on the surface of *Fmr1* KO astrocytes (n=14) than WT (p=0.0489; n=15; Fig.4A). In contrast, levels of the immature, unglycosylated form (~52 kDa) were reduced on the *Fmr1* KO astrocyte surface relative to WT (p=0.0386; Fig.4A). Despite these differences, the total abundance of glycosylated plus immature CD39 did not differ between genotypes (p=0.5799), indicating that glycosylation rather than protein synthesis is altered in FXS.

The membrane-bound ecto-5'-ectonucleotidase enzyme, also known as CD73, converts UMP into uridine and is therefore also important in regulating purinergic ligand availability. Here, no differences were observed in the level of astrocyte-associated CD73 (p=0.5185; n=8) between WT and *Fmr1* KO cultures (Fig. 4B).

### **3.10. Discussion**

Recent research has shown that purinergic signalling pathways are elevated in *Fmr1* KO cortical astrocytes, with potential consequences for astrocytic and neuronal excitation. In order to fully understand the nature of these astrocyte dysfunctions, it is important to consider the ability of astrocytes to secrete and metabolize purinergic ligands. Here, we compared the levels of *Fmr1* KO and WT intracellular nucleoside triphosphates and their metabolites using a novel hydrophilic interaction liquid chromatography (HILIC) method coupled with mass spectrometry. We observed significant dysregulations in the levels of UDP, ATP, AMP, and adenosine intracellular stores within *Fmr1* KO astrocytes, as well as increased glycosylation of the astrocyte membrane-bound CD39 ectonucleotidase responsible for the extracellular metabolism of ATP and UTP. Consistent with our previous P2Y receptor characterization, these differences are indicative of a profoundly dysregulated

purinergic signalling system within *Fmr1* KO cortical astrocytes, and may lead to significant alterations in gliotransmitter release.

***Hydrophilic interaction liquid chromatography coupled with mass spectrometry is a robust method for nucleoside triphosphate detection***

Though purinergic signalling pathways have been known for some time to be active across the majority of cell-types and tissues, the investigation of astrocyte P2Y ligand availability poses a methodological challenge. ATP can be readily quantified through ELISA or luciferase assays, but the detection of UTP is significantly more difficult due to a lack of sensitive, reliable, and commercially available methods. Mass spectrometry is currently considered the most sensitive method for UTP detection, but even still, liquid chromatography/mass spectrometry (LC/MS) approaches have remained challenging to optimize due to substantial difficulties in temporally separating out the various hydrophilic analytes to allow for their quantification. Hydrophilic interaction liquid chromatography (HILIC) columns are generally thought to be most appropriate for this application (Alpert, 1990; Hemström & Irgum, 2006). They permit the quantification of polar and hydrophilic molecules due to the presence of a polar stationary phase that allows these analytes to reversibly bind in the presence of an organic solvent. This binding is reversed using an aqueous mobile phase gradient that promotes temporal separation during elution (Alpert, 1990; Hemström & Irgum, 2006). HILIC has previously been utilized to detect UTP, ATP, and their metabolites with some success (Narayan, 2017), though a number of studies have still found the detection of UTP to be challenging (Galeano Garcia, Zimmermann, & Carazzone, 2019; Kong et al., 2018; Zhang et al., 2014). Here, we found that the use of a basic and highly concentrated aqueous mobile phase (100 mM NH<sub>4</sub>OAc pH 9) ensured the timely elution ATP and UTP, while nucleosides were readily and reproducibly detected under lower aqueous phase concentrations (10 mM NH<sub>4</sub>OAc pH 9). This approach has allowed us to compare the levels of intracellular purinergic signalling molecules between *Fmr1* KO and WT cortical astrocytes, identifying differences that may impact the activation of astrocytic and neuronal purinergic receptors.

### ***Increased intracellular UDP is consistent with elevated P2Y activity in *Fmr1* KO astrocytes***

The most prominent genotypic difference we observed in this study was a nearly 2-fold increase in *Fmr1* KO intracellular UDP relative to WT. This increase in UDP is particularly interesting given recently reported dysregulations in FXS and ASD. Circulating uridine has been previously correlated with the concentration of cerebral UDP, as intravenously administered uridine has been shown to pass through the blood-brain barrier to increase the concentration of UDP within the mouse brain (Steculorum et al., 2015). Elevated levels of the UDP nucleoside precursor uridine are detectable in the plasma of children with ASD (Adams et al., 2011), suggesting that elevated plasma uridine in ASD is consistent with our findings of elevated *Fmr1* KO astrocyte UDP. Conversion of uridine into UDP is accomplished through the action of phosphotransferase enzymes, with uridine kinase first catalyzing the addition of a phosphate to form UMP, followed by UMP kinase-mediated production of UDP. The level and activity of these kinases therefore represents a promising future area of investigation to further characterize FXS astrocyte purinergic dysregulation.

The increased presence of astrocyte intracellular UDP suggests the potential for substantial *Fmr1* KO UDP release to stimulate the activity of astrocytic or neuronal P2Y<sub>6</sub> receptors. UDP uniquely acts as a strong agonist of metabotropic P2Y<sub>6</sub> receptors, with weaker or negligible binding at other purinergic receptor types (Abbracchio et al., 2009). P2Y<sub>6</sub> receptors are in fact one of the two P2Y receptor types found to be elevated in *Fmr1* KO cortical astrocytes (Reynolds et al., 2021), so the increase in intracellular ligand stores may be indicative of significant capacity for upregulated P2Y<sub>6</sub>-mediated signalling. Activation of P2Y<sub>6</sub> and other P2Y receptors leads to PLC/IP3-driven endoplasmic reticulum intracellular calcium release, thereby promoting the propagation of intercellular calcium waves, calcium-dependent gliotransmitter release, and transcription factor activation via signal transduction cascades including the MAPK, Akt, and STAT3 pathways. Thus, the combination of increased receptor expression paired with increased

intracellular ligand stores suggests the potential for widespread calcium wave propagation, neuronal firing, and modulation of gene expression, all of which are generally consistent with FXS symptoms of cortical hyperexcitation.

***Significant alterations in the intracellular levels of *Fmr1* KO adenosine-based purinergic signalling molecules***

The adenosine-based family of purinergic molecules were altered in *Fmr1* KO astrocytes, with significant dysregulations in the intracellular levels of ATP, AMP, and adenosine. Mitochondria are important sources of ATP production, and our detection methods do not discriminate between intracellular ATP used for cellular metabolism versus purinergic signalling. Mitochondrial dysfunctions, including decreased mitochondrial fusion and elevated mitochondrial fragmentation in *Fmr1* KO neurons as well as increased production of reactive oxygen species in *Fmr1* KO astrocytes, have been recently reported in the *Fmr1* KO mouse (Shen et al., 2019; Vandenberg, Dawson, Head, Scott, & Scott, 2021). Recent work has shown reduced ATP synthesis within the *Fmr1* KO cortex (D'Antoni et al., 2020), which is consistent with the reduced ATP levels we observed here. It is also possible that reduced ATP levels may be exacerbated by UDP formation, as both uridine kinase and UMP kinase utilize ATP as a substrate to promote UMP and UDP formation, respectively.

Adenosine-containing gliotransmitters widely target purinergic receptors: ATP agonises all seven ionotropic P2X receptors as well as the majority of P2Y receptors. In contrast, AMP does not directly bind to purinergic receptors, but is an important intermediate in the buildup and breakdown of ATP, and an increase in *Fmr1* KO AMP levels may therefore be a consequence of ATP breakdown (Abbracchio et al., 2009). Activation of ATP-gated P2X receptors promotes the opening of their sodium and calcium channels, thereby permitting an influx of cations. In astrocytes, a rapid influx of calcium triggers the propagation of calcium waves, the activation of signal transduction cascades, and further vesicular gliotransmitter release, with P2X receptors leading to rapid outcomes

and P2Y receptors driving sustained changes (Abbracchio et al., 2009). This finding may suggest that P2Y receptor activity is more likely to be upregulated in the FXS cortex than P2X-mediated signalling, or that P2Y receptors within the *Fmr1* KO cortex are more likely to utilize UTP-derived ligands than ATP-derived ones, even when they also have affinity for ATP/ADP. Given the similarities in intracellular calcium associated with astrocyte P2X and P2Y activation, it is currently unclear how our findings of decreased intracellular ATP contribute to dysregulated FXS purinergic signalling, and it will therefore be crucial to compare the secreted levels of ATP and metabolites in order to address this question.

Intracellular stores of the P1 receptor ligand adenosine were also notably reduced in *Fmr1* KO astrocytes. Adenosine is typically generated through ectonucleotidase-mediated breakdown of ATP following synaptic release of ATP. Its subsequent reuptake by equilibrative and concentrative astrocyte nucleotide transporters likely strongly influences the concentrations of adenosine found intracellularly. This nucleoside binds indiscriminately to G<sub>i/o</sub>-coupled A<sub>1</sub> and A<sub>3</sub> receptors as well as to G<sub>s</sub>-coupled A<sub>2A</sub> and A<sub>2B</sub> receptors, exerting both excitatory and inhibitory effects on the production of cyclic AMP. Of these four receptor types, A<sub>1</sub> receptors are most prevalent in the cortex and are also most sensitive to adenosine (Dunwiddie & Masino, 2001). Agonism of A<sub>1</sub> receptors leads to inhibition of adenylyl cyclase and reduction of voltage-gated calcium channel activity, ultimately reducing the release of gliotransmitters to temper excitatory signalling. A<sub>1</sub> receptor antagonism has been found to increase the onset of seizures in rats, while agonism of A<sub>1</sub> receptors inhibited seizure activity in both mouse and rat models (Amorim et al., 2016; Fabera et al., 2019; Gouder, Fritschy, & Boison, 2003). As seizures are frequently reported in individuals with FXS (Musumeci et al., 1999), reduced levels of intracellular adenosine in *Fmr1* KO astrocytes may be consistent with these findings.

***Increased glycosylation of CD39 ectonucleotidase suggests rapid metabolism of nucleoside triphosphates following Fmr1 KO astrocyte secretion***

While the availability of purinergic molecules for vesicular release is one factor modulating purinergic receptor agonism, it is also important to consider the extracellular processes that occur following vesicular release. Astrocyte membrane-bound ectonucleotidases control the strength and duration of purinergic agonism by metabolizing secreted gliotransmitters to facilitate their reuptake. Increased glycosylation of astrocyte membrane-bound CD39 suggests that the ability of ectonucleotidases to break down purinergic molecules prior to reuptake is enhanced in the FXS cortex. Following gliotransmitter release, purinergic molecules bind to their specific and intended receptor targets on nearby astrocytes and neurons, but also become metabolized at the synapse, converting them into their di- and monophosphate forms, and eventually to their nucleoside bases for astrocyte reuptake. In the context of extracellular ATP metabolism, the action of CD39 has been shown to more rapidly metabolize ATP than ADP. Extracellular ATP was almost completely metabolized within 30 mins *in vitro* to produce a 40% accumulation of ADP; however, ADP was not converted to AMP until 80% of the initially released ATP had been metabolized, taking an additional 2.5 hours (Wink et al., 2003). Though the dynamics of UTP metabolism were not examined by Wink et al. (2003) in this study, ATP and UTP are both metabolized by the same ectonucleotidase, suggesting that UTP/UDP may follow a similar pattern. As receptors such as P2Y<sub>1</sub> and P2Y<sub>6</sub> have higher affinity for diphosphates than triphosphates (ADP>ATP and UDP>UTP, respectively), the action of CD39 may therefore increase the likelihood that these receptors are strongly agonised following UTP release. Conversely, rapid breakdown of CD39 may indicate that activity of receptors with strong affinity for nucleoside triphosphates, such as the P2X receptor family, may be tempered in the *Fmr1* KO cortex.

### ***Challenges detecting secreted purinergic ligands***

In general, aberrant gliotransmitter stores are indicative of dysregulated *Fmr1* KO cortical astrocyte purinergic signalling, which is consistent with our previous work identifying heightened levels of *Fmr1* KO astrocyte P2Y receptors (Reynolds et al., 2021). However, the precise effects of gliotransmitter release on the availability of intracellular purinergic stores are difficult to interpret. On one hand, the presence of select excess intracellular gliotransmitters (*e.g.* UDP) may imply that astrocytes have a heightened capacity for UDP release, promoting subsequent purinergic receptor activation. Conversely, it is also possible that reduced intracellular stores (*e.g.* ATP, adenosine) may indicate recent gliotransmitter release. It will therefore be critical to measure the levels of secreted gliotransmitters to fully understand the interplay between astrocyte ligand availability and receptor expression.

There are significant challenges associated with the quantification of nucleoside mono-, di-, and triphosphates secreted from astrocyte cultures. As a consequence of ectonucleotidase activity, secreted concentrations of ATP and UTP are expected to become quite low, requiring highly sensitive detection methods. The collection of extracellular purinergic ligands for mass spectrometry is further complicated by the fact that the injection of raw culture media or saline buffers into a mass spectrometer leads to a significant reduction in sensitivity, and astrocytes cannot be grown directly in LC/MS solvents such as NH<sub>4</sub>OAc or methanol to facilitate the collection of secreted molecules. As a result, work is ongoing to optimize a solid phase extraction protocol to separate extracellular purinergic targets from the components of culture media prior to liquid chromatography. However, to date, the sensitivity of this protocol is only sufficient to detect secreted nucleosides, even in the presence of ectonucleotidase inhibitors.

Despite these challenges, the identification of altered intracellular purinergic stores and membrane-bound CD39 enzymes in *Fmr1* KO astrocytes lends support to previous findings of elevated FXS purinergic signalling, and lays the groundwork for future research investigating astrocyte purinergic signalling dysregulations and their contribution to FXS symptoms.

### 3.11. References

- Abbracchio, M. P., Burnstock, G., Verkhratsky, A., & Zimmermann, H. (2009). Purinergic signalling in the nervous system: an overview. *Trends Neurosci*, 32(1), 19-29. doi:10.1016/j.tins.2008.10.001
- Adams, J. B., Audhya, T., McDonough-Means, S., Rubin, R. A., Quig, D., Geis, E., . . . Lee, W. (2011). Nutritional and metabolic status of children with autism vs. neurotypical children, and the association with autism severity. *Nutr Metab (Lond)*, 8(1), 34. doi:10.1186/1743-7075-8-34
- Adzic, M., & Nedeljkovic, N. (2018). Unveiling the Role of Ecto-5'-Nucleotidase/CD73 in Astrocyte Migration by Using Pharmacological Tools. *Frontiers in Pharmacology*, 9, 153. doi:10.3389/fphar.2018.00153
- Alpert, A. J. (1990). Hydrophilic-interaction chromatography for the separation of peptides, nucleic acids and other polar compounds. *Journal of Chromatography A*, 499, 177-196. doi:doi.org/10.1016/S0021-9673(00)96972-3
- Amorim, B. O., Hamani, C., Ferreira, E., Miranda, M. F., Fernandes, M. J. S., Rodrigues, A. M., . . . Covolan, L. (2016). Effects of A1 receptor agonist/antagonist on spontaneous seizures in pilocarpine-induced epileptic rats. *Epilepsy Behav*, 61, 168-173. doi:10.1016/j.yebeh.2016.05.036
- Brown, V., Jin, P., Ceman, S., Darnell, J. C., O'Donnell, W. T., Tenenbaum, S. A., . . . Warren, S. T. (2001). Microarray Identification of FMRP-Associated Brain mRNAs and Altered mRNA Translational Profiles in Fragile X Syndrome. *Cell*, 107(4), 477-487. doi:doi.org/10.1016/S0092-8674(01)00568-2
- D'Antoni, S., de Bari, L., Valenti, D., Borro, M., Bonaccorso, C. M., Simmaco, M., . . . Catania, M. V. (2020). Aberrant mitochondrial bioenergetics in the cerebral cortex of the Fmr1 knockout mouse model of fragile X syndrome. *Biol Chem*, 401(4), 497-503. doi:10.1515/hsz-2019-0221
- Dobolyi, A., Juhasz, G., Kovacs, Z., & Kardos, J. (2011). Uridine function in the central nervous system. *Curr Top Med Chem*, 11(8), 1058-1067. doi:10.2174/156802611795347618
- Dunwiddie, T. V., & Masino, S. A. (2001). The Role and Regulation of Adenosine in the Central Nervous System. *Annual Review of Neuroscience*, 24(1), 31-55. doi:10.1146/annurev.neuro.24.1.31

- Fabera, P., Parizkova, M., Uttl, L., Vondrakova, K., Kubova, H., Tsenov, G., & Mares, P. (2019). Adenosine A1 Receptor Agonist 2-chloro-N6-cyclopentyladenosine and Hippocampal Excitability During Brain Development in Rats. *Frontiers in Pharmacology*, 10, 656. doi:10.3389/fphar.2019.00656
- Farzin, F., Perry, H., Hessel, D., Loesch, D., Cohen, J., Bacalman, S., . . . Hagerman, R. (2006). Autism spectrum disorders and attention-deficit/hyperactivity disorder in boys with the fragile X premutation. *J Dev Behav Pediatr*, 27(2 Suppl), S137-144. doi:10.1097/00004703-200604002-00012
- Galeano Garcia, P., Zimmermann, B. H., & Carrazzone, C. (2019). Hydrophilic Interaction Liquid Chromatography Coupled to Mass Spectrometry and Multivariate Analysis of the De Novo Pyrimidine Pathway Metabolites. *Biomolecules*, 9(8). doi:10.3390/biom9080328
- Gouder, N., Fritschy, J. M., & Boison, D. (2003). Seizure suppression by adenosine A1 receptor activation in a mouse model of pharmacoresistant epilepsy. *Epilepsia*, 44(7), 877-885. doi:10.1046/j.1528-1157.2003.03603.x
- Hemström, P., & Irgum, K. (2006). Hydrophilic interaction chromatography. *Journal of Separation Science*, 29(12), 1784-1821. doi:doi.org/10.1002/jssc.200600199
- Higashimori, H., Schin, C. S., Chiang, M. S., Morel, L., Shoneye, T. A., Nelson, D. L., & Yang, Y. (2016). Selective Deletion of Astroglial FMRP Dysregulates Glutamate Transporter GLT1 and Contributes to Fragile X Syndrome Phenotypes In Vivo. *J Neurosci*, 36(27), 7079-7094. doi:10.1523/jneurosci.1069-16.2016
- Hodges, J. L., Yu, X., Gilmore, A., Bennett, H., Tjia, M., Perna, J. F., . . . Zuo, Y. (2017). Astrocytic Contributions to Synaptic and Learning Abnormalities in a Mouse Model of Fragile X Syndrome. *Biological Psychiatry*, 82(2), 139-149. doi:doi.org/10.1016/j.biopsych.2016.08.036
- Jacobs, S., & Doering, L. C. (2009). Primary dissociated astrocyte and neuron co-culture. In L. C. Doering (Ed.), *Protocols for Neural Cell Culture (Fourth Edition ed., pp. 269-284)*. New York, NY: Humana.
- Jacobs, S., & Doering, L. C. (2010). Astrocytes Prevent Abnormal Neuronal Development in the Fragile X Mouse. *The Journal of Neuroscience*, 30(12), 4508-4514. doi:10.1523/jneurosci.5027-09.2010

- Kong, Z., Jia, S., Chabes, A. L., Appelblad, P., Lundmark, R., Moritz, T., & Chabes, A. (2018). Simultaneous determination of ribonucleoside and deoxyribonucleoside triphosphates in biological samples by hydrophilic interaction liquid chromatography coupled with tandem mass spectrometry. *Nucleic Acids Research*, 46(11), e66-e66. doi:10.1093/nar/gky203
- Lie, A. A., Blümcke, I., Beck, H., Wiestler, O. D., Elger, C. E., & Schoen, S. W. (1999). 5'-Nucleotidase activity indicates sites of synaptic plasticity and reactive synaptogenesis in the human brain. *J Neuropathol Exp Neurol*, 58(5), 451-458. doi:10.1097/00005072-199905000-00004
- Musumeci, S. A., Hagerman, R. J., Ferri, R., Bosco, P., Bernardina, B. D., Tassinari, C. A., . . . Elia, M. (1999). Epilepsy and EEG Findings in Males with Fragile X Syndrome. *Epilepsia*, 40(8), 1092-1099. doi:doi.org/10.1111/j.1528-1157.1999.tb00824.x
- Narayan, V. (2017). HPLC Analysis of Nucleotides. (Master of Applied Science (Research)). Queensland University of Technology.
- Pieretti, M., Zhang, F. P., Fu, Y. H., Warren, S. T., Oostra, B. A., Caskey, C. T., & Nelson, D. L. (1991). Absence of expression of the FMR-1 gene in fragile X syndrome. *Cell*, 66(4), 817-822. doi:10.1016/0092-8674(91)90125-i
- Reynolds, K. E., Wong, C. R., & Scott, A. L. (2021). Astrocyte-mediated purinergic signaling is upregulated in a mouse model of Fragile X syndrome. *Glia*, 69(7), 1816-1832. doi:10.1002/glia.23997
- Shen, M., Wang, F., Li, M., Sah, N., Stockton, M. E., Tidei, J. J., . . . Zhao, X. (2019). Reduced mitochondrial fusion and Huntingtin levels contribute to impaired dendritic maturation and behavioral deficits in Fmr1-mutant mice. *Nature Neuroscience*, 22(3), 386-400. doi:10.1038/s41593-019-0338-y
- Steculorum, S. M., Paeger, L., Bremser, S., Evers, N., Hinze, Y., Idzko, M., . . . Brüning, J. C. (2015). Hypothalamic UDP Increases in Obesity and Promotes Feeding via P2Y6-Dependent Activation of AgRP Neurons. *Cell*, 162(6), 1404-1417. doi:10.1016/j.cell.2015.08.032
- Sutcliffe, J. S., Nelson, D. L., Zhang, F., Pieretti, M., Caskey, C. T., Saxe, D., & Warren, S. T. (1992). DNA methylation represses FMR-1 transcription in fragile X syndrome. *Hum Mol Genet*, 1(6), 397-400. doi:10.1093/hmg/1.6.397
- Turner, G., Webb, T., Wake, S., & Robinson, H. (1996). Prevalence of fragile X syndrome. *Am J Med Genet*, 64(1), 196-197.

- Vandenberg, G. G., Dawson, N. J., Head, A., Scott, G. R., & Scott, A. L. (2021). Astrocyte-mediated disruption of ROS homeostasis in Fragile X mouse model. *Neurochemistry International*, 146, 105036. doi:doi.org/10.1016/j.neuint.2021.105036
- Verkerk, A. J. M. H., Pieretti, M., Sutcliffe, J. S., Fu, Y.-H., Kuhl, D. P. A., Pizzuti, A., . . . Warren, S. T. (1991). Identification of a gene (FMR-1) containing a CGG repeat coincident with a breakpoint cluster region exhibiting length variation in fragile X syndrome. *Cell*, 65(5), 905-914. doi:doi.org/10.1016/0092-8674(91)90397-H
- Wallingford, J., Scott, A. L., Rodrigues, K., & Doering, L. C. (2017). Altered Developmental Expression of the Astrocyte-Secreted Factors Hevin and SPARC in the Fragile X Mouse Model. *Frontiers in Molecular Neuroscience*, 10, 268-268. doi:10.3389/fnmol.2017.00268
- Wink, M. R., Braganhol, E., Tamajusuku, A. S. K., Casali, E. A., Karl, J., Barreto-Chaves, M. L., . . . Battastini, A. M. O. (2003). Extracellular adenine nucleotides metabolism in astrocyte cultures from different brain regions. *Neurochemistry International*, 43(7), 621-628. doi:doi.org/10.1016/S0197-0186(03)00094-9
- Youngs, S. A., Murray, A., Dennis, N., Ennis, S., Lewis, C., McKechnie, N., . . . Jacobs, P. (2000). FRAXA and FRAXE: the results of a five year survey. *J Med Genet*, 37(6), 415-421. doi:10.1136/jmg.37.6.415
- Zhang, R., Watson, D. G., Wang, L., Westrop, G. D., Coombs, G. H., & Zhang, T. (2014). Evaluation of mobile phase characteristics on three zwitterionic columns in hydrophilic interaction liquid chromatography mode for liquid chromatography-high resolution mass spectrometry based untargeted metabolite profiling of *Leishmania* parasites. *Journal of Chromatography A*, 1362, 168-179. doi:doi.org/10.1016/j.chroma.2014.08.039
- Zhong, X., Malhotra, R., Woodruff, R., & Guidotti, G. (2001). Mammalian Plasma Membrane Ecto-nucleoside Triphosphate Diphosphohydrolase 1, CD39, Is Not Active Intracellularly: THE N-GLYCOSYLATION STATE OF CD39 CORRELATES WITH SURFACE ACTIVITY AND LOCALIZATION. *Journal of Biological Chemistry*, 276(44), 41518-41525. doi:doi.org/10.1074/jbc.M104415200
- Zhou, S., Liu, G., Guo, J., Kong, F., Chen, S., & Wang, Z. (2019). Pro-inflammatory Effect of Downregulated CD73 Expression in EAE Astrocytes. *Frontiers in Cellular Neuroscience*, 13(233). doi:10.3389/fncel.2019.00233

Zimmermann, H. (1996). BIOCHEMISTRY, LOCALIZATION AND FUNCTIONAL ROLES OF ECTO-NUCLEOTIDASES IN THE NERVOUS SYSTEM. *Progress in Neurobiology*, 49(6), 589-618. doi:doi.org/10.1016/0301-0082(96)00026-3

## **Chapter Four:**

### **Converging purinergic and immune signalling pathways drive IL-6 secretion by Fragile X cortical astrocytes via STAT3**

#### **4.1. Preface**

As discussed in previous chapters, abnormal astrocyte-mediated function is believed to influence the development of FXS cortical pathology. In Chapters 2 and 3, *Fmr1* KO cortical astrocytes were shown to engage in elevated P2Y-mediated purinergic signalling, a pathway that modulates signalling factor release and has also been linked to immune regulatory processes through the phosphorylation of STAT3. Recent evidence suggests an elevated immune response in the FXS cortex, driven by dysregulated secretion of FXS astrocyte soluble factors such as interleukin-6 (IL-6) and tenascin C (TNC). This chapter will therefore investigate the link between elevated astrocyte purinergic signalling and the TNC-STAT3-IL6 immune regulatory pathway in *Fmr1* KO cortical astrocytes, and will aim to determine whether blockade of this pathway can minimize pathological cytokine release in FXS.

#### **4.2. Study Significance**

The research presented here is the first to suggest that purinergic signalling and immune regulatory pathways converge to drive pro-inflammatory responses in FXS cortical astrocytes. In this work, purinergic agonism enhanced both TNC secretion and STAT3 phosphorylation, two processes linked to elevated IL-6 secretion in FXS. Importantly, this link suggests that by controlling excess astrocyte purinergic signalling, the effects of cortical immune signalling can also be mitigated by means of reduced STAT3 phosphorylation. Further investigation into the purinergic regulation of pro-inflammatory pathways may therefore provide new insight to target cortical astrocyte dysregulation in FXS.

### 4.3. Aims and Hypotheses

This research was designed to address the second aim of this thesis work:

Aim 2: Determine whether purinergic signalling alters the activation of the immune-regulating STAT3 signal transduction pathway in *Fmr1* KO cortical astrocytes.

Hypothesis: Purinergic agonism promotes the phosphorylation of astrocyte STAT3, with downstream consequences for cortical immune regulation in the *Fmr1* KO mouse cortex.

### 4.4. Publication Status

The following manuscript has been submitted for publication in *Journal of Neuroimmunology* and is currently under review.

**Title: Converging purinergic and immune signalling pathways drive IL-6 secretion by Fragile X cortical astrocytes via STAT3**

**Authors:**

Kathryn E. Reynolds<sup>1</sup>, Victoria Krasovska<sup>1</sup> & Angela L. Scott<sup>1</sup>

1. Department of Pathology and Molecular Medicine, McMaster University, Hamilton, Ontario, Canada

**Correspondence:**

Angela L. Scott  
Department of Pathology and Molecular Medicine  
McMaster University  
1200 Main Street West, Hamilton, Ontario L8N 3Z5, Canada.

scottan@mcmaster.ca

**Funding Sources:**

This work was funded by McMaster University and a partnership grant from Brain Canada and the Azrieli Foundation (BC ANRP MIRI2013-3352). KR was funded by a Canadian Institutes of Health Research Canada Graduate Scholarship (CIHR CGS-D).

**Acknowledgements:**

We sincerely thank Amanda Poxon, Chloe Wong, and Laurie Doering for the range of technical assistance and support provided for the successful completion of this work.

**Conflict of Interest:**

None

**Keywords:**

Fragile X syndrome, astrocyte, cortex, purinergic signalling, interleukin-6, STAT3, tenascin C

**Highlights:**

- Purinergic and immune signalling pathways converged in Fragile X cortical astrocytes
- Purinergic agonism promoted astrocyte Tenascin C release and STAT3 phosphorylation
- Fragile X cortical astrocytes secreted excess pro-inflammatory IL-6
- Reduced STAT3 and TLR4 activity normalized IL-6 release from Fragile X astrocytes

#### **4.5. Author Contributions**

This study was designed by V. Krasovska, K.E. Reynolds, and A.L. Scott. K.E. Reynolds designed and performed all experiments and data analysis involving UTP treatments (Figures 1,2). V. Krasovska designed and performed experiments involving TNC treatment, STAT3 knockdown, TAK242 treatment, and IL-6 receptor detection (Figures 2-5), while K.E. Reynolds analyzed, presented, and interpreted this data in a purinergic context. The manuscript was written by K.E. Reynolds, and all figures were created by K.E. Reynolds. The manuscript was edited by A.L. Scott and reviewed by V. Krasovska prior to submission. Relevant images and data have been reproduced in this manuscript with permission from V. Krasovska (see Appendix: Copyright Transfer Agreements). Data from experiments carried out by V. Krasovska can also be found in its original format in V. Krasovska's Master of Science thesis:

Krasovska, V. (2018). *Activation of TLR4 by Tenascin C through the induction of Interleukin-6 in the Fragile X mouse model* [Master of Science Thesis, McMaster University]. MacSphere: <http://hdl.handle.net/11375/23708>.

#### **4.6. Abstract**

The symptoms of Fragile X syndrome (FXS) are driven in part by abnormal glial-mediated function. FXS astrocytes release elevated levels of immune-related factors interleukin-6 (IL-6) and tenascin C (TNC), and also demonstrate increased purinergic signalling, a pathway linked to signalling factor release. Here, in cortical astrocytes from the *Fmr1* knockout (KO) FXS mouse model, purinergic agonism enhanced TNC secretion and STAT3 phosphorylation, two processes linked to elevated IL-6 secretion in FXS, while STAT3 knockdown and TLR4 antagonism normalized *Fmr1* KO IL-6 release. We therefore suggest that purinergic signalling and immune regulatory pathways cooperatively converge to drive FXS cortical pro-inflammatory responses.

#### 4.7. Introduction

Fragile X syndrome (FXS), the most common heritable form of autism spectrum disorders (ASD), is characterized by an absence of the FMRP protein resulting from expanded and hypermethylated CGG repeats within the *Fmr1* gene (Pieretti et al., 1991). FMRP is an RNA-binding protein involved in translational regulation and mRNA localization, and its absence in the FXS brain widely affects numerous cortical signalling pathways and leads to many cognitive-related symptoms, including intellectual disability, sensory hypersensitivity, and seizures (reviewed in Zoghbi & Bear, 2012). These neurological deficits appear to largely stem from pathology within key brain regions, including the cortex, hippocampus and striatum, that present with significant imbalances to excitatory-inhibitory activity (Gibson, Bartley, Hays, & Huber, 2008), as well as aberrant synaptogenesis and neurotransmitter release (Zoghbi & Bear, 2012). Due to the myriad of functions and downstream targets of FMRP, the underlying molecular mechanisms remain poorly understood. Interestingly, several studies have associated FXS with dysregulation of immune-related pathways as similarly found for ASDs. In this context, examination of glia, the immune cells of the CNS, has revealed that abnormal astrocyte-mediated function may be a prominent component of FXS neurological pathology (Krasovska & Doering, 2018; Yuskaitis, Beurel, & Jope, 2010).

Expression and secretion of astrocyte soluble factors involved in both synaptogenesis and immune function have recently been shown to be upregulated in primary cortical astrocyte cultures derived from the *Fmr1* knockout (KO) mouse model of FXS. Specifically, our recent work has identified increased expression and secretion of the glycoprotein tenascin C (TNC) and the pro-inflammatory cytokine interleukin-6 (IL-6) (Krasovska & Doering, 2018). TNC, which contributes to extracellular matrix (ECM) remodeling, neuronal migration, and synaptic plasticity (Jones & Bouvier, 2014; Stamenkovic et al., 2017), also drives secretion of pro-inflammatory cytokines IL-6, interleukin-1 $\beta$  (IL-1 $\beta$ ), interleukin-8 (IL-8), and tumour necrosis factor  $\alpha$  (TNF $\alpha$ ) through activation of toll-like receptor 4 (TLR4) (El-Hage, Podhaizer, Sturgill, & Hauser, 2011;

Jones & Bouvier, 2014; Maqbool et al., 2016; Midwood et al., 2009). TLR4-stimulated release of pro-inflammatory factors has been linked to the activation of the signal transducer of transcription 3 (STAT3) transcription factor (Greenhill et al., 2011). Phosphorylation of STAT3 induces dimerization and translocation into the nucleus, where it initiates production of pro-inflammatory cytokines, including IL-6 (reviewed in Wang & Sun, 2014). Heightened levels of IL-6 promote excess excitatory synaptogenesis and reduce inhibitory synaptogenesis, consistent with excitatory-inhibitory neuronal connectivity imbalances noted in ASD (Gibson et al., 2008; Wei et al. 2012). Indeed, elevated levels of IL-6 have been reported in the brain (Li et al., 2009), plasma (Ashwood et al., 2011), and lymphoblasts (Malik et al., 2011) of individuals with ASD.

Astrocyte-mediated immune signalling is regulated, at least in part, by the purinergic signalling system. Purinergic signalling is mediated by purine or pyrimidine nucleotides (*e.g.* ATP and UTP, respectively) and nucleosides that differentially act on either P2 or P1 receptors (Abbracchio, Burnstock, Verkhratsky, & Zimmermann, 2009). Activation of the P2Y receptor subfamily promotes the expression and release of IL-6 in various cell types. For example, UTP stimulated IL-6 secretion in thyrocytes (Caraccio et al., 2005), while IL-6 mRNA was upregulated in cardiac fibroblasts following UTP treatment (Braun, Lu, Aroonsakool, & Insel, 2010). UTP activation of subfamily members P2Y<sub>2</sub> and P2Y<sub>4</sub> was shown to phosphorylate STAT3 in rat cortical astrocytes (Washburn & Neary, 2006), while P2Y<sub>2</sub> agonism also promoted STAT3 activation in human keratinocyte cultures (Jokela et al., 2017). Lack of FMRP is correlated with purinergic upregulation, as *Fmr1* KO mouse cortical astrocytes were recently found to display elevated P2Y<sub>2</sub> and P2Y<sub>6</sub> receptor expression and prolonged activation via ATP and UTP, an effect prevented when treated with a pan purinergic receptor antagonist (Reynolds, Wong, & Scott, 2021; Tran & Neary, 2006). Given this, we aimed to determine if elevated astrocyte purinergic signalling drove the TNC-TLR4-STAT3-IL6 relationship, and whether blockade of this pathway would minimize pathological IL-6 release in FXS. Briefly, we found that P2Y agonism enhanced TNC secretion and STAT3 activation, and both STAT3 knockdown and TLR4 antagonism were sufficient to normalize pathological

IL-6 release by *Fmr1* KO astrocytes. This suggests that further investigation of purinergic regulation of pro-inflammatory pathways may provide new insight to target cortical astrocyte dysregulation in FXS.

#### **4.8. Methods**

**Animals.** WT and *Fmr1*<sup>-/-</sup> mice (*Fmr1* KO; FVB.129P2[B6]-*Fmr1*<sup>tm1Cgr</sup>) were housed and bred in the McMaster University Central Animal Facility. All experiments and mouse handling procedures followed the guidelines set by the Canadian Council on Animal Care and were approved by the McMaster Animal Research Ethics Board (Animal Utilization Protocol 17-04-11).

**Primary Cortical Astrocyte Culture.** Primary cortical astrocyte cultures were created from WT and *Fmr1* KO mice using a glial-selective primary culture protocol described by Jacobs & Doering (2009). Mouse pups were euthanized by decapitation at postnatal day (P) 1-3, and skin, skull, meninges, and hippocampus were removed to isolate cortical tissue. Cortical tissue was combined from a total of three pups in each culture, then dissociated in calcium- and magnesium-free Hanks' buffered saline solution (Invitrogen, Waltham, MA, USA) plus 1 mg/mL DNase (Roche Applied Science) and 0.25% trypsin (Invitrogen). Dissociated cells were seeded in a glial-selective medium containing minimum essential media, 0.6% glucose, and 10% horse serum (Invitrogen). Primary cultures were maintained at 37°C and 5% CO<sub>2</sub> in a humidified incubator for 6-8 days, or until >75% confluent. Astrocytes were then seeded onto 6-well plates (100,000 cells per well) or 12 mm coverslips (5,000 cells per well) coated with poly-L-lysine (1 mg/mL; Sigma-Aldrich, St. Louis, MO, USA) and laminin (10 µg/mL; Invitrogen) for collection, treatment, transfection, and/or imaging.

A total of 6 experimental samples per genotype (n=6), from separate primary astrocyte cultures (3 pups/culture) produced from individual litters were utilized to detect secreted TNC following UTP treatment. Cell-associated WT naïve and 1 µM UTP-treated groups also utilized 6 separate cultures from individual litters (n=6), while a total of 3

cultures obtained from separate litters (n=3) were utilized to detect cell-associated TNC in the WT 100  $\mu$ M UTP condition. All *Fmr1* KO cell-associated TNC treatment groups were comprised of 5 experimental samples obtained from separate cultures produced from individual litters (n=5). For WT UTP-treated pSTAT3:STAT3 analysis, 3 samples per treatment group (n=3) were produced from separate cultures created from individual litters. Four samples per treatment group (n=4) were produced from individual cultures and litters for all *Fmr1* KO UTP-treated pSTAT3:STAT3 conditions, as well as for both genotypes of exTNC-treated astrocytes in pSTAT3:STAT3 and s/IL-6R experiments. Four separate primary cultures of each genotype, obtained from individual mouse litters (n=4), were transfected with STAT3 siRNA and analyzed in STAT3 knockdown experiments; ELISA was performed with duplicate technical replicates, which were averaged to create each data point. Four individual litters and cultures (n=4) were obtained per genotype for TLR4 Western blotting, while three distinct litters and cultures of each genotype (n=3), analyzed in duplicate, were utilized for TLR4 antagonism ELISAs.

**Treatments.** WT and *Fmr1* KO primary cortical astrocytes seeded on 6 well plates (Corning, NY, USA) were grown for an additional 4.5 days *in vitro* (DIV) in serum-free minimum essential media (Invitrogen) supplemented with 0.6% glucose, achieving >75% confluency. After 4 DIV, astrocytes in P2Y agonism experiments were treated for 12 h with UTP (ThermoFisher, Waltham, MA, USA) at concentrations of 1  $\mu$ M and 100  $\mu$ M, diluted in 0.1 M phosphate-buffered saline (PBS; Life Technologies, Waltham, MA, USA). Alternatively, astrocytes in exogenous TNC experiments were treated for 3 h with exogenous chicken TNC (exTNC; Millipore Cat# CC118) at a concentration of 10  $\mu$ g/mL, while astrocytes used in TLR4 antagonist experiments were treated for 6 h with 5  $\mu$ g/mL TAK242 (Millipore Cat# 614316). When TNC was tested for its ability to rescue reduced IL-6 release after TLR4 antagonism, 10  $\mu$ g/mL exTNC was applied for 24 h following TAK242 treatment. Following treatment, astrocyte-conditioned media (ACM) was removed from cells and filtered using a 0.22  $\mu$ m syringe filter. Secreted protein was concentrated using a 10 kDa molecular weight cut-off ultrafiltration device (Vivaspin, GE Healthcare, Chicago, IL, USA), and flash frozen in isopentane until quantification. In

addition to ACM removal, astrocyte cultures were trypsinized (0.05% trypsin-EDTA; Invitrogen) and pelleted for collection prior to Western blotting.

**Western Blotting.** UTP-treated astrocyte samples were homogenized in 1X Brain Extraction Buffer (25 mM HEPES pH 7.3, 150 mM KCl, 8% glycerol, 0.1% NP-40, one Roche ULTRA protease inhibitor tablet, and one Roche PhoSTOP phosphatase inhibitor tablet) (Reynolds et al., 2021), while exogenous TNC-treated astrocyte samples were homogenized in RIPA lysis buffer (150 mM NaCl, 1% NP-40, 0.5% deoxycholic acid, 1% SDS, 50 mM Tris, one Roche ULTRA protease inhibitor tablet, one Roche PhoSTOP phosphatase inhibitor tablet) (Krasovska & Doering, 2018). Following homogenization, the protein concentration of each cell-associated and ACM sample was determined using a DC protein assay (Bio-Rad, Mississauga, ON, CA).

ACM and cell-associated samples containing 30 µg of protein were combined with sample buffer (2.5% β-mercaptoethanol in Laemmli sample buffer, Bio-Rad), boiled at 95°C for 5 mins, and loaded onto 4-15% precast polyacrylamide stain-free gels (Bio-Rad). Proteins were separated via electrophoresis, activated with UV light (302nm) to permit visualization of ‘total protein’ (tryptophan) via Bio-Rad stain-free technology, and transferred onto polyvinylidene difluoride (PVDF) membranes (Bio-Rad) using the Trans-Blot Turbo Transfer System (Bio-Rad). The membranes were imaged for total loaded protein using a ChemiDoc Imaging System (Bio-Rad), then blocked for 1h in 5% non-fat milk solution diluted in Tris-buffered saline solution with Tween-20 (TBS-T). Each membrane was incubated overnight at 4°C in TBS-T containing one of the following primary antibodies: Tenascin C (rat monoclonal; 1:250; R&D Systems, Minneapolis, MN, USA Cat# MAB2138, RRID:AB\_2203818; ~250 kDa), STAT3 (mouse monoclonal; 1:1000; Cell Signaling Technology, Danvers, MA, USA Cat# 9139, RRID:AB\_331757; ~86 kDa), phosphorylated STAT3 (Tyr 705) (pSTAT3; rabbit polyclonal; 1:1000; Cell Signaling Technology Cat# 9131, RRID:AB\_331586; ~86 kDa), TLR4 (mouse monoclonal; 1:250; Novus Biologicals, Centennial, CO, USA Cat# NB100-56566, RRID:AB\_2205129; ~95 kDa), and IL-6R (rabbit polyclonal; 1:500; Abcam, Cat#

ab128008, RRID:AB\_11142611; ~60 kDa and ~52 kDa bands). Following incubation, the membranes were then washed 3 x 10 minutes in TBS-T and incubated in TBS-T containing horseradish peroxidase conjugated secondary antibody against rat (1:10,000; Abcam), mouse (1:5000; GE Healthcare Life Sciences) or rabbit (1:2500; GE Healthcare Life Sciences) for 1 h at room temperature. Membranes were developed using Clarity enhanced chemiluminescence substrate (Bio-Rad) and a ChemiDoc Imaging System (Bio-Rad).

Densitometry measurements were conducted using Image Lab Software 6.0.1 (Bio-Rad). Each band corresponding to either TNC (~250 kDa), STAT3 (~86 kDa), pSTAT3 (~86 kDa), TLR4 (~95 kDa), or IL-6R (~60 kDa and ~52 kDa) was first normalized to total protein within the same lane, and then to a cross-gel control sample which permitted direct comparison of band densities across multiple membranes. These values were then expressed as a fold change of the average densitometry value, relative to mean control protein levels. To determine the proportion of pSTAT3 relative to total STAT3 within paired samples, the normalized pSTAT3 density was divided by the normalized STAT3 density for each set of identical samples.

***STAT3 siRNA Knockdown and ELISA.*** WT and *Fmr1* KO primary cortical astrocytes were transfected using liposome-mediated transfection reagent Lipofectamine RNAiMAX (Invitrogen) with 50 nM STAT3 siRNA(1) or siRNA(2), according to manufacturer instructions, then maintained for 3 DIV prior to ACM collection and/or treatment with exogenous TNC. In the STAT3 siRNA+exTNC experimental condition, cells were first transfected with STAT3 siRNA(1), incubated for 3 DIV, then treated with exogenous chicken TNC (10 µg/mL; Millipore Cat# CC118) for 3 h prior to ACM collection. ACM was filtered using a 0.22 µm syringe filter, then concentrated with a 10 kDa molecular weight cutoff ultrafiltration device (Vivaspin, GE Healthcare, Chicago, IL, USA). Secreted IL-6 in ACM was quantified using an enzyme-linked immunosorbent assay (ELISA; Invitrogen Cat# KMC0061) according to manufacturer instructions.

Post-transfection cell survival was determined by the use of a dead cell dye from the BLOCK-iT Transfection Optimization Kit (Invitrogen). Dead cell dye-stained cells were counted at 10x objective magnification using a Zeiss Axio Imager.M2 epifluorescent microscope (Carl Zeiss, Oberkochen, Germany), and expressed as a percentage of total cultured cells. Transfection efficacy was determined by transfecting primary cortical astrocytes with 25% STAT3 siRNA and 75% fluorescent oligonucleotide (Invitrogen), visualizing fluorescent cells at 10x objective magnification, and counting the percentage of fluorescent cells versus total cells within the analyzed fields of view. Samples obtained from three separate cultures produced from individual litters (n=3) were analyzed for each genotype.

***Immunocytochemistry.*** Representative IL-6R immunocytochemistry was carried out with primary cortical astrocyte cultures plated on PLL/laminin-coated 12 mm coverslips (5000 cells/coverslip; Neuvitro, Vancouver, WA, USA). Following a protocol previously described by Cheng et al. (2016), plated astrocytes were fixed with 4% paraformaldehyde (Sigma-Aldrich), then permeabilized with 0.1% Triton-X-100 (BDH Chemicals, Radnor, PA, USA). Non-specific binding was blocked with 1% bovine serum albumin (Sigma-Aldrich), then a combination of IL-6R (rabbit polyclonal; 1:500; Abcam, Cat# ab128008, RRID:AB\_11142611) and GFAP (chicken, 1:2000; CH22102; Neuromics, Minneapolis, MN, USA) primary antibodies were prepared in PBS and applied overnight at 4°C. Donkey anti-rabbit Alexa Fluor 488 (1:200; Invitrogen Cat# A-11008) and rabbit anti-chicken tetramethylrhodamine (TRITC) (1:100; Jackson ImmunoResearch, West Grove, PA, USAA Cat# 303-025-003) secondary antibodies were applied for 3 h at room temperature prior to coverslip mounting with ProLong Gold Antifade Mountant with 4', 6-diamidino-2-phenylindole (Life Technologies, Carlsbad, CA, USA). Representative images of immunolabelled astrocytes were acquired using a Zeiss Axio Imager.M2 epifluorescent microscope (Carl Zeiss), AxioCam 506 camera (Carl Zeiss), and ZEN Blue (Carl Zeiss) acquisition software.

**Statistical Analysis.** All graphing and statistical analyses were conducted using GraphPad Prism Software 9.0 (GraphPad Software Inc., San Diego, CA, USA). Comparisons between two means were performed using unpaired two-tailed t-tests. Repeated measures one-way analysis of variance (ANOVA) followed by a Sidak multiple comparisons test was used to compare data sets within a single genotype with three or more paired samples. However, in the case of intracellular TNC following 12 h UTP treatment, a mixed-effects model followed by a Sidak multiple comparisons test was used due to one missing *Fmr1* KO paired sample per treatment group resulting from low sample yield. Two-way ANOVA followed by a Sidak multiple comparisons test was chosen to detect differences between multiple treatment groups when genotypes were directly compared, as in IL-6 ELISA experiments. Results of both t-tests and multiple comparisons tests were deemed significant when  $p < 0.05$ . All results are presented as means  $\pm$  standard error of the mean (SEM).

#### 4.9. Results

##### ***UTP increases secretion of TNC in WT but not Fmr1 KO cortical astrocytes***

Previous research from our group has shown that TNC release and cellular expression are both upregulated in FXS (Krasovska & Doering, 2018). To determine whether these cortical TNC levels are influenced by P2Y receptor activation, we treated WT and *Fmr1* KO primary astrocyte cultures with exogenous UTP, then compared secreted and cell-associated TNC levels using Western blotting. In WT cortical astrocytes, treatment with 1  $\mu$ M UTP led to a significant increase in secreted TNC present in ACM after 12 h ( $n=6$ ;  $p=0.0223$ ; Fig.1A,B) relative to naïve controls, but not in cell-associated TNC ( $n=6$ ;  $p=0.0797$ ; Fig.1D,E). In contrast, application of a higher concentration of purinergic agonist, 100  $\mu$ M UTP, did not significantly impact either TNC secretion ( $n=6$ ;  $p=0.1389$ ; Fig.1A,B) or cell-associated expression ( $n=3$ ;  $p=0.6162$ ; Fig.1D,E).

While WT astrocytes modulated TNC secretion in response to UTP treatment, P2Y receptor activation did not lead to any differences for *Fmr1* KO astrocytes. Neither 1  $\mu$ M UTP nor 100  $\mu$ M UTP treatment impacted the secretion of TNC relative to *Fmr1* KO naïve

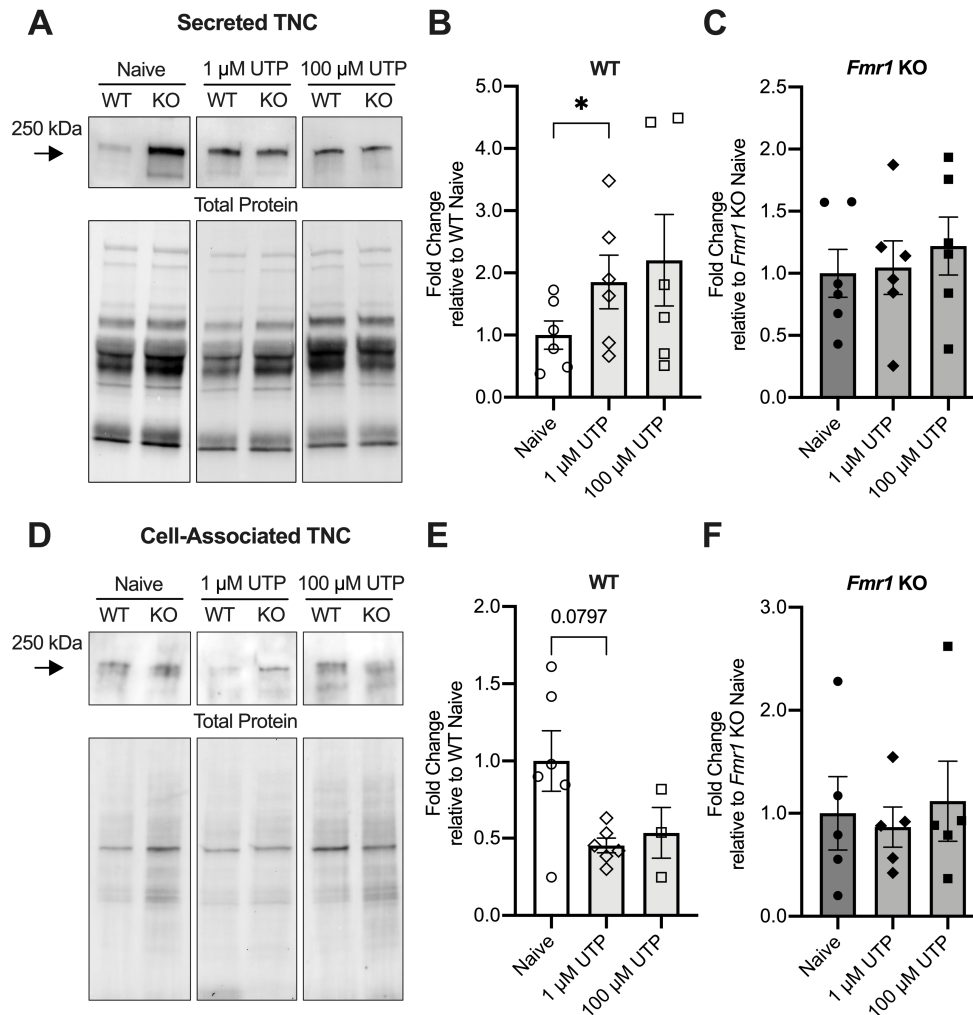


Figure 1. Secreted and cell-associated TNC following application of exogenous UTP to WT and *Fmr1* KO cortical astrocyte cultures. A. Representative Western blotting images of TNC (~250 kDa) detected in WT and *Fmr1* KO astrocyte-conditioned media following 12 h cell treatment with 1  $\mu$ M UTP, 100  $\mu$ M UTP, or naïve controls (n=6), plus corresponding total protein images utilized as loading controls for densitometry. B. TNC secretion from WT UTP-treated astrocytes relative to WT naïve levels, showing elevated TNC secretion following 1  $\mu$ M UTP treatment. C. *Fmr1* KO UTP-treated astrocytes relative to *Fmr1* KO naïve levels, showing no difference in secreted TNC following exogenous UTP application. D. Representative Western blotting images of cell-associated TNC (~250 kDa) detected in WT (naïve/1  $\mu$ M UTP n=6; 100  $\mu$ M UTP n=3) and *Fmr1* KO (n=5) astrocyte cultures following 12h UTP treatment, plus corresponding total protein images. Cell-associated TNC levels were unchanged following UTP treatment in both (E) WT and (F) *Fmr1* KO astrocyte cultures, relative to their respective naïve levels. All data presented as means  $\pm$  SEM. Significant differences between treatments denoted by \*; p<0.05.

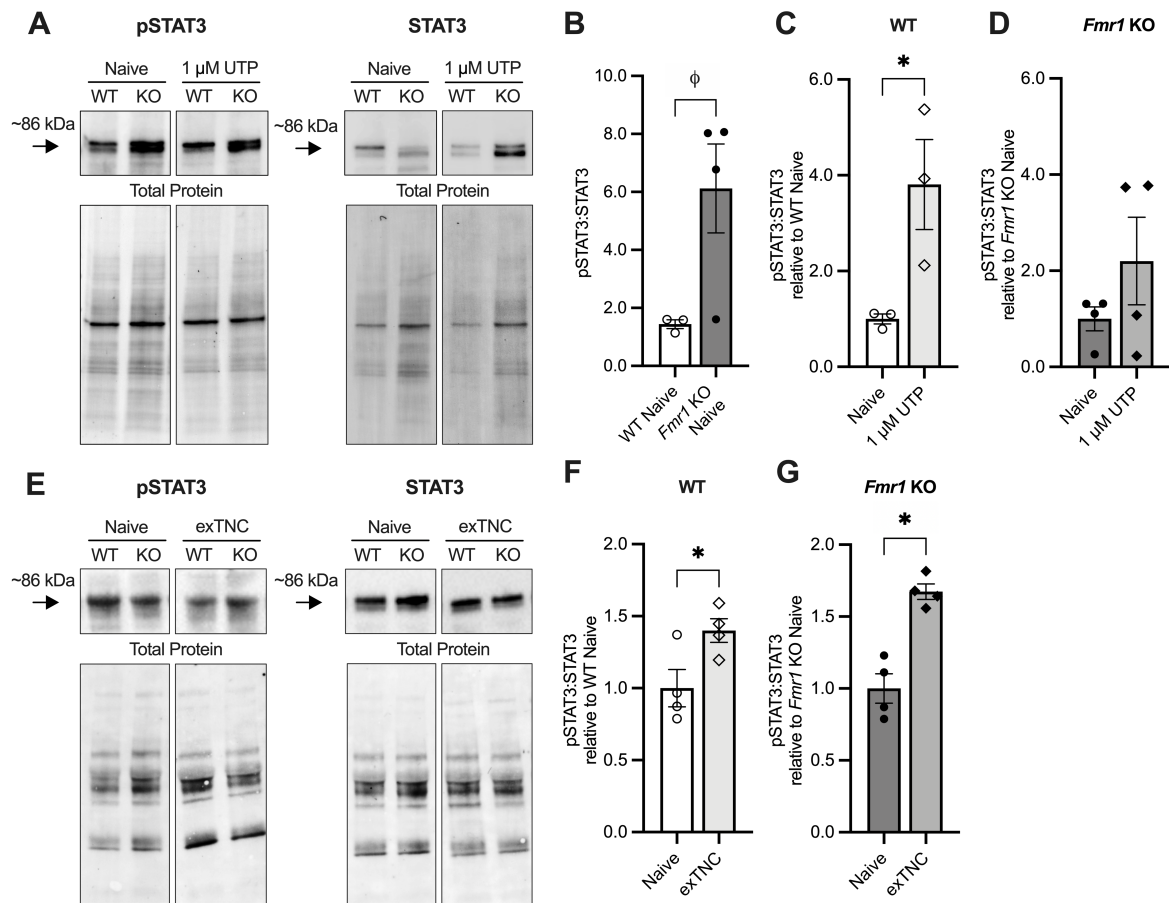


Figure 2. Proportion of tyrosine-phosphorylated STAT3 vs total STAT3 in WT and *Fmr1* KO cortical astrocyte cultures treated with exogenous UTP and TNC. A. Representative Western blots of tyrosine-705 phosphorylated STAT3 (pSTAT3;  $\sim$ 86 kDa) and total STAT3 ( $\sim$ 86 kDa) in WT (n=3) and *Fmr1* KO (n=4) primary astrocytes following 12h treatment with 1  $\mu$ M UTP. Corresponding total protein images were utilized as loading controls for densitometry. B. Comparison between pSTAT3:STAT3 in WT vs *Fmr1* KO naïve astrocytes, indicating a significantly higher proportion of pSTAT3 relative to STAT3 in *Fmr1* KO astrocytes. C-D. Comparison between pSTAT3:STAT3 in naïve vs 1  $\mu$ M UTP-treated (C) WT and (D) *Fmr1* KO astrocytes, relative to their respective naïve controls. E. Representative Western blots of pSTAT3 and total STAT3 in WT and *Fmr1* KO primary astrocytes (n=4) following 3 h treatment with 10  $\mu$ g/mL exogenous TNC (exTNC), plus corresponding total protein images. F-G. Comparison between pSTAT3:STAT3 in naïve vs exTNC-treated (F) WT and (G) *Fmr1* KO astrocytes relative to their respective naïve controls, showing increased pSTAT3 relative to STAT3 following exTNC treatment in both genotypes. All data presented as means  $\pm$  SEM. Significant differences between genotypes denoted by  $\phi$ ; significant differences between treatments denoted by \*;  $p < 0.05$ .

controls (n=6; p=0.9633 and p=0.1204 respectively; Fig.1A,C). Cell-associated TNC levels were also unchanged following treatment with either concentration of UTP (n=5; p=0.9631 and p=0.9169 respectively; Fig.1D,F).

***UTP and TNC increase the proportion of tyrosine-705 phosphorylated STAT3 in both WT and Fmr1 KO cortical astrocytes***

We have also recently demonstrated that exogenous TNC (exTNC) treatment increases astrocyte production and secretion of IL-6 (Krasovska & Doering, 2018), a process which is regulated in part by tyrosine-705 phosphorylation of STAT3. We therefore investigated the proportion of tyrosine-705 phosphorylated STAT3 (pSTAT3) relative to total STAT3 in *Fmr1* KO and WT astrocytes following both UTP and exTNC treatments. To determine the proportion of pSTAT3, samples were probed for both pSTAT3 and total STAT3 using Western blotting, and normalized densitometry volumes from both pSTAT3 and STAT3 blots were subsequently divided and expressed in relation to naïve controls. Given that the pSTAT3 and STAT3 antibodies were applied to separate Western blots with different affinities and enhanced chemiluminescent substrate exposure times, the resultant normalized values represent relative proportions, not absolute quantifications.

In naïve astrocytes, the baseline proportion of pSTAT3:STAT3 was elevated in *Fmr1* KO cells (n=4) relative to WT (n=3; p=0.0498; Fig.2B). However, the total amount of astrocyte intracellular STAT3 present was not impacted by genotype (data not shown). Treatment with 1  $\mu$ M UTP also increased pSTAT3 relative to total STAT3 in WT astrocytes (n=3; p=0.0414; Fig.2C). In contrast, UTP treatment did not further enhance the pSTAT3:STAT3 proportion in *Fmr1* KO astrocytes (n=4; p=2506; Fig.2D) relative to naïve *Fmr1* KO controls. When both WT and *Fmr1* KO astrocytes were treated with 10  $\mu$ g/mL exTNC, the proportion of phosphorylated STAT3 to total STAT3 also significantly increased in both genotypes, relative to their respective naïve controls (WT p=0.0399 and *Fmr1* KO p=0.0011; Fig.2F-G).

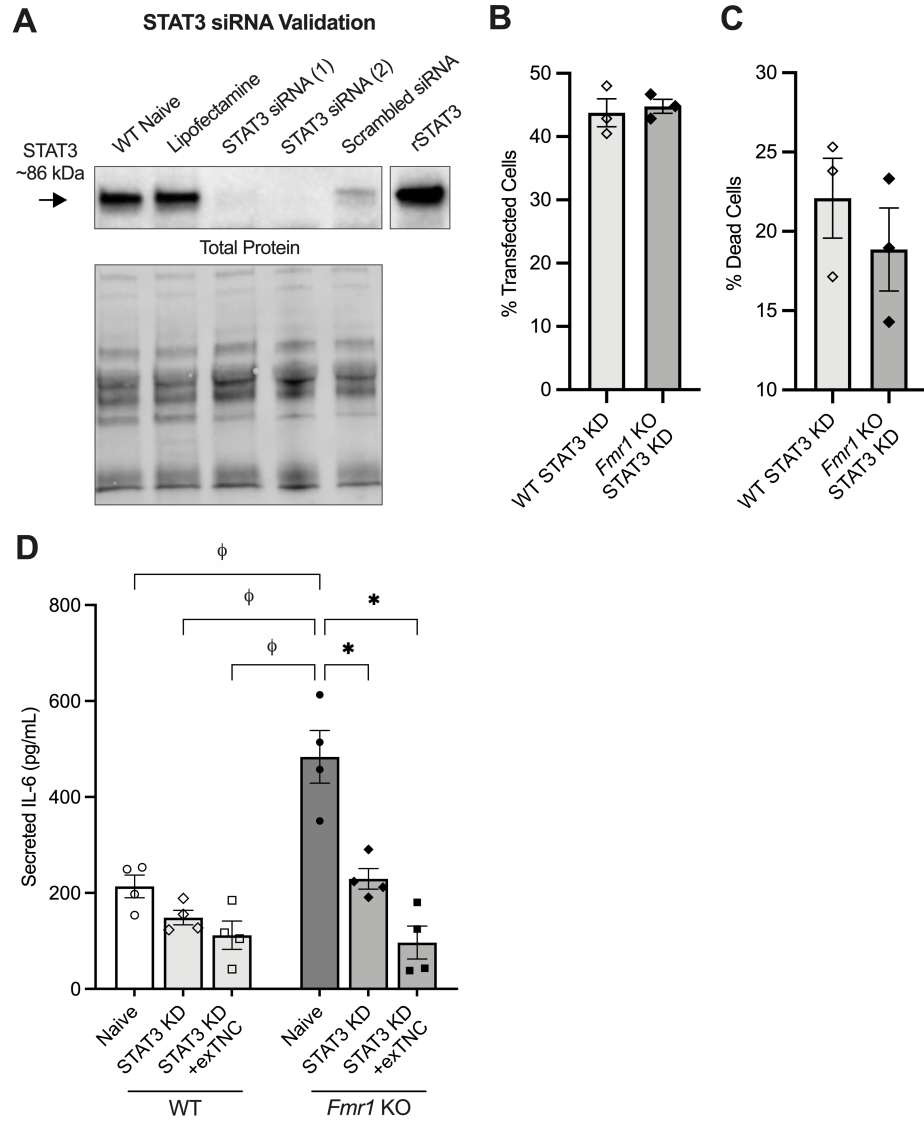


Figure 3. IL-6 secretion from WT and *Fmr1* KO cortical astrocytes following STAT3 knockdown. A. STAT3 siRNA validation Western blot and corresponding total protein loading control demonstrating STAT3 (~86 kDa) levels in WT primary cortical astrocytes following transfection with STAT3 siRNA, lipofectamine (no siRNA), scrambled siRNA control, and recombinant STAT3 (rSTAT3). B. Transfection efficiency in WT vs *Fmr1* KO astrocytes (n=3) transfected with STAT3 siRNA plus a fluorescent oligonucleotide, showing no difference in transfection efficiency between genotypes. C. Analysis of post-transfection cell survival in WT vs *Fmr1* KO astrocytes (n=3) stained with dead cell dye, showing no difference in cell death between genotypes. D. Quantification of IL-6 (pg/mL) secreted from WT and *Fmr1* KO cortical astrocyte cultures (n=4) following STAT3 siRNA knockdown and exogenous TNC (exTNC) treatment, showing that elevated IL-6 secretion from *Fmr1* KO naïve astrocytes was reduced to WT levels following *Fmr1* KO STAT3 knockdown.

***STAT3 knockdown decreases IL-6 secretion from Fmr1 KO but not WT cortical astrocytes, and is unable to be rescued by exogenous TNC***

Given that both UTP and TNC elevated the proportion of tyrosine-phosphorylated, active STAT3 in cortical astrocytes, we aimed to determine the downstream impact that the STAT3 pathway might have on cytokine release in the *Fmr1* KO cortex relative to WT. We have previously shown that cortical astrocyte-secreted levels of IL-6 are elevated in the FXS mouse (Krasovska & Doering, 2018), while LPS stimulation of glial IL-6 production can be reduced by both STAT3 knockdown and pharmacological STAT3 inhibition (Beurel & Jope, 2009). We therefore tested whether STAT3 differentially regulated IL-6 secretion in WT versus *Fmr1* KO cortical astrocytes by knocking down STAT3 expression in astrocyte primary culture and measuring secreted levels of IL-6.

To validate siRNA knockdown, WT primary cortical astrocyte cultures were first transfected with one of two distinct STAT3 siRNAs (STAT3 siRNA(1) and siRNA(2)), then probed for STAT3 using Western blotting. Both siRNAs were observed to visibly decrease astrocyte STAT3 levels in knockdown conditions, in comparison to naïve astrocytes, a lipofectamine-transfected negative control, a scrambled siRNA-transfected negative control, and recombinant STAT3 protein (Fig.3A). STAT3 siRNA(1) was subsequently chosen for future knockdown experiments. Transfection efficacy was determined to be approximately 40-45% in both WT and *Fmr1* KO astrocytes ( $p=0.4229$ ; Fig.3B) through the use of co-transfection with a fluorescent oligonucleotide. Cell viability was not significantly impacted between genotypes following STAT3 knockdown with siRNA(1) ( $p=0.7055$ ; Fig.3C).

Using ELISA, we observed a ~100% increase of IL-6 secretion from naïve *Fmr1* KO astrocytes ( $n=4$ ; 483.601 pg/mL) compared to naïve WT astrocytes ( $n=4$ ; 213.598 pg/mL;  $p=0.0002$ ; Fig.3D). STAT3 knockdown decreased IL-6 secretion from *Fmr1* KO astrocytes to 229.35 pg/mL ( $p=0.0004$ ; Fig.3D), and essentially normalized it to WT naïve levels ( $p>0.9999$ ; Fig.3D). Conversely, in WT ACM, STAT3 knockdown did not

significantly impact IL-6 secretion in comparison to WT controls (148.631 pg/mL;  $p=0.9427$ ; Fig.3D).

TNC increases secretion of IL-6 from both *Fmr1* KO and WT astrocytes, as demonstrated by our recent work (Krasovska & Doering, 2018). To determine whether this increase occurs in the absence of STAT activation, we treated STAT3 knockdown astrocytes of both genotypes ( $n=4$ ) with 10  $\mu\text{g/mL}$  exTNC for 3 h prior to ACM collection. *Fmr1* KO IL-6 secretion from exTNC-treated cells was not statistically different from that observed from *Fmr1* KO astrocytes with STAT3 knockdown ( $p=0.1355$ ; Fig.3D), but was significantly reduced in comparison to *Fmr1* KO naïve controls ( $n=4$ ;  $p<0.0001$ ; Fig.3D). WT IL-6 secretion following exTNC treatment remained unchanged relative to both WT STAT3 knockdown ( $p=0.9998$ ; Fig.3D) and WT naïve conditions ( $p=0.4557$ ; Fig.3D).

#### ***TLR4 antagonist TAK242 reduces IL-6 secretion from both WT and Fmr1 KO astrocytes***

As astrocyte IL-6 secretion is linked to TNC binding of TLR4 receptors (Krasovska & Doering, 2018; Zuliani-Alvarez et al., 2017), we next aimed to determine whether pathological *Fmr1* KO IL-6 secretion could also be normalized by blocking the TLR4 receptor. It was first important to determine whether the levels of TLR4 receptors differed between WT and *Fmr1* KO astrocytes, as excess receptor availability could drive elevated cytokine expression. Consistent with our previously published findings in cortical homogenates (Krasovska & Doering, 2018), TLR4 expression was indeed unaltered between WT and *Fmr1* KO astrocytes in vitro ( $p=0.2903$ ; Fig.4A,B). In naïve conditions, we again observed a substantial increase in IL-6 secretion from *Fmr1* KO astrocytes relative to WT ( $n=3$ ;  $p=0.0026$ ; Fig.4C). Blockade of TLR4 in astrocyte cultures was achieved using a specific TLR4 antagonist TAK242. TAK242 selectively binds to an intracellular domain of TLR4 and prevents it from interacting with adaptor molecules and initiating downstream signalling events (Matsunaga et al., 2010). Using TAK242 (5  $\mu\text{g/mL}$ ) led to a dramatic decrease of IL-6 secretion (to 66.8248 pg/mL) from *Fmr1* KO astrocytes.

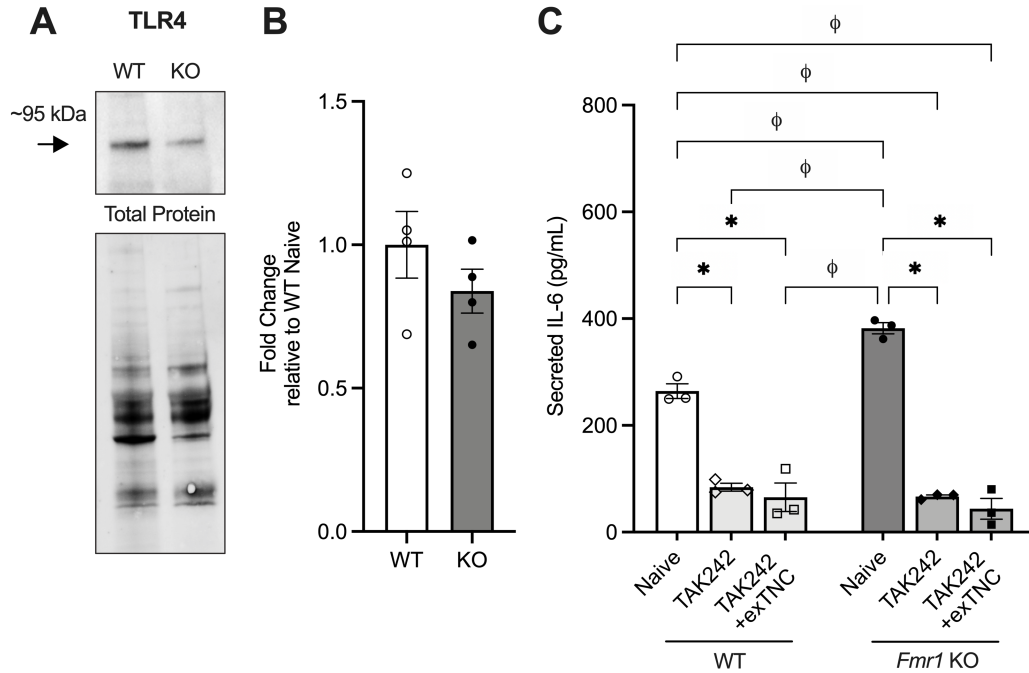


Figure 4. IL-6 secretion from WT and *Fmr1* KO cortical astrocytes following TLR4 antagonism. A. Representative Western blots of cell-associated TLR4 (~95 kDa) in WT and *Fmr1* KO astrocyte cultures. Corresponding total protein images were utilized as loading controls to permit quantification. B. TLR4 receptor levels did not differ between WT and *Fmr1* KO astrocytes *in vitro*. C. Quantification of IL-6 (pg/mL) secreted from WT and *Fmr1* KO cortical astrocyte cultures (n=3) following TLR4 antagonism with 5 ug/mL TAK242 plus co-treatment with 10  $\mu$ g/mL exTNC, demonstrating significant reduction in IL-6 secretion from both genotypes following TAK242 treatment. All data presented as means  $\pm$  SEM. Significant between-genotype differences denoted by  $\phi$ ; significant within-genotype differences denoted by \*;  $p < 0.05$ .

This TAK242-induced decrease in secretion represented a significant difference relative to both *Fmr1* KO naïve ( $p < 0.0001$ ) and WT naïve ( $p < 0.0001$ ; Fig.4C). WT IL-6 secretion was also reduced relative to WT controls following TAK242 treatment, to a concentration of 84.1343 pg/mL ( $p < 0.0001$ ; Fig.4C).

When cells were co-treated with both exTNC and TAK242, both *Fmr1* KO and WT astrocytes were unable to rescue their respective naïve levels of IL-6 secretion (43.7437 pg/mL,  $p < 0.0001$  for *Fmr1* KO TAK242+exTNC and 65.3814 pg/mL,  $p < 0.0001$  for WT TAK242+exTNC; Fig.4C) and maintained secretion levels comparable to TAK242-only treatment (*Fmr1* KO  $p = 0.9966$  and WT  $p = 0.9996$ ; Fig.4C). All TAK242 treatment conditions across both genotypes reduced IL-6 secretion to comparably low concentrations in contrast to naïve levels, suggesting that TLR4 activity is necessary for astrocyte IL-6 release regardless of genotype.

#### ***TNC upregulates IL-6 receptor levels associated with Fmr1 KO but not WT cortical astrocytes***

While IL-6 production and secretion is known to be elevated by activation of STAT3, STAT3 can also be activated by binding of IL-6 to cell-associated or soluble IL-6 receptors (Legendre, Bogdanowicz, Boumediene, & Pujol, 2005). We therefore compared the presence of IL-6/soluble IL-6 receptors (s/IL-6R) between WT and *Fmr1* KO cortical astrocytes ( $n = 4$ ), both in the presence and absence of exogenous TNC. Baseline levels of s/IL-6R were visibly unchanged between WT and *Fmr1* KO naïve astrocytes, signifying equivalent capacity for IL-6 binding (Fig.5B). However, 3 h treatment with 10  $\mu\text{g/mL}$  exogenous TNC elevated cell-associated IL-6R levels in *Fmr1* KO astrocytes ( $p = 0.0209$ ; Fig.5C) relative to *Fmr1* KO naïve cells. No differences were observed following exTNC treatment in WT astrocytes ( $p = 0.9912$ ; Fig.5D). Representative immunocytochemistry confirmed s/IL-6R distribution within diffusely located puncta, as well as nuclear-adjacent regions consistent with potential receptor synthesis and distal regions consistent with potential membrane association (Fig.5A).

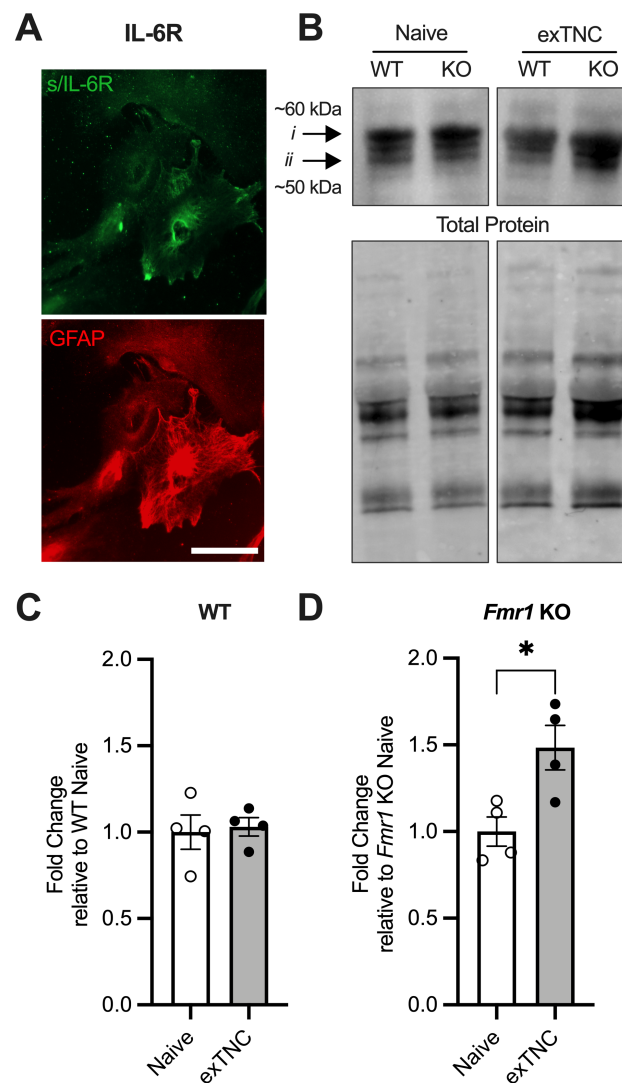


Figure 5. Soluble/bound IL-6 receptor (s/IL-6R) association with WT and *Fmr1* KO cortical astrocytes following 3 h treatment with TNC. A. Representative epifluorescent images showing distribution of cell-associated s/IL-6R in WT primary cortical astrocyte cultures (s/IL-6R, green; GFAP, red). Scale bar: 25 µm. B. Representative Western blots of cell-associated s/IL-6R detected in WT and *Fmr1* KO primary astrocyte cultures (n=4) following 3 h treatment with 10 µg/mL exogenous TNC (exTNC). s/IL-6R is represented by a band at ~52 kDa (*i*), while IL-6 coupled with s/IL-6R is represented by a band at ~60 kDa (*ii*). Corresponding total protein images were utilized as loading controls for densitometry. C. Cell-associated s/IL-6R levels were unchanged following exTNC treatment in WT astrocyte cultures, but (D) exTNC increased cell-associated s/IL-6R in *Fmr1* KO astrocyte cultures relative to *Fmr1* KO naïve levels. All data presented as means +/- SEM. Significant differences between treatments denoted by \*; p<0.05.

#### 4.10. Discussion

Absence of FMRP within the FXS cortex widely impacts signaling cascades, leading to aberrant release of soluble factors mediating various functions (Higashimori et al., 2016; Reynolds et al., 2021; Wallingford, Scott, Rodrigues, & Doering, 2017). In particular, our group has recently reported evidence of elevated IL-6 and TNC in *Fmr1* KO astrocytes, suggesting a potential immune mechanism associated with FXS (Krasovska & Doering, 2018). Here, we found that astrocyte secretion of TNC, which drives IL-6 release through activation of the TLR4 receptor (El-Hage et al., 2011; Maqbool et al., 2016; Midwood et al., 2009), was upregulated following P2Y receptor agonism, as was phosphorylation of the transcription factor STAT3 (Fig.6). Pathological IL-6 release from *Fmr1* KO astrocytes was normalized by both STAT3 knockdown and TLR4 antagonism and could not be rescued with exogenous TNC, emphasizing the role of STAT3 and TLR4 in cortical IL-6 regulation. Taken together, our findings suggest that purinergic signalling and immune regulatory pathways cooperatively converge to drive pro-inflammatory responses in the FXS cortex.

##### ***TNC secretion is elevated by P2Y receptor agonism***

Astrocyte soluble proteins with crucial roles in early postnatal cortical development, including potential immune responses, may be modulated through the action of purinergic receptors. Exogenous UTP stimulates select G protein-coupled P2Y receptors, including astrocyte P2Y<sub>2</sub>, P2Y<sub>4</sub>, and P2Y<sub>6</sub>, to promote signal transduction and modulate protein release (Abbracchio et al., 2009). Here, astrocyte TNC secretion was elevated following 1  $\mu$ M UTP treatment in WT astrocytes, a concentration roughly comparable to purine levels produced by local signalling events (Dobolyi et al., 1998). The lack of effect of a 100-fold higher UTP dose suggests that sustained P2Y activation causes WT astrocytes to shut down TNC secretion in a compensatory manner. Lower level P2Y receptor agonism appears to drive WT TNC secretion towards *Fmr1* KO naïve levels, indicating a potential mechanism underlying this FXS dysregulation. TNC is not the only

FXS-linked astrocyte soluble factor to be modulated by P2Y agonism, as we and others have recently demonstrated that exogenous UTP heightened release of the astrocyte-secreted synaptogenic protein TSP-1, through proposed mechanisms including MAPK and Akt phosphorylation (Reynolds et al., 2021; Tran & Neary, 2006). These genotypic differences in P2Y-driven TNC secretion provide additional evidence for widespread astrocyte dysfunction associated with a lack of FMRP. While there was a trend towards a significant decrease in astrocyte-associated levels of WT TNC, this was insignificant in our hands, and overall, we did not observe any differences in cell-associated TNC levels in either genotype following UTP treatment. However, relatively small sample sizes, coupled with a not-insignificant degree of variability within both secreted and cell-associated treatment groups throughout this study, may be considered a limitation of this work. Future work investigating additional UTP treatment durations, as well as quantifying TNC mRNA transcripts versus secretion, may clarify the role played by UTP in TNC regulation.

***Exogenous UTP and TNC increase tyrosine STAT3 phosphorylation in primary cortical astrocytes***

Phosphorylation of the STAT3 transcription factor is one method by which local astrocytes increase production of pro-inflammatory cytokines such as IL-6. STAT3 is phosphorylated at either serine or tyrosine residues, though it is tyrosine phosphorylation in conjunction with Janus kinase 1 (JAK1) that promotes nuclear translocation of STAT3 to impact gene expression (Guschin et al., 1995). Here, we observed a greater proportion of tyrosine-705 phosphorylated pSTAT3 relative to STAT3 in naïve cortical *Fmr1* KO versus WT astrocytes. STAT3 phosphorylation requires glycogen synthase kinase – 3 (GSK3) (Beurel & Jope, 2008), which is translationally regulated by FMRP (Luo et al., 2010) and proportionally more active within the cortex, hippocampus, and striatum of the *Fmr1* KO mouse brain (Yuskaitis, Mines, et al., 2010). Interestingly, GSK3 activity is also promoted by P2 receptor activation in astrocytes (Neary & Kang, 2006) and correlated with TLR4-driven cytokine release (Martin, Rehani, Jope, & Michalek, 2005). Although not

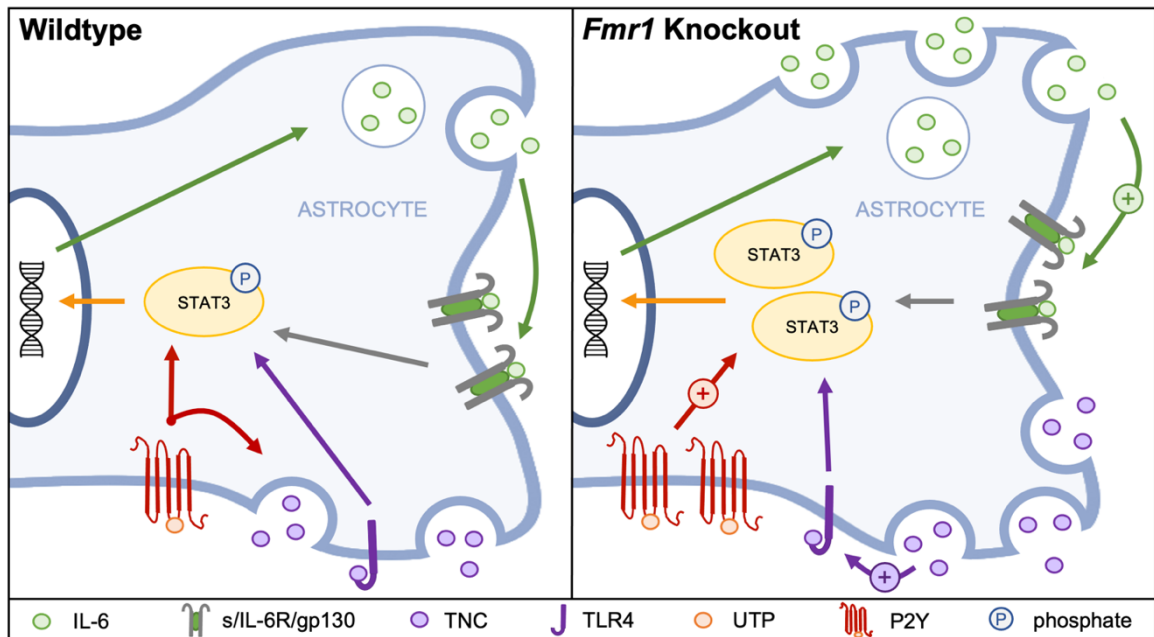


Figure 6. Proposed model of purinergic and immune interactions in cortical astrocytes. TNC (purple circles) binding at TLR4 receptors (purple) promotes STAT3 phosphorylation, nuclear translocation, and ultimately the production, secretion, and signalling of pro-inflammatory cytokines, including IL-6 (green circles). P2Y receptor (red) activation also promotes STAT3 phosphorylation, and drives wildtype secreted TNC release (left panel) in the direction of naïve *Fmr1* KO levels (right panel). The convergence of these signalling events on STAT3 phosphorylation, as well as the known FXS upregulations in purinergic P2Y receptor expression and TNC secretion, suggest a potential underlying mechanism of elevated IL-6 in FXS.

tested here, it is likely that GSK3 activation also contributes to increased *Fmr1* KO pro-inflammatory cytokine secretion.

Baseline elevations of both TNC secretion and STAT3 phosphorylation in *Fmr1* KO astrocytes are reminiscent of the upregulation of astrocyte purinergic and synaptic factors observed by our group (Reynolds et al., 2021; Wallingford et al., 2017). The lack of influence exogenous UTP had on *Fmr1* KO astrocytes in terms of either TNC or pSTAT3 levels suggests that P2Y-mediated activation of these factors was already maximized. The significant action of UTP to induce both secretion of TNC and activation of STAT3 on WT cells further confirms that P2Y receptor activation sufficiently promotes immune signaling factors.

While STAT3 phosphorylation following UTP treatment may result from elevated TNC release in WT astrocytes, it is important to note that UTP-P2Y binding can also promote JAK/STAT pathway activation independent of TNC. Previous research demonstrating STAT3 phosphorylation following P2Y antagonism in rat cortical astrocyte cultures identified P2Y-coupled MAPK as a mediator between metabotropic P2Y receptors and STAT3 phosphorylation (Washburn & Neary, 2006). Purinergic signalling and TNC-TLR4 binding should therefore be thought of as complementary but not necessarily co-dependent processes. This is supported by the increases we observed in exTNC-driven pSTAT3:STAT within both WT and *Fmr1* KO astrocytes, side-stepping purinergic-mediated processes.

### ***STAT3 inhibition prevents aberrant IL-6 secretion from Fmr1 KO cortical astrocytes***

As previously mentioned, the STAT3-IL-6 relationship is bi-directional. On one hand, STAT3 activation promotes IL-6 production, while the presence of IL-6 can also increase STAT3 phosphorylation via IL-6 receptor activation (Beurel & Joep, 2009; Lam et al., 2008). This relationship emphasizes the importance of mitigating pathological IL-6 levels in the *Fmr1* KO cortex. In agreement with our previous findings (eg. Krasovska & Doering, 2018), we observed that IL-6 secretion from *Fmr1* KO astrocytes was indeed

strongly and consistently elevated relative to WT levels. Here, reduced levels of STAT3 following knockdown in *Fmr1* KO astrocytes effectively tempered overactive IL-6 secretion to levels present in WT naïve conditions. Notably, STAT3 inhibition did not significantly impact IL-6 secretion in WT astrocytes, suggesting alternative mechanisms of IL-6 regulation.

The NF- $\kappa$ B family of transcription factors is also activated by TNC and plays a central role in the production of IL-6 and other pro-inflammatory cytokines (Shimojo et al., 2015; Sparacio, Zhang, Vilcek, & Benveniste, 1992; Tong, Zhang, Shen, & Zhang, 2020), providing an alternate pathway of cytokine regulation that helps to explain the lack of effect of STAT3 knockdown in WT astrocytes. Alternatively, the differential responses of *Fmr1* KO and WT astrocytes may be a potential consequence of simply reducing excess STAT3 phosphorylation in FXS astrocytes. *Fmr1* KO IL-6 secretion also remained tempered when STAT3 knockdown was paired with exogenous TNC treatment, and since we have recently shown that exogenous TNC treatment increased IL-6 in both WT and *Fmr1* KO astrocytes (Krasovska & Doering, 2018), this suggests that STAT3 activation may be a crucial and necessary step in the TNC-TLR4-IL-6 pathway.

***IL-6 secretion is robustly inhibited by the TLR4 antagonist TAK242 in primary cortical astrocytes***

Consistent with the TNC-TLR4-STAT3-IL-6 relationship described here, acute antagonism of TLR4 was strongly effective at limiting IL-6 secretion from both *Fmr1* KO and WT astrocytes. This suggests that TNC binding at this receptor is a critical component driving pathologically upregulated IL-6 release from *Fmr1* KO astrocytes. The inability of exTNC to rescue IL-6 secretion in TAK242-treated WT and *Fmr1* KO astrocytes reinforces the role of TLR4 in the initiation of IL-6 secretion. This is consistent with our previous reported work showing that TLR4 antagonism by LPS-RS reduced IL-6 release from *Fmr1* KO astrocytes (Krasovska & Doering, 2018), though this antagonism was found to be transient when studied for longer treatment periods. Studies in *TLR4* KO mouse

gastrointestinal tract also indicate that knockout of TLR4 is insufficient to impact IL-6 mRNA and protein levels, indicating that IL-6 expression can be influenced but is not dependent of the presence of TLR4 (Khan, Bowen, & Wardill, 2019).

As previously mentioned, TNC is well-known to utilize the NF- $\kappa$ B transcription factor family in the regulation of IL-6 levels, in addition to the JAK/STAT pathway (Shimojo et al., 2015; Tong et al., 2020). It is therefore unsurprising that TLR4 antagonism was more effective than STAT3 knockdown in mitigating IL-6 release, since TLR4 signals activation of either transcription factor family. In addition, a fast-acting TLR4 pathway has also been identified to trigger calcium-mediated activation of the cAMP response element-binding protein to promote rapid IL-6 release (Song et al., 2007). While NF- $\kappa$ B and STAT3 are typically thought to act in distinct ways, they can work together to cooperatively activate their respective transcription factors (reviewed in Grivennikov & Karin, 2010; Lam et al., 2008). These transcription factors are also not specific to the TNC-TLR4-IL-6 axis, as NF- $\kappa$ B and STAT3 can be activated by a host of other processes, including purinergic signalling, to ultimately influence pro-inflammatory cytokine levels.

### ***Impact of elevated IL-6 on cortical physiology and neurological disease***

Findings in this study highly corroborated our previous work reporting astrocyte IL-6 upregulation in the *Fmr1* KO mouse model (Krasovska & Doering, 2018), as well as heightened IL-6 levels in the brains of individuals with ASD (Ashwood et al., 2011). Overexpression of IL-6 in the mouse brain has been associated with neurological impairment similar to FXS, such as dendritic aberrations, astrocyte reactivity, and increased seizure activity (Campbell et al., 1993). IL-6 overexpression was inversely proportional to mouse health in these studies, suggesting that IL-6 elevations may underlie several FXS symptoms.

It is important to also consider the effect of IL-6 secretion on other cell types within the central nervous system (CNS). IL-6 binding at soluble IL-6R receptors forms a complex along with glycoprotein 130 (gp130) (Hibi et al., 1990; Taga et al., 1989), which can

activate not only JAK/STAT, but also MAPK and PI3K/Akt signal transduction pathways to propagate pro-inflammatory signaling (Legendre et al., 2005; Zegeye et al., 2018). While this IL-6 trans-signaling occurs in a myriad of cortical cell types, including astrocytes, it remains unclear which cell types are primarily responsible for the production and secretion of these soluble IL-6 receptors. Interestingly, UTP-mediated activation of metalloproteinases ADAM 10 or 17 has been shown to increase IL-6 receptor cleavage in astrocytoma cells, which may provide yet another mechanism driving inflammation in FXS (Camden et al., 2015). IL-6 receptors are also highly expressed in microglia, another prominent immune cell within the CNS, where they induce activation of similar transcription factors and release of additional pro-inflammatory cytokines (Erta, Quintana, & Hidalgo, 2012). In addition, stress-induced upregulation of TLR4 in neonate mice also leads to the production and secretion of pro-inflammatory factors, exacerbating the neuroinflammatory response (Yao et al., 2013).

Despite the undesirable roles of pro-inflammatory cytokines, it is important to consider that they can also be advantageous within the brain. IL-6 has been shown to influence oligodendrocyte differentiation and exert neurotrophic effects to protect against degeneration and infection (reviewed in Rothaug, Becker-Pauly, & Rose-John, 2016). Lack of cerebral IL-6 is detrimental to learning and memory, as IL-6 blockade in rat orbitofrontal cortex resulted in reversal learning impairment (Donegan, Girotti, Weinberg, & Morilak, 2014). Moreover, IL-6 knockout mice perform poorly on behavioural learning tasks (Baier, May, Scheller, Rose-John, & Schifflholz, 2009). Potential therapeutic investigation may therefore aim for reduction of IL-6 levels, rather than complete abolishment, in order to preserve the beneficial anti-inflammatory processes within the *in vivo* FXS cortex.

#### **4.11. Conclusion**

In this work, we suggest a potential convergence of purinergic and immune signalling pathways in FXS cortical astrocytes, whereby elevated purinergic signalling exacerbates STAT3 activation to impact pro-inflammatory cytokine release. Here,

purinergic signalling promoted both TNC secretion and STAT3 phosphorylation, two processes linked to elevated IL-6 secretion in FXS. Pathological levels of *Fmr1* KO astrocyte-secreted IL-6 were reduced by inhibiting both STAT3 and TLR4 receptors. Therefore, mitigation of either P2Y purinergic receptors or one of the players along the TNC-TLR4-STAT3-IL-6 axis may provide a promising strategy to lessen cortical pro-inflammatory cytokine release in FXS.

#### 4.12. References

- Abbracchio, M. P., Burnstock, G., Verkhatsky, A., & Zimmermann, H. (2009). Purinergic signalling in the nervous system: an overview. *Trends Neurosci*, 32(1), 19-29. doi:10.1016/j.tins.2008.10.001
- Ashwood, P., Krakowiak, P., Hertz-Picciotto, I., Hansen, R., Pessah, I., & Van de Water, J. (2011). Elevated plasma cytokines in autism spectrum disorders provide evidence of immune dysfunction and are associated with impaired behavioral outcome. *Brain, Behavior, and Immunity*, 25(1), 40-45. doi:10.1016/j.bbi.2010.08.003
- Baier, P. C., May, U., Scheller, J., Rose-John, S., & Schifflholz, T. (2009). Impaired hippocampus-dependent and -independent learning in IL-6 deficient mice. *Behavioural Brain Research*, 200(1), 192-196. doi:10.1016/j.bbr.2009.01.013
- Beurel, E., & Jope, R. S. (2008). Differential regulation of STAT family members by glycogen synthase kinase-3. *The Journal of Biological Chemistry*, 283(32), 21934-21944. doi:10.1074/jbc.M802481200
- Beurel, E., & Jope, R. S. (2009). Lipopolysaccharide-induced interleukin-6 production is controlled by glycogen synthase kinase-3 and STAT3 in the brain. *J Neuroinflammation*, 6, 9. doi:10.1186/1742-2094-6-9
- Braun, O. Ö., Lu, D., Aroonsakool, N., & Insel, P. A. (2010). Uridine triphosphate (UTP) induces profibrotic responses in cardiac fibroblasts by activation of P2Y2 receptors. *Journal of Molecular and Cellular Cardiology*, 49(3), 362-369. doi:10.1016/j.yjmcc.2010.05.001
- Campbell, I. L., Abraham, C. R., Masliah, E., Kemper, P., Inglis, J. D., Oldstone, M. B., & Mucke, L. (1993). Neurologic disease induced in transgenic mice by cerebral overexpression of interleukin 6. *Proc Natl Acad Sci USA*, 90(21), 10061-10065. doi:10.1073/pnas.90.21.10061
- Caraccio, N., Monzani, F., Santini, E., Cuccato, S., Ferrari, D., Callegari, M. G., . . . Solini, A. (2005). Extracellular adenosine 5'-triphosphate modulates interleukin-6 production by human thyrocytes through functional purinergic P2 receptors. *Endocrinology*, 146(7), 3172-3178. doi:10.1210/en.2004-1527
- Cheng, C., Lau, S. K., & Doering, L. C. (2016). Astrocyte-secreted thrombospondin-1 modulates synapse and spine defects in the fragile X mouse model. *Mol Brain*, 9(1), 74. doi:10.1186/s13041-016-0256-9

- Dobolyi, Á., Reichart, A., Szikra, T., Szilágyi, N., Kékesi, A. K., Karancsi, T., . . . Juhász, G. (1998). Analysis of purine and pyrimidine bases, nucleosides and deoxynucleosides in brain microsamples (microdialysates and micropunches) and cerebrospinal fluid. *Neurochemistry International*, 32(3), 247-256. doi:10.1016/S0197-0186(97)00090-9
- Donegan, J. J., Girotti, M., Weinberg, M. S., & Morilak, D. A. (2014). A novel role for brain interleukin-6: facilitation of cognitive flexibility in rat orbitofrontal cortex. *The Journal of Neuroscience*, 34(3), 953-962. doi:10.1523/JNEUROSCI.3968-13.2014
- El-Hage, N., Podhaizer, E. M., Sturgill, J., & Hauser, K. F. (2011). Toll-like receptor expression and activation in astroglia: differential regulation by HIV-1 Tat, gp120, and morphine. *Immunol Invest*, 40(5), 498-522. doi:10.3109/08820139.2011.561904
- Erta, M., Quintana, A., & Hidalgo, J. (2012). Interleukin-6, a Major Cytokine in the Central Nervous System. *International Journal of Biological Sciences*, 8(9), 1254-1266. doi:10.7150/ijbs.4679
- Gibson, J. R., Bartley, A. F., Hays, S. A., & Huber, K. M. (2008). Imbalance of neocortical excitation and inhibition and altered UP states reflect network hyperexcitability in the mouse model of fragile X syndrome. *J Neurophysiol*, 100(5), 2615-2626. doi:10.1152/jn.90752.2008
- Greenhill, C. J., Rose-John, S., Lissilaa, R., Ferlin, W., Ernst, M., Hertzog, P. J., . . . Jenkins, B. J. (2011). IL-6 Trans-Signaling Modulates TLR4-Dependent Inflammatory Responses via STAT3. *The Journal of Immunology*, 186(2), 1199. doi:10.4049/jimmunol.1002971
- Grivennikov, S. I., & Karin, M. (2010). Dangerous liaisons: STAT3 and NF-kappaB collaboration and crosstalk in cancer. *Cytokine & Growth Factor Reviews*, 21(1), 11-19. doi:10.1016/j.cytogfr.2009.11.005
- Guschin, D., Rogers, N., Briscoe, J., Witthuhn, B., Watling, D., Horn, F., . . . et al. (1995). A major role for the protein tyrosine kinase JAK1 in the JAK/STAT signal transduction pathway in response to interleukin-6. *Embo J*, 14(7), 1421-1429.
- Hibi, M., Murakami, M., Saito, M., Hirano, T., Taga, T., & Kishimoto, T. (1990). Molecular cloning and expression of an IL-6 signal transducer, gp130. *Cell*, 63(6), 1149-1157. doi:10.1016/0092-8674(90)90411-7

- Higashimori, H., Schin, C. S., Chiang, M. S. R., Morel, L., Shoneye, T. A., Nelson, D. L., & Yang, Y. (2016). Selective Deletion of Astroglial FMRP Dysregulates Glutamate Transporter GLT1 and Contributes to Fragile X Syndrome Phenotypes In Vivo. *The Journal of Neuroscience*, 36(27), 7079. doi:10.1523/JNEUROSCI.1069-16.2016
- Jacobs, S., & Doering, L. C. (2009). Primary dissociated astrocyte and neuron co-culture. In L. C. Doering (Ed.), *Protocols for Neural Cell Culture* (4th ed., pp. 269–284). New York, NY: Humana.
- Jokela, T., Kärnä, R., Rauhala, L., Bart, G., Pasonen-Seppänen, S., Oikari, S., . . . Tammi, R. H. (2017). Human Keratinocytes Respond to Extracellular UTP by Induction of Hyaluronan Synthase 2 Expression and Increased Hyaluronan Synthesis. *The Journal of Biological Chemistry*, 292(12), 4861-4872. doi:10.1074/jbc.M116.760322
- Jones, E. V., & Bouvier, D. S. (2014). Astrocyte-secreted matricellular proteins in CNS remodelling during development and disease. *Neural Plast*, 2014, 321209. doi:10.1155/2014/321209
- Khan, S., Bowen, J. M., & Wardill, H. R. (2019). TLR4 mediates Il-6 production in irinotecan-induced mucositis. *bioRxiv*, 715417. doi:10.1101/715417
- Krasovska, V., & Doering, L. C. (2018). Regulation of IL-6 Secretion by Astrocytes via TLR4 in the Fragile X Mouse Model. *Frontiers in Molecular Neuroscience*, 11, 272-272. doi:10.3389/fnmol.2018.00272
- Lam, L. T., Wright, G., Davis, R. E., Lenz, G., Farinha, P., Dang, L., . . . Staudt, L. M. (2008). Cooperative signaling through the signal transducer and activator of transcription 3 and nuclear factor- $\kappa$ B pathways in subtypes of diffuse large B-cell lymphoma. *Blood*, 111(7), 3701-3713. doi:10.1182/blood-2007-09-111948
- Legendre, F., Bogdanowicz, P., Boumediene, K., & Pujol, J. P. (2005). Role of interleukin 6 (IL-6)/IL-6R-induced signal transducers and activators of transcription and mitogen-activated protein kinase/extracellular. *J Rheumatol*, 32(7), 1307-1316.
- Li, X., Chauhan, A., Sheikh, A. M., Patil, S., Chauhan, V., Li, X.-M., . . . Malik, M. (2009). Elevated immune response in the brain of autistic patients. *Journal of Neuroimmunology*, 207(1), 111-116. doi:10.1016/j.jneuroim.2008.12.002
- Luo, Y., Shan, G., Guo, W., Smrt, R. D., Johnson, E. B., Li, X., . . . Zhao, X. (2010). Fragile X Mental Retardation Protein Regulates Proliferation and Differentiation of Adult Neural Stem/Progenitor Cells. *PLOS Genetics*, 6(4), e1000898. doi:10.1371/journal.pgen.1000898

- Malik, M., Sheikh, A. M., Wen, G., Spivack, W., Brown, W. T., & Li, X. (2011). Expression of inflammatory cytokines, Bcl2 and cathepsin D are altered in lymphoblasts of autistic subjects. *Immunobiology*, 216(1), 80-85. doi:10.1016/j.imbio.2010.03.001
- Maqbool, A., Spary, E. J., Manfield, I. W., Ruhmann, M., Zuliani-Alvarez, L., Gamboa-Esteves, F. O., . . . Turner, N. A. (2016). Tenascin C upregulates interleukin-6 expression in human cardiac myofibroblasts via toll-like receptor 4. *World J Cardiol*, 8(5), 340-350. doi:10.4330/wjc.v8.i5.340
- Martin, M., Rehani, K., Jope, R. S., & Michalek, S. M. (2005). Toll-like receptor-mediated cytokine production is differentially regulated by glycogen synthase kinase 3. *Nat Immunol*, 6(8), 777-784. doi:10.1038/ni1221
- Midwood, K., Sacre, S., Piccinini, A. M., Inglis, J., Trebaul, A., Chan, E., . . . Foxwell, B. (2009). Tenascin-C is an endogenous activator of Toll-like receptor 4 that is essential for maintaining inflammation in arthritic joint disease. *Nat Med*, 15(7), 774-780. doi:10.1038/nm.1987
- Neary, J. T., & Kang, Y. (2006). P2 purinergic receptors signal to glycogen synthase kinase-3 $\beta$  in astrocytes. *Journal of Neuroscience Research*, 84(3), 515-524. doi:10.1002/jnr.20969
- Pieretti, M., Zhang, F. P., Fu, Y. H., Warren, S. T., Oostra, B. A., Caskey, C. T., & Nelson, D. L. (1991). Absence of expression of the FMR-1 gene in fragile X syndrome. *Cell*, 66(4), 817-822. doi:10.1016/0092-8674(91)90125-i
- Reynolds, K. E., Wong, C. R., & Scott, A. L. (2021). Astrocyte-mediated purinergic signaling is upregulated in a mouse model of Fragile X syndrome. *Glia*, 69(7):1816-1832. doi:10.1002/glia.23997
- Rothaug, M., Becker-Pauly, C., & Rose-John, S. (2016). The role of interleukin-6 signaling in nervous tissue. *Biochimica et Biophysica Acta (BBA) - Molecular Cell Research*, 1863(6, Part A), 1218-1227. doi:10.1016/j.bbamcr.2016.03.018
- Shimojo, N., Hashizume, R., Kanayama, K., Hara, M., Suzuki, Y., Nishioka, T., . . . Imanaka-Yoshida, K. (2015). Tenascin-C may accelerate cardiac fibrosis by activating macrophages via the integrin  $\alpha$ V $\beta$ 3/nuclear factor- $\kappa$ B/interleukin-6 axis. *Hypertension*, 66(4), 757-766. doi:10.1161/hypertensionaha.115.06004
- Song, J., Duncan, M. J., Li, G., Chan, C., Grady, R., Stapleton, A., & Abraham, S. N. (2007). A Novel TLR4-Mediated Signaling Pathway Leading to IL-6 Responses in Human Bladder Epithelial Cells. *PLOS Pathogens*, 3(4), e60. doi:10.1371/journal.ppat.0030060

- Sparacio, S. M., Zhang, Y., Vilcek, J., & Benveniste, E. N. (1992). Cytokine regulation of interleukin-6 gene expression in astrocytes involves activation of an NF-kappa B-like nuclear protein. *J Neuroimmunol*, 39(3), 231-242. doi:10.1016/0165-5728(92)90257-1
- Stamenkovic, V., Stamenkovic, S., Jaworski, T., Gawlak, M., Jovanovic, M., Jakovcevski, I., . . . Andjus, P. R. (2017). The extracellular matrix glycoprotein tenascin-C and matrix metalloproteinases modify cerebellar structural plasticity by exposure to an enriched environment. *Brain Struct Funct*, 222(1), 393-415. doi:10.1007/s00429-016-1224-y
- Taga, T., Hibi, M., Hirata, Y., Yamasaki, K., Yasukawa, K., Matsuda, T., . . . Kishimoto, T. (1989). Interleukin-6 triggers the association of its receptor with a possible signal transducer, gp130. *Cell*, 58(3), 573-581. doi:10.1016/0092-8674(89)90438-8
- Tong, X., Zhang, J., Shen, M., & Zhang, J. (2020). Silencing of Tenascin-C Inhibited Inflammation and Apoptosis Via PI3K/Akt/NF-κB Signaling Pathway in Subarachnoid Hemorrhage Cell Model. *J Stroke Cerebrovasc Dis*, 29(1), 104485. doi:10.1016/j.jstrokecerebrovasdis.2019.104485
- Tran, M. D., & Neary, J. T. (2006). Purinergic signaling induces thrombospondin-1 expression in astrocytes. *Proc Natl Acad Sci USA*, 103(24), 9321-9326. doi:10.1073/pnas.0603146103
- Wallingford, J., Scott, A. L., Rodrigues, K., & Doering, L. C. (2017). Altered Developmental Expression of the Astrocyte-Secreted Factors Hevin and SPARC in the Fragile X Mouse Model. *Frontiers in molecular neuroscience*, 10, 268-268. doi:10.3389/fnmol.2017.00268
- Wang, S. W., & Sun, Y. M. (2014). The IL-6/JAK/STAT3 pathway: potential therapeutic strategies in treating colorectal cancer. *Int J Oncol*, 44(4), 1032-1040. doi:10.3892/ijo.2014.2259
- Washburn, K. B., & Neary, J. T. (2006). P2 purinergic receptors signal to STAT3 in astrocytes: Difference in STAT3 responses to P2Y and P2X receptor activation. *Neuroscience*, 142(2), 411-423. doi:10.1016/j.neuroscience.2006.06.034
- Yao, L., Kan, E. M., Lu, J., Hao, A., Dheen, S. T., Kaur, C., & Ling, E. A. (2013). Toll-like receptor 4 mediates microglial activation and production of inflammatory mediators in neonatal rat brain following hypoxia: role of TLR4 in hypoxic microglia. *J Neuroinflammation*, 10, 23. doi:10.1186/1742-2094-10-23

- Yuskaitis, C. J., Beurel, E., & Jope, R. S. (2010). Evidence of reactive astrocytes but not peripheral immune system activation in a mouse model of Fragile X syndrome. *Biochim Biophys Acta*, 1802(11), 1006-1012. doi:10.1016/j.bbadis.2010.06.015
- Yuskaitis, C. J., Mines, M. A., King, M. K., Sweatt, J. D., Miller, C. A., & Jope, R. S. (2010). Lithium ameliorates altered glycogen synthase kinase-3 and behavior in a mouse model of fragile X syndrome. *Biochemical Pharmacology*, 79(4), 632-646. doi:10.1016/j.bcp.2009.09.023
- Zegeye, M. M., Lindkvist, M., Fälker, K., Kumawat, A. K., Paramel, G., Grenegård, M., . . . Ljungberg, L. U. (2018). Activation of the JAK/STAT3 and PI3K/AKT pathways are crucial for IL-6 trans-signaling-mediated pro-inflammatory response in human vascular endothelial cells. *Cell Communication and Signaling*, 16(1), 55. doi:10.1186/s12964-018-0268-4
- Zoghbi, H. Y., & Bear, M. F. (2012). Synaptic dysfunction in neurodevelopmental disorders associated with autism and intellectual disabilities. *Cold Spring Harb Perspect Biol*, 4(3). doi:10.1101/cshperspect.a009886
- Zuliani-Alvarez, L., Marzeda, A. M., Deligne, C., Schwenzer, A., McCann, F. E., Marsden, B. D., . . . Midwood, K. S. (2017). Mapping tenascin-C interaction with toll-like receptor 4 reveals a new subset of endogenous inflammatory triggers. *Nature Communications*, 8(1), 1595-1595. doi:10.1038/s41467-017-01718-7

## Chapter Five:

### Astrocyte-derived purinergic signalling mediates neurite outgrowth and excitability in the Fragile X mouse cortex

#### 5.1. Preface

In the preceding chapters, novel dysregulations in P2Y-mediated purinergic signalling were identified within *Fmr1* KO cortical astrocytes. Taken together, these findings indicate that astrocyte purinergic signalling is upregulated in the FXS cortex and may influence the establishment of neuronal connections. However, the direct impact of this upregulation on FXS neurons has remained unclear. This chapter will therefore investigate the impact of purinergic secretions on neurite outgrowth and explore the impact of selective P2Y receptor antagonism on neuronal firing, in order to determine the neuronal consequences of elevated *Fmr1* KO astrocyte purinergic signalling.

#### 5.2. Study Significance

This work indicates that astrocyte soluble factors such as UTP are crucial for the modulation of neurite extension, a process which may impact the establishment of neural networks. This study also utilizes microelectrode arrays to record neuronal firing at repeated intervals over the first ~5 weeks of development *in vitro*, thereby providing a detailed characterization of *Fmr1* KO *in vitro* neuronal activity. Furthermore, the work presented in this chapter identifies P2Y<sub>2</sub> antagonism as a novel approach to mitigate heightened *Fmr1* KO neuronal burst frequency, thereby providing a potential drug target for future therapeutic investigation. Overall, these findings suggest that the activity of upregulated astrocyte P2Y purinergic receptors underlies pathological FXS neuronal excitation, providing future directions for therapeutic development.

### 5.3. Aims and Hypotheses

This research was designed to address the third aim of this thesis work:

Aim 3: Determine the functional outcomes of purinergic signalling on neural circuitry.

Hypothesis: Elevated astrocyte purinergic signalling increases neuronal activity and connectivity in *Fmr1* KO co-cultures, and can be targeted for potential therapeutic interventions.

### 5.4. Publication Status

The following manuscript will be submitted to *Molecular Autism* following approval from all co-authors.

**Title: Astrocyte-derived purinergic signalling mediates neurite outgrowth and excitability in the Fragile X mouse cortex**

**Authors:**

Kathryn E. Reynolds<sup>1</sup>, Eileen Huang<sup>1</sup>, Monica Sabbineni<sup>1</sup>, Eliza Wiseman<sup>1</sup>, Nadeem Murtaza<sup>1,2</sup>, Karun K. Singh<sup>1,2</sup> & Angela L. Scott<sup>1</sup>

1. Department of Pathology and Molecular Medicine, McMaster University, Hamilton, Ontario, Canada
2. McMaster Stem Cell and Cancer Research Institute, McMaster University, Hamilton, Ontario, Canada

**Correspondence:**

Angela L. Scott

Department of Pathology and Molecular Medicine

McMaster University  
1200 Main Street West, Hamilton, Ontario L8N 3Z5, Canada.  
scottan@mcmaster.ca

**Conflict of Interest:**

None

**5.4. Author Contributions**

This study was designed by K.E. Reynolds and A.L. Scott. K.E. Reynolds performed microelectrode array experiments with assistance from E. Huang, as well as training and guidance from N. Murtaza and K. K. Singh. M. Sabbineni and E. Wiseman assisted with neurite outgrowth and Sholl analysis on neurons that were cultured, stained, and imaged by K.E. Reynolds. K.E. Reynolds performed Western blotting, as well as all data analysis and interpretation for all experiments. The manuscript was written by K.E. Reynolds with editorial assistance from A.L. Scott.

**5.5. Abstract**

Increased neuronal excitation is commonly observed in Fragile X syndrome (FXS), the most prevalent heritable form of intellectual disability and autism spectrum disorder (ASD). While this aberrant circuitry is typically studied from a neuron-centric perspective, astrocytes are known to regulate neuronal connectivity by releasing soluble factors that influence neurite extension and synaptogenesis, utilizing pathways such as the nucleoside triphosphate-mediated purinergic signalling system to facilitate this astrocyte-neuron communication. We have recently shown that UTP-mediated purinergic signalling is upregulated in *Fmr1* KO mouse cortical astrocytes and impacts secretion of the synaptogenic protein TSP-1, suggesting that this signalling pathway may be linked to the establishment of excess neuronal excitation in FXS. To determine the extent to which elevated astrocyte purinergic signalling impacts *Fmr1* KO neurons during early postnatal development, we sought to identify whether dysregulated purinergic signalling promotes

altered morphology and activity in *Fmr1* KO mouse cortical neurons. The presence of *Fmr1* KO astrocyte soluble factors increased neurite extension in both wildtype and *Fmr1* KO neurons, yet prevented excess UTP-driven outgrowth and branching in a manner consistent with potential saturation effects, indicating that astrocyte-secreted factors such as UTP are crucial for the modulation of early neuronal outgrowth. Hyperexcitable firing was also observed in *Fmr1* KO neuron-astrocyte co-cultures grown on microelectrode arrays, along with moderate culture-wide deficits in neuronal firing synchrony. The selective P2Y<sub>2</sub> purinergic receptor antagonist AR-C 118925XX normalized this aberrant *Fmr1* KO activity and transiently corrected aberrant synchrony, while the nonspecific purinergic antagonist suramin was less effective at tempering *Fmr1* KO neuronal firing. These results demonstrate the importance of astrocyte soluble factors in the development of neural circuitry, and suggest that the activity of P2Y purinergic receptors may underlie pathological FXS neuronal excitation.

## **5.6. Introduction**

Elevated excitatory signalling is a well-known hallmark of Fragile X syndrome (FXS), the most common monogenic form of autism spectrum disorder (ASD) and intellectual disability. FXS arises due to the presence of excess CGG repeats within the *Fmr1* gene, triggering hypermethylation and subsequently preventing transcription of the RNA-binding protein FMRP (Fu et al., 1991; Pieretti et al., 1991; Sutcliffe et al., 1992; Verkerk et al., 1991). FMRP is crucial for appropriate cortical development and maturation, as this protein regulates the expression of a plethora of developmentally significant proteins within the cerebral cortex and throughout the central nervous system (Darnell et al., 2011). This absence of FMRP-driven regulatory function therefore has numerous consequences for the creation, refinement, and hyperexcitation of cortical networks, which are thought to underlie common symptoms of FXS such as seizures and sensory hyperresponsivity (Ethridge et al., 2016; Ethridge et al., 2017).

Studies using the *Fmr1* knockout (KO) mouse model of FXS highlight that the absence of neuronal and astrocyte FMRP leads to atypical neuronal morphology, connectivity, and activity during early postnatal development. *Fmr1* KO neurons are characterized by aberrant neurite outgrowth and arborization, excess immature dendritic spines, and increased synaptic puncta (Galvez, Gopal, & Greenough, 2003; Jacobs & Doering, 2010; Wallingford, Scott, Rodrigues, & Doering, 2017). These structural phenotypes are correlated with network-level findings of a bias toward heightened neuronal excitation paired with deficits in inhibitory activity, which is also reflected to a considerable degree in individuals with ASD (e.g. Brown, Singel, Hepburn, & Rojas, 2013; Ethridge et al., 2016; Gibson, Bartley, Hays, & Huber, 2008; Puts et al., 2017). While these FXS dysregulations are often studied from a neuron-centric perspective, astrocytes are also affected by the absence of FMRP, and they powerfully modulate neuronal connectivity by releasing soluble factors that influence the processes of neurite extension and synaptogenesis. The presence of *Fmr1* KO astrocyte-secreted factors in culture media is sufficient for wildtype neurons to assume a disordered *Fmr1* KO-like dendritic structure *in vitro* (Jacobs & Doering, 2010), while *in vivo*, astrocyte-specific silencing of *Fmr1* alters mouse motor neuron morphology and impairs acquisition of motor skills (Jennifer L. Hodges et al., 2017), highlighting the ability of *Fmr1* KO astrocytes to drive FXS neuronal phenotypes. A broader understanding of the ways in which astrocytes contribute to the early postnatal development of aberrant FXS cortical circuitry will therefore be critical in the search for novel therapeutic approaches.

Astrocytic regulation of the neuronal environment can be modulated through a variety of pathways, including the purinergic signalling system, which has recently been shown to be upregulated in *Fmr1* KO mouse cortical astrocytes (Reynolds, Wong, & Scott, 2021). Both neurons and glia express the excitatory G<sub>q</sub>-coupled P2Y family of purinergic receptors, which are activated by the nucleoside di- and triphosphates ATP, ADP, UTP, and/or UDP. P2Y activation initiates phospholipase C-inositol triphosphate-mediated calcium release pathways, thereby promoting propagation of astrocyte intercellular calcium waves, vesicular release of purinergic neuro/gliotransmitters and proteins, and regulation

of gene expression (reviewed in Abbracchio, Burnstock, Verkhratsky, & Zimmermann, 2009). Consistent with the development of a hyperexcitable FXS cortex, P2Y<sub>2</sub> and P2Y<sub>6</sub> receptor expression is elevated in *Fmr1* KO mouse cortical astrocytes, and is correlated with increased ATP- and UTP-driven mobilization of intracellular calcium stores (Reynolds et al., 2021). Through the disordered release of astrocyte soluble factors, heightened astrocyte purinergic signalling can influence neuronal morphology, as P2Y<sub>2</sub> activation significantly elevates neurite outgrowth in PC12 cells by modulating actin cytoskeleton remodeling (Peterson et al., 2013; Pooler, Guez, Benedictus, & Wurtman, 2005). Stimulation of P2Y receptors with exogenous UTP also increases expression and secretion of astrocyte thrombospondin-1 (TSP-1), which promotes the creation of immature excitatory synapses (Eroglu et al., 2009; Tran & Neary, 2006). Thus, disordered astrocyte purinergic pathways may impact both neuronal structure and connectivity during early postnatal development, with implications for the formation of hyperexcitable neuronal networks in FXS.

While *Fmr1* KO cortical astrocytes demonstrate purinergic signalling aberrations, the extent to which this affects *Fmr1* KO neurons during early postnatal development has remained unclear. We therefore sought to determine whether dysregulated purinergic signalling promotes altered *Fmr1* KO mouse cortical neuron morphology and activity. Exogenous UTP promoted outgrowth and branching when combined with wildtype astrocyte-conditioned media, yet the presence of *Fmr1* KO astrocyte soluble factors increased neurite extension in both wildtype and *Fmr1* KO neurons in the absence of UTP, indicating that astrocyte-secreted factors such as UTP are crucial for the modulation of early neuronal outgrowth. Hyperexcitable firing was also observed in *Fmr1* KO neuron-astrocyte co-cultures grown on microelectrode arrays, and was normalized following chronic P2Y<sub>2</sub> antagonism, implicating astrocyte P2Y<sub>2</sub> receptors in the facilitation of neuronal hyperexcitability.

## 5.7. Methods

**Animals.** Two genotypes of mice, wildtype (WT) and *Fmr1*<sup>-/-</sup> (*Fmr1* KO; FVB.129P2(B6)-*Fmr1*<sup>tm1Cgr</sup>), were bred and housed at the McMaster Health Sciences Central Animal Facility. All mouse housing conditions and experimental protocols were authorized by the McMaster Animal Ethics Board (Animal Utilization Protocol 17-04-11), following Canadian Council on Animal Care policies. Timed pregnant dams were removed for neuronal dissection once embryos reached approximately embryonic day (E) 15, while pups of both sexes were removed at postnatal day (P) 1-3 for astrocyte dissection.

**Primary Astrocyte Culture.** Cortices from three P1-3 WT or *Fmr1* KO mice, euthanized by decapitation, were pooled to obtain each primary astrocyte culture. Following protocols described in Jacobs and Doering (2009), whole brains were placed in into ice-cold calcium- and magnesium-free Hanks' buffered saline solution (CMF-HBSS; Invitrogen, Waltham, MA, USA). Using a Zeiss Stemi SR stereo microscope (Carl Zeiss, Oberkochen, Germany), olfactory bulbs, meninges, and hippocampi were detached to isolate both hemispheres of the cerebral cortex. Cortical hemispheres were dissociated in 1 mg/mL DNase (Roche Applied Science) and 0.25% trypsin (Invitrogen), then seeded in glial-selective media (minimum essential media (Gibco, Waltham, MA, USA), 10% horse serum (Gibco), and 0.6% D-(+)-glucose (Sigma-Aldrich, St. Louis, MO, USA)). Primary astrocyte cultures were grown within a humidified incubator (37°C, 5% CO<sub>2</sub>; NuAire, Plymouth, MN, USA) for a total of 6-8 days *in vitro* (DIV), with half media changes 24 h post-plating and every subsequent 48-72 h.

Once cultures achieved 75-90% confluence, they were utilized to produce astrocyte-conditioned media (ACM), or replated on top of neurons within microelectrode arrays (see Microelectrode Arrays). To produce ACM, glial-selective media was replaced with neuronal maintenance media (NMM) containing NeuroCult Basal Medium (StemCell Technologies, Vancouver, ON, Canada), 2% SM1 neuronal supplement (StemCell Technologies), 0.1125% Glutamax (Invitrogen), and 0.1% glutamine (Invitrogen).

Astrocyte cultures were maintained at 37°C and 5% CO<sub>2</sub> for an additional 48 h to allow for the accumulation of astrocyte-secreted factors within the media.

**Primary Neuron Culture.** Timed pregnant WT and *Fmr1* KO dams were euthanized with CO<sub>2</sub> once embryos reached ~E15. Following abdominal sterilization with 95% ethanol, uterine horns were removed through a midline incision through the skin and abdominal wall, and rinsed in sterile ice-cold CMF-HBSS (Invitrogen). Three embryos from each litter were randomly selected for dissection. Skin, skull, olfactory bulbs, meninges, and hippocampi were removed from one cortical hemisphere per embryo under a Zeiss Stemi SR stereo microscope (Carl Zeiss). Cortical tissue was dissociated in CMF-HBSS plus 0.25% trypsin, using a series of mechanical dissociation steps outlined in Jacobs and Doering (2009). Neurons intended for neurite outgrowth and Sholl analyses were then resuspended in ACM and plated on 1 mg/mL poly-L-lysine (Sigma-Aldrich)/10 µg/mL laminin (Invitrogen)-coated 12 mm coverslips (Neuvitro, Vancouver, WA), at a density of 7000 cells/coverslip.

The two different genotypes of neurons and ACM (WT and *Fmr1* KO) were combined to create four separate groups: WT neurons cultured with WT ACM (WTN WTACM), WT neurons cultured with *Fmr1* KO ACM (WTN KOACM), *Fmr1* KO neurons cultured with WT ACM (KON WTACM), and *Fmr1* KO neurons cultured with *Fmr1* KO ACM (KON KOACM). Each combination was plated in duplicate, and cultured four times using separate litters, for a total of eight coverslips (n) per combination. Neurons were treated 24 h and 72 h after plating with phosphate buffered saline vehicle (PBS; Life Technologies) or one of the following concentrations of UTP (diluted in PBS; ThermoFisher): 0.1 µM, 1 µM, 10 µM, or 100 µM. Primary neuron cultures were maintained at 37°C and 5% CO<sub>2</sub> for a total of 5DIV, without media changes.

**Immunocytochemistry.** Primary neuron cultures and neuron-astrocyte co-cultures were processed for immunocytochemistry using protocols outlined in Cheng, Lau, and Doering (2016). Neurons cultured in ACM were fixed in 100% ice-cold acetone (BioShop,

Burlington, ON) at 5DIV for analysis, while co-cultures were fixed at 7DIV for representative imaging. Fixed cells were permeabilized with 0.1% Triton X-100 (BDH Chemicals, Radnor, PA, USA) and blocked with 1% bovine serum albumin (BSA; Sigma-Aldrich). Neurons were incubated in anti-MAP2 primary antibody (mouse monoclonal; 1:250 in PBS; Invitrogen Cat# 13-1500, RRID:AB\_2533001) overnight at 4°C, then in goat anti-mouse fluorescein isothiocyanate (FITC) (1:100 in PBS; Jackson ImmunoResearch, West Grove, PA, USA Cat# 115-095-166, RRID:AB\_2338601) secondary antibody for 3 h at room temperature. Co-cultures were also incubated in anti-MAP2 primary antibody as well as anti-gial fibrillary acidic primary antibody (GFAP; chicken polyclonal; 1:1000; OriGene, Rockville, MD, USA Cat# TA309150), followed by donkey anti-mouse AlexaFluor 594 (1:500; Invitrogen Cat# 21203, RRID:AB\_141633) and donkey anti-chicken FITC (1:100; Jackson ImmunoResearch Cat# 703-095-155, RRID:AB\_2340356) secondary antibodies. Prolong Gold antifade mounting medium plus 4',6-diamidino-2-phenylindole (DAPI; Invitrogen) was used to stain nuclei with DAPI and mount the coverslips onto slides. Neurons were imaged by a blinded experimenter at x20 objective magnification, using a Zeiss Axio Imager.M2 epifluorescent microscope (Carl Zeiss) fitted with an AxioCam 506 camera (Carl Zeiss) and ZEN Blue acquisition software (Carl Zeiss).

***Neurite Outgrowth and Sholl Analysis.*** Neurite outgrowth and complexity in UTP-treated neurons were simultaneously assessed using Fiji software (ImageJ; National Institutes of Health, Bethesda, MD, USA). All analyses were performed by experimenters who were blinded to the treatment conditions and hypotheses. Each treatment group consisted of 8 coverslips isolated from embryos of four separate dams (n=8; n=6 for the following groups: WTN WTACM 10  $\mu$ M UTP, WTN KOACM 1  $\mu$ M UTP, KON WT ACM 10  $\mu$ M UTP, and KON KOACM 10  $\mu$ M UTP). Five images representative of the total neuronal population were taken per coverslip. From those images, ~4 neurons per image were randomly chosen for analysis, for a total of ~20 neurons analyzed per n and ~120-160 neurons analyzed per condition. Each neurite of a selected neuron was traced from proximal to distal end using the Simple Neurite Tracer Fiji plugin, and radius step size was set to 10  $\mu$ m for Sholl analysis. Traces began outside the soma at the base of each neurite to ensure

that the soma was excluded from outgrowth measurements. Results of both neurite outgrowth and Sholl analyses were expressed as fold change relative to PBS vehicle control.

**Western Blotting.** Western blotting lysates were prepared from WT and *Fmr1* KO mouse primary neuron cultures to compare levels of neuronal P2Y receptors. For P2Y<sub>1</sub> quantification, experimental samples consisted of 3 WT (n=3) and 5 *Fmr1* KO (n=5) cultures from individual litters, while for P2Y<sub>2</sub> western blotting, 6 (n) separate neuron cultures per genotype, from individual timed pregnancies, were used. Experimental samples for P2Y<sub>4</sub> western blotting were obtained from 4 WT (n=4) and 3 *Fmr1* KO (n=3) cultures isolated from separate litters, and 5 (n) separate neuron cultures per genotype, from individual timed pregnancies, were used for P2Y<sub>6</sub> western blotting. Following dissociation protocols described above (see Primary Neuron Culture), neurons were plated on 1 mg/mL PLL- and 10 µg/mL laminin-coated 6-well plates (Corning, NY, USA) and maintained for 5DIV, then lifted using 0.05% trypsin-ethylenediaminetetraacetic acid (trypsin-EDTA; Gibco). Pelleted cultured neurons were flash frozen in liquid nitrogen and stored at -80°C until homogenization with RIPA lysis buffer (150 mM NaCl, 1% NP-40, 0.5% deoxycholic acid, 1% SDS, 50 mM Tris, Roche ULTRA protease inhibitor, Roche PhoSTOP phosphatase inhibitor), as described in Krasovska & Doering (2018). Total protein levels within each lysate were quantified using a DC protein assay (BioRad, Mississauga, ON, Canada) to determine gel loading dilutions.

Western blotting samples were comprised of 5 µg protein lysate per lane, diluted in Laemmli sample buffer plus 2.5% β-mercaptoethanol (BioRad). Following gel electrophoresis using polyacrylamide TGX 4-12% gradient gels (BioRad), proteins were transferred to polyvinylidene difluoride (PVDF) (BioRad) membranes, which were then agitated in a blocking solution of 5% non-fat milk in 1X Tris-buffered saline solution with Tween-20 (TBS-T). Membranes were incubated overnight at 4°C with primary antibodies against the following P2Y receptors: P2Y<sub>1</sub> (rabbit polyclonal; 1:200; Alomone Labs, Jerusalem, Israel Cat# APR-009, RRID:AB\_2040070; band at ~66 kDa) (Cui et al., 2016),

P2Y<sub>2</sub> (rabbit polyclonal; 1:200; Alomone Labs Cat# APR-010, RRID:AB\_2040078; band at ~47 kDa) (Cui et al., 2016), P2Y<sub>4</sub> (rabbit polyclonal; 1:200; Alomone Labs Cat# APR-006, RRID:AB\_2040080; band at ~50 kDa) (D'Ambrosi, Iafrate, Saba, Rosa, & Volonté, 2007; Sage & Marcus, 2002), and P2Y<sub>6</sub> (rabbit polyclonal; 1:200; Alomone Labs Cat# APR-106, RRID:AB\_2040082; band at ~65 kDa) (D'Ambrosi et al., 2007; Koizumi et al., 2007). Membranes were subsequently incubated in donkey-anti rabbit horseradish peroxidase secondary antibody (1:2500; GE Healthcare Cat# NA934) for 2 h, then developed in Clarity MAX enhanced chemiluminescence (ECL) substrate (BioRad) and imaged using a ChemiDoc imaging system (BioRad). Following development, membranes were stripped using Blot Restore Solution (MilliporeSigma) and re-probed with  $\beta$ -actin primary antibody (mouse monoclonal; 1:5000; MilliporeSigma Cat# A5441, RRID:AB\_476744) and donkey-anti mouse horseradish peroxidase secondary antibody (1:2500; GE Healthcare Cat# NA931V) to serve as a loading control. Bands of interest were quantified and normalized to  $\beta$ -actin using ImageLab 6.0.1 software (BioRad). P2Y receptor levels were expressed as fold change relative to WT means.

***Neuron-Astrocyte Co-Cultures.*** WT and *Fmr1* KO neurons intended for co-culture on microelectrode arrays were dissected according to protocols described above (see Primary Neuron Culture), then resuspended in NeuroCult Neuronal Plating Medium (NMM, STEMCELL Technologies, Vancouver, BC, Canada) supplemented with 2% STEMCELL Modified-1 Neuronal Supplement (SM1, STEMCELL Technologies). Neurons were seeded at a density of 30,000 cells per well on Axion 48-well Cytoview plates (Axion Biosystems, Atlanta, GA, USA) containing 16 microelectrodes per well with a 0.32 cm<sup>2</sup> total recording electrode area, pre-coated with 0.1% polyethylenimine (PEI) in borate buffer (pH 8.4). After 24 h, confluent astrocytes of the same genotype (see Primary Astrocyte Culture) were added to the culture at a density of 60,000 cells per well. On-plate reservoirs were filled with 5-7 mL of sterile water to increase humidity and to prevent evaporation of cell suspensions and media. Co-cultures were maintained in a humidified incubator at 37°C and 5% CO<sub>2</sub>, with media changes 2x per week and >24 h prior to recording, as media changes temporarily dysregulate neuronal firing. Between 5-11DIV,

cells received half media changes consisting of BrainPhys Neuronal Medium (STEMCELL Technologies, Vancouver, BC, Canada) supplemented with 2% SM1. Starting at 12DIV, half media changes consisted of BrainPhys Neuronal Medium with 2% SM1 and 7.5 mM glucose.

***Microelectrode Array Recording and Analysis.*** Neuronal firing activity was recorded every 2-3 days, from 7-35DIV, using the Axion MaestroPro multiwell plate recording system (Axion Biosystems) set to detect spontaneous real-time neural spikes. All recordings were carried out for 10 min at a temperature of 37°C, in the absence of CO<sub>2</sub> regulation. Wells in which less than 9 of the 16 total electrodes (<50%) detected neuronal activity, defined as a minimum spike rate of 5 spikes per minute, were removed prior to data analysis unless they recovered to  $\geq 9/16$  active electrodes in subsequent recordings.

P2Y antagonist treatments were applied to culture media 2x per week and >24 h prior to recording, starting at 5DIV and continuing until 31DIV. Cultures were treated with the specific P2Y<sub>2</sub> antagonist AR-C 118925XX (AR-C; 1  $\mu$ M and 10  $\mu$ M in 50% PBS/50% DMSO; Tocris Bioscience, Bristol, UK) or general P2 antagonist suramin (0.1  $\mu$ M in 50% PBS/50% DMSO; Tocris Bioscience). Some cultures were unable to be recorded for the full experimental period due to external factors. The WT naïve experimental sample consisted of a total of 13 wells (n=13) obtained from 7 individual timed pregnancies and cultures, with 6 wells remaining at 35DIV, while the *Fmr1* KO naïve experimental sample was comprised of 15 wells (n=15) from 6 separate dams and cultures and was reduced to 8 wells by 35DIV. WT AR-C 118925XX 1  $\mu$ M experimental samples were composed of 14 wells (n=14) at 7DIV/8 wells at 35DIV, while 13 WT wells (n=14) at 7DIV/7 wells at 35DIV were treated with 10  $\mu$ M antagonist, each derived from 7 individual timed pregnancies and cultures. *Fmr1* KO 1  $\mu$ M AR-C samples consisted of 12 wells (n=12) at 7DIV/3 wells at 31DIV obtained from 7 individual dams and cultures, while *Fmr1* KO 10  $\mu$ M samples were made up of 11 wells (n=11) at 7DIV/7 wells at 35DIV obtained from 6 individual dams and cultures. Suramin experimental samples were composed of 10 WT wells (n=10) at 7DIV and reduced to 8 wells by 35DIV, as well as 9 *Fmr1* KO wells (n=9)

at 7 DIV/5 wells at 35DIV, each obtained from 5 individual timed pregnancies and cultures per genotype.

To ensure that recordings detected synaptic firing and not gap junction activity, a reversible treatment of AMPA and NMDA receptor blockers, 10  $\mu$ M CNQX plus 10  $\mu$ M AP-5 (MilliporeSigma, Oakville, ON, CA), was applied at 7DIV, 10DIV, and 12DIV. Combined CNQX+AP-5 treatments were applied to separate wells (WT n=14 from 7 separate timed pregnancies; *Fmr1* KO n=12 from 6 individual timed pregnancies) for a 10 min incubation period plus 10 min recording time, then the culture media was removed and replaced in order to restore neuronal firing. All analysis of firing activity was completed using AxIS Metric software (Axion Biosystems) with default settings applied for neural spike, burst, and network burst parameters. Relevant measured metrics, processed by the Neural Statistics Compiler (Axion), are defined in Table 1.

**Statistical Analysis.** GraphPad Prism 9.1.0 software (GraphPad Software, San Diego, CA, USA) was used for all graphing and statistical analyses. Neuronal outgrowth and complexity analyses between three or more means within a single genotype were performed by fitting the data to a mixed model followed by post-hoc Holm-Sidak multiple comparisons tests; the mixed model was chosen in place of a one-way repeated measures analysis of variance (ANOVA) due to missing replicates in 10  $\mu$ M UTP conditions. Comparisons between three or more means across different genotypes were performed using two-way ANOVA with post-hoc Holm-Sidak corrections. All statistical results were considered significant at  $p < 0.05$ , and reported statistics are adjusted p values obtained from Holm-Sidak correction unless otherwise specified. Western blotting comparisons, made between two means, were performed using two-tailed, unpaired t-tests with significance at  $p < 0.05$ . All data is presented as means  $\pm$  SEM.

Time series comparisons of MEA metrics between WT and *Fmr1* KO naïve groups were performed using mixed models, chosen in place of two-way repeated measures ANOVA due to missing values at later time points, as some cultures were unable to be

followed for the full 35DIV due to external factors. Differences between WT and *Fmr1* KO treatment groups over time were initially analyzed using three-way ANOVA, then parameters of interest at select time points were further compared between genotypes and treatments using two-way ANOVA followed by post-hoc Holm-Sidak multiple comparisons tests. All line graphs present data as means  $\pm$  SEM, while box plots present the median and interquartile range with whiskers extending to minimum and maximum values. All statistical comparisons were considered significant at  $p < 0.05$ .

## 5.8. Results

### ***UTP increases cortical neurite outgrowth when combined with WT but not Fmr1 KO astrocyte-conditioned media***

Given that purinergic signalling is elevated in *Fmr1* KO astrocytes, we investigated the impact of elevated purinergic signalling on neuronal morphology by treating neuron cultures with varying concentrations of UTP. In order to isolate the effect of neurons vs astrocyte soluble factors, WT and *Fmr1* KO neurons were combined with WT and *Fmr1* KO astrocyte-conditioned media (ACM) to form four distinct genotype conditions, as shown in Fig.1A. In WT neurons grown in WT ACM and treated with high-dose UTP (10  $\mu$ M and 100  $\mu$ M) over 5DIV (Fig.1B-D), we observed an increase in maximal neurite extension (*i.e.* the length of the neuron's longest neurite, presumably the axon) relative to PBS vehicle (n=8) treatment ( $p=0.0258$  for both treatment conditions; 10  $\mu$ M n=6 and 100  $\mu$ M n=8). However, incubation with lower concentrations of UTP (0.1  $\mu$ M and 1  $\mu$ M) did not influence this neurite length ( $p=0.1029$  for both treatment conditions; n=8). Surprisingly, an even more robust effect of UTP was observed in *Fmr1* KO neurons grown in WT ACM (Fig.1E). Within this mixed genotype condition, sustained treatment with all four concentrations of exogenous UTP significantly elevated maximal neurite extension (0.1  $\mu$ M UTP  $p=0.0133$ , n=8; 1  $\mu$ M UTP  $p=0.0054$ , n=8; 10  $\mu$ M UTP  $p=0.0063$ , n=6; and 100  $\mu$ M UTP  $p=0.0063$ , n=8) relative to PBS vehicle (n=8).

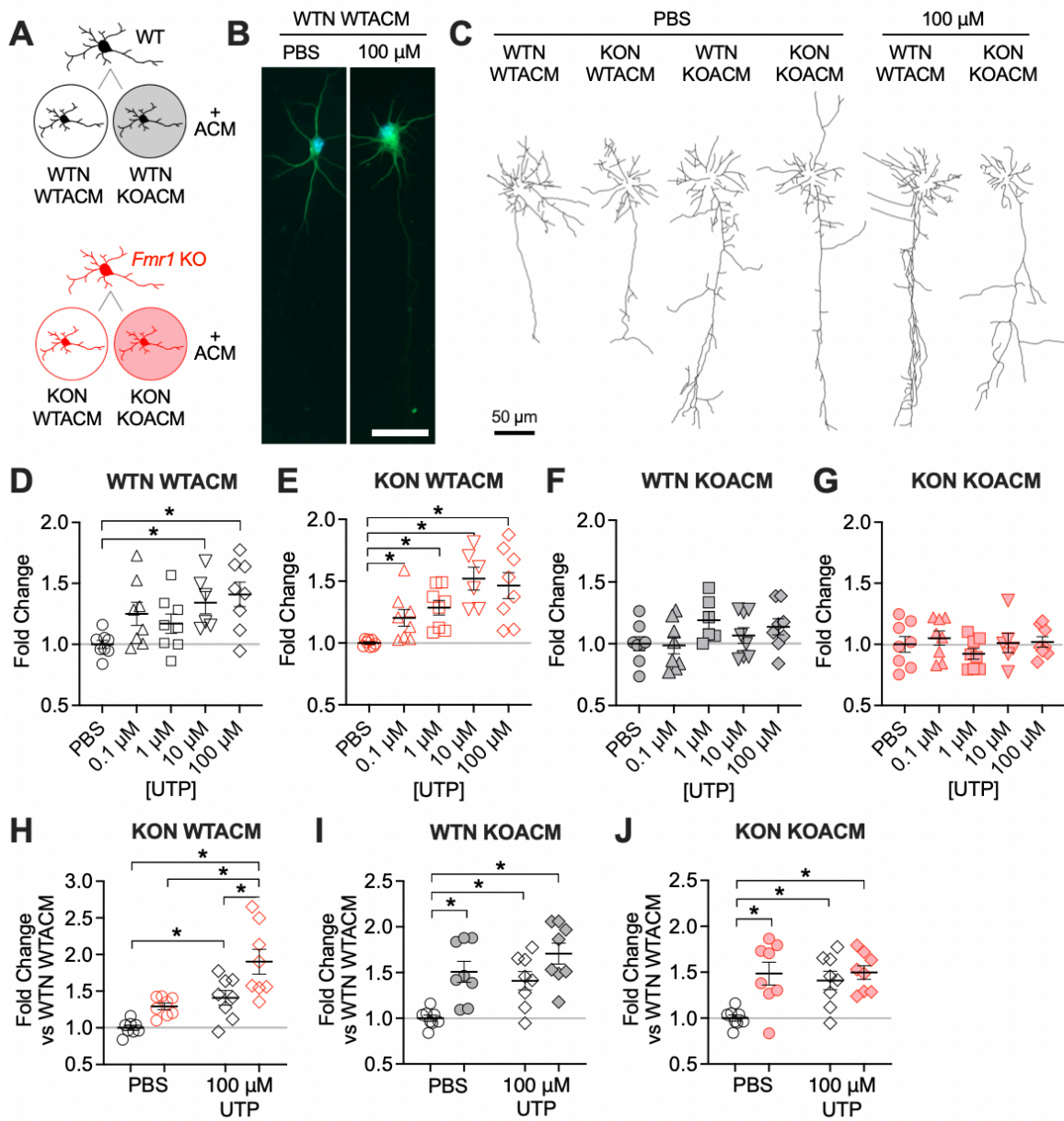


Figure 1. Extension of the longest neurite in WT and *Fmr1* KO primary neurons cultured for 5DIV in combination with either WT or *Fmr1* KO astrocyte-conditioned media, and treated with the P2Y agonist UTP (0.1  $\mu$ M, 1  $\mu$ M, 10  $\mu$ M, or 100  $\mu$ M, or PBS control). A. Schematic outlining the four different genotype conditions within neurite outgrowth experiments. WT and *Fmr1* KO neurons (N) were each cultured in media (ACM) containing WT or *Fmr1* KO astrocyte soluble factors. B. Representative immunofluorescence showing WTN WTACM treated with PBS (control) or 100  $\mu$ M UTP. Scale bar: 50  $\mu$ m. C. Representative neurite traces of all four genotype conditions following PBS treatment, as well as WTN WTACM and KON KOACM following treatment with 100  $\mu$ M UTP. UTP treatment increased the length of the longest neurite (*i.e.* the putative axon) in (D) WTN WTACM and (E) KON WTACM conditions, but not in (F) WTN KOACM or (G) KON KOACM. Between-genotype comparisons of PBS vs 100  $\mu$ M UTP treatment in (H) KON WTACM, (I) WTN KOACM, and (J) KON KOACM groups relative to WTN WTACM, demonstrating excess baseline outgrowth in KOACM-grown neurons, and showing that 100  $\mu$ M UTP treatment permits WTN WTACM to reach this level of excess outgrowth. All data presented as means  $\pm$  SEM, with gray horizontal lines indicating control means. n=8, with the exception of n=6 for 10  $\mu$ M WTN WTACM, KON WTACM, KON KOACM, and 1  $\mu$ M WTN KOACM. Significant differences between groups denoted by \*; p<0.05.

In contrast, we did not observe any changes in maximal neurite extension when neurons of either genotype were grown in culture media pre-conditioned by *Fmr1* KO astrocytes. In WT neurons grown in *Fmr1* KO ACM (Fig.1F), neither low-dose UTP (0.1  $\mu$ M  $p=0.9001$ ,  $n=8$  and 1  $\mu$ M  $p=0.4953$ ,  $n=6$ ) nor high-dose UTP (10  $\mu$ M  $p=0.7486$ ,  $n=8$  and 100  $\mu$ M  $p=0.4953$ ,  $n=8$ ) impacted the length of the longest neurite relative to PBS vehicle treatment ( $n=8$ ). Similarly, the maximal neurite extension of *Fmr1* KO neurons grown in *Fmr1* KO ACM (Fig.1G) was unaffected by UTP at any of the concentrations we tested (0.1  $\mu$ M UTP  $p=0.7718$ ,  $n=8$ ; 1  $\mu$ M UTP  $p=0.5419$ ,  $n=8$ ; 10  $\mu$ M UTP  $p=0.9726$ ,  $n=6$ ; and 100  $\mu$ M UTP  $p=0.9726$ ,  $n=8$ ).

#### ***UTP increases WT maximal neurite length to Fmr1 KO levels***

When we compared maximal neurite lengths between the PBS controls of our four genotype conditions ( $n=8$ ), we saw that neurons grown in WT ACM exhibited shorter baseline neurite extension than neurons grown in *Fmr1* KO ACM (Fig.1C). Both vehicle-treated WT and *Fmr1* KO neurons grown in *Fmr1* KO ACM grew significantly longer neurites than those in the WTN WTACM condition ( $p=0.0047$  and  $p=0.0034$ , respectively; Fig.1C,I,J), while the maximal neurite length of *Fmr1* KO neurons in WT ACM did not significantly differ from that of WTN WTACM ( $p=0.1036$ ; Fig.1C,H).

Treatment with 100  $\mu$ M UTP elevated WTN WTACM outgrowth to levels comparable with the PBS controls of *Fmr1* KO ACM-grown neurons ( $p=0.8743$  versus KON KOACM, Fig.1C,J;  $p=0.4839$  versus WTN KOACM, Fig.1C,I). When *Fmr1* KO neurons were grown in WT ACM, their maximal neurite length was also significantly longer than that of 100  $\mu$ M UTP-treated WTN WTACM ( $p=0.0084$ ; Fig.1H), though this additional extension following exogenous UTP treatment was not seen in either genotype of cells grown with *Fmr1* KO ACM (WTN KOACM  $p=0.1129$ , Fig.1I and KON KOACM  $p=0.8743$ , Fig.1J).

***UTP increases complexity of cortical neurons grown in WT but not Fmr1 KO astrocyte-conditioned media***

Given that UTP influenced the maximum length to which neurons grown with WT secreted factors could extend their neurites, we wondered if UTP also influenced these neurites' levels of branching and complexity. We utilized Sholl analysis to record the number of neurites that intersected concentric circles radiating from the centre of the neuronal soma, with an increased number of Sholl intersections being indicative of a more complex dendritic arbor. The total number of Sholl intersections followed a similar pattern across the four genotype conditions and treatment groups: it rose sharply at radii between 10-20  $\mu\text{m}$  from the neuronal soma, then declined with increasing distance from the soma, reaching a plateau between  $\sim$ 80-120  $\mu\text{m}$  radii (see example WTN WTACM and KON KOACM plots and traces in Fig.2B,C). The baseline (PBS) number of Sholl intersections was considerably more variable in mixed genotype groups than in WTN WTACM, but did not significantly differ from that of WTN WTACM (KON WTACM  $p=0.0670$ ; WTN KOACM  $p=0.5978$ ; KON KOACM  $p=0.5978$  when compared with WTN WTACM; Fig.2H).

In WT neurons grown in WTACM (Fig.2B,E), we found that UTP did indeed influence neurite complexity: 10  $\mu\text{M}$  and 100  $\mu\text{M}$  UTP treatments led to an increase in the total number of Sholl intersections (10  $\mu\text{M}$  UTP  $p=0.0115$ ,  $n=6$  and 100  $\mu\text{M}$  UTP  $p=0.0130$ ,  $n=8$ ) relative to PBS vehicle ( $n=8$ ), but 0.1  $\mu\text{M}$  and 1  $\mu\text{M}$  UTP did not ( $p=0.2017$  and  $p=0.0608$ ;  $n=8$ ). Similar to our neurite outgrowth findings, *Fmr1* KO neurons grown in WTACM also increased their complexity in response to exogenous UTP (Fig.2F), with all four UTP treatment concentrations exhibiting elevated total Sholl intersections ( $p=0.0274$  for all comparisons;  $n=8/10$   $\mu\text{M}$  UTP  $n=6$ ) relative to PBS. However, neither WT neurons (0.1  $\mu\text{M}$  UTP  $p=0.5836$ ,  $n=8$ ; 1  $\mu\text{M}$  UTP  $p=0.3251$ ,  $n=6$ ; 10  $\mu\text{M}$  UTP  $p=0.4986$ ,  $n=8$ ; 100  $\mu\text{M}$  UTP  $p=0.5836$ ,  $n=8$ ) nor *Fmr1* KO neurons (0.1  $\mu\text{M}$  UTP  $p=0.2301$ ,  $n=8$ ; 1  $\mu\text{M}$  UTP  $p=0.9661$ ,  $n=8$ ; 10  $\mu\text{M}$  UTP  $p=0.9984$ ,  $n=6$ ; 100  $\mu\text{M}$  UTP  $p=0.8527$ ,  $n=8$ ) demonstrated

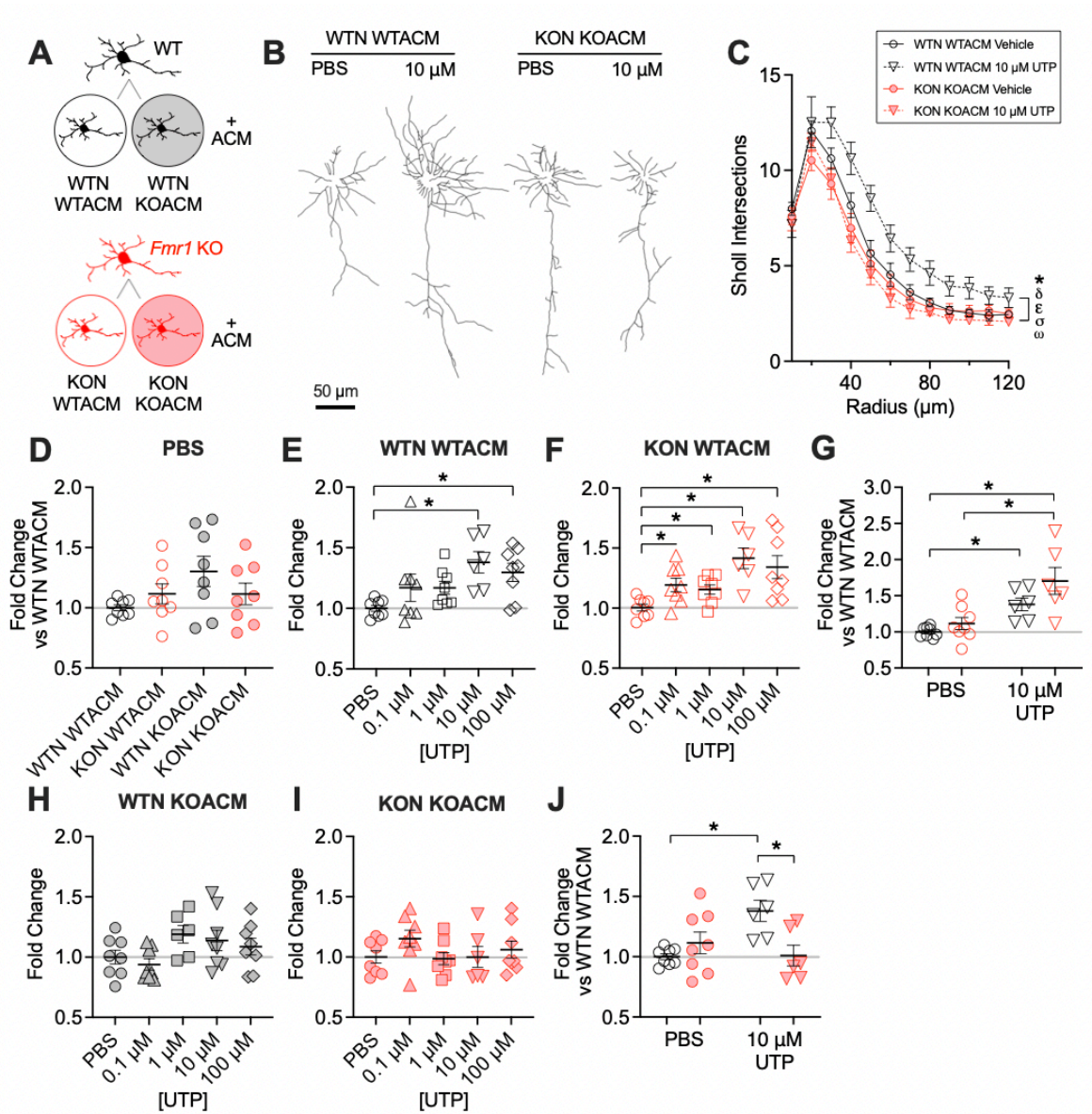


Figure 2. Sholl analysis of WT and *Fmr1* KO primary neurons cultured in WT or *Fmr1* KO astrocyte-conditioned media in the presence of UTP (0.1  $\mu$ M, 1  $\mu$ M, 10  $\mu$ M, 100  $\mu$ M, or PBS control). A. WT and *Fmr1* KO neurons (N) were each cultured for 5DIV in media (ACM) containing either WT or *Fmr1* KO astrocyte soluble factors, creating four separate genotype groups for neurite complexity experiments. B. Representative traces of WT neurons in WTACM and *Fmr1* KO neurons in *Fmr1* KO ACM, both treated with PBS (control) and 10  $\mu$ M UTP. C. Number of Sholl intersections at each radius from the neuronal soma, in WTN WTACM and KON KOACM conditions treated with PBS and 10  $\mu$ M UTP. Significant main effects and interactions ( $p < 0.05$ ) denoted by the following characters: \* genotype;  $\delta$  Sholl radius;  $\epsilon$  treatment;  $\sigma$  genotype x radius;  $\omega$  genotype x treatment. D. Between-genotypes comparison of baseline Sholl intersections when cultured neurons were treated with PBS. UTP treatment (10-100  $\mu$ M) increased the total number of Sholl intersections in (E) WTN WTACM and (F) KON WTACM conditions, but not in (H) WTN KOACM or (I) KON KOACM. Comparisons of (G) KON WTACM and (J) KON WTACM in relation to WTN WTACM show differences in the overall branching levels between genotypes. All data presented as means  $\pm$  SEM, with gray horizontal lines indicating control means.  $n=8$ ;  $n=6$  for 10  $\mu$ M WTN WTACM, KON WTACM, KON KOACM, and 1  $\mu$ M WTN KOACM. Significant differences between groups denoted by \*;  $p < 0.05$ .

differences in the number of Sholl intersections relative to vehicle (n=8) when grown in *Fmr1* KO ACM (Fig.2H,I).

While neurons grown with WT secreted factors demonstrated similar elevated numbers of Sholl intersections following 10  $\mu$ M UTP treatment (WTN WTACM 10  $\mu$ M UTP vs KON WTACM 10  $\mu$ M UTP: p=0.8992; Fig.2G), KON KOACM neurons formed significantly less complex arbors than WTN WTACM when both groups were treated with 10  $\mu$ M UTP (p=0.0018; Fig.2J). This can be seen clearly in the example Sholl plots and neurite traces in Fig.2B,C, where the purinergic-mediated increase in WTN WTACM arborization is broadly distributed throughout all Sholl radii, with significant effects of treatment ( $\epsilon$ ; p=0.0006), genotype (\*; p<0.0001) and Sholl radius ( $\delta$ ; p<0.0001), as well as significant interactions of genotype x radius ( $\sigma$ ; p=0.0188) and genotype x treatment ( $\omega$ ; p<0.0001). Surprisingly, these effects on neurite complexity were most prominent following 10  $\mu$ M concentration of UTP, as the number of WTN WTACM vs KON KOACM Sholl intersections following 100  $\mu$ M UTP treatment did not differ (p=0.4165; data not shown).

### ***P2Y<sub>2</sub> receptor expression is decreased in *Fmr1* KO neurons***

Select members of the P2Y receptor family possess high affinity for UTP, so we investigated the expression of these receptors on WT and *Fmr1* KO primary neurons to determine whether their differential expression might contribute to aberrant FXS neuronal signalling. Notably, neuronal P2Y<sub>2</sub> receptor levels were significantly reduced in *Fmr1* KO primary neuron cultures relative to WT (p=0.0315; n=6; Fig. 3B). However, not all P2Y receptors were similarly dysregulated in *Fmr1* KO neurons, as P2Y<sub>6</sub> receptor expression did not differ between WT and *Fmr1* KO neurons (p=0.7802; n=5; Fig. 3D). Similarly, neuronal P2Y<sub>1</sub> (p=0.2119; WT n=3 and *Fmr1* KO n=5; Fig. 3A) and P2Y<sub>4</sub> (p=0.8484; WT n=4 and *Fmr1* KO n=3; Fig. 3C) receptors were not differentially expressed between the two genotypes.

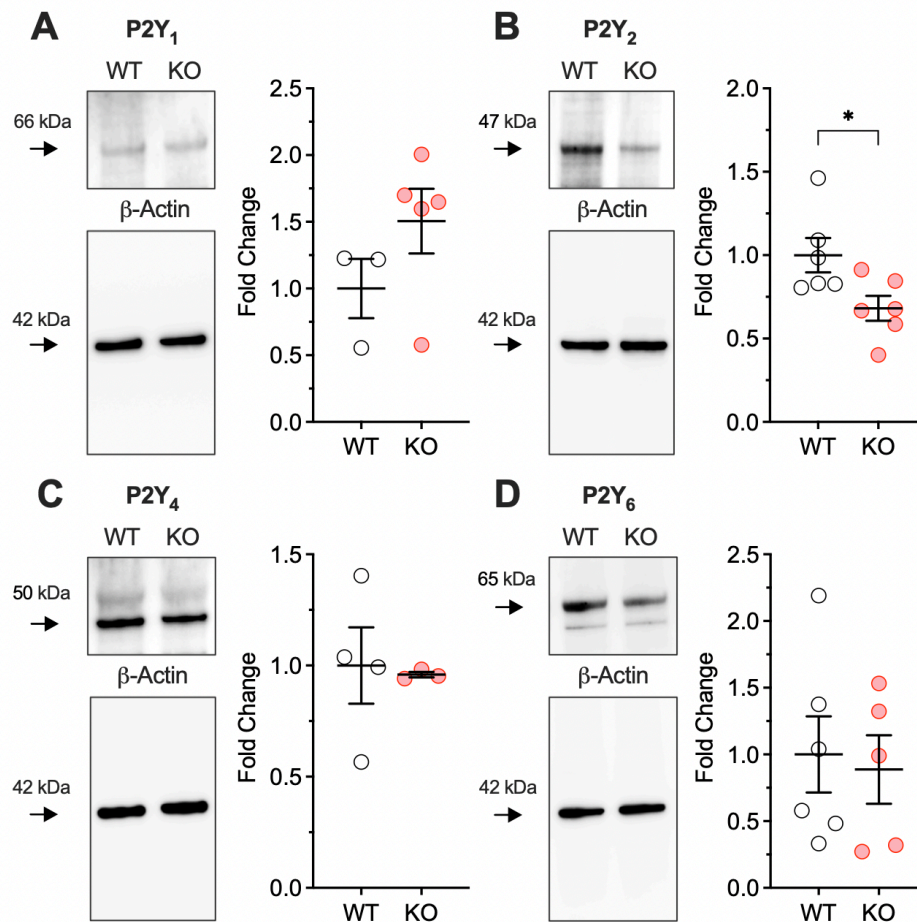


Figure 3. Quantification of P2Y<sub>1</sub>, P2Y<sub>2</sub>, P2Y<sub>4</sub>, and P2Y<sub>6</sub> excitatory purinergic receptors in neurons cultured from WT and *Fmr1* KO embryonic (E15) cortex. Representative western blots and  $\beta$ -actin loading controls are shown on each left panel, and neuron-associated receptor levels, expressed as fold change relative to WT means, are shown on each right panel. Expression of (B) neuronal P2Y<sub>2</sub> (47 kDa; n=6) was reduced in *Fmr1* KO cultures relative to WT, while (A) P2Y<sub>1</sub> (66 kDa; WT n=3/*Fmr1* KO n=5), (C) P2Y<sub>4</sub> (50 kDa; WT n=4; *Fmr1* KO n=3), and (D) P2Y<sub>6</sub> (65 kDa; n=5) receptor expression did not differ between genotypes. All data presented as means  $\pm$  SEM. Significant differences between treatments denoted by \*;  $p < 0.05$ .

### ***Fmr1 KO neuronal activity is elevated after 3 weeks in co-culture***

As our neurite outgrowth data has shown that astrocyte secreted factors powerfully influence neurite extension during early development, we wanted to understand how this early modulation of outgrowth impacts the formation of neural circuits over time. This led us to establish astrocyte-neuron co-cultures on microelectrode arrays (MEAs). MEAs are electrophysiology preparations which permit the recording of a simplified neural circuit *in vitro*, which we utilized to record neuronal firing activity 3x per week throughout the first 7-35 days of network development. Representative immunofluorescent images of 7DIV co-cultures are shown in FIG.4A, demonstrating the association between neurons and astrocytes in co-culture. Definitions and graphics explaining the MEA parameters we analyzed are presented in Table 1 and Fig.4B.

To ensure that measured neuronal firing recorded was a result of synaptic activity and not general excitability (*e.g.* gap junction activity), we first applied AMPA and NMDA receptor blockers CNQX (10  $\mu$ M) and AP-5 (10  $\mu$ M) to inhibit synaptic firing. Mean firing rates of naïve versus CNQX+AP-5-treated cells were not significantly different between either genotype at 7DIV, but by 10-12DIV, there was a visible decrease in the amount of activity detected from both WT and *Fmr1* KO CNQX+AP-5-treated cultures. In WT cultures, significant effects of treatment ( $\epsilon$ ;  $p < 0.0001$ ), time ( $\delta$ ;  $p < 0.0001$ ), and treatment x time ( $\psi$ ;  $p < 0.0001$ ; Fig.4D) were reported, along with significant post-hoc differences between treatment groups at 10DIV and 12DIV (7DIV  $p = 0.1587$ ; 10DIV and 12DIV both  $p < 0.0001$ ); in *Fmr1* KOs, significant main effects of treatment ( $\epsilon$ ;  $p < 0.0001$ ), time ( $\delta$ ;  $p = 0.0124$ ), and treatment x time ( $\psi$ ;  $p = 0.0412$ ; Fig.4D) were also found, along with significant differences revealed by post-hoc comparisons at 10DIV and 12DIV (7DIV  $p = 0.7704$ ; 10DIV  $p = 0.0187$  and 12DIV;  $p = 0.0008$ ).

We also compared the number of “active” electrodes, defined as detecting  $>5$  spikes per minute, between genotypes throughout the duration of the experiment in order to ensure that each MEA measurement reflected similar levels of healthy and actively firing neurons.

Wells with at least 9/16 (50%) active electrodes at >10DIV were retained for analysis of firing characteristics. Among these selected wells, a mean of 12.68 of the 16 available electrodes per well consistently detected neuronal firing in WT co-cultures (n=13 at 7DIV and n=6 by 35DIV) once synaptic activity was established, versus 11.77 of 16 electrodes in *Fmr1* KO co-cultures (p=0.2115; n=15 at 7DIV and n=8 by 35DIV; Fig.4E). A significant effect of time was noted ( $\delta$ ; p=0.0040), as the number of active electrodes was low during the earliest stages of recording, but rapidly stabilized as cultures developed networks.

To determine the general firing characteristics of WT vs *Fmr1* KO neurons in co-culture, we utilized weighted mean firing rate, which measures the total number of spikes within the 10 min recording period normalized to the number of active electrodes. Within the first 14DIV, *Fmr1* KO neurons demonstrated a nonsignificant trend toward reduced weighted mean firing rate in comparison to WTs (effects of genotype; p=0.0690 and time  $\delta$ ; p<0.0001; Fig.4F left panel), though as the cultures matured, this reversed to a nonsignificant but apparent trend toward an increased *Fmr1* KO weighted mean firing rate (effect of genotype; p=0.1644; Fig.4F right panel). While weighted mean firing rate indicates the number of spikes, the synchrony index indicates how these spikes are temporally related to each other, with values close to 1 indicating a high degree of neuronal synchrony. Surprisingly, *Fmr1* KO firing synchrony was significantly reduced relative to WT throughout 35DIV, with significant effects of genotype (\*; p=0.0247; Fig.4G) as well as time ( $\delta$ ; p=0.0363).

Clearer genotypic differences were observed between the activity and connectivity of neurons within a regional network centred around a singular electrode. Most strikingly, the frequency of neuronal bursting events was elevated in naïve *Fmr1* KO neuron-astrocyte co-culture relative to WT. These bursting events are visualized in Fig.4C over a representative 30 s of the total 10 min recording, where each row signifies the neuronal firing recorded across each of the 16 MEA electrodes, and neuronal bursts are indicated by blue boxes. Neuronal burst frequency steadily increased with maturation and was visibly

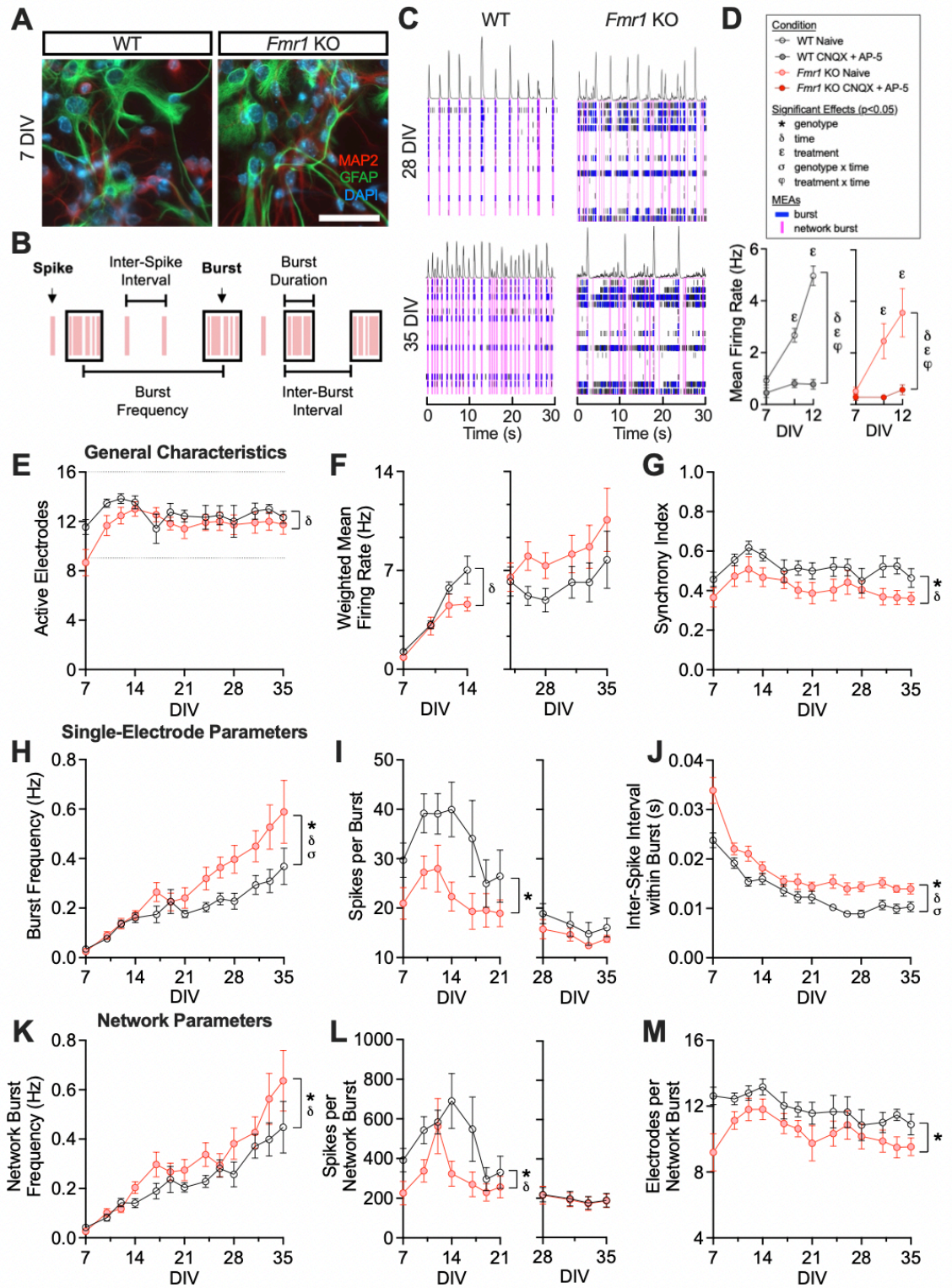


Figure 4. Firing characteristics of WT and *Fmr1* KO co-cultured neurons between 7-35DIV. Neurons were co-cultured on microelectrode arrays (MEAs) with their respective genotype of astrocytes, then recorded 3x weekly (10 min/recording) from 7-35DIV. A. Representative images of WT and *Fmr1* KO co-cultures at 7DIV, with neurons labelled in red (MAP2), astrocytes labelled in green (GFAP), and nuclei stained in blue (DAPI). Scale bar: 50  $\mu$ m. B. Schematic demonstrating the various MEA parameters measured at a single electrode, adapted from Axion Biosystems (2017) and Botelho et al. (Neucyte). Spikes are shown as pink lines, and bursts are shown as black boxes. C. Representative raster plots of WT and *Fmr1* KO neuronal firing at 28DIV and 35DIV. Representative neuronal spikes from a single electrode are shown on the top row of each plot, and each subsequent row indicates the activity recorded at a single electrode over a 30 s recording period. Blue bars indicate neuronal burst events, and pink boxes indicate network burst events. D. Mean firing rate of WT and *Fmr1* KO naïve (WT n=13; *Fmr1* KO n=15) and CNQX+AP-5-treated (WT n=15; *Fmr1* KO n=12) cultures. The AMPA and NMDA receptor blockers CNQX (10  $\mu$ M) and AP-5 (10  $\mu$ M) were applied to cells for 10 min prior to recording, then immediately removed after recording to restore neuronal firing. WT and *Fmr1* KO synaptic activity was effectively blocked by CNQX+AP-5 at 10DIV and 12DIV, but not 7DIV. E. Wells with at least 9/16 (>50%) active electrodes at  $\geq$ 10DIV were retained for analysis of firing characteristics. Though some cultures were unable to be recorded for the full 35DIV, the number of active electrodes in analyzed wells did not differ between WT (n=13 at 7DIV; n=6 by 35DIV) and *Fmr1* KO (n=15 at 7DIV; n=8 by 35DIV) throughout the duration of the experiment. F. Weighted mean firing rate throughout the 7-35DIV recording period did not significantly differ between WT and *Fmr1* KO neurons, though synchrony index (G) was reduced in *Fmr1* KO neurons throughout the experiment. H. At single electrodes, *Fmr1* KO neurons demonstrated increased burst frequency as the co-cultures matured. The number of spikes per burst (I) were reduced in *Fmr1* KO neurons over the first 21 DIV, but were normalized to WT levels between 28-35DIV, while the mean inter-spike interval within bursts (J) was elevated in *Fmr1* KO neurons throughout the duration of the experiment. Throughout the entire neural network, network burst frequency (K) was elevated in *Fmr1* KO neurons, and the number of spikes per burst (L) were reduced in *Fmr1* KO neurons over the first 21DIV but were normalized to WT levels between 28-35DIV. M. The number of electrodes participating in a network burst, indicating the level of connectivity within the culture, were also decreased in *Fmr1* KO cultures relative to WT. Data points represent means  $\pm$  SEM. Main effects/interactions were considered significant at  $p < 0.05$ .

consistent between genotypes within the first two weeks in culture, but began to diverge at 21DIV (Fig.4H). We observed significant effects of genotype (\*;  $p=0.0064$ ) and time ( $\delta$ ;  $p<0.0001$ ) on neuronal bursting frequency throughout the 7-35DIV recording period, as well as a significant interaction of genotype x time ( $\sigma$ ;  $p=0.0091$ ). The number of neuronal spikes within each bursting event was significantly higher in WT versus *Fmr1* KO co-cultures during the earliest stages of development (7-21DIV; significant effect of genotype \*;  $p=0.0071$ ; Fig.4I left panel) but became remarkably consistent between genotypes with maturation. By 28DIV, *Fmr1* KO neuronal bursting events contained the same number of spikes as their respective WT bursting events (28-35DIV;  $p=0.4506$ ; Fig.4I right panel), indicating that the frequency of these coordinated firing events had increased in *Fmr1* KO co-cultured neurons, but their magnitude had not. The average time between the spikes that comprise a bursting event, or the mean inter-spike interval within bursts, was significantly elevated in *Fmr1* KO cultures (Fig.4J), with significant effects of genotype (\*;  $p=0.0002$ ) and time ( $\delta$ ;  $p<0.0001$ ), as well as a significant interaction between genotype x time ( $\sigma$ ;  $p=0.0447$ ). Accordingly, the variability between inter-burst intervals was elevated in *Fmr1* KO (significant effects of genotype;  $p=0.0367$  and time;  $p=0.0094$ ), though the duration of the bursts did not differ between genotypes ( $p=0.3300$ ) (data not shown).

Looking at the MEA culture as a single entity also revealed elevated activity and decreased connectivity throughout the culture. The frequency of network bursts, shown with pink boxes in Fig.4C, was increased in *Fmr1* KO co-culture in comparison to WT (Fig.4K), with significant effects of both genotype (\*;  $p=0.0241$ ) and time ( $\delta$ ;  $p<0.0001$ ). Similar to single-electrode bursts, the number of spikes per network burst was reduced in *Fmr1* KO cultures relative to WT during the first two weeks of recording (7-21DIV; \*  $p=0.0165$ ; Fig.4L left panel), then normalized by the end of the recording period (28-35DIV;  $p=0.9730$ ; Fig.4L right panel). Reduced synchrony throughout the culture is reflected in the number of electrodes associated with each network burst (Fig.4M), which was significantly reduced in *Fmr1* KO co-cultures versus WT (significant main effect of genotype \*;  $p=0.0296$ ). This indicates that while *Fmr1* KO neurons in co-culture

demonstrated greater local excitability than WTs, they did not show as robust connectivity between the more distant networks of neurons within the culture dish.

### ***P2Y<sub>2</sub> antagonism normalizes *Fmr1* KO neuronal bursting***

Given that *Fmr1* KO co-cultured neurons demonstrated heightened activity in the form of increased burst and network burst frequency, we hypothesized that elevated *Fmr1* KO astrocyte P2Y<sub>2</sub> receptor levels (Reynolds, Wong & Scott, 2021) might contribute to this excitatory phenotype. We therefore treated WT and *Fmr1* KO co-cultures with the specific P2Y<sub>2</sub> antagonist AR-C 118925XX at concentrations of 1  $\mu$ M (WT n=14 at 7DIV/n=8 at 35DIV and *Fmr1* KO n=12 at 7DIV/n=2 at 35DIV) or 10  $\mu$ M (WT n=13 at 35DIV/n=7 at 35DIV and *Fmr1* KO n=11 at 35DIV/n=7 at 35DIV) over the 7-35DIV MEA recording period in order to isolate the effect of the P2Y<sub>2</sub> receptor on neuronal firing. Here, we have highlighted the most relevant activity and synchrony effects when this chronic antagonism was applied indiscriminately to both neuronal and astrocyte P2Y<sub>2</sub> receptors.

Most strikingly, AR-C 118925XX treatment led to a robust decrease in the rapid firing of neurons over time, which was evident when comparing burst frequency between naïve and AR-C 118925XX-treated cultures. As seen in Fig.5A, *Fmr1* KO naïve and 1  $\mu$ M AR-C 118925XX-treated co-cultures followed a similar burst frequency trajectory for the first 7-24DIV, then at 26DIV, AR-C-treated *Fmr1* KO neurons rapidly decreased their bursting frequency, as AR-C appeared to normalize *Fmr1* KO bursting to WT naïve levels. Here, we observed significant main effects of treatment ( $\epsilon$ ;  $p < 0.0001$ ), genotype ( $*$ ;  $p < 0.0001$ ), and time ( $\delta$ ;  $p < 0.0001$ ) on burst frequency over the 7-35DIV period, as well as significant interactions between treatment x time ( $\psi$ ;  $p = 0.0005$ ), genotype x time ( $\sigma$ ;  $p = 0.0093$ ), and treatment x genotype ( $\omega$ ;  $p = 0.0212$ ). The 1  $\mu$ M and 10  $\mu$ M AR-C 118925XX treatments were similar in their ability to decrease neuronal burst activity within a single genotype (AR-C 118925XX 1  $\mu$ M vs 10  $\mu$ M: WT  $p = 0.7874$  and *Fmr1* KO  $p = 0.6510$ ), allowing the data from both treatment concentrations to be pooled together for further comparison. A significant increase in *Fmr1* KO naïve burst frequency was observed

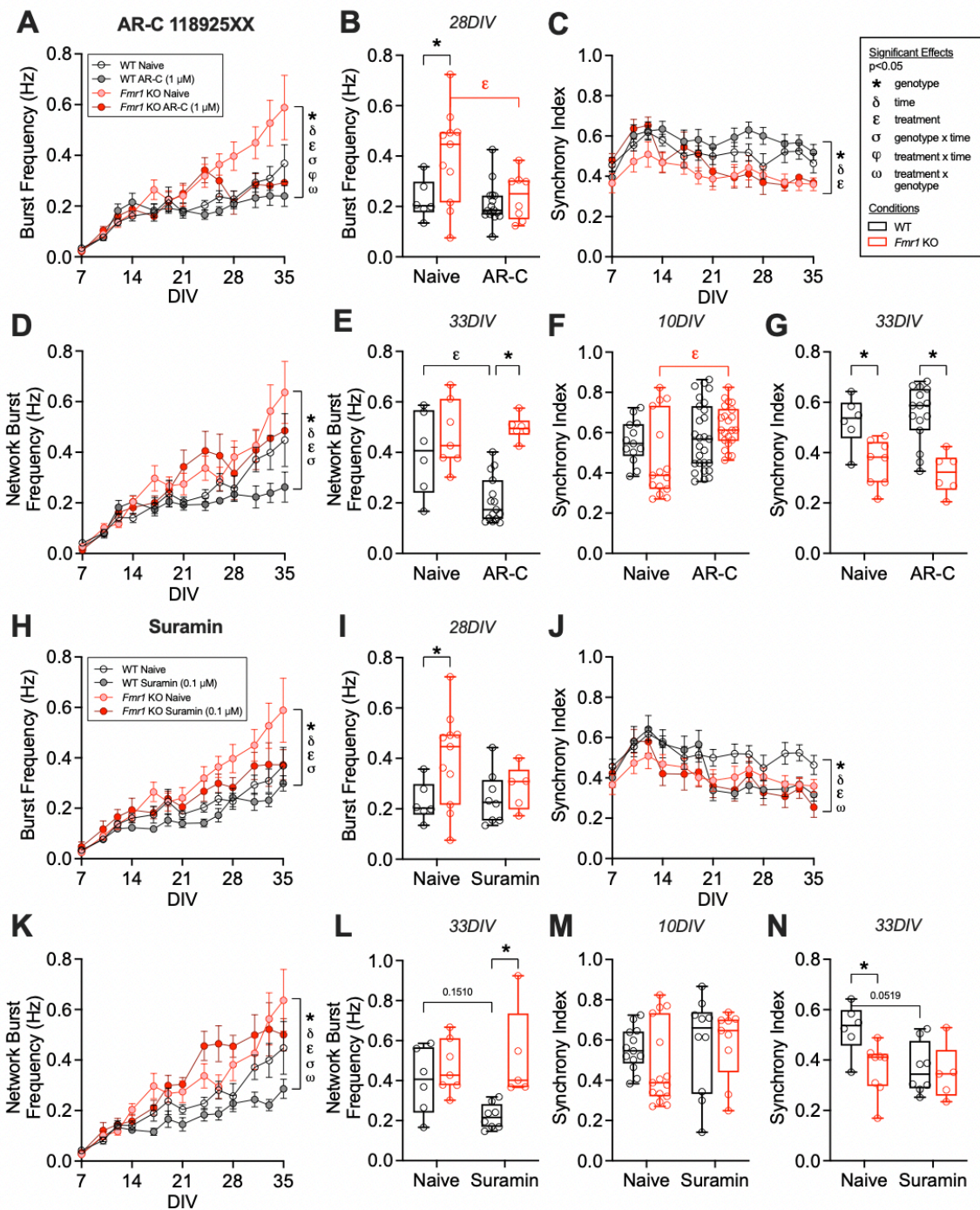


Figure 5. Normalization of aberrant neuronal *Fmr1* KO bursting with P2Y<sub>2</sub> antagonism. WT and *Fmr1* KO neurons were co-cultured on microelectrode arrays (MEAs) with their respective genotype of astrocytes, then treated 2x weekly with the selective P2Y<sub>2</sub> antagonist AR-C 118925XX (1 μM and 10 μM) or the pan-purinergic antagonist suramin (0.1 μM) in an attempt to correct aberrant neuronal activity and synchrony. Cultures were recorded 3x weekly (10 min/recording) from 7-35DIV. A. Single-electrode burst frequency between 7-35DIV following treatment with 1 μM AR-C 118925XX. Pooling both AR-C 118925XX treatment concentrations, which did not significantly differ from each other, revealed a significant decrease in burst frequency at 28DIV (B) that normalized *Fmr1* KO bursting to WT levels. C. Culture-wide synchrony index of 1 μM AR-C 118925XX-treated neurons. A transient elevation in *Fmr1* KO AR-C 118925XX (pooled) synchrony index was evident at 10 DIV (F) but was not retained by 33DIV (G). D. Network burst frequency of naïve and AR-C 118925XX-treated neurons between 7-35DIV, highlighting a significant decrease in WT network burst frequency at 33DIV (E) following pooled AR-C 118925XX treatment. H. Single electrode burst frequency of suramin-treated neurons between 7-35DIV, which did not significantly reduce *Fmr1* KO burst frequency at 28DIV (I). J. Synchrony index of naïve and suramin-treated neurons over 7-35DIV, with specific comparisons highlighted at 10DIV (M) and 33DIV (N). K. Network burst frequency following suramin treatment, showing a reduction in WT network burst frequency at 33DIV (L). Naïve: WT n=13 at 7DIV/n=6 by 35DIV and *Fmr1* KO n=15 at 7DIV/n=8 by 35DIV. AR-C 118925XX 1 μM: WT n=14 at 7DIV/n=8 at 35DIV and *Fmr1* KO n=12 at 7DIV/n=2 at 35DIV; AR-C 118925XX 10 μM: WT n=13 at 35DIV/n=7 at 35DIV and *Fmr1* KO n=11 at 35DIV/n=7 at 35DIV. Suramin: WT n=10 at 7DIV/n=8 at 35DIV; *Fmr1* KO n=9 at 7DIV/n=5 at 35DIV. Data points on line graphs represent means +/- SEM, while box plots denote the interquartile range with whiskers extending to minimum and maximum values. Both main effects/interactions (line graphs) and post-hoc comparisons between treatments and genotypes (box plots) were considered significant at p<0.05.

relative to WT naïve ( $p=0.0383$ ) at 28DIV, but this elevated burst frequency was normalized in *Fmr1* KO pooled AR-C 118925XX-treated neurons ( $p=0.0383$ ; Fig.5B).

P2Y<sub>2</sub> antagonism also impacted the coordinated firing of neurons within networks (*i.e.* network bursts), though differences were most evident between WT treatment groups, as WT AR-C neurons demonstrated decreased network burst frequency relative to WT naïve within the final recording week (Fig.5D). Following 1  $\mu$ M AR-C 118925XX treatment, we observed significant main effects of treatment ( $\epsilon$ ;  $p=0.0109$ ), genotype (\*;  $p<0.0001$ ), and time ( $\delta$ ;  $p<0.0001$ ), as well as a significant interaction between genotype x time ( $\sigma$ ;  $p<0.0008$ ). When both AR-C 118925XX treatments were pooled together (AR-C 118925XX 1  $\mu$ M vs 10  $\mu$ M: WT  $p=0.2503$  and *Fmr1* KO  $p=0.5912$ ), the network burst frequency of WT AR-C 118925XX-treated cultures was significantly lesser than that of WT naïve at 33DIV ( $p=0.0061$ ), yet also reduced in comparison to *Fmr1* AR-C 118925XX-treated neurons ( $p<0.0001$ ; Fig.5E). While specific P2Y<sub>2</sub> antagonism decreased the frequency of bursts at a single electrode, it did not significantly alter *Fmr1* KO network burst frequency relative to *Fmr1* KO naïve (33DIV  $p=0.6524$ ).

In addition, the synchrony index of *Fmr1* KO neurons undergoing P2Y<sub>2</sub> antagonist treatment was transiently normalized within the first  $\sim 2$  weeks *in vitro*. However, *Fmr1* KO AR-C synchrony lessened with time, and returned to *Fmr1* KO naïve levels by  $\sim 24$ DIV. Significant main effects of treatment ( $\epsilon$ ;  $p=0.0019$ ), genotype (\*;  $p<0.0001$ ), and time ( $\delta$ ;  $p<0.0001$ ) were noted when genotypes and treatment groups were compared over the full 7-35DIV period (Fig.5C). Pooling both AR-C treatments (1  $\mu$ M vs 10  $\mu$ M: WT  $p=0.1883$  and *Fmr1* KO;  $p=0.4561$ ) and focusing at the 10DIV time point, a significant increase in the synchrony index of *Fmr1* KO AR-C 118925XX-treated cultures was found relative to *Fmr1* KO naïve ( $p=0.0144$ ; Fig.5F), but by 33DIV, only genotypic differences remained (WT vs *Fmr1* KO AR-C 118925XX  $p=0.4844$ ; WT vs *Fmr1* KO naïve  $p=0.4844$ ; Fig.5G).

We also attempted to investigate the effect of the selective P2Y<sub>6</sub> antagonist MRS 2578 on neuronal activity and connectivity. However, we experienced significant issues

determining an adequate treatment concentration, as MRS 2578 co-cultures did not consistently survive for 35DIV even after a 100-fold decrease in the treatment concentrations suggested in the literature. It remains unclear whether these effects result from specific P2Y<sub>6</sub> antagonism or are an unintended consequence of the molecule itself, and further investigation using a different form of P2Y<sub>6</sub> blockade will be important to make this distinction.

### ***General P2 antagonism has little effect on neuronal activity and synchrony***

Numerous P2Y receptors are expressed on both cortical neurons and glia, and it is possible that these receptors may be capable of compensating for selective inhibition of P2Y<sub>2</sub>. Thus, we also treated co-cultures with the pan-purinergic antagonist suramin (0.1  $\mu$ M; WT n=10 at 7DIV/n=8 at 35DIV and *Fmr1* KO n=9 at 7DIV/n=5 at 35DIV) to see whether nonselective inhibition led to a more robust reduction of *Fmr1* KO neuronal activity. Similar to AR-C, we observed significant main effects of treatment ( $\epsilon$ ;  $p < 0.0001$ ), genotype ( $*$ ;  $p < 0.0001$ ), and time ( $\delta$ ;  $p < 0.0001$ ) on neuronal burst frequency (Fig.5H), as well as a significant interaction between genotype x time ( $\sigma$ ;  $p = 0.0149$ ). Suramin-treated *Fmr1* KO burst frequency appeared to somewhat diverge from *Fmr1* KO naïve levels after ~1 month *in vitro*, though this effect was less pronounced than that of AR-C 118925XX and was not statistically significant at 28DIV (*Fmr1* KO naïve vs *Fmr1* KO suramin;  $p = 0.4342$ ; Fig.5I).

Network burst frequency differed between genotypes and treatments (Fig.5K), with significant main effects of treatment ( $\epsilon$ ;  $p = 0.0475$ ), genotype ( $*$ ;  $p < 0.0001$ ), and time ( $\delta$ ;  $p < 0.0001$ ), as well as interactions between genotype x time ( $\sigma$ ;  $p < 0.0001$ ) and genotype x treatment ( $\omega$ ;  $p = 0.0005$ ), as a result of prominently decreased network bursting activity in suramin-treated WT cells. This reduced activity was evident at 33DIV (Fig.5L), where WT suramin treatment resulted in significantly lower network burst frequency than in *Fmr1* KO suramin-treated neurons ( $p = 0.0120$ ), and trended toward a nonsignificant decrease relative to WT naïve ( $p = 0.1510$ ).

We also observed significant main effects of both treatment ( $\epsilon$ ;  $p=0.0027$ ), genotype ( $*$ ;  $p<0.0001$ ), and time ( $\delta$ ;  $p<0.0001$ ) on synchrony index (Fig.5J), as well as a significant interaction between the two ( $\omega$ ;  $p=0.0423$ ). However, the direction of this effect was quite different than that of AR-C 118925XX, as it appeared to selectively reduce WT synchrony. At 33DIV, this effect was very nearly significant (Fig.5N) with a trend toward a decrease in WT suramin synchrony relative to WT naïve ( $p=0.0519$ ), though suramin affected neither WT nor *Fmr1* KO synchrony at 10DIV (WT naïve vs WT suramin;  $p=0.9820$  and *Fmr1* KO naïve vs *Fmr1* KO suramin;  $p=0.6558$ ).

## 5.9. Discussion

Our current findings indicate that astrocytes modulate both the morphology and the activity of neurons to influence the FXS neuronal phenotype. Here, putative axons were significantly extended in control-treated conditions when neurons of either genotype were grown with *Fmr1* KO ACM, while P2Y receptor activation elevated neurite outgrowth and branching in the presence of WT but not *Fmr1* KO ACM, suggesting that astrocyte-secreted factors such as UTP drive maximal neurite extension. *Fmr1* KO neurons demonstrated hyperexcitation in the form of increased neuronal burst frequency following several weeks in co-culture, which was normalized to WT levels through chronic application of the selective P2Y<sub>2</sub> antagonist AR-C 118925XX. As we have recently found that P2Y<sub>2</sub> expression is increased in *Fmr1* KO cortical astrocytes, we suggest that this beneficial effect of treatment is due to the reduction of elevated purinergic signalling in *Fmr1* KO astrocytes, which influences the neuronal environment to regulate localized cortical excitation.

### ***Neurite outgrowth and complexity is influenced by purinergic signalling***

Dysregulated neurite outgrowth and branching can greatly impact the ability of neurons to establish appropriate neuronal networks during early cortical development. Neurons extend their axons via actin-rich growth cones that probe the neuronal environment in search of attractive or repulsive cues to influence axonal length and

direction (reviewed in Dent, Gupton, & Gertler, 2011; Gillespie, 2003). Rapid actin depolymerization and repolymerization cycles facilitate the addition of actin monomers to extend the axon, while neurotrophins influence the direction of the extension (Marsick, Flynn, Santiago-Medina, Bamberg, & Letourneau, 2010). Purinergic modulation of the actin-severing protein cofilin has been found to elevate both neurite outgrowth and branching *in vitro* (Peterson et al., 2013; Pooler et al., 2005), suggesting that purinergic mechanisms may underlie the formation of neural networks. Here, treatment with UTP was capable of influencing the extension of the longest neurite (presumably the axon) and the complexity of arborization as predicted: UTP-treated WT neurons grown in WT ACM significantly increased their maximal neurite outgrowth and number of Sholl intersections, while surprisingly, *Fmr1* KO neurons grown in WT ACM were even more responsive to UTP. These patterns indicate that along with WT neurons, *Fmr1* KO neurons retain their ability to modulate neurite length through purinergic-driven pathways when cultured in the appropriate astrocytic environment.

As neurite extension and branching are regulated in part by purinergic signalling, we sought to determine whether neuronal purinergic receptors were differentially expressed on WT vs *Fmr1* KO neurons. P2Y<sub>2</sub> receptor levels were unexpectedly decreased in *Fmr1* KO cortical neuron cultures, while P2Y<sub>1</sub>, P2Y<sub>4</sub>, and P2Y<sub>6</sub> levels were unchanged. This is contrary to the elevated neurite extension seen in WTACM-grown *Fmr1* KO neurons following UTP treatment, as previous literature suggests that the P2Y<sub>2</sub> receptor is responsible for purinergic-mediated outgrowth (Peterson et al., 2013; Pooler et al., 2005). Though a lack of P2Y<sub>2</sub> receptors may be a limiting factor for *Fmr1* KO neuronal extension, it is possible that UTP may also be acting on additional neuronal P2Y receptors to facilitate outgrowth. While UTP/UDP-sensitive P2Y<sub>4</sub> and P2Y<sub>6</sub> receptors have not yet been identified as specific regulators of neurite extension, intracellular calcium release has previously been shown to activate brain-derived neurotrophic factor (Finkbeiner, 2000), which promotes neurite lengthening (Rabacchi et al., 1999). Excitatory P2Y GPCRs also broadly activate the PI3K/Akt signalling pathway (Sanchez et al., 2001) to influence axonal

elongation (Heine et al., 2015; Van Kolen & Slegers, 2006), suggesting another mechanism by which P2Y receptors could cooperatively utilize exogenous UTP to drive outgrowth.

It is also important to consider that these neuronal P2Y<sub>2</sub> levels reflect the baseline receptor expression in the absence of astrocytic input. This excitatory receptor downregulation may suggest that, to a certain degree, *Fmr1* KO neurons in isolation are able to compensate for elevated astrocyte P2Y receptor expression. However, P2Y receptor levels are known to be modulated by ongoing excitatory activity *in vivo*. Astrocyte P2Y<sub>2</sub>, in particular, has been found to be upregulated through ERK-mediated pathways in response to UTP and guanosine availability (Ballerini et al., 2006), as well as BzATP-mediated activation of the excitatory P2X<sub>7</sub> purinergic receptor (D'Alimonte et al., 2007). It is therefore likely that excitatory purinergic receptor levels are dynamically modulated throughout early cortical development, especially given that astrocyte purinergic pathways are known to be upregulated (Reynolds et al., 2021).

### ***Neurite outgrowth and branching is primarily astrocyte-driven***

While UTP effectively increased neurite outgrowth and branching in our control group of WTN WTACM neurons, neuronal genotype did not at all determine the capacity for additional UTP-driven neurite extension or complexity. Further, neuronal genotype also did not determine the longest neurite length in control-treated cultures. Instead, FMRP-associated astrocyte soluble factors significantly increased maximal neurite length yet completely inhibited the ability of neurons to extend their longest outgrowths or form new branches following purinergic agonism. It is possible that neurons treated with *Fmr1* KO soluble factors, including UTP and UDP, may have reached maximal UTP-driven extension within control conditions due to upregulated *Fmr1* KO astrocyte purinergic secretions, making the presence of excess UTP unable to further drive outgrowth. Notably, 100  $\mu$ M UTP treatment in WTN WTACM cultures led to a maximal neurite length very similar to both control-treated WT and *Fmr1* KO neurons grown in *Fmr1* KO ACM, in accordance with this hypothesis. It remains unclear whether UTP is indeed present in higher amounts

within *Fmr1* KO ACM, as current techniques pose significant challenges for the quantification of cortical and astrocyte-secreted UTP. However, the presence of increased levels of the UTP precursor uridine in the plasma of individuals with ASD (Adams et al., 2011) suggests the potential for elevated UTP synthesis and secretion within the FXS brain.

Neurotrophic factors, which powerfully influence neuronal growth processes including axonal growth and direction, may also underlie the excess outgrowth of KOACM-grown neurons. Astrocyte-secreted neurotrophin-3 (NT-3), which promotes axonal growth (Fornaro et al., 2020) and regeneration (Grill, Murai, Blesch, Gage, & Tuszynski, 1997), is translationally regulated by FMRP. This neurotrophin is elevated in both *Fmr1* KO mice (Yang et al., 2012) and in individuals with ASD (Sajdel-Sulkowska, Xu, & Koibuchi, 2009), and these upregulations are reflected by increased NT-3 levels within *Fmr1* KO cortical astrocyte media (Yang et al., 2012). Correcting NT-3 at the level of the astrocyte affects connectivity in a physiologically meaningful way, including the normalization of aberrant trace fear conditioning in *Fmr1* KO mice (Yang et al., 2012). NT-3 and UTP/UDP may therefore be part of a host of *Fmr1* KO astrocyte secretions which promote axonal extension of cultured neurons, driving neurons to quickly reach their “ceiling” of neurite extension.

These strong effects of ACM indicate that neuronal outgrowth and complexity during early development are highly dependent on astrocytic regulation of the neuronal environment. As neuronal FMRP is expressed within dendrites and axonal growth cones (Antar, Dichtenberg, Plociniak, Afroz, & Bassell, 2005), and its absence in *Drosophila* leads to axonal overgrowth and mistargeting in select brain regions (Morales et al., 2002; Pan, Zhang, Woodruff, & Broadie, 2004), we had anticipated some degree of difference in baseline and/or UTP-driven outgrowth and branching between neuronal genotypes. However, we show here that in mouse cortical neurons, absence of neuronal FMRP is not sufficient to influence neurite extension. This is consistent with previous research indicating that astrocytes influence neuronal dysregulation in FXS; for instance, Jacobs and Doering (2010) observed that WT hippocampal neurons assumed a disordered *Fmr1* KO-

like dendritic morphology when grown in *Fmr1* KO ACM, while J. L. Hodges et al. (2017) found that astrocyte-specific silencing of *Fmr1* was sufficient to alter mouse motor neuron morphology and alter acquisition of motor skills. It is therefore clear that FXS therapeutic approaches must take into account the contribution of astrocytes to the neuronal environment in order to meaningfully influence neuronal morphology and connectivity, as astrocytes exert substantial influence on neuronal growth processes.

### ***Fmr1* KO neurons in co-culture display hallmarks of hyperexcitation**

Having found that the morphology of cortical neurons is highly influenced by astrocyte secretions, we sought to investigate how this astrocyte-driven aberrant neuronal morphology impacts the formation of neuronal circuits over time. Microelectrode arrays (MEAs) were an ideal tool for this research question, as they utilize electrophysiology to obtain population-level measurements of neuronal activity, synchrony, and oscillation, and allow for repeated and non-invasive recordings. In co-culture with *Fmr1* KO cortical astrocytes, *Fmr1* KO cortical neurons demonstrated both increased burst frequency and increased network burst frequency after ~3 weeks *in vitro*, consistent with the development of a hyperexcitable cortex. Upon further investigation, we noted that the magnitude of these *Fmr1* KO bursts and network bursts were initially reduced during the first ~2 weeks of recording, during time frames typically associated with neurite elongation and synaptogenesis, and occurring concurrently with a transient trend toward a potential reduction in weighted mean firing rate. However, once the frequency of bursts increased (>24DIV), these events contained the same number of neuronal spikes as WTs, indicating an overall heightened local excitatory output.

These findings are consistent with elevated neuronal firing reported in *Fmr1* KO rat visual cortex following a transient early period of hypoexcitability (Berzhanskaya, Phillips, Shen, & Colonnese, 2016), suggesting that *Fmr1* KO neuronal networks may mature at different rates than WTs, potentially as a result of altered processes during cortical development. Numerous other studies in both *Fmr1* KO rodent models and iPSCs support

neuronal hyperexcitability within the first two months of postnatal development, both across large MEA-measured networks (Graef et al., 2020; Liu et al., 2018) and within more localized interactions (Gonçalves, Anstey, Golshani, & Portera-Cailliau, 2013; Zhang et al., 2014). In contrast, several studies of human iPSC-derived neurons have shown early deficits in neuronal firing (Telias, Kuznitsov-Yanovsky, Segal, & Ben-Yosef, 2015), possibly indicating variability of FXS phenotypes across regions and developmental stages.

### ***Neuronal burst frequency is regulated in part by P2Y<sub>2</sub> receptor activation***

Our findings suggest a role for P2Y<sub>2</sub> receptors in heightened *Fmr1* KO burst frequency, as excess bursting was normalized to WT levels following treatment with the specific P2Y<sub>2</sub> antagonist AR-C 118925XX. We have recently shown that P2Y-mediated excitatory signalling is elevated in *Fmr1* KO cortical astrocytes; specifically, levels of astrocyte P2Y<sub>2</sub> receptors were elevated both *in vitro* and in acutely dissected astrocytes, and P2Y agonism led to increased duration of astrocyte intracellular calcium responses (Reynolds et al., 2021). The binding of UTP to G<sub>q</sub>-coupled P2Y receptors including P2Y<sub>2</sub> activates phospholipase C, which initiates inositol triphosphate-mediated release of intracellular calcium stores from the endoplasmic reticulum (Abbracchio, Burnstock, Verkhratsky, & Zimmermann, 2009). This released calcium is transmitted to other astrocytes, leading to the spread of astrocyte calcium waves and the subsequent initiation of excitatory processes which affect both astrocytes and the neuronal environment. Purinergic-driven release of astrocyte intracellular calcium prompts release of gliotransmitters including glutamate and ATP (Scemes & Giaume, 2006), an event which would increase the likelihood of neurons reaching their threshold for action potentials. Purinergic agonism is also associated with both the expression and release of astrocyte soluble factors, including pro-synaptogenic proteins such as TSP-1. Indeed, this P2Y<sub>2</sub>-mediated effect occurred soon after the *Fmr1* KO and WT naïve burst frequency trajectories began to diverge, at a time point consistent with a potential correction of synaptic dysregulation.

Given that P2Y<sub>2</sub> receptor expression was reduced in *Fmr1* KO neuronal cultures, it is likely that the effects of AR-C 118925XX primarily occurred as a result of antagonizing overexpressed astrocyte P2Y<sub>2</sub> receptors to correct upregulated *Fmr1* KO astrocyte purinergic signalling. This is consistent with the idea that astrocytes exert a strong influence on the neuronal environment to modulate neuronal function. Interestingly, P2Y<sub>2</sub> antagonism was effective at reducing burst frequency in *Fmr1* KO neurons, and network burst frequency in WT neurons. This may suggest that increased levels of P2Y<sub>2</sub> antagonism are required to have a substantial effect throughout the culture, as WT cultures contain lower levels of astrocyte P2Y<sub>2</sub> receptors than WTs.

P2Y<sub>2</sub>-specific inhibition through AR-C 118925XX was surprisingly more effective at reducing neuronal bursting than nonspecific P2 antagonism using suramin. This may be an effect of treatment concentration, or a result of compensatory processes, as a widespread inhibition of purinergic activity may prompt the upregulation of other excitatory signalling pathways. As suramin has recently shown promise in the mitigation of ASD symptoms within clinical trials (Naviaux et al., 2017), the ability of AR-C 118925XX to normalize *Fmr1* KO burst frequency while only targeting a single P2Y receptor suggests that it may be an interesting candidate for future therapeutic research. Given the similarly increased P2Y<sub>6</sub> expression in *Fmr1* KO cortical astrocytes, the impact of P2Y<sub>6</sub> antagonism on neuronal burst frequency should also be further explored to determine whether it may also act as a potential modulator of neuronal excitation.

### ***Astrocyte-mediated control of neuronal excitability***

The time frames in which *Fmr1* KO neuronal activity and connectivity were altered are broadly associated with neurite elongation, synaptogenesis, and network refinement. Though elevated *Fmr1* KO neuronal bursting may arise through intrinsic neuronal factors such as FXS channelopathies (for review, see Deng & Klyachko, 2021), numerous astrocyte-mediated developmental events take place within the first several weeks of network formation to modulate neuronal connectivity. In addition to powerfully

influencing neurite extension and branching during the first week of postnatal development, as discussed above, astrocytes transiently express and release numerous proteins critical to the development and maturation of synapses. An abundance of synaptic puncta and immature dendritic spines have been reported in FXS models (Galvez et al., 2003; Wallingford, Scott, Rodrigues, & Doering, 2017), suggesting that the creation of additional excitatory synapses may be one factor contributing to the hyperexcitability of FXS neurons. Indeed, several astrocyte soluble factors that promote excitatory synaptogenesis have recently been found to be expressed at elevated levels in *Fmr1* KO cortical astrocytes during the first several weeks of cortical development. These include hevin, interleukin-6, and in particular the purinergic-regulated protein TSP-1 (Krasovska & Doering, 2018; Reynolds et al., 2021; Wallingford et al., 2017). As TSP-1 promotes the formation of postsynaptically silent synapses that become active due to later recruitment of AMPA receptors (Christopherson et al., 2005), it is possible that excess synaptogenesis may occur during the first ~2-3 weeks of development yet not impact burst frequency until ~24DIV. However, the timing and mechanism behind the maturation of immature synapses, and their potential dysregulation in FXS, have yet to be elucidated.

Excess excitatory synapses may alternately be preserved due to a lack of pruning and refinement as the neuronal network develops. Approximately 50% of synapses are typically pruned following synaptogenesis to promote network efficiency and coordination (Lossi and Merighi, 2003). An increase in *Fmr1* KO bursting after ~1 month in culture is indeed consistent with an early failure in pruning. Though synaptic pruning is typically studied in the context of microglial mediation, this process is also regulated by astrocytes through the activity of phagocytic receptors (Chung et al., 2013). Lack of pruning is hypothesized to underlie hyperexcitable FXS connectivity (Bagni & Greenough, 2005), and the absence of postsynaptic FMRP is indeed associated with pruning deficits (Patel, Loerwald, Huber, & Gibson, 2014). A combination of excess synaptogenesis and inadequate synaptic refinement may therefore potentially lead to a tendency towards overall hyperexcitable bursting in *Fmr1* KO neurons.

Astrocytic regulation of neuronal activity is not just restricted to the formation and maintenance of neuronal connections, as astrocytes regulate neuro- and gliotransmitter release through purinergic mechanisms. Glutamate receptors are well-known to be dysregulated in the FXS cortex, with excess excitatory glutamatergic signalling paired with a lack of inhibitory GABAergic signalling (El Idrissi et al., 2005; Fatemi & Folsom, 2011). In particular, astrocyte-specific conditional *Fmr1* KO mice display reduced cortical GLT1 glutamate transporter expression, which inhibits synaptic glutamate reuptake and leaves excess glutamate present in the synaptic cleft to promote neuronal firing. The resulting dendritic morphology and elevated excitatory signalling can be rescued by correcting astrocyte GLT1 expression (Higashimori et al., 2016), demonstrating the importance of astrocyte-mediated control of the synaptic environment. In fact, the GLT1 transporter may act synergistically alongside purinergic signalling, as pharmacological elevation of GLT1 transporters and inhibition of ATP-specific P2X7 purinergic receptors were significantly more effective against induced seizure activity in rats when administered in combination, rather than in isolation (Soni, Koushal, Reddy, Deshmukh, & Kumar, 2015). Elevated ATP levels drive additional gliotransmitter release to further promote excitatory signalling, so the excess availability of glutamate may therefore be another contributing factor leading to elevated burst frequency in *Fmr1* KO co-cultured neurons.

### ***Fmr1* KO neurons in co-culture display reduced local and global synchronicity**

While we hypothesized that *Fmr1* KO neurons would develop hyperexcitable characteristics, their connectivity and firing synchrony are less clearly understood. In addition to excess *Fmr1* KO cortical burst frequency, we observed a number of deficits in the synchronicity of *Fmr1* KO neuronal firing, both within local and culture-wide networks. At the level of a single electrode, the duration between spikes within a burst (*i.e.* inter-spike interval within bursts) was elevated in *Fmr1* KO cultures during time frames associated within increased burst frequency. This indicates that while neurons in local networks engaged in bursts more frequently, their firing within those bursts was less tightly regulated. The time frame between bursts was also somewhat more variable in *Fmr1* KO cultures than

WT, suggesting that while bursting activity may have been more frequent, it occurred more randomly. Unfortunately, one drawback to the MEA method is that it is impossible to determine whether the spikes within a sustained bursting event represent repeated firing of a limited number of neurons, or single action potentials generated by numerous neurons within a localized region. Looking more broadly at the connectivity of the entire culture, the synchrony index and the number of electrodes participating in network bursts were both moderately reduced throughout the duration of the study, suggesting that *Fmr1* KO neurons on separate electrodes were less connected than WT. However, we can assume that a lack of culture-wide synchrony cannot be attributed to a generalized failure of neurons to transmit action potentials, as intact FXS synapses are fully functional (Bureau, Shepherd, & Svoboda, 2008; Li, Pelletier, Perez Velazquez, & Carlen, 2002). Together, these findings indicate that *Fmr1* KO cortical neurons within this developmental period may demonstrate an overall desynchronization of activity that is independent from the level of localized neuronal excitation.

FXS is typically thought of as a disorder of overconnectivity and hypersynchrony, yet previous studies have reported both over- and underconnectivity across various brain regions, as well as both increased and decreased synchrony of firing (Ethridge et al., 2017; Gonçalves et al., 2013; Paluszkiwicz, Olmos-Serrano, Corbin, & Huntsman, 2011; Müller et al., 2011; Testa-Silva et al., 2012). For instance, overall neuronal connectivity in children with ASDs is transiently reduced relative to typically developing children, but is regionally elevated in the frontal cortex, indicating that connectivity is differentially regulated across brain regions and developmental stages (Dajani & Uddin, 2016). It is currently somewhat unclear how deficits in firing synchronicity in MEAs compare with these findings of *in vivo* activity between brain regions, given the small size of MEA wells, the lack of cortical layer and region specification, and the presence of only two cortical cell-types. In this simplified system, it is also important to consider the fact that a lack of connectivity may be expected following chronic overexcitation, as cells attempt to engage in compensatory processes throughout the 7-35DIV in the absence of other cortical cell-types.

It is possible that P2Y<sub>2</sub>-mediated intracellular calcium responses are sufficient to excite neurons locally, but not throughout the entirety of the MEA culture. Astrocyte calcium waves are powerful upregulators of excitatory activity, but are spatially limited due to factors such as the short lifetime of calcium ions, as well as the rapid activity of ectonucleotidase enzymes which restrict UTP/ATP-driven effects (reviewed in Scemes & Giaume, 2006). Elevated astrocyte purinergic signalling may therefore potentially lead to regional pockets of excitation (*i.e.* bursts) yet culture-wide asynchronous firing. Accordingly, while specific P2Y<sub>2</sub> antagonism reduced burst frequency, it did not have a lasting impact on synchronicity or connectivity throughout the culture dish. Both *Fmr1* KO firing synchrony across multiple electrodes and the number of spikes per burst were initially elevated following treatment with AR-C 118925XX, indicating that P2Y<sub>2</sub> antagonism is in fact able to modulate synchronous firing to a certain degree, but these effects did not persist throughout the duration of the experiment. In contrast, suramin treatment had a nearly significant effect on WT synchrony index, potentially suggesting that suramin may be binding another receptor which could be targeted to further explore therapeutic modulation of firing synchrony.

Many prospective therapeutic approaches have aimed to restore the excitation-inhibition balance in FXS, due to the fact that hyperexcitable firing is associated with common symptoms such as seizures and sensory hyperresponsivity. Seizures are in fact linked to the heightened purinergic signalling we previously observed in *Fmr1* KO cortical astrocytes, as elevated P2Y<sub>2</sub> receptor levels are observed in the brains of individuals with epilepsy, and increased levels of astrocyte P2Y<sub>2</sub> receptors are positively correlated with epileptiform activity (Alves et al., 2017; Sukigara et al., 2014). Increased burst and network burst frequencies during early development may potentially indicate a predisposition toward seizure-like events as cortical networks mature. Epileptiform activity typically emerges by 9 years of age in individuals with FXS, while other genetic epilepsies require neuronal networks to be established in culture for several months *in vitro* prior to the detection of epileptiform activity (Musumeci et al., 1999); therefore, a potentially epileptic phase of firing may therefore not be fully captured in this experiment.

## 5.10. Summary

Our current findings demonstrate that *Fmr1* KO astrocyte soluble factors, potentially including UTP, are vital to neurite elongation processes which initiate the formation of neural networks. These neural networks are dysregulated in the *Fmr1* KO cortex, leading to hyperexcitation in the form of elevated burst frequency that can be normalized with specific P2Y<sub>2</sub> antagonism. It remains unclear whether reducing burst frequency alone will have a sufficient impact on FXS symptoms, or whether simultaneously improving longer-range connectivity will also be necessary. Future research *in vivo* will therefore be required to determine the efficacy of P2Y<sub>2</sub>-specific interventions.

## 5.11. References

- Abbracchio, M. P., Burnstock, G., Verkhratsky, A., & Zimmermann, H. (2009). Purinergic signalling in the nervous system: an overview. *Trends Neurosci*, 32(1), 19-29. doi:10.1016/j.tins.2008.10.001
- Adams, J. B., Audhya, T., McDonough-Means, S., Rubin, R. A., Quig, D., Geis, E., . . . Lee, W. (2011). Nutritional and metabolic status of children with autism vs. neurotypical children, and the association with autism severity. *Nutr Metab (Lond)*, 8(1), 34. doi:10.1186/1743-7075-8-34
- Alves, M., Gomez-Villafuertes, R., Delanty, N., Farrell, M. A., O'Brien, D. F., Miras-Portugal, M. T., . . . Engel, T. (2017). Expression and function of the metabotropic purinergic P2Y receptor family in experimental seizure models and patients with drug-refractory epilepsy. *Epilepsia*, 58(9), 1603-1614. doi:https://doi.org/10.1111/epi.13850
- Antar, L. N., Dichtenberg, J. B., Plociniak, M., Afroz, R., & Bassell, G. J. (2005). Localization of FMRP-associated mRNA granules and requirement of microtubules for activity-dependent trafficking in hippocampal neurons. *Genes Brain Behav*, 4(6), 350-359. doi:10.1111/j.1601-183X.2005.00128.x
- Bagni, C., & Greenough, W. T. (2005). From mRNP trafficking to spine dysmorphogenesis: the roots of fragile X syndrome. *Nature Reviews Neuroscience*, 6(5), 376-387. doi:10.1038/nrn1667
- Ballerini, P., Di Iorio, P., Caciagli, F., Rathbone, M. P., Jiang, S., Nargi, E., . . . Ciccarelli, R. (2006). P2Y2 receptor up-regulation induced by guanosine or UTP in rat brain cultured astrocytes. *Int J Immunopathol Pharmacol*, 19(2), 293-308. doi:10.1177/039463200601900207
- Berzhanskaya, J., Phillips, M. A., Shen, J., & Colonnese, M. T. (2016). Sensory hypoexcitability in a rat model of fetal development in Fragile X Syndrome. *Sci Rep*, 6, 30769. doi:10.1038/srep30769
- Brown, M. S., Singel, D., Hepburn, S., & Rojas, D. C. (2013). Increased glutamate concentration in the auditory cortex of persons with autism and first-degree relatives: a (1)H-MRS study. *Autism Res*, 6(1), 1-10. doi:10.1002/aur.1260
- Bureau, I., Shepherd, G. M. G., & Svoboda, K. (2008). Circuit and Plasticity Defects in the Developing Somatosensory Cortex of Fmr1 Knock-Out Mice. *The Journal of Neuroscience*, 28(20), 5178-5188. doi:10.1523/jneurosci.1076-08.2008

- Cea-Del Rio, C. A., & Huntsman, M. M. (2014). The contribution of inhibitory interneurons to circuit dysfunction in Fragile X Syndrome. *Frontiers in Cellular Neuroscience*, 8(245). Doi:10.3389/fncel.2014.00245
- Cheng, C., Lau, S. K., & Doering, L. C. (2016). Astrocyte-secreted thrombospondin-1 modulates synapse and spine defects in the fragile X mouse model. *Mol Brain*, 9(1), 74. doi:10.1186/s13041-016-0256-9
- Christopherson KS, Ullian EM, Stokes CC, Mallowney CE, Hell JW, Agah A, Lawler J, Mosher DF, Bornstein P, Barres BA. (2005). Thrombospondins are astrocyte-secreted proteins that promote CNS synaptogenesis. *Cell*. 120(3), 421-33. doi: 10.1016/j.cell.2004.12.020. PMID: 15707899.
- Chung, W. S., Clarke, L. E., Wang, G. X., Stafford, B. K., Sher, A., Chakraborty, C., . . . Barres, B. A. (2013). Astrocytes mediate synapse elimination through MEGF10 and MERTK pathways. *Nature*, 504(7480), 394-400. doi:10.1038/nature12776
- Cui, J. D., Xu, M. L., Liu, E. Y. L., Dong, T. T. X., Lin, H. Q., Tsim, K. W. K., & Bi, C. W. C. (2016). Expression of globular form acetylcholinesterase is not altered in P2Y1R knock-out mouse brain. *Chem Biol Interact*, 259(Pt B), 291-294. doi:10.1016/j.cbi.2016.06.028
- D'Alimonte, I., Ciccarelli, R., Diiorio, P., Nargi, E., Buccella, S., Giuliani, P., . . . Ballerini, P. (2007). Activation of P2X7 Receptors Stimulates the Expression of P2Y2 Receptor mRNA in Astrocytes Cultured from Rat Brain. *International Journal of Immunopathology and Pharmacology*, 20(2), 301-316. doi:10.1177/039463200702000210
- D'Ambrosi, N., Iafrate, M., Saba, E., Rosa, P., & Volonté, C. (2007). Comparative analysis of P2Y4 and P2Y6 receptor architecture in native and transfected neuronal systems. *Biochimica et Biophysica Acta (BBA) - Biomembranes*, 1768(6), 1592-1599. doi:10.1016/j.bbamem.2007.03.020
- Dajani, D. R., & Uddin, L. Q. (2016). Local brain connectivity across development in autism spectrum disorder: A cross-sectional investigation. *Autism Res*, 9(1), 43-54. doi:10.1002/aur.1494
- Darnell, J. C., Van Driesche, S. J., Zhang, C., Hung, K. Y., Mele, A., Fraser, C. E., . . . Darnell, R. B. (2011). FMRP stalls ribosomal translocation on mRNAs linked to synaptic function and autism. *Cell*, 146(2), 247-261. doi:10.1016/j.cell.2011.06.013
- Deng, P. Y., & Klyachko, V. A. (2021). Channelopathies in fragile X syndrome. *Nat Rev Neurosci*, 22(5), 275-289. doi:10.1038/s41583-021-00445-9

- Dent, E. W., Gupton, S. L., & Gertler, F. B. (2011). The growth cone cytoskeleton in axon outgrowth and guidance. *Cold Spring Harb Perspect Biol*, 3(3). doi:10.1101/cshperspect.a001800
- El Idrissi, A., Ding, X. H., Scalia, J., Trenkner, E., Brown, W. T., & Dobkin, C. (2005). Decreased GABA(A) receptor expression in the seizure-prone fragile X mouse. *Neurosci Lett*, 377(3), 141-146. doi:10.1016/j.neulet.2004.11.087
- Eroglu, C., Allen, N. J., Susman, M. W., O'Rourke, N. A., Park, C. Y., Ozkan, E., . . . Barres, B. A. (2009). Gabapentin receptor alpha2delta-1 is a neuronal thrombospondin receptor responsible for excitatory CNS synaptogenesis. *Cell*, 139(2), 380-392. doi:10.1016/j.cell.2009.09.025
- Ethridge, L. E., White, S. P., Mosconi, M. W., Wang, J., Byerly, M. J., & Sweeney, J. A. (2016). Reduced habituation of auditory evoked potentials indicate cortical hyperexcitability in Fragile X Syndrome. *Transl Psychiatry*, 6(4), e787. doi:10.1038/tp.2016.48
- Ethridge, L. E., White, S. P., Mosconi, M. W., Wang, J., Pedapati, E. V., Erickson, C. A., . . . Sweeney, J. A. (2017). Neural synchronization deficits linked to cortical hyperexcitability and auditory hypersensitivity in fragile X syndrome. *Molecular Autism*, 8(1), 22. Doi:10.1186/s13229-017-0140-1
- Fatemi, S. H., & Folsom, T. D. (2011). Dysregulation of fragile X mental retardation protein and metabotropic glutamate receptor 5 in superior frontal cortex of individuals with autism: a postmortem brain study. *Molecular Autism*, 2(1), 6. doi:10.1186/2040-2392-2-6
- Finkbeiner, S. (2000). Calcium regulation of the brain-derived neurotrophic factor gene. *Cell Mol Life Sci*, 57(3), 394-401. doi:10.1007/pl00000701
- Fornaro, M., Giovannelli, A., Foggetti, A., Muratori, L., Geuna, S., Novajra, G., & Perroteau, I. (2020). Role of neurotrophic factors in enhancing linear axonal growth of ganglionic sensory neurons in vitro. *Neural Regeneration Research*, 15(9), 1732-1739. doi:10.4103/1673-5374.276338
- Fu, Y. H., Kuhl, D. P., Pizzuti, A., Pieretti, M., Sutcliffe, J. S., Richards, S., . . . et al. (1991). Variation of the CGG repeat at the fragile X site results in genetic instability: resolution of the Sherman paradox. *Cell*, 67(6), 1047-1058. doi:10.1016/0092-8674(91)90283-5
- Galvez, R., Gopal, A. R., & Greenough, W. T. (2003). Somatosensory cortical barrel dendritic abnormalities in a mouse model of the fragile X mental retardation syndrome. *Brain Res*, 971(1), 83-89. doi:10.1016/s0006-8993(03)02363-1

- Gibson, J. R., Bartley, A. F., Hays, S. A., & Huber, K. M. (2008). Imbalance of neocortical excitation and inhibition and altered UP states reflect network hyperexcitability in the mouse model of fragile X syndrome. *Journal of neurophysiology*, 100(5), 2615-2626. doi:10.1152/jn.90752.2008
- Gillespie, L. N. (2003). Regulation of axonal growth and guidance by the neurotrophin family of neurotrophic factors. *Clinical and Experimental Pharmacology and Physiology*, 30(10), 724-733. doi:10.1046/j.1440-1681.2003.03909.x
- Gonçalves, J. T., Anstey, J. E., Golshani, P., & Portera-Cailliau, C. (2013). Circuit level defects in the developing neocortex of Fragile X mice. *Nat Neurosci*, 16(7), 903-909. doi:10.1038/nn.3415
- Graef, J. D., Wu, H., Ng, C., Sun, C., Villegas, V., Qadir, D., . . . Wallace, O. (2020). Partial FMRP expression is sufficient to normalize neuronal hyperactivity in Fragile X neurons. *Eur J Neurosci*, 51(10), 2143-2157. doi:10.1111/ejn.14660
- Grill, R., Murai, K., Blesch, A., Gage, F. H., & Tuszynski, M. H. (1997). Cellular Delivery of Neurotrophin-3 Promotes Corticospinal Axonal Growth and Partial Functional Recovery after Spinal Cord Injury. *The Journal of Neuroscience*, 17(14), 5560-5572. doi:10.1523/jneurosci.17-14-05560.1997
- Haberl, M. G., Zerbi, V., Veltien, A., Ginger, M., Heerschap, A., & Frick, A. (2015). Structural-functional connectivity deficits of neocortical circuits in the *Fmr1* (-/y) mouse model of autism. *Science Advances*, 1(10), e1500775-e1500775. doi:10.1126/sciadv.1500775
- Heine, C., Sygnecka, K., Scherf, N., Grohmann, M., Bräsigg, A., & Franke, H. (2015). P2Y1 receptor mediated neuronal fibre outgrowth in organotypic brain slice co-cultures. *Neuropharmacology*, 93, 252-266. doi:10.1016/j.neuropharm.2015.02.001
- Higashimori, H., Schin, C. S., Chiang, M. S., Morel, L., Shoneye, T. A., Nelson, D. L., & Yang, Y. (2016). Selective Deletion of Astroglial FMRP Dysregulates Glutamate Transporter GLT1 and Contributes to Fragile X Syndrome Phenotypes In Vivo. *J Neurosci*, 36(27), 7079-7094. doi:10.1523/jneurosci.1069-16.2016
- Hodges, J. L., Yu, X., Gilmore, A., Bennett, H., Tjia, M., Perna, J. F., . . . Zuo, Y. (2017). Astrocytic Contributions to Synaptic and Learning Abnormalities in a Mouse Model of Fragile X Syndrome. *Biological Psychiatry*, 82(2), 139-149. doi:https://doi.org/10.1016/j.biopsych.2016.08.036

- Hodges, J. L., Yu, X., Gilmore, A., Bennett, H., Tjia, M., Perna, J. F., . . . Zuo, Y. (2017). Astrocytic Contributions to Synaptic and Learning Abnormalities in a Mouse Model of Fragile X Syndrome. *Biol Psychiatry*, 82(2), 139-149. doi:10.1016/j.biopsych.2016.08.036
- Jacobs, S., & Doering, L. C. (2009). Primary dissociated astrocyte and neuron co-culture. In L. C. Doering (Ed.), *Protocols for Neural Cell Culture* (Fourth Edition ed., pp. 269-284). New York, NY: Humana.
- Jacobs, S., & Doering, L. C. (2010). Astrocytes Prevent Abnormal Neuronal Development in the Fragile X Mouse. *The Journal of Neuroscience*, 30(12), 4508-4514. doi:10.1523/jneurosci.5027-09.2010
- Koizumi, S., Shigemoto-Mogami, Y., Nasu-Tada, K., Shinozaki, Y., Ohsawa, K., Tsuda, M., . . . Inoue, K. (2007). UDP acting at P2Y6 receptors is a mediator of microglial phagocytosis. *Nature*, 446(7139), 1091-1095. doi:10.1038/nature05704
- Krasovska, V., & Doering, L. C. (2018). Regulation of IL-6 Secretion by Astrocytes via TLR4 in the Fragile X Mouse Model. *Front Mol Neurosci*, 11, 272. doi:10.3389/fnmol.2018.00272
- Li, J., Pelletier, M. R., Perez Velazquez, J.-L., & Carlen, P. L. (2002). Reduced Cortical Synaptic Plasticity and GluR1 Expression Associated with Fragile X Mental Retardation Protein Deficiency. *Molecular and Cellular Neuroscience*, 19(2), 138-151. doi:https://doi.org/10.1006/mcne.2001.1085
- Liu, X. S., Wu, H., Krzisch, M., Wu, X., Graef, J., Muffat, J., . . . Jaenisch, R. (2018). Rescue of Fragile X Syndrome Neurons by DNA Methylation Editing of the FMR1 Gene. *Cell*, 172(5), 979-992.e976. doi:10.1016/j.cell.2018.01.012
- Lossi L, Merighi A. In vivo cellular and molecular mechanisms of neuronal apoptosis in the mammalian CNS. (2003). *Prog Neurobiol*. 69(5), 287-312. doi: 10.1016/s0301-0082(03)00051-0. PMID: 12787572.
- Marsick, B. M., Flynn, K. C., Santiago-Medina, M., Bamburg, J. R., & Letourneau, P. C. (2010). Activation of ADF/cofilin mediates attractive growth cone turning toward nerve growth factor and netrin-1. *Dev Neurobiol*, 70(8), 565-588. doi:10.1002/dneu.20800
- Morales, J., Hiesinger, P. R., Schroeder, A. J., Kume, K., Verstreken, P., Jackson, F. R., . . . Hassan, B. A. (2002). Drosophila Fragile X Protein, DFXR, Regulates Neuronal Morphology and Function in the Brain. *Neuron*, 34(6), 961-972. doi:10.1016/S0896-6273(02)00731-6

- Müller, R.-A., Shih, P., Keehn, B., Deyoe, J. R., Leyden, K. M., & Shukla, D. K. (2011). Underconnected, but How? A Survey of Functional Connectivity MRI Studies in Autism Spectrum Disorders. *Cerebral Cortex*, 21(10), 2233-2243. doi:10.1093/cercor/bhq296
- Musumeci, S. A., Hagerman, R. J., Ferri, R., Bosco, P., Bernardina, B. D., Tassinari, C. A., . . . Elia, M. (1999). Epilepsy and EEG Findings in Males with Fragile X Syndrome. *Epilepsia*, 40(8), 1092-1099. doi:https://doi.org/10.1111/j.1528-1157.1999.tb00824.x
- Naviaux, R. K., Curtis, B., Li, K., Naviaux, J. C., Bright, A. T., Reiner, G. E., . . . Townsend, J. (2017). Low-dose suramin in autism spectrum disorder: a small, phase I/II, randomized clinical trial. *Ann Clin Transl Neurol*, 4(7), 491-505. doi:10.1002/acn3.424
- Paluszkiewicz, S. M., Olmos-Serrano, J. L., Corbin, J. G., & Huntsman, M. M. (2011). Impaired inhibitory control of cortical synchronization in fragile X syndrome. *Journal of Neurophysiology*, 106(5), 2264-2272. doi:10.1152/jn.00421.2011
- Pan, L., Zhang, Y. Q., Woodruff, E., & Broadie, K. (2004). The Drosophila Fragile X Gene Negatively Regulates Neuronal Elaboration and Synaptic Differentiation. *Current Biology*, 14(20), 1863-1870. doi:10.1016/j.cub.2004.09.085
- Patel, A. B., Loerwald, K. W., Huber, K. M., & Gibson, J. R. (2014). Postsynaptic FMRP promotes the pruning of cell-to-cell connections among pyramidal neurons in the L5A neocortical network. *J Neurosci*, 34(9), 3413-3418. doi:10.1523/jneurosci.2921-13.2014
- Peterson, T. S., Thebeau, C. N., Ajit, D., Camden, J. M., Woods, L. T., Wood, W. G., . . . Weisman, G. A. (2013). Up-regulation and activation of the P2Y(2) nucleotide receptor mediate neurite extension in IL-1 $\beta$ -treated mouse primary cortical neurons. *Journal of Neurochemistry*, 125(6), 885-896. doi:10.1111/jnc.12252
- Pieretti, M., Zhang, F. P., Fu, Y. H., Warren, S. T., Oostra, B. A., Caskey, C. T., & Nelson, D. L. (1991). Absence of expression of the FMR-1 gene in fragile X syndrome. *Cell*, 66(4), 817-822. doi:10.1016/0092-8674(91)90125-i
- Pooler, A. M., Guez, D. H., Benedictus, R., & Wurtman, W. J. (2005). Uridine enhances neurite outgrowth in nerve growth factor-differentiated pheochromocytoma cells. *Neuroscience*, 134, 207-214.

- Puts, N. A. J., Wodka, E. L., Harris, A. D., Crocetti, D., Tommerdahl, M., Mostofsky, S. H., & Edden, R. A. E. (2017). Reduced GABA and altered somatosensory function in children with autism spectrum disorder. *Autism Res*, 10(4), 608-619. doi:10.1002/aur.1691
- Rabacchi, S. A., Kruk, B., Hamilton, J., Carney, C., Hoffman, J. R., Meyer, S. L., . . . Baird, D. H. (1999). BDNF and NT4/5 promote survival and neurite outgrowth of pontocerebellar mossy fiber neurons. *J Neurobiol*, 40(2), 254-269.
- Reynolds, K. E., Wong, C. R., & Scott, A. L. (2021). Astrocyte-mediated purinergic signaling is upregulated in a mouse model of Fragile X syndrome. *Glia*, 69(7), 1816-1832. doi:10.1002/glia.23997
- Sage, C. L., & Marcus, D. C. (2002). Immunolocalization of P2Y4 and P2Y2 purinergic receptors in strial marginal cells and vestibular dark cells. *J Membr Biol*, 185(2), 103-115. doi:10.1007/s00232-001-0116-z
- Sajdel-Sulkowska, E. M., Xu, M., & Koibuchi, N. (2009). Increase in cerebellar neurotrophin-3 and oxidative stress markers in autism. *Cerebellum*, 8(3), 366-372. doi:10.1007/s12311-009-0105-9
- Sanchez, S., Sayas, C. L., Lim, F., Diaz-Nido, J., Avila, J., & Wandosell, F. (2001). The inhibition of phosphatidylinositol-3-kinase induces neurite retraction and activates GSK3. *Journal of neurochemistry*, 78(3), 468-481. doi:10.1046/j.1471-4159.2001.00453.x
- Scemes, E., & Giaume, C. (2006). Astrocyte calcium waves: what they are and what they do. *Glia*, 54(7), 716-725. doi:10.1002/glia.20374
- Soni, N., Koushal, P., Reddy, B. V., Deshmukh, R., & Kumar, P. (2015). Effect of GLT-1 modulator and P2X7 antagonists alone and in combination in the kindling model of epilepsy in rats. *Epilepsy Behav*, 48, 4-14. doi:10.1016/j.yebeh.2015.04.056
- Sukigara, S., Dai, H., Nabatame, S., Otsuki, T., Hanai, S., Honda, R., . . . Itoh, M. (2014). Expression of Astrocyte-Related Receptors in Cortical Dysplasia With Intractable Epilepsy. *Journal of Neuropathology & Experimental Neurology*, 73(8), 798-806. doi:10.1097/nen.0000000000000099
- Sutcliffe, J. S., Nelson, D. L., Zhang, F., Pieretti, M., Caskey, C. T., Saxe, D., & Warren, S. T. (1992). DNA methylation represses FMR-1 transcription in fragile X syndrome. *Hum Mol Genet*, 1(6), 397-400. doi:10.1093/hmg/1.6.397

- Telias, M., Kuznitsov-Yanovsky, L., Segal, M., & Ben-Yosef, D. (2015). Functional Deficiencies in Fragile X Neurons Derived from Human Embryonic Stem Cells. *J Neurosci*, 35(46), 15295-15306. doi:10.1523/jneurosci.0317-15.2015
- Testa-Silva, G., Loebel, A., Giugliano, M., de Kock, C. P., Mansvelter, H. D., & Meredith, R. M. (2012). Hyperconnectivity and slow synapses during early development of medial prefrontal cortex in a mouse model for mental retardation and autism. *Cereb Cortex*, 22(6), 1333-1342. doi:10.1093/cercor/bhr224
- Tran, M. D., & Neary, J. T. (2006). Purinergic signaling induces thrombospondin-1 expression in astrocytes. *Proceedings of the National Academy of Sciences of the United States of America*, 103(24), 9321-9326. doi:10.1073/pnas.0603146103
- Van Kolen, K., & Slegers, H. (2006). Integration of P2Y receptor-activated signal transduction pathways in G protein-dependent signalling networks. *Purinergic Signal*, 2(3), 451-469. doi:10.1007/s11302-006-9008-0
- Verkerk, A. J. M. H., Pieretti, M., Sutcliffe, J. S., Fu, Y.-H., Kuhl, D. P. A., Pizzuti, A., . . . Warren, S. T. (1991). Identification of a gene (FMR-1) containing a CGG repeat coincident with a breakpoint cluster region exhibiting length variation in fragile X syndrome. *Cell*, 65(5), 905-914. doi:https://doi.org/10.1016/0092-8674(91)90397-H
- Wallingford, J., Scott, A. L., Rodrigues, K., & Doering, L. C. (2017). Altered Developmental Expression of the Astrocyte-Secreted Factors Hevin and SPARC in the Fragile X Mouse Model. *Frontiers in Molecular Neuroscience*, 10, 268-268. doi:10.3389/fnmol.2017.00268
- Wallingford, J., Scott, A. L., Rodrigues, K., & Doering, L. C. (2017). Altered Developmental Expression of the Astrocyte-Secreted Factors Hevin and SPARC in the Fragile X Mouse Model. *Front Mol Neurosci*, 10, 268. doi:10.3389/fnmol.2017.00268
- Yang, Q., Feng, B., Zhang, K., Guo, Y. Y., Liu, S. B., Wu, Y. M., . . . Zhao, M. G. (2012). Excessive astrocyte-derived neurotrophin-3 contributes to the abnormal neuronal dendritic development in a mouse model of fragile X syndrome. *PLoS Genet*, 8(12), e1003172. doi:10.1371/journal.pgen.1003172
- Zhang, Y., Bonnan, A., Bony, G., Ferezou, I., Pietropaolo, S., Ginger, M., . . . Frick, A. (2014). Dendritic channelopathies contribute to neocortical and sensory hyperexcitability in *Fmr1(-/y)* mice. *Nat Neurosci*, 17(12), 1701-1709. doi:10.1038/nn.3864

## 6. Chapter Six:

### Discussion and Conclusions

The P2Y-specific purinergic signalling pathway employs UTP and its metabolites to agonise a host of metabotropic receptors expressed by the cells of the brain, and is widely used by astrocytes to facilitate glial-glial and glial-neuronal communication (Abbracchio, Burnstock, Verkhratsky, & Zimmermann, 2009). Mounting evidence suggests that astrocyte dysregulations in FXS may influence the development of neuronal circuitry, and indeed, the structural and functional hallmarks of FXS are consistent with the outcomes of increased astrocyte and neuronal P2Y receptor activation (*e.g.* Galvez, Gopal, & Greenough, 2003; Hodges et al., 2017; Jacobs & Doering, 2010; Wallingford, Scott, Rodrigues, & Doering, 2017). This considerable overlap, paired with evidence of elevated circulatory purinergic precursors in children with ASD (Adams et al., 2011), suggests a role for astrocyte P2Y receptors in the establishment of aberrant FXS circuitry. The overall objective of this thesis work was therefore two-fold: firstly, to establish whether purinergic signalling is dysregulated within astrocytes of the *Fmr1* KO mouse cortex, and secondly, to determine whether astrocyte purinergic dysregulations contribute to the aberrant neuronal-glial interactions observed in FXS. Collectively, the studies within this thesis provide the first reported evidence that purinergic signalling is upregulated in *Fmr1* KO mouse cortical astrocytes, and also demonstrate that elevated purinergic signalling modulates the establishment and activity of cortical neuronal circuitry in a manner consistent with the symptoms of FXS. Additionally, the findings presented here suggest that specific P2Y antagonism should be further explored as a potential approach to normalize excess neuronal excitation and related symptoms within this neurodevelopmental disorder.

## **Purinergic signalling is elevated in *Fmr1* KO cortical astrocytes**

Given that P2Y-mediated astrocyte purinergic signalling is crucial for bidirectional astrocyte-neuron communication and possesses significant functional overlap with the processes dysregulated in FXS, it was hypothesized that the expression of astrocyte purinergic receptors and/or ligands is dysregulated within the *Fmr1* KO mouse cortex. In agreement with this hypothesis, Chapters Two and Three demonstrate that components of the *Fmr1* KO astrocyte purinergic signalling system are elevated at the receptor, ligand, and enzyme levels. *Fmr1* KO P2Y<sub>2</sub> and P2Y<sub>6</sub> receptor expression was increased both *in vitro* and in acutely dissociated astrocytes relative to WT, and was correlated with prolonged *Fmr1* KO UTP-evoked intracellular calcium responses that were indicative of probable intercellular calcium wave propagation. This UTP-driven intracellular calcium release could be prevented with general purinergic antagonism in the form of suramin treatment, further implicating astrocyte P2Y receptors in PLC-IP<sub>3</sub>-mediated release of intracellular calcium from the endoplasmic reticulum. Not only were astrocyte P2Y<sub>2</sub> and P2Y<sub>6</sub> receptor levels increased, but these cells also exhibited dysregulated intracellular levels of purinergic molecules: for instance, *Fmr1* KO astrocyte intracellular UDP levels were elevated, suggesting the presence of excess vesicular stores available for calcium-dependent secretion. Further, elevated glycosylation of the astrocyte-bound ectonucleotidase CD39 indicated that *Fmr1* KO astrocytes have an increased ability to metabolize extracellular purinergic signalling molecules into their diphosphate and monophosphate forms, implying that *Fmr1* KO receptors with high affinity for diphosphates (*e.g.* P2Y<sub>6</sub>) may become more easily agonised.

Together, this combination of elevated receptor expression, increased ligand availability, and heightened ectonucleotidase glycosylation reveals a substantial and novel increase in P2Y-mediated signalling within *Fmr1* KO cortical astrocytes. This indicates the potential for significantly upregulated astrocyte intercellular communication through the propagation of calcium waves, as P2Y-mediated intracellular calcium release permits gap junction-mediated spreading of calcium between astrocytes (Scemes & Giaume, 2006).

Increased astrocyte calcium signalling can also trigger the release of gliotransmitters and soluble factors to promote both short-term neuronal excitation and longer-term synaptic modulation, respectively, while also prompting second messenger-mediated regulation of gene expression (Abbracchio et al., 2009). Elevated astrocyte purinergic signalling in FXS is therefore capable of influencing not only local astrocyte activity, but also broadly driving sustained changes in neural circuitry.

Notably, a similar increase in astrocyte P2Y receptor expression has been identified in epilepsy, a neurological disorder which frequently co-occurs with FXS and is characterized by pathologically upregulated neuronal excitation (Musumeci et al., 1999). In particular, P2Y<sub>2</sub>, P2Y<sub>4</sub>, and P2Y<sub>6</sub> receptor levels were elevated in mouse models of seizure disorders, while individuals with cortical dysplasia displayed astrocyte-specific increases in P2Y<sub>2</sub> and P2Y<sub>4</sub> expression, suggesting that excess astrocyte P2Y stimulation may be linked with the onset of seizures (Alves et al., 2017; Sukigara et al., 2014). Further, excess astrocyte intracellular calcium oscillations and associated calcium-dependent glutamate release preceded epileptiform activity across a number of *in vitro* and *in vivo* models of epilepsy (Tian et al., 2005), while anticonvulsant treatment abolished these excess astrocyte intracellular calcium transients, leading Tian et al. (2005) to propose that altered astrocyte calcium signalling may therefore drive seizure pathology. Taken together, these findings suggest a prominent role of astrocyte P2Y receptors and associated calcium transients in the development of pathologically hyperexcitable circuitry.

### **Elevated purinergic signalling influences astrocyte secretion of synaptogenic factors**

Astrocyte intracellular calcium has been linked to the expression and release of astrocyte soluble proteins, some of which are known to aid in the establishment and refinement of synaptic connections. Notably, expression and secretion of astrocyte TSP-1, a glycoprotein associated with the formation of immature synapses, has been shown to be regulated by the action of P2Y receptors (Tran & Neary, 2006). Given this, it was hypothesized that elevated astrocyte purinergic signalling in FXS would lead to increased

downstream soluble factor expression and release. Indeed, as shown in Chapter 2, expression and secretion of TSP-1 were both increased in *Fmr1* KO cortical astrocytes following high concentrations of exogenous UTP. This was correlated with increased levels of TSP-1 in whole cortical tissue at postnatal days 7 and 14, a time frame associated with peak levels of synaptogenesis (Semple et al., 2003). The increased *Fmr1* KO IL-6 levels observed in Chapter 4 are also consistent with elevations in astrocyte synaptogenic factor secretion, as IL-6 has been shown to promote excitatory synaptogenesis (Wei et al., 2011).

This intracellular upregulation is likely mediated by the action of purinergic-coupled signal transduction pathways, as the activation of UTP/UDP-sensitive P2Y receptors initiates a number of calcium-dependent and calcium-independent signal transduction cascades that influence gene expression, including activation of MAPK, Akt, and STAT3 pathways. Previous research has suggested that TSP-1 expression in particular is regulated through MAPK and Akt signal transduction cascades downstream of P2Y receptors (Tran & Neary, 2006), providing a potential mechanism behind the specific upregulations seen here. TSP-1 has previously been thought to be regulated by P2Y<sub>4</sub> (Tran & Neary, 2006), though the upregulations of astrocyte P2Y<sub>2</sub> and P2Y<sub>6</sub> suggest a potential role for one or both of these receptors, perhaps in addition to P2Y<sub>4</sub>. Given the increased CD39 glycosylation in *Fmr1* KO astrocytes, it is possible that the exogenous UTP treatment provided in these experiments may have been rapidly metabolized to UDP during the 12h treatment period, thereby permitting substantial activation of over-abundant P2Y<sub>6</sub>.

These findings of altered synaptogenic protein levels are consistent with previous work showing increased astrocyte expression of synaptic factors in the *Fmr1* KO mouse. During time periods associated with synaptogenesis, *Fmr1* KO cortical astrocytes were found to transiently express increased levels of the pro-synaptogenic protein hevin alongside reduced levels of anti-synaptogenic SPARC; and furthermore, these changes were correlated with an early developmental increase in the density of synaptic puncta (Wallingford, Scott, Rodrigues, & Doering, 2017). Similarly, in patients with FXS and ASD, the density of dendritic spines on cortical pyramidal neurons was found to be elevated

(Hutsler & Zhang, 2010; Irwin et al., 2001). The increase in TSP-1 expression and secretion reported here therefore suggests that upregulated P2Y-mediated astrocyte soluble factor secretion may contribute to the early development of excess synaptic connections, thereby potentially influencing aberrant FXS circuitry.

### **Purinergic-immune links in the FXS cortex**

Cell-associated and secreted levels of the synaptic plasticity-associated glycoprotein TNC have also previously been shown to be elevated in *Fmr1* KO cortical astrocytes (Krasovska & Doering, 2018), and their purinergic regulation was further explored here in relation to JAK/STAT pathway activation and immune responses. TNC is an extracellular matrix glycoprotein which is transiently expressed during early development and has been associated with synaptic plasticity; specifically, the activity of voltage-gated calcium channels to promote long-term potentiation (Šekeljić & Andjus, 2012). In Chapter 4, secretion of TNC and phosphorylation of the STAT3 transcription factor were both increased in WT astrocytes following UTP-mediated P2Y receptor activation, in a manner consistent with upregulated *Fmr1* KO TNC release (Krasovska & Doering, 2018). P2Y-driven phosphorylation of STAT3 has previously been shown in other cell-types and, like TSP-1, has been found to be mediated by the action of MAPK, providing a likely mechanism (Jokela et al., 2017; Washburn & Neary, 2006). Expression of TNC was also reported to be regulated by MAPK in breast carcinoma, as tumours with increased MAPK signalling pathway activation demonstrated elevated TNC expression, while pharmacological inhibition of MAPK substantially reduced TNC levels (Maschler, Grunert, Danielopol, Beug, & Wirl, 2004). Similar to TSP-1, MAPK signalling pathways may therefore be involved in the purinergic regulation of both astrocyte TNC and the phosphorylation of STAT3. The finding that both TNC release and STAT3 phosphorylation are promoted by P2Y activation suggests novel links between P2Y receptor activity and immune regulatory function within FXS cortical astrocytes, which may shed light on immune responses within the FXS cortex.

Inhibition of STAT3 activity prevented pathological upregulation of IL-6 in *Fmr1* KO astrocytes, suggesting that increased IL-6 expression may occur in part due to P2Y-mediated initiation of STAT3 phosphorylation. Importantly, this link suggests that by controlling excess astrocyte purinergic signalling, the effects of cortical immune signalling may also be mitigated by means of reduced STAT3 phosphorylation. While cytokines such as IL-6 can exert both neuroprotective and pro-inflammatory roles, long-term elevation of IL-6, as seen in FXS, is damaging. Increased levels of IL-6 are associated with the progression of neurodegeneration, and are observed in a number of neurological diseases including Alzheimer's disease, Parkinson's disease, and multiple sclerosis (Rothaug, Becker-Pauly, & Rose-John, 2016); concordantly, STAT3 phosphorylation is also associated with deficits in learning and memory impairments in a mouse model of Alzheimer's disease (Chen et al., 2013). Furthermore, in mouse models, overexpression of IL-6 within the brain was correlated with the onset of FXS-like characteristics including cognitive deficits and seizures, consistent with its role as an upregulator of excitatory synaptogenesis (Wei et al., 2011). The degree of IL-6 overexpression was inversely correlated with mouse health in IL-6 overexpression studies, implying that elevated IL-6 levels in FXS may potentially influence the development of certain FXS symptoms (Campbell et al., 1993; Wei et al., 2012). Other pro-inflammatory cytokines such as TNF $\alpha$  and IL-1 $\beta$  have been found to be regulated by STAT3 phosphorylation, and like IL-6, are also elevated within rodent models of the ASD brain (Huang et al., 2019). Pharmacologically targeting the FXS purinergic signalling system may therefore lead to mitigation of pathological FXS cytokine levels by way of STAT3 modulation, represent an interesting future direction in the search for novel therapeutic approaches.

### **Elevated purinergic signalling increases neurite outgrowth and complexity**

As purinergic signalling pathways have been found to promote neurite outgrowth and complexity, the impact of P2Y agonism on these processes was studied to investigate the ability of *Fmr1* KO neurons to extend their processes and permit neural network formation. Activation of P2Y<sub>2</sub> receptors with UTP/cytokine co-treatment has previously

been shown to upregulate neurite outgrowth and branching as a result of calcium-dependent processes (Peterson et al., 2013; Pooler, Guez, Benedictus, & Wurtman, 2005). This neurite extension was linked to phosphorylation of cofilin, an actin-severing protein that cycles between phosphorylated and unphosphorylated states to promote actin polymerization and depolymerization, respectively; thereby driving the dynamic actin cytoskeleton remodeling processes that are crucial for the extension of neurites (Basu & Lamprecht, 2018; Figge, Loers, Schachner, & Tilling, 2012; Peterson et al., 2013).

As shown in Chapter 5, extension of cortical neurites was determined firstly by the genotype of astrocyte used to prepare astrocyte-conditioned media, and secondly, by the presence of UTP as a P2Y agonist. When neurons were grown in the presence of *Fmr1* KO astrocyte soluble factors, putative axons were lengthened regardless of neuronal genotype. However, exogenous UTP was unable to promote additional outgrowth and branching within this ACM condition, in a manner consistent with potential P2Y-specific saturation effects. Conversely, UTP treatment promoted outgrowth of WT ACM-grown neurons to levels observed in control-treated neurons grown with *Fmr1* KO ACM, in a manner consistent with previous findings of UTP-driven neurite outgrowth (Peterson et al., 2013; Pooler et al., 2005). Surprisingly, this effect was not dampened by the reduced P2Y<sub>2</sub> expression observed in *Fmr1* KO neurons, suggesting that outgrowth effects may result from the simultaneous agonism of multiple excitatory P2Y receptor types. These results are significant to the study of FXS neural circuits as they suggest that *Fmr1* KO astrocyte secretions, including UTP and/or UDP, may drive the formation of aberrant neuronal circuitry.

The concept of UTP saturation in *Fmr1* KO media is supported by similar effects seen in Chapter 4: UTP treatment elevated WT astrocyte TNC secretion in a manner consistent with control *Fmr1* KO astrocyte secretion levels, but UTP was unable to further increase *Fmr1* KO TNC secretion. Despite the identification of increased intracellular UDP in *Fmr1* KO astrocytes, quantification of secreted purinergic factors will ultimately be required to determine whether UTP and/or UDP are indeed elevated in *Fmr1* KO ACM to

facilitate these effects on neurite outgrowth. Alternately, increased neurite length may be concurrently driven by additional *Fmr1* KO astrocyte secretions; for instance, neurotrophins are widely known to promote axonal extension and guidance. Interestingly, TNC has also been found to regulate neurite outgrowth through the presence of specific fibronectin domains that facilitate both neurite extension and guidance (Meiners et al. 1999). TNC levels in hippocampal astrocytes were upregulated following experimental lesion, which Deller et al. (1997) suggested may indicate a role for TNC in reinnervation following brain injury. Increased secretion of TNC from *Fmr1* KO cortical astrocytes, possibly driven by increased P2Y activity, may therefore potentially contribute to the *Fmr1* KO ACM-specific neurite extension observed in this work.

Regardless of the precise mechanism, the effects of ACM reported within this chapter indicate that neuronal outgrowth and complexity are highly dependent on astrocytic regulation of the neuronal environment. Astrocyte-driven neuronal regulation has previously been observed in FXS, with *Fmr1* KO cortical astrocytes promoting an FXS-like phenotype in wildtype hippocampal neurons, while astrocyte-specific loss of FMRP led to dysregulated neuronal circuitry and physiologically relevant behavioural impairments (Hodges et al., 2017; Jacobs & Doering, 2010). The present findings therefore suggest that the astrocyte-specific alterations in purinergic signalling reported in Chapters 2 and 3 may be capable of strongly influencing the development of neuronal circuitry.

### **Elevated neuronal excitation in ASD and FXS**

To further explore the development of neuronal circuitry in the presence of both neurons and astrocytes, astrocyte-neuron co-cultures were established on microelectrode arrays and their firing characteristics were recorded over the first five weeks of development. In this experiment, astrocyte and neuronal genotypes were matched within each culture to create simplified signalling systems representative of early developmental activity within the *Fmr1* KO vs wildtype cortex. Given the excitatory nature of astrocyte purinergic signalling and its demonstrated effects on synaptic factor secretion,

gliotransmitter release, and neurite outgrowth, it was hypothesized that elevated astrocyte purinergic signalling would increase neuronal activity and connectivity in cortical *Fmr1* KO co-cultures.

Consistent with this hypothesis, *Fmr1* KO cortical neurons demonstrated increased burst frequency and network burst frequency after ~3 weeks *in vitro*, as seen in Chapter 5. However, reductions in the synchrony of *Fmr1* KO firing were coincident with these increases in neuronal burst and network burst frequency, though it is unclear to what extent reduced synchrony within a culture dish is correlated with the brain-wide connectivity deficits observed in individuals with FXS. The elevations in *Fmr1* KO neuronal burst frequency observed here are corroborated by numerous recent findings of early *Fmr1* KO postnatal hyperexcitability (*e.g.* Gonçalves, Anstey, Golshani, & Portera-Cailliau, 2013; Graef et al., 2020; Liu et al., 2018; Zhang et al., 2014). Previous studies have shown that neuronal hyperactivity is not detectable in *Fmr1* KO rats until ~3 postnatal weeks (Berzhanskaya et al. 2016), suggesting that increased *Fmr1* KO neuronal burst frequency may be associated with differential establishment or maturation of neuronal networks; for instance, altered release of *Fmr1* KO synaptogenic factors could be a factor in this delayed onset of hyperexcitation. While synaptogenesis peaks *in vivo* between 3-14DIV and continues at lower levels until ~28DIV (Schüz & Palm, 1989), levels of the presynaptic marker synaptophysin were found to be elevated in cortical neuron cultures at 21DIV and 28DIV relative to the first two weeks of *in vitro* development (Harrill et al., 2015). This suggests that the onset of excess *Fmr1* KO burst frequency occurred at a time frame in which the majority of cortical excitatory synapses have been newly established *in vitro*, consistent with the hypothesis that these differences may be synapse-related. However, it will be important to determine the timing and mechanism of *Fmr1* KO TSP-1-induced synapse maturation, as well as dysregulations in *Fmr1* KO synaptic pruning, to fully understand the synaptic mechanisms that may underlie this excess neuronal activity.

Findings of excess neuronal burst frequency and network burst frequency in the *Fmr1* KO mouse also contribute to the growing body of evidence supporting the

excitation/inhibition imbalance hypothesis of ASD. This hypothesis posits that glutamatergic signalling is upregulated while GABAergic signalling is reduced in ASD. Indeed, metabotropic glutamate receptors have been found to be elevated in the cortex of children with FXS, while a lack of inhibitory GABAergic signalling has been noted in the *Fmr1* KO mouse (El Idrissi et al., 2005; Fatemi & Folsom, 2011). Cortical astrocytes release glutamate through calcium-dependent mechanisms; and accordingly, increased intracellular calcium levels are associated with upregulated vesicular glutamate release, suggesting that excess *Fmr1* KO astrocyte purinergic receptor expression may drive elevated excitatory neuronal signalling (Scemes & Giaume, 2006). Not only can astrocytes control glutamatergic release into the synapse, but they also facilitate its reuptake to modulate the duration of its effects. Cortical astrocyte expression of the GLT1 glutamate transporter was found to be reduced in an astrocyte-specific conditional *Fmr1* KO mouse model, potentially exacerbating the effects of elevated calcium-driven glutamate release by retaining glutamate within the FXS synapse (Higashimori et al., 2016). Activity of the GLT1 transporter is associated with synergistic purinergic effects, as increased GLT1 reuptake paired with purinergic P2X<sub>7</sub> receptor inhibition was significantly more effective than single administration of either pharmacological treatment in the mitigation of seizures (Soni et al., 2015). Increased glutamate availability may therefore be a contributing factor in the elevation of *Fmr1* KO burst frequency, and may be driven in part by the action of elevated *Fmr1* KO astrocyte purinergic receptors.

### **Purinergic normalization of *Fmr1* KO neuronal burst frequency**

Purinergic signalling was indeed implicated in the hyperexcitation of *Fmr1* KO co-cultured neurons, as excess *Fmr1* KO neuronal bursting was normalized at 28 DIV by treatment with the P2Y<sub>2</sub> antagonist AR-C 118925XX. It is likely that this correction of neuronal activity primarily results from antagonizing aberrant purinergic signalling in astrocytes, the neural cell-type in which expression of P2Y<sub>2</sub> is significantly elevated. In contrast, P2Y<sub>2</sub> expression in *Fmr1* KO neurons was reduced, and accordingly, antagonism of already poorly expressed receptors would not be expected to have a significant impact

on neuronal activity. The work presented throughout this thesis suggests that astrocytes exert a strong influence on the neuronal environment by regulating neurite outgrowth and promoting secretion of synaptogenic factors, lending support to the idea that astrocyte P2Y<sub>2</sub> activity promotes neuronal firing.

Not only was P2Y<sub>2</sub>-specific antagonism able to correct excess neuronal burst frequency, but it was in fact more effective at reducing this excitation than pan-purinergic antagonism with suramin. Since this thesis work was initiated, treatment with the nonspecific purinergic antagonist suramin has shown clinical promise in the mitigation of purinergic-driven metabolic syndrome and ASD symptoms (Naviaux et al., 2017). Suramin acts broadly on P2Y<sub>1</sub>, P2Y<sub>2</sub>, P2Y<sub>6</sub>, P2Y<sub>11</sub>, and P2Y<sub>13</sub> receptors as well as several P2X<sub>7</sub> and ryanodine receptors to exert its effects, and has historically been used in clinical settings to treat African sleeping sickness (trypanosomiasis) and river blindness (onchocerciasis) (Barrett, Boykin, Brun, & Tidwell, 2007; Jacobson et al., 2006; Schulz-Key, Karam, & Prost, 1985; von Kugelgen & Hoffmann, 2016). However, as a consequence of this nonspecific targeting of receptors, as well as the fact that the purinergic signalling pathway is both complex and highly expressed throughout the body, systemic delivery of suramin remains highly prone to adverse reactions when used long-term. Previous clinical trials for suramin use in adrenocortical carcinoma, hormone-refractory metastatic prostate cancer, and HIV/AIDS have all failed due to a combination of limited efficacy, excess adverse effects, and fatalities due to drug toxicity (Arlt, Reincke, Siekmann, Winkelmann, & Allolio, 1994; Kaplan et al., 1987; Rosen et al., 1996). This history of adverse effects following chronic treatment, coupled with the fact that suramin does not readily cross the blood-brain barrier (Hawking, 1940), suggest that suramin may ultimately be unsuitable for specific and long-lasting correction of astrocyte dysfunction in FXS.

In contrast, the ability of AR-C 118925XX to normalize *Fmr1* KO burst frequency while only binding to a single P2Y receptor suggests that it may be a promising candidate for future therapeutic research. AR-C 118925XX is currently the only well-characterized selective P2Y<sub>2</sub> antagonist to date, and has only become commercially available within

recent years (Muoboghare, Drummond, & Kennedy, 2019). To the author's knowledge, the research presented here is the first to specifically investigate the role of AR-C 118925XX in either cortical cell culture or in FXS. However, this competitive antagonist has been successfully utilized in mouse tumour progression studies to mitigate growth of pancreatic ductal adenocarcinoma and prolong mouse life expectancy, suggesting that it may be safe for future experimentation *in vivo* in animal models (Hu et al., 2019).

Given that P2Y<sub>6</sub> receptor levels were elevated in *Fmr1* KO cortical astrocytes, and both intracellular UDP levels and membrane-bound CD39 glycosylation suggest an abundance of *Fmr1* KO UDP, it is logical that inhibiting P2Y<sub>6</sub> activity could also have a beneficial effect on neuronal burst frequency. However, neuronal firing activity following P2Y<sub>6</sub> inhibition could not be determined in these experiments due to the fact that specific chronic antagonism of P2Y<sub>6</sub> negatively impacted long-term co-culture survival. As P2Y<sub>6</sub> knockout mice do not exhibit substantial developmental impairments (Bar et al., 2008), these observations are likely to be an unintended toxicity related to treatment with this particular compound, rather than an indication that P2Y<sub>6</sub> receptor activity is necessary for astrocyte and/or neuronal survival.

### **Future Directions**

Given the experimental difficulties experienced here with P2Y<sub>6</sub> antagonism in microelectrode arrays, it remains unclear what role elevated astrocyte P2Y<sub>6</sub> receptors play in *Fmr1* KO neuronal hyperexcitation. Future research utilizing another approach to P2Y<sub>6</sub> inhibition, such as siRNA knockdown, will be crucial to determine whether blocking this receptor subtype may also reduce hyperexcitation in FXS.

It will also be important to characterize the differences in purinergic secretion between WT and *Fmr1* KO astrocytes in order to determine the degree to which P2Y-mediated purinergic signalling is dysregulated in the FXS cortex. While the current intracellular LC/MS data demonstrates increased levels of astrocyte UDP, and thereby suggests that vesicular UDP release may be elevated, it remains unclear whether these

intracellular levels are in fact correlated with the true levels of UDP secretion. UDP and/or UTP secretion from FXS astrocytes is hypothesized to be increased based on the current findings: for example, patterns of neurite outgrowth in the presence of *Fmr1* KO ACM are consistent with an elevated concentration of purinergic secretions in culture media, while secretion of TNC appears to be saturated regardless of UTP treatment. To answer this outstanding question, research is currently ongoing to develop novel LC/MS sample preparation methods that facilitate sensitive detection of *Fmr1* KO and WT purinergic secretions.

Additionally, the further exploration of astrocyte purinergic receptor subtypes will elucidate whether FXS purinergic dysregulations are largely restricted to the P2Y receptor family, or whether P1 and/or P2X receptors are similarly dysregulated. In particular, the adenosine A<sub>1</sub> receptor is an interesting target for future studies. A<sub>1</sub> receptor activity is associated with anti-epileptic effects, while antagonism of this receptor promotes seizure activity (Amorim et al., 2016; Fabera et al., 2019; Gouder, Fritschy, & Boison, 2003). As intracellular adenosine levels were found here to be reduced in *Fmr1* KO astrocytes, further characterization of A<sub>1</sub> receptor expression and activity may suggest a potential link between altered adenosine availability and the epileptic symptoms of FXS and ASD.

## **Summary**

In order to provide a solid foundation for the development of new and effective treatment strategies for FXS and ASD, it is crucial to understand the dysfunctions in astrocyte signalling that occur within the FXS cortex, as well as their impacts on neuronal circuitry. The work presented within this thesis demonstrates, for the first time, that P2Y receptor-specific purinergic signalling pathways are elevated in *Fmr1* KO cortical astrocytes. Furthermore, the upregulation of *Fmr1* KO astrocyte purinergic signalling is shown to lead to aberrant neuronal synaptogenic protein expression and secretion, heightened immune responses, elevated neurite extension, and increased neuronal burst frequency, consistent with cortical excitation-driven FXS symptoms. As *Fmr1* KO burst

frequency can be corrected *in vitro* with specific P2Y<sub>2</sub> antagonism, these results suggest that the targeted inhibition of P2Y receptors may warrant further investigation as a potential therapeutic approach to combat FXS symptoms.

## 6.1. References

- Abbracchio, M. P., Burnstock, G., Verkhratsky, A., & Zimmermann, H. (2009). Purinergic signalling in the nervous system: an overview. *Trends Neurosci*, 32(1), 19-29. doi:10.1016/j.tins.2008.10.001
- Alves, M., Gomez-Villafuertes, R., Delanty, N., Farrell, M. A., O'Brien, D. F., Miras-Portugal, M. T., . . . Engel, T. (2017). Expression and function of the metabotropic purinergic P2Y receptor family in experimental seizure models and patients with drug-refractory epilepsy. *Epilepsia*, 58(9), 1603-1614. doi:10.1111/epi.13850
- Amorim, B. O., Hamani, C., Ferreira, E., Miranda, M. F., Fernandes, M. J. S., Rodrigues, A. M., . . . Covolan, L. (2016). Effects of A1 receptor agonist/antagonist on spontaneous seizures in pilocarpine-induced epileptic rats. *Epilepsy Behav*, 61, 168-173. doi:10.1016/j.yebeh.2016.05.036
- Arlt, W., Reincke, M., Siekmann, L., Winkelmann, W., & Allolio, B. (1994). Suramin in adrenocortical cancer: limited efficacy and serious toxicity. *Clinical Endocrinology*, 41, 299-307.
- Bar, I., Guns, P. J., Metallo, J., Cammarata, D., Wilkin, F., Boeynants, J. M., . . . Robaye, B. (2008). Knockout mice reveal a role for P2Y6 receptor in macrophages, endothelial cells, and vascular smooth muscle cells. *Mol Pharmacol*, 74(3), 777-784. doi:10.1124/mol.108.046904
- Barrett, M. P., Boykin, D. W., Brun, R., & Tidwell, R. R. (2007). Human African trypanosomiasis: pharmacological re-engagement with a neglected disease. *Br J Pharmacol*, 152(8), 1155-1171. doi:10.1038/sj.bjp.0707354
- Basu, S., & Lamprecht, R. (2018). The Role of Actin Cytoskeleton in Dendritic Spines in the Maintenance of Long-Term Memory. *Frontiers in Molecular Neuroscience*, 11, 143-143. doi:10.3389/fnmol.2018.00143
- Berzhanskaya J, Phillips MA, Shen J, Colonnese MT. (2016). Sensory hypo-excitability in a rat model of fetal development in Fragile X Syndrome. *Sci Rep*. 6, 30769. doi: 10.1038/srep44515.
- Campbell, I. L., Abraham, C. R., Masliah, E., Kemper, P., Inglis, J. D., Oldstone, M. B., & Mucke, L. (1993). Neurologic disease induced in transgenic mice by cerebral overexpression of interleukin 6. *Proceedings of the National Academy of Sciences of the United States of America*, 90(21), 10061-10065. doi:10.1073/pnas.90.21.10061

- Chen, E., Xu, D., Lan, X., Jia, B., Sun, L., Zheng, J. C., & Peng, H. (2013). A novel role of the STAT3 pathway in brain inflammation-induced human neural progenitor cell differentiation. *Curr Mol Med*, 13(9), 1474-1484. doi:10.2174/15665240113139990076
- Deller T, Haas CA, Naumann T, Joester A, Faissner A, Frotscher M. (1997). Up-regulation of astrocyte-derived tenascin-C correlates with neurite outgrowth in the rat dentate gyrus after unilateral entorhinal cortex lesion. *Neuroscience*. 81(3), 829-46. doi: 10.1016/s0306-4522(97)00194-2.
- El Idrissi, A., Ding, X. H., Scalia, J., Trenkner, E., Brown, W. T., & Dobkin, C. (2005). Decreased GABA(A) receptor expression in the seizure-prone fragile X mouse. *Neurosci Lett*, 377(3), 141-146. doi:10.1016/j.neulet.2004.11.087
- Fabera, P., Parizkova, M., Uttl, L., Vondrakova, K., Kubova, H., Tsenov, G., & Mares, P. (2019). Adenosine A1 Receptor Agonist 2-chloro-N6-cyclopentyladenosine and Hippocampal Excitability During Brain Development in Rats. *Frontiers in Pharmacology*, 10, 656. doi:10.3389/fphar.2019.00656
- Fatemi, S. H., & Folsom, T. D. (2011). Dysregulation of fragile X mental retardation protein and metabotropic glutamate receptor 5 in superior frontal cortex of individuals with autism: a postmortem brain study. *Molecular Autism*, 2(1), 6. doi:10.1186/2040-2392-2-6
- Figge, C., Loers, G., Schachner, M., & Tilling, T. (2012). Neurite outgrowth triggered by the cell adhesion molecule L1 requires activation and inactivation of the cytoskeletal protein cofilin. *Molecular and Cellular Neuroscience*, 49(2), 196-204. doi:doi.org/10.1016/j.mcn.2011.10.002
- Fornaro, M., Giovannelli, A., Foggetti, A., Muratori, L., Geuna, S., Novajra, G., & Perroteau, I. (2020). Role of neurotrophic factors in enhancing linear axonal growth of ganglionic sensory neurons in vitro. *Neural Regeneration Research*, 15(9), 1732-1739. doi:10.4103/1673-5374.276338
- Gonçalves, J. T., Anstey, J. E., Golshani, P., & Portera-Cailliau, C. (2013). Circuit level defects in the developing neocortex of Fragile X mice. *Nat Neurosci*, 16(7), 903-909. doi:10.1038/nn.3415
- Gouder, N., Fritschy, J. M., & Boison, D. (2003). Seizure suppression by adenosine A1 receptor activation in a mouse model of pharmacoresistant epilepsy. *Epilepsia*, 44(7), 877-885. doi:10.1046/j.1528-1157.2003.03603.x

- Graef, J. D., Wu, H., Ng, C., Sun, C., Villegas, V., Qadir, D., . . . Wallace, O. (2020). Partial FMRP expression is sufficient to normalize neuronal hyperactivity in Fragile X neurons. *Eur J Neurosci*, 51(10), 2143-2157. doi:10.1111/ejn.14660
- Harrill, J. A., Chen, H., Streifel, K. M., Yang, D., Mundy, W. R., & Lein, P. J. (2015). Ontogeny of biochemical, morphological and functional parameters of synaptogenesis in primary cultures of rat hippocampal and cortical neurons. *Molecular Brain*, 8(1), 10. doi:10.1186/s13041-015-0099-9
- Hawking, F. (1940). Concentration of Bayer 205 (Germanin) in human blood and cerebrospinal fluid after treatment. *Transactions of The Royal Society of Tropical Medicine and Hygiene*, 34(1), 37-52. doi:10.1016/s0035-9203(40)90088-8
- Higashimori, H., Schin, C. S., Chiang, M. S., Morel, L., Shoneye, T. A., Nelson, D. L., & Yang, Y. (2016). Selective Deletion of Astroglial FMRP Dysregulates Glutamate Transporter GLT1 and Contributes to Fragile X Syndrome Phenotypes In Vivo. *J Neurosci*, 36(27), 7079-7094. doi:10.1523/jneurosci.1069-16.2016
- Hodges, J. L., Yu, X., Gilmore, A., Bennett, H., Tjia, M., Perna, J. F., . . . Zuo, Y. (2017). Astrocytic Contributions to Synaptic and Learning Abnormalities in a Mouse Model of Fragile X Syndrome. *Biological Psychiatry*, 82(2), 139-149. doi:doi.org/10.1016/j.biopsych.2016.08.036
- Hu, L. P., Zhang, X. X., Jiang, S. H., Tao, L. Y., Li, Q., Zhu, L. L., . . . Zhang, Z. G. (2019). Targeting Purinergic Receptor P2Y2 Prevents the Growth of Pancreatic Ductal Adenocarcinoma by Inhibiting Cancer Cell Glycolysis. *Clin Cancer Res*, 25(4), 1318-1330. doi:10.1158/1078-0432.Ccr-18-2297
- Huang L, Otrokocsi L, Sperl agh B. Role of P2 receptors in normal brain development and in neurodevelopmental psychiatric disorders. (2019). *Brain Res Bull*. 151, 55-64. doi: 10.1016/j.brainresbull.2019.01.030.
- Jacobs, S., & Doering, L. C. (2010). Astrocytes Prevent Abnormal Neuronal Development in the Fragile X Mouse. *The Journal of Neuroscience*, 30(12), 4508-4514. doi:10.1523/jneurosci.5027-09.2010
- Jacobson, K. A., Costanzi, S., Joshi, B. V., Besada, P., Shin, D. H., Ko, H., . . . Mamedova, L. (2006). Agonists and antagonists for P2 receptors. *Novartis Foundation symposium*, 276, 58-281. doi:10.1002/9780470032244.ch6

- Jokela, T., Kärnä, R., Rauhala, L., Bart, G., Pasonen-Seppänen, S., Oikari, S., . . . Tammi, R. H. (2017). Human Keratinocytes Respond to Extracellular UTP by Induction of Hyaluronan Synthase 2 Expression and Increased Hyaluronan Synthesis. *The Journal of Biological Chemistry*, 292(12), 4861-4872. doi:10.1074/jbc.M116.760322
- Kaplan, L. D., Wolfe, P. R., Volberding, P. A., Feorino, P., Levy, J. A., Abrams, D. I., . . . Gottlieb, M. S. (1987). Lack of response to suramin in patients with AIDS and AIDS-related complex. *The American Journal of Medicine*, 82, 615-620.
- Krasovska, V., & Doering, L. C. (2018). Regulation of IL-6 Secretion by Astrocytes via TLR4 in the Fragile X Mouse Model. *Frontiers in Molecular Neuroscience*, 11, 272-272. doi:10.3389/fnmol.2018.00272
- Liu, X. S., Wu, H., Krzisch, M., Wu, X., Graef, J., Muffat, J., . . . Jaenisch, R. (2018). Rescue of Fragile X Syndrome Neurons by DNA Methylation Editing of the FMR1 Gene. *Cell*, 172(5), 979-992.e976. doi:10.1016/j.cell.2018.01.012
- Maschler, S., Grunert, S., Danielopol, A., Beug, H., & Wirl, G. (2004). Enhanced tenascin-C expression and matrix deposition during Ras/TGF-beta-induced progression of mammary tumor cells. *Oncogene*, 23(20), 3622-3633. doi:10.1038/sj.onc.1207403
- Meiners S, Nur-e-Kamal MS, Mercado ML. Identification of a neurite outgrowth-promoting motif within the alternatively spliced region of human tenascin-C. (2001). *J Neurosci*. 21(18), 7215-25. doi: 10.1523/JNEUROSCI.21-18-07215.2001.
- Muoboghare, M. O., Drummond, R. M., & Kennedy, C. (2019). Characterisation of P2Y(2) receptors in human vascular endothelial cells using AR-C118925XX, a competitive and selective P2Y(2) antagonist. *Br J Pharmacol*, 176(16), 2894-2904. doi:10.1111/bph.14715
- Naviaux, R. K., Curtis, B., Li, K., Naviaux, J. C., Bright, A. T., Reiner, G. E., . . . Townsend, J. (2017). Low-dose suramin in autism spectrum disorder: a small, phase I/II, randomized clinical trial. *Ann Clin Transl Neurol*, 4(7), 491-505. doi:10.1002/acn3.424
- Peterson, T. S., Thebeau, C. N., Ajit, D., Camden, J. M., Woods, L. T., Wood, W. G., . . . Weisman, G. A. (2013). Up-regulation and activation of the P2Y(2) nucleotide receptor mediate neurite extension in IL-1 $\beta$ -treated mouse primary cortical neurons. *Journal of Neurochemistry*, 125(6), 885-896. doi:10.1111/jnc.12252
- Pooler, A. M., Guez, D. H., Benedictus, R., & Wurtman, W. J. (2005). Uridine enhances neurite outgrowth in nerve growth factor-differentiated pheochromocytoma cells. *Neuroscience*, 134, 207-214.

- Rosen, P. J., Mendoza, E. F., Landaw, E. M., Mondino, B., Graves, M. C., McBride, J. H., . . . Beldegrun, A. (1996). Suramin in hormone-refractory metastatic prostate cancer: a drug with limited efficacy. *Journal of Clinical Oncology*, 14(5), 1626-1636.
- Rothaug, M., Becker-Pauly, C., & Rose-John, S. (2016). The role of interleukin-6 signaling in nervous tissue. *Biochimica et Biophysica Acta (BBA) - Molecular Cell Research*, 1863(6, Part A), 1218-1227. doi:10.1016/j.bbamcr.2016.03.018
- Scemes, E., & Giaume, C. (2006). Astrocyte calcium waves: what they are and what they do. *Glia*, 54(7), 716-725. doi:10.1002/glia.20374
- Schulz-Key, H., Karam, M., & Prost, A. (1985). Suramin in the treatment of onchocerciasis: the efficacy of low doses on the parasite in an area with vector control. *Trop Med Parasitol*, 36(4), 244-248.
- Schüz, A., & Palm, G. (1989). Density of neurons and synapses in the cerebral cortex of the mouse. *Journal of Comparative Neurology*, 286(4), 442-455. doi:doi.org/10.1002/cne.902860404
- Šekeljić, V., & Andjus, P. R. (2012). Tenascin-C and its functions in neuronal plasticity. *The International Journal of Biochemistry & Cell Biology*, 44(6), 825-829. doi:doi.org/10.1016/j.biocel.2012.02.014
- Semple BD, Blomgren K, Gimlin K, Ferriero DM, Noble-Haeusslein LJ. (2013). Brain development in rodents and humans: Identifying benchmarks of maturation and vulnerability to injury across species. *Prog Neurobiol*. 106-107,1-16. doi: 10.1016/j.pneurobio.2013.04.001.
- Sukigara, S., Dai, H., Nabatame, S., Otsuki, T., Hanai, S., Honda, R., . . . Itoh, M. (2014). Expression of astrocyte-related receptors in cortical dysplasia with intractable epilepsy. *J Neuropathol Exp Neurol*, 73(8), 798-806. doi:10.1097/nen.0000000000000099
- Tian GF, Azmi H, Takano T, Xu Q, Peng W, Lin J, Oberheim N, Lou N, Wang X, Zielke HR, Kang J, Nedergaard M. (2005). An astrocytic basis of epilepsy. *Nat Med*. 11(9), 973-81. doi: 10.1038/nm1277.
- Tran, M. D., & Neary, J. T. (2006). Purinergic signaling induces thrombospondin-1 expression in astrocytes. *Proceedings of the National Academy of Sciences of the United States of America*, 103(24), 9321-9326. doi:10.1073/pnas.0603146103

- von Kugelgen, I., & Hoffmann, K. (2016). Pharmacology and structure of P2Y receptors. *Neuropharmacology*, 104, 50-61. doi:10.1016/j.neuropharm.2015.10.030
- Wallingford, J., Scott, A. L., Rodrigues, K., & Doering, L. C. (2017). Altered Developmental Expression of the Astrocyte-Secreted Factors Hevin and SPARC in the Fragile X Mouse Model. *Frontiers in Molecular Neuroscience*, 10, 268-268. doi:10.3389/fnmol.2017.00268
- Washburn, K. B., & Neary, J. T. (2006). P2 purinergic receptors signal to STAT3 in astrocytes: Difference in STAT3 responses to P2Y and P2X receptor activation. *Neuroscience*, 142(2), 411-423. doi:10.1016/j.neuroscience.2006.06.034
- Wei H, Zou H, Sheikh AM, Malik M, Dobkin C, Brown WT, Li X. (2011). IL-6 is increased in the cerebellum of autistic brain and alters neural cell adhesion, migration and synaptic formation. *J Neuroinflammation*. 8, 52. doi: 10.1186/1742-2094-8-52.
- Wei, H., Chadman, K. K., McCloskey, D. P., Sheikh, A. M., Malik, M., Brown, W. T., & Li, X. (2012). Brain IL-6 elevation causes neuronal circuitry imbalances and mediates autism-like behaviors. *Biochimica et Biophysica Acta (BBA) - Molecular Basis of Disease*, 1822(6), 831-842. doi:doi.org/10.1016/j.bbadis.2012.01.011
- Yang, Q., Feng, B., Zhang, K., Guo, Y. Y., Liu, S. B., Wu, Y. M., . . . Zhao, M. G. (2012). Excessive astrocyte-derived neurotrophin-3 contributes to the abnormal neuronal dendritic development in a mouse model of fragile X syndrome. *PLoS Genet*, 8(12), e1003172. doi:10.1371/journal.pgen.1003172
- Zhang, Y., Bonnan, A., Bony, G., Ferezou, I., Pietropaolo, S., Ginger, M., . . . Frick, A. (2014). Dendritic channelopathies contribute to neocortical and sensory hyperexcitability in *Fmr1(-/y)* mice. *Nat Neurosci*, 17(12), 1701-1709. doi:10.1038/nn.3864

## 7. Appendix: Copyright Transfer Agreements

### 7.1. Copyright Transfer Agreement: GLIA

GLIA

Published by Wiley (the "Owner")

#### COPYRIGHT TRANSFER AGREEMENT

Date: March 17, 2021

Contributor name: ANGELA, LEE SCOTT

Contributor address:

Manuscript number: GLIA-00260-2020.R2

Re: Manuscript entitled Astrocyte-mediated purinergic signaling is upregulated in a mouse model of Fragile X syndrome (the "Contribution")

for publication in GLIA (the "Journal")

published by Wiley Periodicals LLC ("Wiley")

Dear Contributor(s):

Thank you for submitting your Contribution for publication. In order to expedite the editing and publishing process and enable the Owner to disseminate your Contribution to the fullest extent, we need to have this Copyright Transfer Agreement executed. If the Contribution is not accepted for publication, or if the Contribution is subsequently rejected, this Agreement shall be null and void.

**Publication cannot proceed without a signed copy of this Agreement.**

---

#### A. COPYRIGHT

1. The Contributor assigns to the Owner, during the full term of copyright and any extensions or renewals, all copyright in and to the Contribution, and all rights therein, including but not limited to the right to publish, republish, transmit, sell, distribute and otherwise use the Contribution in whole or in part in electronic and print editions of the Journal and in derivative works throughout the world, in all languages and in all media of expression now known or later developed, and to license or permit others to do so. For the avoidance of doubt, "Contribution" is defined to only include the article submitted by the Contributor for publication in the Journal (including any embedded rich media) and does not extend to any supporting information submitted with or referred to in the Contribution ("Supporting Information"). To the extent that any Supporting Information is submitted to the Journal, the Owner is granted a perpetual, non-exclusive license to publish, republish, transmit, sell, distribute and otherwise use this Supporting Information in whole or in part in electronic and print editions of the Journal and in derivative works throughout the world, in all languages and in all media of expression now known or later developed, and to license or permit others to do so. If the Contribution was shared as a preprint, the Contributor grants to the Owner exclusivity as to any rights retained by the Contributor in the preprint.

2. Reproduction, posting, transmission or other distribution or use of the final Contribution in whole or in part in any medium by the Contributor as permitted by this Agreement requires a citation to the Journal suitable in form and content as follows: (Title of Article, Contributor, Journal Title and Volume/Issue, Copyright © [year], copyright owner as specified in the Journal, Publisher). Links to the final article on the publisher website are encouraged where appropriate.

## B. RETAINED RIGHTS

Notwithstanding the above, the Contributor or, if applicable, the Contributor's employer, retains all proprietary rights other than copyright, such as patent rights, in any process, procedure or article of manufacture described in the Contribution.

## C. PERMITTED USES BY CONTRIBUTOR

**1. Submitted Version.** The Owner licenses back the following rights to the Contributor in the version of the Contribution as originally submitted for publication (the "Submitted Version"):

a. The right to self-archive the Submitted Version on: the Contributor's personal website; a not for profit subject-based preprint server or repository; a Scholarly Collaboration Network (SCN) which has signed up to the STM article sharing principles [<http://www.stm-assoc.org/stm-consultations/scn-consultation-2015/>] ("Compliant SCNs"); or the Contributor's company/ institutional repository or archive. This right extends to both intranets and the Internet. The Contributor may replace the Submitted Version with the Accepted Version, after any relevant embargo period as set out in paragraph C.2(a) below has elapsed. The Contributor may wish to add a note about acceptance by the Journal and upon publication it is recommended that Contributors add a Digital Object Identifier (DOI) link back to the Final Published Version.

b. The right to transmit, print and share copies of the Submitted Version with colleagues, including via Compliant SCNs, provided that there is no systematic distribution of the Submitted Version, e.g. posting on a listserv, network (including SCNs which have not signed up to the STM sharing principles) or automated delivery.

**2. Accepted Version.** The Owner licenses back the following rights to the Contributor in the version of the Contribution that has been peer-reviewed and accepted for publication, but not final (the "Accepted Version"):

a. The right to self-archive the Accepted Version on: the Contributor's personal website; the Contributor's company/institutional repository or archive; Compliant SCNs; and not for profit subject-based repositories such as PubMed Central, all subject to an embargo period of 12 months for scientific, technical and medical (STM) journals and 24 months for social science and humanities (SSH) journals following publication of the Final Published Version. There are separate arrangements with certain funding agencies governing reuse of the Accepted Version as set forth at the following website: <http://www.wileyauthors.com/funderagreements>. The Contributor may not update the Accepted Version or replace it with the Final Published Version. The Accepted Version posted must contain a legend as follows: This is the accepted version of the following article: FULL CITE, which has been published in final form at [Link to final article]. This article may be used for non-commercial purposes in accordance with the Wiley Self-Archiving Policy [<http://www.wileyauthors.com/self-archiving>].

b. The right to transmit, print and share copies of the Accepted Version with colleagues, including via Compliant SCNs (in private research groups only before the embargo and publicly after), provided that there is no systematic distribution of the Accepted Version, e.g. posting on a listserv, network (including SCNs which have not signed up to the STM sharing principles) or automated delivery.

**3. Final Published Version.** The Owner hereby licenses back to the Contributor the following rights with respect to the final published version of the Contribution (the "Final Published Version"):

a. Copies for colleagues. The personal right of the Contributor only to send or transmit individual copies of the Final Published Version in any format to colleagues upon their specific request, and to share copies in private

sharing groups in Compliant SCNs, provided no fee is charged, and further provided that there is no systematic external or public distribution of the Final Published Version, e.g. posting on a listserve, network or automated delivery.

**b. Re-use in other publications.** The right to re-use the Final Published Version or parts thereof for any publication authored or edited by the Contributor (excluding journal articles) where such re-used material constitutes less than half of the total material in such publication. In such case, any modifications must be accurately noted.

**c. Teaching duties.** The right to include the Final Published Version in teaching or training duties at the Contributor's institution/place of employment including in course packs, e-reserves, presentation at professional conferences, in-house training, or distance learning. The Final Published Version may not be used in seminars outside of normal teaching obligations (e.g. commercial seminars). Electronic posting of the Final Published Version in connection with teaching/training at the Contributor's company/institution is permitted subject to the implementation of reasonable access control mechanisms, such as user name and password. Posting the Final Published Version on the open Internet is not permitted.

**d. Oral presentations.** The right to make oral presentations based on the Final Published Version.

#### **4. Article Abstracts, Figures, Tables, Artwork and Selected Text (up to 250 words).**

**a.** Contributors may re-use unmodified abstracts for any non-commercial purpose. For online uses of the abstracts, the Owner encourages but does not require linking back to the Final Published Version.

**b.** Contributors may re-use figures, tables, artwork, and selected text up to 250 words from their Contributions, provided the following conditions are met:

(i) Full and accurate credit must be given to the Final Published Version.

(ii) Modifications to the figures and tables must be noted. Otherwise, no changes may be made.

(iii) The re-use may not be made for direct commercial purposes, or for financial consideration to the Contributor.

(iv) Nothing herein will permit dual publication in violation of journal ethical practices.

#### **D. CONTRIBUTIONS OWNED BY EMPLOYER**

**1.** If the Contribution was written by the Contributor in the course of the Contributor's employment as a "work-made-for-hire" in the course of employment, the Contribution is owned by the company/institution which must execute this Agreement (in addition to the Contributor's signature). In such case, the company/institution hereby agrees to the terms of use set forth in paragraph A above and assigns to the Owner, during the full term of copyright, all copyright in and to the Contribution for the full term of copyright throughout the world as specified in paragraph A above.

**2.** In addition to the rights specified as retained in paragraph B above and the rights granted back to the Contributor pursuant to paragraph C above, the Owner hereby grants back, without charge, to such company/institution, its subsidiaries and divisions, the right to make copies of and distribute the Final Published Version internally in print format or electronically on the Company's internal network. Copies so used may not be resold or distributed externally. However, the company/institution may include information and text from the Final Published Version as part of an information package included with software or other products offered for sale or license or included in patent applications. Posting of the Final Published Version by the company/institution on a public access website may only be done with written permission, and payment of any applicable fee(s). Also, upon payment of the applicable reprint fee, the company/institution may distribute print copies of the Final Published Version externally.

#### **E. GOVERNMENT CONTRACTS**

In the case of a Contribution prepared under U.S. Government contract or grant, the U.S. Government may reproduce, without charge, all or portions of the Contribution and may authorize others to do so, for official U.S. Government purposes only, if the U.S. Government contract or grant so requires. (U.S. Government, U.K. Government, and other government employees: see notes at end.)

#### **F. COPYRIGHT NOTICE**

The Contributor and the company/institution agree that any and all copies of the Final Published Version or any part thereof distributed or posted by them in print or electronic format as permitted herein will include the notice of copyright as stipulated in the Journal and a full citation to the Journal.

#### **G. CONTRIBUTOR'S REPRESENTATIONS**

The Contributor represents that: (i) the Contributor and all co-Contributors have the full power, authority and capability to enter into this Agreement, to grant the rights and license granted herein and to perform all obligations hereunder; (ii) neither the Contributor nor any co-Contributor has granted exclusive rights to, or transferred their copyright in, any version of the Contribution to any third party; (iii) the Contribution is the Contributor's original work, all individuals identified as Contributors actually contributed to the Contribution, and all individuals who contributed are included; (iv) if the Contribution was prepared jointly, the Contributor has informed the co-Contributors of the terms of this Agreement and has obtained their signed written permission to execute this Agreement on their behalf; (v) the Contribution is submitted only to this Journal and has not been published before, has not been included in another manuscript, and is not currently under consideration or accepted for publication elsewhere; (vi) if excerpts from copyrighted works owned by third parties are included, the Contributor shall obtain written permission from the copyright owners for all uses as set forth in the standard permissions form and the Journal's Author Guidelines, and show credit to the sources in the Contribution; (vii) the Contribution and any submitted Supporting Information contain no libelous or unlawful statements, do not infringe upon the rights (including without limitation the copyright, patent or trademark rights) or the privacy of others, do not breach any confidentiality obligation, do not violate a contract or any law, do not contain material or instructions that might cause harm or injury, and only utilize data that has been obtained in accordance with applicable legal requirements and Journal policies; and (viii) there are no conflicts of interest relating to the Contribution, except as disclosed. Accordingly, the Contributor represents that the following information shall be clearly identified on the title page of the Contribution: (1) all financial and material support for the research and work; (2) any financial interests the Contributor or any co-Contributors may have in companies or other entities that have an interest in the information in the Contribution or any submitted Supporting Information (e.g., grants, advisory boards, employment, consultancies, contracts, honoraria, royalties, expert testimony, partnerships, or stock ownership); and (3) indication of no such financial interests if appropriate.

Notwithstanding acceptance, the Owner or Wiley may (but is not obliged to) require changes to the Contribution, including changes to the length of the Contribution, and/or elect not to publish the Contribution if for any reason, in the Owner's or Wiley's reasonable judgment, such publication would be inconsistent with the Core Practices and associated guidelines set forth by the Committee on Publication Ethics (a not-for-profit organization based in the UK: <https://publicationethics.org/core-practices>) or would result in legal liability, violation of Wiley's ethical guidelines, or violation of journal ethical practices.

#### **H. USE OF INFORMATION**

The Contributor acknowledges that, during the term of this Agreement and thereafter, the Owner (and Wiley where Wiley is not the Owner) may process the Contributor's personal data, including storing or transferring data outside of the country of the Contributor's residence, in order to process transactions related to this Agreement and to communicate with the Contributor, and that the Publisher has a legitimate interest in processing the Contributor's personal data. By

entering into this Agreement, the Contributor agrees to the processing of the Contributor's personal data (and, where applicable, confirms that the Contributor has obtained the permission from all other contributors to process their personal data). Wiley shall comply with all applicable laws, statutes and regulations relating to data protection and privacy and shall process such personal data in accordance with Wiley's Privacy Policy located at: <https://www.wiley.com/en-us/privacy>.

---

I agree to the COPYRIGHT TRANSFER AGREEMENT as shown above, consent to execution and delivery of the Copyright Transfer Agreement electronically and agree that an electronic signature shall be given the same legal force as a handwritten signature, and have obtained written permission from all other contributors to execute this Agreement on their behalf.

Contributor's signature (type name here): Angela Scott

Date: March 17, 2021

---

**SELECT FROM OPTIONS BELOW:**

**Contributor-owned work**

**U.S. Government work**

*Note to U.S. Government Employees*

*A contribution prepared by a U.S. federal government employee as part of the employee's official duties, or which is an official U.S. government publication, is called a "U.S. government work", and is in the public domain in the United States. If the Contribution was not prepared as part of the employee's duties, is not an official U.S. government publication, or if at least one author is **not** a U.S. government employee, it is not a U.S. government work. If at least one author is **not** a U.S. government employee, then the non-government author should also sign the form, selecting the appropriate ownership option. If more than one author is not a U.S. government employee, one may sign on behalf of the others.*

**U.K. Government work (Crown Copyright)**

*Note to U.K. Government Employees*

*The rights in a contribution prepared by an employee of a UK government department, agency or other Crown body as part of his/her official duties, or which is an official government publication, belong to the Crown and must be made available under the terms of the Open Government Licence. Contributors must ensure they comply with departmental regulations and submit the appropriate authorisation to publish. If your status as a government employee legally prevents you from signing this Agreement, please contact the Journal production editor. If this selection does not apply to at least one author in the group, this author should also sign the form, indicating transfer of those rights which that author has and selecting the appropriate additional ownership selection option. If this applies to more than one author, one may sign on behalf of the others.*

**Other**

Including Other Government work or Non-Governmental Organisation work

*Note to Non-U.S., Non-U.K. Government Employees or Non-Governmental Organisation Employees*

*If you are employed by the Australian Government, the World Bank, the World Health Organization, the International Monetary Fund, the European Atomic Energy Community, the Jet Propulsion Laboratory at California Institute of Technology, the Asian Development Bank, the Bank of International Settlements, USDA Agricultural Research Services, or are a Canadian Government civil servant, please download a copy of the license agreement from <http://www.wileyauthors.com/licensingFAQ> and upload the form to the Wiley Author Services Dashboard. If*

*your status as a government or non-governmental organisation employee legally prevents you from signing this Agreement, please contact the Journal production editor.*

Name of Government/Non-Governmental Organisation:

---

**[ ] Company/institution owned work (made for hire in the course of employment)**

If you are an employee of Amgen, please download a copy of the company addendum from <http://www.wileyauthors.com/licensingFAQ> and return your signed license agreement along with the addendum. If this selection does not apply to at least one author in the group, this author should also sign the form, indicating transfer of those rights which that author has and selecting the appropriate additional ownership selection option. If this applies to more than one author, one may sign on behalf of the others.

Name of Company/Institution:

---

Authorized Signature of Employer:

---

Date:

---

Signature of Employee:

---

Date:

---

---

## 7.2. Copyright Transfer Agreement: Victoria Krasovska (Pagnan)

Kathryn Reynolds  
PhD Candidate

McMaster University  
HSC 1R15A  
1280 Main Street West  
Hamilton, ON  
L8S 4L8

September 30, 2021

Victoria Krasovska  
21-88 Decorso Drive  
Guelph, ON  
N1L 0A1

Dear Victoria,

As you know, I am completing a Ph.D. at McMaster University entitled ASTROCYTE-MEDIATED PURINERGIC SIGNALLING IN THE FRAGILE X MOUSE CORTEX.

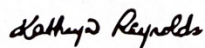
In your capacity as my co-author for the submitted manuscript entitled DYSREGULATED PURINERGIC SIGNALLING MOLECULES IN FRAGILE X MOUSE CORTICAL ASTROCYTES, which will comprise Chapter Four of my sandwich thesis, I would like your permission to reprint images and data collected as part of the following work in my thesis:

Krasovska, V. (2018). *Activation of TLR4 by Tenascin C through the induction of Interleukin-6 in the Fragile X mouse model* [Master of Science Thesis, McMaster University]. MacSphere: <http://hdl.handle.net/11375/23708>.

I am also requesting that you grant irrevocable, nonexclusive license to McMaster University and to the National Library of Canada to reproduce this material as a part of the thesis. Proper acknowledgement of your copyright of the reprinted material will be given in the thesis. If these arrangements meet with your approval, please sign where indicated below and return this letter to me.

Thank you very much.

Sincerely,



Kathryn Reynolds

PERMISSION GRANTED FOR THE USE REQUESTED ABOVE

McMaster University

Authorized by: Victoria Krasovska

Title: Co-Author

Date: September 30, 2021

Signature: 